



**University of  
Nottingham**  
UK | CHINA | MALAYSIA

Connecting MicroRNA and Autophagy  
Disturbances in  
Amyotrophic Lateral Sclerosis (ALS)

**Sophie Foggin, BSc**

School of Life Sciences

University of Nottingham

**2022**

This dissertation is submitted for the degree of Doctor of Philosophy

## Declaration

I confirm that the work in this thesis is my own. Images from other sources, or work that has been generated through collaborative projects, have been otherwise acknowledged in the text.

**Sophie Foggin**

## Acknowledgements

I must extend my sincere gratitude to my two supervisors, Professor Robert Layfield and Dr. Federico Dajas-Bailador, for their guidance and enthusiasm, which proved extremely motivating, and for their patience, kindness and nurture, which allowed me to develop and flourish. They have been a constant source of inspiration and have ensured my PhD experience will be remembered with great fondness.

To those who provided me with guidance and support in the lab, especially Dr. Alex Rathbone, Barry Shaw, Dr. Raquel Mesquita-Ribeiro and Dr. Daniel Scott, I am so grateful. Thanks must also go to the SLIM team, for their help and instruction with microscopy. I must also thank the Motor Neurone Disease Association for sponsoring this project and allowing this to be possible.

My unreserved thanks go to those both past and present from the Layfield, Dajas-Bailador and Serres labs and to those further afield, who have become true friends. Their daily laughter, fun and support over the last four years has meant more than I can explain.

I would especially like to thank my family, particularly my mum and grandparents. Without their endless support and encouragement I would never be where I am. Finally, thanks go particularly to Ben, for his love and friendship, always.

## Abstract

Growing evidence implicates miRNA dysregulation as a hallmark of Amyotrophic Lateral Sclerosis (ALS) and there has been increasing interest in their potential as biomarkers of disease. However, no miRNA biomarker signature is currently clinically available. In Chapter 3, we perform a systematic literature review to collate 727 miRNAs reported as dysregulated between ALS patients and controls across 27 studies and note overlap of many miRNAs. However, the number of ALS-relevant predicted gene targets does not correlate with miRNAs reported as more frequently dysregulated in ALS compared to randomly chosen miRNAs, not dysregulated in ALS. We establish a pipeline to identify a candidate miRNA, miR-340-5p, dysregulated in ALS and implicated in autophagy, a biochemical pathway relevant to ALS. In addition, miR-340 is known to regulate NRF2, a transcription factor which mediates antioxidant signalling, a process defective in ALS.

In Chapter 4 we use a live cell autophagy assay to show overexpression of miR-340 is associated with reduced lysosomal incorporation of a *SQSTM1/p62* reporter construct, indicative of inhibited autophagy. MiR-340 is predicted to target the ALS-associated gene, *TBK1*, a critical autophagy regulator. Dual luciferase reporter assays suggest miR-340 can bind a specific region in the *TBK1* 3'UTR, and western blotting confirmed a decrease of TBK1 protein levels in HeLa cells overexpressing miR-340. We also show that miR-340 overexpression reduces Ser-403 phosphorylation of p62 in HeLa cells, a process mediated by TBK1, which suggests miR-340 impacts on proteins of relevance to ALS, downstream of TBK1 signalling.

In Chapter 5 we inhibit endogenous miR-340 in human primary astrocytes and observe an increase in NRF2 protein by western blotting, which indicates miR-340 may be an attractive potential therapeutic target. Consistent with the complexity of miRNA-mediated translational regulation, TBK1 protein levels are not similarly increased. Further to NRF2 and TBK1, we also identify other ALS and autophagy-relevant targets of miR-340, by mRNA sequencing of HeLa cells overexpressing miR-340. One such possible target, *UNC13A*, is associated with the mislocalisation of TDP-43, seen in almost all ALS cases. Recently, it has been highlighted that 'direct' and

'indirect' mRNA targets of a miRNA might contribute distinctly to motor neurone dysfunction and we establish a pipeline to determine potential 'direct' and 'indirect' mRNA targets of a miRNA using mRNA sequencing data.

We also investigate a downstream impact of impaired autophagy, specifically, its effect on the extracellular vesicle proteome, due to the increasing interest in the role of extracellular vesicles in the pathogenesis of ALS. Upon treatment with an autophagy inhibitor, bafilomycin, we observe changes in the secreted exosomal autophagy and ALS-related proteins. This identifies a potential increase in exosomal TBK1 in cells with impaired autophagy.

This work has established a novel role of the ALS-dysregulated miR-340 in pathways of relevance to ALS. Our findings contribute to knowledge of miRNA regulation of autophagy-relevant proteins implicated in ALS, and explores ALS-relevant consequences of autophagy dysfunction. Overall, we demonstrate the potential of miR-340 as a therapeutic target in ALS. The work presented in this thesis contributes to the growing knowledge of the pathomechanisms of ALS.

## Publications

**Foggin, S.**, Mesquita-Ribeiro, R., Dajas-Bailador, F., Layfield, R. (2019) 'Biological significance of microRNA biomarkers in ALS-innocent bystanders or disease culprits?', *Frontiers in Neurology*, 10(578). doi: 10.3389/fneur.2019.00578.

## Abstracts

**Foggin, S.**, Mesquita-Ribeiro, R., Dajas-Bailador, F., Layfield, R. 'Deregulation of TBK1-Mediated Autophagy by ALS-Associated MicroRNA-340' (Abstract). In: European Network for the Cure of ALS; 2021 May 12-14; Virtual.

**Foggin, S.**, Mesquita-Ribeiro, R., Dajas-Bailador, F., Layfield, R. 'Deregulation of TBK1-Mediated Autophagy by ALS-Associated MicroRNA-340' (Abstract). In: 31st International Symposium on ALS/MND; 2020 Dec 9-11; Virtual.

## List of Abbreviations

ALS – Amyotrophic lateral sclerosis  
ALS2 – Gene encoding alsin  
AMPK – AMP-activated protein kinase  
ARE – Antioxidant response element  
ATG – Autophagy related gene  
BCA – Bicinchroninic acid  
Bcl-2 – B cell lymphoma 2  
BECN1 – Gene encoding Beclin-1  
BRCA1 – Breast cancer type 1  
C21orf2 – Gene encoding cilia and flagella associated protein 410  
C9orf72 – Chromosome 9 open reading frame 72  
CHMP2B - Charged Multivesicular Body Protein 2B  
CNS – Central nervous system  
CSF – Cerebrospinal fluid  
DCTN1 – Gene encoding dynactin subunit 1  
DEPTOR - DEP Domain Containing MTOR Interacting Protein  
DGCR8 - DiGeorge syndrome chromosomal region 8  
DMSO – Dimethyl sulphoxide  
DRP – Dipeptide repeat protein  
DTX4 – Deltex E3 Ubiquitin ligase 4  
DYRK2 - Dual specificity tyrosine phosphorylation regulated kinase 2  
ESCRT - Endosomal sorting complex required for transport  
ER – Endoplasmic reticulum  
ERGIC – ER-Golgi intermediate compartment  
EV – Extracellular vesicle  
fALS – Familial amyotrophic lateral sclerosis  
FIP200 - Family-interacting protein of 200 kDa  
FTD – Frontotemporal dementia  
FUS – Fused in sarcoma  
FYCO1 - FYVE and coiled-coil domain containing 1  
GFAP – Glial fibrillary acidic protein  
GO – Gene ontology

GWAS – Genome wide association study  
H2DCFDA - DCFH-DA, 2',7'-Dichlorodihydrofluorescein diacetate  
hnRNP – Heterogenous nuclear ribonuclear protein  
*HNRNPA1* – Gene encoding heterogeneous nuclear ribonucleoprotein H  
*HNRNPA2B1* – Gene encoding heterogeneous nuclear ribonucleoprotein A2/B1  
*HNRNPA3* – Gene encoding heterogeneous nuclear ribonucleoprotein A3  
hnRNPH – Heterogenous nuclear ribonuclear protein H  
HRP – Horseradish peroxidase  
hsa – Homo Sapien miRNA prefix  
ICC - Immunocytochemistry  
ILV – Intraluminal vesicle  
INF – Interferon  
iPSC – Induced pluripotent stem cell  
JNK1 – C-Jun N terminal protein kinase  
LAMP – Lysosome associated membrane protein  
LC/MS/MS – Liquid chromatography tandem mass spectrometry  
LIR – LC3 interacting region  
KEAP1 – Kelch ECH associating protein  
MeSH – Medical subject headings  
MAP1LC3 – Microtubule associated proteins 1A/1B light chain 3  
*MAPT* – Gene encoding microtubule associated protein tau  
*MATR3* – Gene encoding Matrin-3  
miRISC – MicroRNA Induced Silencing Complex  
miRNA – Micro-ribonucleic acid  
miTG – miRNA targeted gene score  
mLST8 – Mammalian lethal with SEC13 protein 8  
MND – Motor neurone disease  
MRE – MicroRNA response element  
mRNA – Messenger ribonucleic acid  
MS – Mass spectrometry  
mTOR – Mammalian target of rapamycin  
MVB – Multivesicular body  
NBR1 – Next to BRCA1 gene 1  
NDP-52 – Nuclear domain 10 protein 52

NEFH – Neurofilament heavy  
*NEK1* – Gene encoding nima related kinase 1  
NEFL – Neurofilament light  
NRF2 – Nuclear factor erythroid 2-related factor 2  
*OPTN* – Gene encoding optineurin  
*p62/SQSTM1* – Sequestosome 1  
PAS – Phagosome assembly site  
PB1 – RNA-directed RNA polymerase catalytic subunit  
PCC – Pearson’s correlation coefficient  
*PFN1* – Gene encoding profilin 1  
PI3K – Phosphoinositide 3-kinase  
PLEKHM1 – Pleckstrin homology domain-containing family M member 1  
PRAS40 – Proline-rich Akt substrate of 40 kDa  
RAPTOR – Regulatory associated protein of mTOR  
ROS – Reactive oxygen species  
RNA – Ribonucleic acid  
RRM – RNA recognition motif  
sALS – Sporadic amyotrophic lateral sclerosis  
SEC – Size exclusion chromatography  
SMCR8 - Guanine nucleotide exchange protein SMCR8 (Smith-Magenis syndrome chromosomal region candidate gene 8 protein)  
SNAP - Synaptosomal-Associated Protein  
SNARE – SNAP receptor  
*SOD1* – Gene encoding superoxide dismutase 1  
*SPG11* – Gene encoding spatacsin  
STING – Stimulator of interferon genes  
*TARDBP* – Gene encoding Tar DNA binding protein-43 (TDP-43)  
TBK1 – TANK-binding Kinase 1  
TDP-43 – Tar DNA binding protein-43  
TFEB - Transcription factor EB  
TOLLIP – Toll-interacting protein  
TRPB – Transactivation response element RNA-binding protein  
*TUBA4A* – Gene encoding tubulin alpha-4A  
UBA – ubiquitin associated

*UBQLN2* – Gene encoding ubiquilin-2  
ULK – Unc-51 like kinase  
UPS – Ubiquitin proteasome system  
UVRAG - UV radiation resistance associated gene  
VAPB – VAMP Associated Protein B  
VCP – Valosin Containing Protein  
VPS – Vacuolar protein sorting  
WDR41 - WD repeat-containing protein 41  
WIPI – WD-repeat protein Interacting with Phosphoinositides

# List of Figures

Figure 1: Structure of a neurone.

Figure 2: Neurone and astrocyte interaction.

Figure 3: Diagrammatic representation of TDP-43 structure.

Figure 4: Diagrammatic representation of the structure of FUS.

Figure 5: Diagrammatic representation of *C9orf72* DNA and the three RNA transcripts.

Figure 6: Molecular mechanisms of autophagy.

Figure 7: Selective autophagy.

Figure 8: Neuronal autophagy.

Figure 9: The canonical miRNA biogenesis pathway.

Figure 10: Heatmap of miRNAs most frequently reported as dysregulated in ALS.

Figure 11: Tissue distribution of deregulated miRNAs.

Figure 12: Bioinformatic processes identified miR-340 as a candidate TBK1-targeting miRNA.

Figure 13: T-coffee alignment showing conservation of mammalian miR-340-5p gene sequences.

Figure 14: Diagrammatic representation of the KEAP1:NRF2 pathway.

Figure 15: Diagrammatic representation of the relationship between TBK1 and NRF2 signalling.

Figure 16: Diagrammatic representation of the STING pathway.

Figure 17: miR-340 reduces NRF2 protein levels in HeLa cells.

Figure 18: Live HeLa cells transfected with miR-340 show inhibited autophagic flux that phenocopies pharmacological inhibition of autophagy.

Figure 19: Western blotting for endogenous autophagy markers with miR-340 mimic in HeLa cells.

Figure 20: Dual luciferase reporter assay shows miR-340 can directly target TBK1.

Figure 21: Western blotting for TBK1 in mouse N2A cells with miR-340 mimic and control.

Figure 22: Western blotting for Ser-403 phosphorylated p62.

Figure 23: Direct vs indirect modulation of NRF2 by miR-340.

Figure 24: TBK1 inhibition with BX-795 decreases NRF2 protein levels.

Figure 25: Western blotting for STING in HeLa cells.

Figure 26: Use of the miR-340 inhibitor in HeLa cells.

Figure 27: Impact of miR-340 inhibition in cells with high levels of miR-340 compared to low.

Figure 28: Astrocytic neuroprotection.

Figure 29: Western blotting for NRF2 and TBK1 protein in human primary astrocytes.

Figure 30: Diagrammatic model of regulation of TBK1 levels under normal conditions or endogenous miR-340 inhibition.

Figure 31: Summary of gene expression distribution from human primary astrocytes treated with miR-340 inhibitor or control inhibitor.

Figure 32: Summary of gene expression distribution from HeLa cells transfected with miR-340 mimic or control.

Figure 33: Comparison of mRNAs with significantly altered expression upon miR-340 overexpression, with known ALS and autophagy genes.

Figure 34: Gene ontology of mRNAs with statistically significantly altered expression by miR-340 overexpression compared to control.

Figure 35: Identifying potential miR-340 direct and indirect gene targets.

Figure 36: Representation of Amin and colleagues' findings in mice with decreasing miR-218 expression.

Figure 37: Exosome biogenesis and overlap with the autophagy pathway.

Figure 38: Venn diagram showing the overlap between ALS<sup>o</sup>D genes, the detected human exosomal proteins reported on Exocarta and the top 100 exosomal proteins reported on Exocarta.

Figure 39: Characterisation of purified exosomes from N2A cells.

Figure 40: Western blotting for exosomal markers from N2A derived exosomes or N2A cell lysate.

Figure 41: Number of proteins detected from N2A-derived exosomes in all replicates of DMSO or all replicates of bafilomycin treated cells.

Figure 42: Western blotting for Tbk1 to validate mass spectrometry results of Tbk1 in exosome samples from N2A cells treated with bafilomycin or DMSO control.

Figure 43: Fold change of Alix and Flotillin-1 for DMSO or bafilomycin treated exosomes (second exosome fraction (F2) only) for each of the three biological replicates.

Figure 44: Western blotting for Tbk1 in N2A cells treated with DMSO and bafilomycin.

## List of Tables

Table 1: List of miRNAs used in this thesis, their nucleotide sequence and purchase information.

Table 2: 5-20 % gel solution components.

Table 3: Oligonucleotides used for cloning.

Table 4: Primers used for SDM.

Table 5: PCR reaction for site directed mutagenesis.

Table 6: : List of cell permeable miRNA inhibitors used in Chapter 5, their nucleotide sequence and purchase information.

Table 7: Mature miRNAs found dysregulated in five or more different studies reporting altered miRNA levels in ALS patients compared to controls out of a maximum of 27.

Table 8: ALS deregulated and non-deregulated miRNAs and ALS gene target predictions.

Table 9: MITG scores (predicted likelihood of gene targeting) of TBK1 and NFE2L2.

Table 10: Known targets of hsa-miR-340-5p.

Table 11: Summary of findings of miR-340 mimic and inhibitor.

Table 12: Noteworthy mRNAs from sequencing of human primary astrocytes treated with miR-340 inhibitor or control inhibitor.

Table 13: Noteworthy mRNAs from sequencing of miR-340 mimic or control transfected HeLa cells.

Table 14: Impact of miR-340 overexpression on protein and mRNA levels of TBK1, NRF2, p62 and STING in HeLa cells

Table 15: ALS-relevant mRNAs with altered expression induced by miR-340 overexpression in HeLa cells.

Table 16: Autophagy-relevant mRNAs with altered expression induced by miR-340 overexpression in HeLa cells.

Table 17: ALS-relevant genes with altered expression in HeLa cells with overexpressed miR-340 classed as 'direct' or 'indirect' targets of miR-340.

Table 18: Differentially expressed miRNAs found in ALS patient-derived exosomes.

Table 19: Number of proteins detected across all six samples of N2A-derived exosomes, present in at least one DMSO repeat and at least one bafilomycin repeat.

Table 20: Mass spectrometry analysis of exosomal autophagy proteins unique to bafilomycin A1 treated N2As.

Table 21: Mass spectrometry analysis of exosomal ALS-related proteins unique to bafilomycin A1 treated N2As.

Table 22: Mass spectrometry analysis of exosomal autophagy proteins detected in at least one replicate of bafilomycin treated exosomes or at least one replicate of DMSO treated exosomes.

Table 23: Mass spectrometry analysis of exosomal ALS-related proteins detected in at least one replicate of bafilomycin treated exosomes or at least one replicate of DMSO treated exosomes.

# Table of Contents

<b>Chapter 1 - Introduction</b> .....	<b>1</b>
<b>1.1 Amyotrophic Lateral Sclerosis</b> .....	<b>1</b>
1.1.1 The Nervous System: Neurones and Astrocytes .....	2
1.1.2 Disease Genetics .....	4
1.1.3 Molecular and Cellular Mechanisms in ALS .....	5
<b>1.2 Autophagy</b> .....	<b>18</b>
1.2.1 Molecular Mechanisms .....	18
1.2.2 Selective Autophagy.....	24
1.2.3 Autophagy in Neurones.....	26
1.2.4 Autophagic Dysregulation in Amyotrophic Lateral Sclerosis.....	28
<b>1.3 MicroRNAs</b> .....	<b>35</b>
1.3.1 Biogenesis and Function.....	35
1.3.2 MiRNA Target Predictions .....	40
1.3.3 MiRNAs in Neurones .....	41
1.1.1 MiRNAs as Biomarkers of ALS .....	42
1.3.4 MicroRNAs in Autophagy .....	44
1.3.5 MicroRNAs as Therapeutics .....	44
<b>1.4 Summary and Thesis Aims</b> .....	<b>45</b>
<b>Chapter 2 - Materials and Methods</b> .....	<b>47</b>
<b>2.1 Identification of ALS-Associated, Patient-Relevant MiRNAs from a Systematic Literature Review</b> .....	<b>47</b>
2.1.1 Studies of Deregulated MicroRNAs in ALS Patients .....	47
2.1.2 Heatmaps .....	47
2.1.3 Bioinformatic MicroRNA Target Predictions of ALS Genes .....	47
<b>2.2 Investigation of ALS-Relevant miR-340 as a regulator of Autophagy</b> .....	<b>48</b>
2.2.1 Bioinformatic Autophagy-Targeting MicroRNA Predictions.....	48
2.2.2 Cell Culture.....	48
2.2.3 MicroRNA Transfections .....	48
2.2.4 Western Blotting .....	49
2.2.5 Immunocytochemistry .....	52
2.2.6 Analysis of Immunocytochemistry Images.....	52
2.2.7 Live Cell Autophagic Flux Assay.....	53

2.2.8	Luciferase Reporter Assay .....	54
2.2.9	HeLa Cell Treatment with BX-795 .....	58
<b>2.3</b>	<b>Investigation of miR-340 Function in Human Astrocytes .....</b>	<b>58</b>
2.3.1	Seeding and Treatment of Cells for RNA Extraction.....	58
2.3.2	TRIzol Extraction of RNA.....	59
2.3.3	mRNA Sequencing .....	59
2.3.4	Bioinformatics to Determine Direct and Indirect mRNA Targets of miR-340 .....	59
<b>2.4</b>	<b>Investigation of Autophagy Failure – Impact on Extracellular Vesicle Proteomes .....</b>	<b>60</b>
2.4.1	Cell Culture for Exosome Purification .....	60
2.4.2	Bafilomycin Treatment of N2A cells Cultured for Exosome Purification.....	60
2.4.3	Purification of Exosomes using Size Exclusion Chromatography .....	60
2.4.4	Preparation of Exosome Samples for Western Blotting and Mass Spectrometry.....	61
2.4.5	Treatment and Western Blotting of N2A Cells.....	62
<b>2.5</b>	<b>Statistical Analysis .....</b>	<b>62</b>
<b><i>Chapter 3 - Identification of ALS-Associated miRNAs from a Systematic Literature Review.....</i></b>		
		<b>63</b>
<b>3.1</b>	<b>Introduction .....</b>	<b>63</b>
3.1.1	Experimental Aims .....	63
<b>3.2</b>	<b>Results and Discussion.....</b>	<b>65</b>
3.2.1	Review of Studies of miRNA Expression in ALS Patients .....	65
3.2.2	ALS Patient-Deregulated MicroRNAs .....	66
3.2.3	Correlating Deregulated MicroRNAs with Target Gene Predictions .....	70
3.2.4	Tissue Distribution of Deregulated MicroRNAs.....	75
3.2.5	Analysis of Deregulated MiRNAs with Relevance to Autophagy.....	78
<b>3.3</b>	<b>Conclusions and Future Directions.....</b>	<b>84</b>
<b><i>Chapter 4 - Investigation of ALS-Relevant miR-340 as a Regulator of Autophagy 86</i></b>		
<b>4.1</b>	<b>Introduction .....</b>	<b>86</b>
4.1.1	The miR-340-5p Gene .....	86
4.1.2	Established Gene Targets of hsa-miR-340-5p .....	87
4.1.3	Known functions of miR-340-5p.....	89
4.1.4	NRF2 .....	91
4.1.5	STING Signalling.....	96
4.1.6	Experimental Aims .....	98

<b>4.2</b>	<b>Results and Discussion.....</b>	<b>100</b>
4.2.1	MiR-340 Overexpression Reduces NRF2 Protein Levels.....	100
4.2.2	Impact of miR-340 on Autophagy in a Live-Cell Model .....	102
4.2.3	<i>TBK1</i> is a Direct Target of miR-340.....	106
4.2.4	Impact of miR-340 on Targets Downstream of TBK1 Signalling .....	111
4.2.5	The miR-340 Inhibitor Has Minimal Effects On Autophagy and Proteins of Interest in HeLa Cells .....	116
<b>4.3</b>	<b>Conclusions and Future Directions.....</b>	<b>123</b>
<b><i>Chapter 5 - Investigation of miR-340 Function in Human Astrocytes.....</i></b>		<b>126</b>
<b>5.1</b>	<b>Introduction .....</b>	<b>126</b>
5.1.1	Astrocytes.....	126
5.1.2	Experimental Aims .....	131
<b>5.2</b>	<b>Results and Discussion.....</b>	<b>132</b>
5.2.1	Impact of miR-340 on NRF2 and TBK1 in Astrocytes.....	132
5.2.2	Exploration of Human miR-340 Targets <i>In Cellulo</i> .....	136
<b>5.3</b>	<b>Conclusions and Future Directions.....</b>	<b>156</b>
<b><i>Chapter 6 - Investigation of Autophagy Failure – Impact on Extracellular Vesicle Proteomes.....</i></b>		<b>159</b>
<b>6.1</b>	<b>Introduction .....</b>	<b>159</b>
6.1.1	Extracellular Vesicles.....	159
6.1.2	Experimental Aims .....	172
<b>6.2</b>	<b>Results and Discussion.....</b>	<b>173</b>
6.2.1	Isolation of Exosomes from N2A Cells.....	173
6.2.2	Impact of Dysfunctional Autophagy on Exosomal Protein Content .....	176
<b>6.3</b>	<b>Conclusions and Future Directions.....</b>	<b>187</b>
<b><i>Chapter 7 - Final Discussion and Conclusions.....</i></b>		<b>189</b>
<b>7.1</b>	<b>Concluding Remarks .....</b>	<b>196</b>
<b>7.2</b>	<b>Future Directions.....</b>	<b>197</b>
<b><i>Chapter 8 - References.....</i></b>		<b>199</b>
<b><i>Chapter 9 - Appendices.....</i></b>		<b>237</b>

# Chapter 1 - Introduction

Amyotrophic lateral sclerosis (ALS) is a complex and terminal disease which results in motor neurone death. The disruption of several cellular and molecular mechanisms, including autophagy, are attributed to this. Growing evidence implicates the dysregulation of microRNAs (miRNAs) in ALS, which regulate protein translation, and many miRNAs influence the translation of autophagy proteins, including those linked to ALS. Their dysregulation may therefore result in autophagic impairment during ALS. The following introduction details the pathways, genes and proteins implicated in ALS, including those critical to autophagy. A more detailed overview of the autophagy pathway and its role in ALS is also presented and the contribution of miRNA dysregulation to ALS is discussed. Membrane-bound extracellular vesicles (EVs) have also been implicated in the pathogenic spread of ALS, and their biogenesis overlaps with the autophagy pathway. A more detailed overview of extracellular vesicles and their implication in ALS is given in section 6.1.1.

## 1.1 Amyotrophic Lateral Sclerosis

ALS, also known as Lou Gehrig's disease, is the most common form of adult-onset motor neurone disease (MND). It generally presents in late middle age and is characterised by the progressive loss of upper and lower motor neurones in the spinal cord, cerebral cortex and brainstem (Tao, Wei and Wu, 2018). This leads to skeletal muscle wasting, as well as dysphagia, dysarthria and paralysis (Watts and Vanryckeghem, 2001; Duffy, Peach and Strand, 2007; Ramirez *et al.*, 2008; Muscaritoli *et al.*, 2012). It is a fatal neurodegenerative disease with a life expectancy of 2-5 years from onset, and death usually occurs due to respiratory failure (Thomsen *et al.*, 2014). ALS affects 1.7-2.3 people per 100,000 world-wide, making it one of the most common motor neurone diseases, and it is the third most common neurodegenerative disease in the 40-60 age group, following Alzheimer's and Parkinson's (Beghi *et al.*, 2006; Cloutier *et al.*, 2015). The only treatment currently available in the UK is Riluzole, which can increase life expectancy by 2-3 months

(Bensimon *et al.*, 1994). The drug Edaravone is approved for use in the USA, China, Japan, Korea, Canada and Switzerland (Rothstein, 2017).

In some ALS cases, patients display impaired cognitive function and develop frontotemporal dementia (FTD) (Lomen-Hoerth, Anderson and Miller, 2002). FTD is a group of disorders resulting from degeneration of cortical neurones and basal ganglia which can also result in language dysfunction and personality changes. Around 15% of ALS patients have presented with symptoms of FTD and around 15% of FTD patients develop ALS (Ringholz *et al.*, 2005; Lillo *et al.*, 2011). Additionally, patients with ALS-FTD usually have shorter life spans than those with the pure forms of disease. As such, ALS and FTD are considered to exist within a disease spectrum.

### 1.1.1 The Nervous System: Neurones and Astrocytes

The nervous system refers to the central and peripheral nervous systems (CNS and PNS respectively). The CNS is comprised of the brain and spinal cord, whilst the PNS consists of cells within the nervous system which exist outside the brain and spinal cord. Both the CNS and PNS contain neuronal and non-neuronal (glial) cells. Motor neurones are encompassed in the CNS, and glial cells in the CNS include astrocytes, oligodendrocytes and microglia. In the PNS, neuronal cells include sensory neurones and glial cells include satellite cells and Schwann cells.

Neurones are polarised cells and typically comprise dendrites, soma (cell body) and axons. Information from neighbouring neurones is received by dendrites which transmit the information to the soma. This information is transmitted along the axon *via* an action potential which moves towards the axon terminals where neurotransmitters are released at synapses (Figure 1). Sensory neurones respond to stimuli such as touch, and transmit information to the central nervous system. Motor neurones receive information from the brain and spinal cord to result in muscle contraction. Interneurones connect neurones to other neurones whether in the CNS or PNS. Axons are myelinated to aid the conduction of the action potential by Schwann cells in the PNS and oligodendrocytes in the CNS (Dodson and Forsythe, 2004; Debanne *et al.*, 2011).

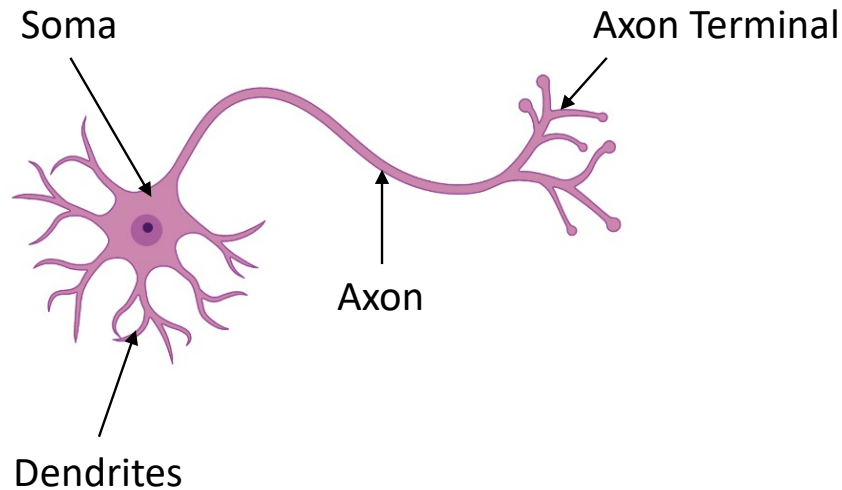


**Figure 1: Structure of a neurone.** The dendrites receive information which is processed in the soma and an action potential is transmitted along the axon towards the axon terminals. Drawn by author using Biorender.

Another form of communication along neurones is axonal transport, which is an important regulated mechanism in neurones due to their polarised nature, and is dysfunctional in ALS (Williamson and Cleveland, 1999; De vos *et al.*, 2007). Most protein synthesis occurs in the soma and transport of cellular components occurs along the axon. Human motor neurones can reach 1 metre in length, demonstrating an additional challenge faced by motor neurones over other cell types. Most transport occurs via microtubules which contain a fast growing 'plus' end and slower growing 'minus' end. The plus end faces towards the axon terminal whilst the minus end faces the soma. Cellular components are moved by retrograde transport by dyneins towards the soma or by anterograde transport by kinesins towards the synapse (Stenoien and Brady, 1999).

Astrocytes are the most common cell type in the CNS and are considered to be 10-50 times more abundant than neurones. They are closely associated with all parts of neurones and their end processes are associated with vascular endothelial cells, enabling them to regulate the blood brain barrier (Dehouck *et al.*, 1990). At the synapses, astrocytes recycle neurotransmitters to help regulate synaptic activity (Figure 2) (Takahashi *et al.*, 1997; Perea and Araque, 2005). They also have a crucial role in antioxidant defence through a protein called Nuclear factor erythroid 2-

related factor 2 (NRF2). NRF2 is a transcription factor which activates the expression of several antioxidant genes (Itoh *et al.*, 1997). Overexpression of NRF2 specifically in ALS mutant mouse astrocytes (not muscle or neurones) delayed disease onset and increased survival (Vargas *et al.*, 2008, 2013). Astrocytes and their relevance to ALS are discussed in more depth in Chapter 5.

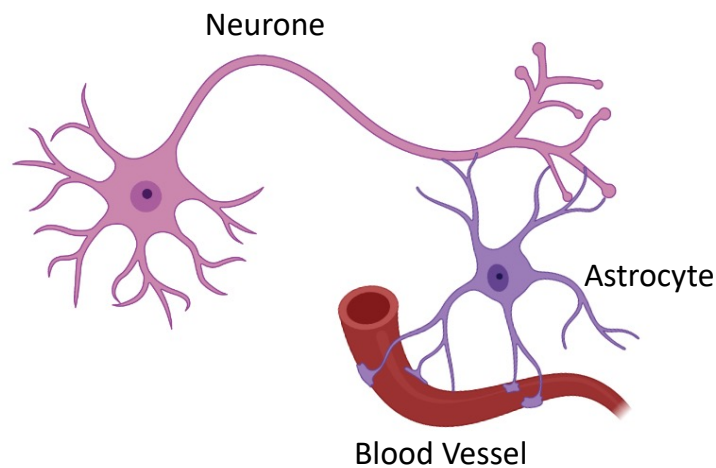


**Figure 2: Neurone and astrocyte interaction.** Astrocytes associate with neurones and are involved in regulating synaptic functions through neurotransmitter recycling as well as regulating the blood brain barrier. Drawn by author using Biorender.

### 1.1.2 Disease Genetics

Around 90% of ALS cases are sporadic (sALS) occurring in individuals with no prior family history of the disease. The remaining 10% are familial (fALS), where at least one other family member is affected and are caused by mutations that are predominantly inherited by autosomal dominance. Over 100 different genes have been identified with mutations in ALS patients which are either causative or disease associated (Dervishi *et al.*, 2018).

Mutations in the gene, chromosome 9 open reading frame 72 (*C9orf72*), are the most common cause of fALS and sALS, accounting for around 40% and 7% of cases respectively. Mutations in this gene are also the most common genetic variant of FTD, accounting for 25% of familial FTD (Renton *et al.*, 2011). The mutation affecting  $\text{Cu}^{2+}/\text{Zn}^{2+}$  superoxide dismutase (SOD1), was the first cause of ALS to be discovered and accounts for about 20% of fALS cases (Rosen *et al.*, 1993). Mutations in TAR DNA

binding protein 43 kDa (TDP-43) and fused in sarcoma (FUS) each account for around 4% of fALS cases (Chiò *et al.*, 2012).

Genes and genetic variants related to ALS have been collated in the Amyotrophic Lateral Sclerosis online Database (ALSoD). Throughout this thesis ALSoD is repeatedly referred to for the use of its collection of known ALS-related genes. ALSoD was last updated in 2020 to include 154 genes implicated in ALS (Abel *et al.*, 2012).

### 1.1.3 Molecular and Cellular Mechanisms in ALS

Whilst diverse, many of the established ALS-associated genes can be broadly grouped into several cellular mechanisms or pathways, implicated in ALS: autophagy and vesicle trafficking (*TBK1*, *OPTN*, *SQSTM1*, *C9orf72*, *UBQLN2*, *VCP*, *VAPB*, *ALS2*, *CHMP2B*, *ANXA11* and *UNC13A*), RNA regulation (*TARDBP*, *FUS*, *HNRNPA1*, *HNRNPA2B1* and *MATR3*), DNA damage control (*FUS*, *C21orf2* and *NEK1*), cytoskeletal dynamics and axonal guidance (*PFN1*, *DCTN1*, *NEFH*, *MAPT*, *SPG11*, *TUBA4* and *KIF5A*), oxidative stress and mitochondrial dysfunction (*CHCHD10* and *SOD1*) and glutamate excitotoxicity (*C9orf72* and *ALS2*) (Weishaupt, Hyman and Dikic, 2016; Gall *et al.*, 2020). In addition, many of these genes overlap with several of these pathways.

#### 1.1.3.1 Oxidative Stress and Mitochondrial Dysfunction

Oxidative stress results from an imbalance of oxidants and antioxidants, causing the levels of reactive oxygen species (ROS) to increase, which has adverse effects on cellular components. An increase in damaging oxidation of proteins, lipids, RNA and DNA are observed in ALS cases (Shibata *et al.*, 2001; Chang *et al.*, 2008; Mitsumoto *et al.*, 2008). The major source of ROS is oxidative phosphorylation in mitochondria, implicating dysfunction of this organelle in ALS. Indeed, mitochondrial damage has been observed in ALS patients (Sasaki, Horie and Iwata, 2007).

##### 1.1.3.1.1 SOD1

$\text{Cu}^{2+}/\text{Zn}^{2+}$  superoxide dismutase is an antioxidant enzyme which functions to protect cells from ROS by catalysing the reaction of free radical superoxide to hydrogen

peroxide and oxygen. The hydrogen peroxide is further broken down into water and oxygen by catalase. It is a 32 kDa homodimer with one copper and one zinc binding site (Valentine, Doucette and Zittin Potter, 2005). Familial *SOD1* ALS patients have shown over a 40% reduction in SOD1 function, resulting in an imbalance of ROS levels. The build-up of ROS subsequently leads to the oxidation of proteins, DNA and RNA which results in toxicity (Saccon *et al.*, 2013).

Mutations in *SOD1* were the first discovered genetic cause of ALS and consist mostly of point mutations (Rosen *et al.*, 1993; Morgan and Orrell, 2016). The most frequently studied mutation in SOD1 is SOD1<sup>G93A</sup>. SOD1 mutations often result in its misfolding and aggregation in spinal motor neurones (Bosco *et al.*, 2010). The toxicity of mutant SOD1 is thought to be through gain of function, since most SOD1 mutant proteins maintain normal enzymatic function (Kirby *et al.*, 2016). Additionally, it is the expression of mutant SOD1, rather than the elimination of endogenous SOD1 that has been suggested to cause ALS phenotypes (Weishaupt, Hyman and Dikic, 2016). For example, *Sod1* knockout mice do not develop ALS to the extent SOD1<sup>G93A</sup> transgenic mice do (Reaume *et al.*, 1996). However, transgenic mice overexpressing wild type SOD1 developed terminal ALS-like symptoms such as loss of spinal ventral neurones (Graffmo *et al.*, 2013).

### ***1.1.3.2 RNA regulation and DNA damage control***

Mutations in several RNA-binding proteins, including TDP-43 and FUS, are associated with ALS. This results in disruption of RNA splicing, miRNA biogenesis, transcription, translation and RNA nuclear-cytoplasmic transport (Buratti *et al.*, 2004, 2010; Polymenidou *et al.*, 2011). Further, ALS-associated mutations in several proteins involved in DNA damage repair may prevent their normal function during ALS pathogenesis (Higelin *et al.*, 2018).

#### **1.1.3.2.1 TAR DNA Binding Protein (TDP-43)**

The gene, *TARDBP* codes for a 43 kDa protein, TDP-43. It is part of the heterogenous nuclear ribonuclear (hnRNP) protein family (Chaudhury, Chander and Howe, 2010). It has a C-terminal glycine rich region where the majority of mutations occur, two

RNA recognition motifs (RRM1 and RRM2) and nuclear localisation and export signals, allowing movement between the nucleus and cytoplasm (Figure 3) (Lagier-Tourenne, Polymenidou and Cleveland, 2010). As an RNA binding protein, TDP-43 plays a role in alternate splicing, RNA transcription and transport, pre-miRNA processing and mRNA stability (Scotter, Chen and Shaw, 2015). Further, TDP-43 is able to stabilise its own mRNA, meaning it can regulate its own protein levels (Ayala *et al.*, 2011).

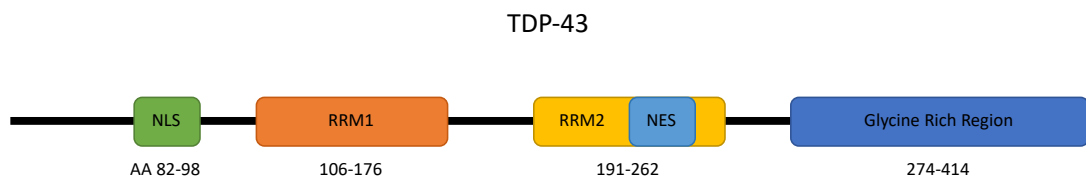


**Figure 3: Diagrammatic representation of TDP-43 structure.** The position in amino acids of each domain are shown. NLS= nuclear localisation signal, RRM= RNA recognition motif, NES= nuclear export signal. Not to scale. Drawn by author.

TDP-43 is also a component of stress granules in the cytoplasm, where protein and mRNA are sequestered, and protein translation is temporarily halted in response to cellular stress (Colombrita *et al.*, 2009; Kozomara, Birgaoanu and Griffiths-Jones, 2019). These stress granules are considered liquid-like compartments that form in both the nucleus and cytoplasm of neurones and are formed by phase separation from the cytoplasm (Molliex *et al.*, 2015).

TDP-43 is normally nuclear, though mutations in *TARDBP* can lead to its mislocalisation to the cytoplasm where it forms ubiquitin-positive, hyperphosphorylated and TDP-43 fragmented aggregates (Neumann *et al.*, 2006; Van Deerlin *et al.*, 2008; Winton *et al.*, 2008). Whilst in the cytoplasm, TDP-43 undergoes several post-translational modifications including ubiquitination, phosphorylation and C-terminal cleavage (Neumann *et al.*, 2006). These aggregates, which define ALS as a TDP-43 proteinopathy are detected first in spinal motor neurones, before spreading to glia and the wider central nervous system (CNS). Around 97% of ALS patients possess phosphorylated cytoplasmic TDP-43 inclusions and in most ALS cases, TDP-43 aggregates are present in patient motor neurones,

regardless of any *TARDBP* mutation (Neumann *et al.*, 2006; Winton *et al.*, 2008). Indeed, the spread of TDP-43 proteinopathy is used to measure the severity and progression of ALS (Brettschneider *et al.*, 2013). Protein aggregates in FTD are often tau positive, though TDP-43 inclusions in the brain are also a hallmark of FTD and many tau-negative FTD patients develop TDP-43 aggregation (Neumann *et al.*, 2006).

TDP-43 in microvesicles, a type of extracellular vesicle (EV) secreted by cells, has been shown to be preferentially taken up by recipient cells and delivers a higher level of toxicity to these cells. Additionally, TDP-43 oligomers are able to spread both cell to cell and along axons, demonstrating a prion-like tendency for TDP-43 (Feiler *et al.*, 2015). However, whether toxicity is due to loss of function of TDP-43 due to its aggregation and subsequent inability to interact with partners, or due to its gain of toxic function through aggregation, remains under experimental examination. Mutations in TDP-43 as well as gain and loss of function of TDP-43 have been shown to produce motor neurone phenotypes (Stallings *et al.*, 2010). For example, overexpression of TDP-43 in a mouse model leads to degeneration of spinal and cortical motor neurones and to the accumulation of TDP-43 aggregates in neurones (Wils *et al.*, 2010). In contrast, another mouse model, with inactivation of the *Tardbp* gene resulted in ALS-like phenotypes such as motor neurone loss. This study also identified the accumulation of ubiquitinated proteins, including TDP-43 in the affected neurones (Wu, Cheng and Shen, 2012). A different mouse model harnessing TDP-43 inactivation also found affected mice displayed ALS phenotypes such as degenerated large motor axons. Further, autolysosomes and autophagosomes accumulated in the affected motor neurone cell bodies, suggesting loss of TDP-43 disrupted normal cellular autophagy (Iguchi *et al.*, 2013). Since both loss and gain of TDP-43 result in ALS phenotypes, the disruption of normal TDP-43, regardless of direction appears mechanistic in the disease.

The reduction of TDP-43 in the nucleus, where it is required for miRNA processing, implicates miRNAs in the pathogenesis of ALS. TDP-43 has been shown to be a necessary component of the nuclear microprocessor complex with Drosha and DGCR8, aiding the binding of this complex to specific primary miRNAs. Additionally it is part of the cytoplasmic Dicer-TRPB complex where it facilitates processing of a

subset of pre-miRNAs regulated by TDP-43 in the nucleus, through binding to their terminal loops (Kawahara and Mieda-Sato, 2012). The mislocalisation of TDP-43 to the cytoplasm resulted in reduction of TDP-43 regulated miRNAs by the Dicer-TRPB complex (Kawahara and Mieda-Sato, 2012). Knockdown of TDP-43 has been shown to downregulate the expression of several miRNAs in human SH-SY5Y cells including hsa-miR-181a-1-3p, hsa-miR-132-5p, hsa-miR-143-3p and hsa-miR-335-5p (Kawahara and Mieda-Sato, 2012). Note this is regulation of a miRNA biogenesis by a protein as opposed to regulation of protein expression levels by an miRNA.

#### 1.1.3.2.2 Fused in Sarcoma (FUS)

Human FUS is a 526 amino acid protein with an RNA recognition motif, SYGQ (serine, tyrosine, glycine, glutamine) rich region, zinc finger motif, nuclear localisation and export signal, an RNA recognition motif (RRM) and multiple RGG (arginine, glycine, glycine) rich regions (Figure 4) (Kirby *et al.*, 2016). FUS is an hnRNP due to its involvement in transcription, splicing, mRNA stabilisation and transport as well as miRNA processing (Ishigaki *et al.*, 2012; Morlando *et al.*, 2012; Zhou *et al.*, 2013; Yang *et al.*, 2014; Udagawa *et al.*, 2015).

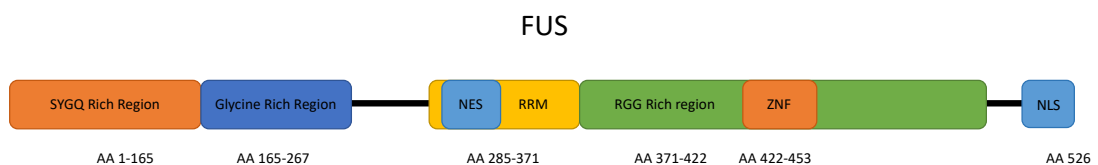


**Figure 4: Diagrammatic representation of the structure of FUS.** The position in amino acids of each domain are shown. NLS= nuclear localisation signal, RRM= RNA recognition motif, NES= nuclear export signal, ZNF=zinc finger region. Not to scale. Drawn by author.

FUS is normally nuclear, but, similar to TDP-43, mutations can lead to its mislocalisation to the cytoplasm where it can form FUS positive inclusions (Neumann *et al.*, 2009). Most ALS-associated FUS mutations occur in the nuclear localisation signal (NLS) at the C-terminal, and amongst the first discovered were FUS<sup>R521C</sup>, FUS<sup>R521G</sup> and FUS<sup>R521H</sup> (Kwiatkowski *et al.*, 2009; Vance *et al.*, 2009). This disrupts the nuclear-cytoplasmic shuttling of FUS (Ito *et al.*, 2011). Like TDP-43, FUS is incorporated into stress granules during cellular stress, which evolve towards an

aggregated state, made more rapid by ALS-associated FUS mutations and contributes to ALS pathology (Sama *et al.*, 2013; Patel *et al.*, 2015). The cytoplasmic inclusions are immunoreactive for ubiquitin and p62, but not TDP-43, demonstrating FUS acts independently of TDP-43 (Suzuki *et al.*, 2010; Tateishi *et al.*, 2010).

FUS binds RNA through its RNA recognition motif (RRM), zinc finger motif and RGG regions (Prasad *et al.*, 1994; Iko *et al.*, 2004). It binds to RNA specifically via AU-rich stem loops and GGUG motifs (Lerga *et al.*, 2001; Hoell *et al.*, 2011). FUS is also implicated in the regulation of miRNAs and is required for Drosha recruitment to pri-miRNAs (Gregory *et al.*, 2004; Morlando *et al.*, 2012). FUS has also been shown to interact with AGO2, a component of the miRNA induced silencing complex (miRISC) and is required for mature miRNA gene silencing (Zhang *et al.*, 2018). Indeed, reduction of FUS has been shown to alter the expression of over 150 miRNAs, including miR-9-5p, miR-125b-5p, miR-128-3p, miR-132-3p and miR-143-3p, and miR-199a-3p, many of which are relevant to neuronal function (Morlando *et al.*, 2012).

#### 1.1.3.2.3 HNRNPA1/HNRNPA2B1

*HNRNPA1/HNRNPA2B1* genes encode proteins hnRNPA1/2B1 which have prion like domains and have a role in miRNA biogenesis and the packing and transport of mRNA. hnRNPA1 is involved in the recognition of splice sites on mRNA (Buratti *et al.*, 2005). Mutations causing inherited neurodegeneration result in hnRNPA1/2 assembly into stress granules (H. J. Kim *et al.*, 2013).

#### 1.1.3.2.4 MATR3

*MATR3* encodes the protein matrin 3 which has been associated with distal myopathy when mutated (S85C) (Feit *et al.*, 1998). Matrin 3 was found to associate with TDP-43 which was increased by a S85C mutation. Mutations have been identified in both sALS and fALS and an F115C mutation presents much more aggressive symptoms than a S85C mutation (Johnson *et al.*, 2014).

#### 1.1.3.2.5 Never in Mitosis A Related Kinase 1

Never in Mitosis A Related Kinase 1 (NEK1) is involved in the DNA damage response and mutations associated with ALS can cause haploinsufficiency. Human motor neurone-derived iPSCs with *C9orf72* repeat expansion or a *NEK1* mutation were subject to DNA damage with irradiation. Neurones with *C9orf72* repeat expansion showed signs of DNA damage using immunocytochemistry of histone accumulation. The number of cells positive for histones was increased in *C9orf72* repeat expansion differentiated motor neurones, though was more severely increased in *NEK1* mutant differentiated motor neurones (Higelin *et al.*, 2018). This indicates *NEK1* mutations contribute directly to the vulnerability of motor neurones during ALS.

#### 1.1.3.3 Cytoskeletal Dynamics and Axonal Transport

Mutations in several genes associated with axonal transport have been linked with ALS. This leads to impaired trafficking of cellular components in both retrograde and anterograde directions along microtubules (Williamson and Cleveland, 1999; De vos *et al.*, 2007). The significant length of motor neurones (up to one metre long) and their polarised nature, which separates the soma from axon terminals, renders them particularly vulnerable to defective axonal transport .

##### 1.1.3.3.1 Profilin 1

*PFN1* encodes profilin 1 which is an actin binding protein and is involved in membrane trafficking and cytoskeletal dynamics (Witke, 2004). Multiple mutations in *PFN1* have been associated with fALS and account for 1-2% of cases. One study found mice expressing an ALS-associated Pfn1<sup>C71G</sup> mutation experienced motor neurone loss, muscle wasting and death. Further, this study showed the mutation caused the formation of Pfn1 insoluble aggregates and increased the levels of the autophagy marker, p62, in motor neurones. Interestingly, these aggregates formed after motor neurone degeneration, indicating they did not trigger the initial degeneration (Yang *et al.*, 2016).

#### 1.1.3.3.2 Dynactin

Dynactin 1 (*DCTN1*), a subunit of the dynactin complex, binds directly to dynein and both proteins are required for retrograde axonal transport. A dynactin 1 G59S mutation reduces the affinity of dynactin for microtubules and results in aggregation of the mutated dynactin protein and increased cell death in the motor neurone cell line, MN1 (Levy *et al.*, 2006). Dynactin 1 is reduced in motor neurones of sALS patients and knockdown of dynactin in motor neurones was found to impede the transport of autophagosomes (Ikenaka *et al.*, 2013).

#### 1.1.3.3.3 Tubulin Alpha 4A

Mutations in the gene, *TUBA4A*, which codes for the protein tubulin alpha 4A were identified by an exome wide analysis of over 350 patients with fALS (Smith *et al.*, 2014). ALS mutations in *TUBA4A* reduce microtubule repolarisation and stability (Smith *et al.*, 2014). Decreased mRNA of *TUBA4A* have been found in the brain and spinal cord of both sALS and fALS patients (Helferich *et al.*, 2018).

#### 1.1.3.3.4 Neurofilaments

Neurofilaments are intermediate filaments specific to neurones. They are composed of neurofilament protein L (low molecular weight) (NFL), neurofilament protein M (medium molecular weight) (NFM) and neurofilament protein H (high molecular weight) (NFH), and correct stoichiometry of these three proteins is crucial for neuronal function (Szaro and Strong, 2010). A recent study has shown *NEFH* (the gene encoding NFH) to be targeted by several miRNAs shown to be downregulated in ALS patient spinal cord motor neurones. Further, the levels of NEFH were also found increased in ALS patient spinal cord samples, consistent with downregulation of their regulating miRNAs (Campos-Melo, Hawley and Strong, 2018). The *Nefl* (the gene encoding NFL) mRNA levels were reported to be reduced in NSC-34 cells with *SOD1*<sup>G37R</sup> and *SOD1*<sup>G93A</sup> mutations and in *SOD1*<sup>G93A</sup> transgenic mice as well as in human *SOD1* ALS patient spinal motor neurones. Indeed, mutant *SOD1* can bind to the 3' untranslated region (UTR) of *NEFL* mRNA, altering the proportions of the neurofilament subunits (Menzies *et al.*, 2002; Ge *et al.*, 2005). Although

contradicting, it is thought destabilisation of *NEFL* mRNA leads to NFL aggregation in motor neurones, which is a hallmark of ALS (Chen *et al.*, 2014).

#### 1.1.3.3.5 Microtubule Associated Protein Tau

Mutations in the microtubule associated protein tau (*MAPT*) are mostly associated with FTD and are rarely identified in ALS cases. The main pathological outcomes are hyperphosphorylated tau protein filaments in neurones and glia (Spillantini *et al.*, 1997). Normally soluble, in patients with FTD, tau has been observed as both soluble and insoluble. In the latter instance it is accumulated in the cytoplasm (Ghetti *et al.*, 2015).

#### 1.1.3.3.6 Spatacsin

*SPG11* encodes the protein spatacsin. Mutations in this gene can cause juvenile ALS with long term survival through a recessive mode of inheritance. Over a dozen mutations in *SPG11* have been identified in patients with juvenile ALS (Orlacchio *et al.*, 2010). The normal functions of spatacsin are mostly unknown, but it is considered to play a role in intracellular trafficking and endolysosomal homeostasis and interacts with proteins involved in membrane trafficking such as the adaptor protein complex 5, AP5Z1 (Hirst *et al.*, 2013). Mice with *Spg11* knockout experience neuronal degeneration and these neurones show accumulation of autophagosomes with a reduction in lysosomes. The authors suggest this results in too fewer lysosomes available for autophagosome-lysosome fusion, resulting in a build-up of cargo material including p62 and LC3 that would otherwise be degraded (Varga *et al.*, 2015).

#### 1.1.3.4 Autophagy and Vesicle Trafficking

TDP-43 protein aggregates in degenerating motor neurones are present in approximately 98% of all ALS cases (except those caused by mutations in *SOD1* or *FUS*), suggesting impaired protein homeostasis (Neumann *et al.*, 2006). Knockout or reduction of several crucial autophagy related proteins results in neurodegeneration,

implicating autophagy as a specific mechanism dysfunctional in ALS pathogenesis (Hara *et al.*, 2006; Komatsu *et al.*, 2006).

The role of the autophagy-associated proteins p62 (*SQSTM1*), optineurin (*OPTN*) and Tank binding kinase 1 (TBK1) in ALS are described in section 1.2.4 – Autophagic Dysregulation in Amyotrophic Lateral Sclerosis.

#### 1.1.3.4.1 C9orf72

The mutation in *C9orf72* is an extended GGGGCC hexanucleotide repeat expansion in its non-coding region on chromosome 9p21 which was identified through genome wide association studies (GWAS) of sALS patients (Shatunov *et al.*, 2010). Studies have reported *C9orf72*-mutant ALS patients to have slower disease duration and earlier age of disease onset (Byrne *et al.*, 2012; Cooper-Knock *et al.*, 2012; Van Rheenen *et al.*, 2012).

Normally, individuals possess less than eight repeats of this sequence, though in ALS, patients possess one allele where this is expanded up to several thousand times (DeJesus-Hernandez *et al.*, 2011; Renton *et al.*, 2011). These repeats are transcribed in both directions, leading to sense and anti-sense RNA foci, which can be translated in every reading frame to produce five dipeptide repeat proteins (DRPs), poly-GA, poly-GP, poly-GR, poly-PA and poly-PR, through a process called repeat associated, non-ATG dependent (RAN) translation (Ash *et al.*, 2013; Mori *et al.*, 2013). Poly-GA, poly-GP and poly-GR are formed from the sense strand and poly-GP, poly-GR, poly-PA and poly-PR from the antisense strand (Barker *et al.*, 2017). Three RNA transcript variants can be produced from *C9orf72*; a long isoform of 54 kDa produced from variants 2 and 3, and a short isoform of 24 kDa produced from variant 1 (Figure 5) (DeJesus-Hernandez *et al.*, 2011; Renton *et al.*, 2011).

The expression levels of variants 1 and 2 have been found significantly reduced in the cerebellum and frontal cortex of ALS patients with *C9orf72* mutations. Further, a higher expression of variant 1 was associated with ALS survival advantage (van Blitterswijk *et al.*, 2015).

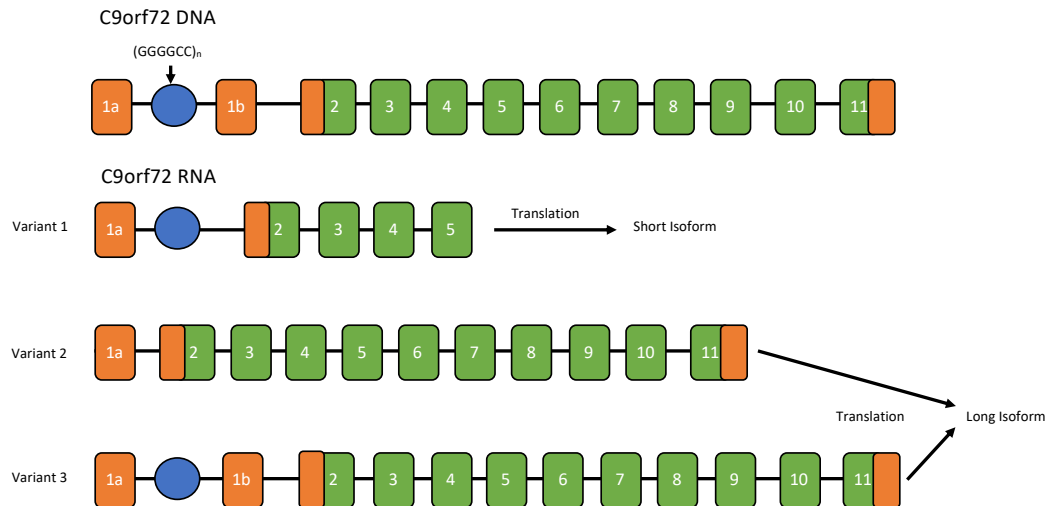


**Figure 5: Diagrammatic representation of C9orf72 DNA and the three RNA transcripts.** The GGGGCC repeat is shown as a blue circle. Variant 1 produces the short isoform of 24 kDa post translation whilst variants 2 and 3 produce the long isoform of 54 kDa. Drawn by author.

RNA foci were postulated to recruit RNA binding proteins, leading to disruption of normal RNA regulating and processing functions. Indeed, pull down assays using repeats of GGGGCC with HEK293T, SH-SY5Y, human cerebellar tissue nucleic acid extracts, combined with mass spectrometry (LC/MS/MS), have shown presence of RNA binding proteins including, but not limited to, hnRNPA1, hnRNPA2/B1, hnRNPA3 and FUS (Mori *et al.*, 2013; Sareen *et al.*, 2013; Cooper-Knock *et al.*, 2014; Haeusler *et al.*, 2014). This was subsequently shown to be associated with neurodegeneration (Davidson *et al.*, 2016). Further, increased levels of the antisense foci correlates with a later age of onset (DeJesus-Hernandez *et al.*, 2017).

TDP-43 neuronal cytoplasmic inclusions which are typical in ALS pathology have been identified in C9orf72 patients, though additionally, the DRPs form ubiquitin and p62 positive aggregates in the spinal cord, cerebellum and hippocampus (Al-Sarraj *et al.*, 2011; Cooper-Knock *et al.*, 2012; Stewart *et al.*, 2012; Mann *et al.*, 2013). It has also been shown only the antisense foci correlated with TDP-43 mislocalisation in motor neurones of ALS patients with C9orf72 mutations (Cooper-Knock *et al.*, 2015).

Reduction or knockout of C9orf72 inhibited autophagy and increased the number of cytoplasmic aggregates of p62 and TDP-43 (Sellier *et al.*, 2016). A more detailed description of C9orf72 in the autophagic pathway is given in section 1.3.4.

#### 1.1.3.4.2 Ubiquilin-2

In both sALS and fALS cases, ubiquilin-2 has been found in cytoplasmic inclusions, colocalised with TDP-43. Ubiquilin 2, as an autophagy receptor can indirectly interact with LC3 *via* its ubiquitin associated (UBA) domain during autophagy (N'Diaye *et al.*, 2009). It can also bind ubiquitinated cargo through its UBA domain and deliver them to the autophagosome. Further, reduction of *UBQLN2* (the gene encoding ubiquilin-2) expression reduces the formation of autophagosomes (Rothenberg *et al.*, 2010). Overexpression of *UBQLN2* constructs containing ALS-associated mutations resulted in the accumulation of polyubiquitinated proteins, including TDP-43, in N2A neuronal like cells (Osaka, Ito and Suzuki, 2016).

#### 1.1.3.4.3 Valosin Containing Protein

In autophagy, valosin containing protein (VCP) stabilises Beclin-1, a key protein during the early stages of autophagy, to promote early autophagosome formation (Furuya *et al.*, 2005). Reductions in VCP or inhibition of its ATPase function reduce the formation of autophagosomes. Several mutations have been identified in *VCP*, which encodes valosin containing protein and causes approximately 1-2% of fALS cases (Johnson *et al.*, 2010). It is an AAA+-ATPase with various roles including DNA repair and protein clearance (Kakizuka, 2008).

#### 1.1.3.4.4 Vesicle Associated Membrane Protein Associated Protein

Vesicle Associated Membrane Protein Associated Protein B (VAPB) plays a role in endoplasmic reticulum (ER) and golgi vesicle secretion and has a role in neurotransmitter release (Skehel *et al.*, 1995; Peretti *et al.*, 2008). It is an integral membrane protein of the ER. Mutations in *VAPB* account for less than 0.6% of ALS cases.

#### 1.1.3.4.5 Alsin

*ALS2* encodes the protein alsin and mutations in this gene have been identified in a rare juvenile onset form of ALS (Yang *et al.*, 2001). Alsin localises on the cytosolic side of the ER and is involved in endosomal vesicle transport. It acts as a guanine

nucleotide exchange factor (GEF) for Rab5 which is key for endocytosis and endosome trafficking. One study has shown that mutations in *ALS2* resulted in mislocalisation of alsin and impaired its activation of Rab5 (Otomo *et al.*, 2011). *ALS2* Knockout resulted in an accumulation of Rab5-positive vesicles and resulted in their transformation from endosomes to lysosomes (Lai *et al.*, 2009).

#### 1.1.3.4.6 Charged Multivesicular protein 2B

*CHMP2B* encodes charged multivesicular protein 2B which is a subunit of the endosomal sorting complex required for transport (ESCRT-III) machinery (Teis, Saksena and Emr, 2008). Cells overexpressing ALS-associated *CHMP2B* mutations were found to increase autophagosomes and cause ubiquitinated protein aggregation of ubiquitinated proteins and p62 (Filimonenko *et al.*, 2007).

#### 1.1.3.4.7 Unc-13 Homolog A

*UNC13A* was first associated with ALS in 2009, through a genome-wide association study and has been shown to modify survival and susceptibility to ALS (Van Es *et al.*, 2009; Diekstra *et al.*, 2012). A major role of TDP-43 is to prevent cryptic exon inclusion during RNA splicing and was shown to repress a cryptic exon splicing event in *UNC13A* (Ling *et al.*, 2015; Ma *et al.*, 2022). Consequently, nuclear reduction of TDP-43 resulted in the inclusion of this cryptic exon and was recently found to lead to *UNC13A* protein loss. Knockdown of TDP-43 also promoted the inclusion of this cryptic exon. Two polymorphisms associated with ALS and FTD in *UNC13A* also overlap with TDP-43 binding sites (Brown *et al.*, 2022). ALS risk-associated single nucleotide polymorphisms (SNPs) in *UNC13A* are located in the intron containing the cryptic exon and they promote the inclusion of this exon (Ma *et al.*, 2022).

*UNC13A* also has a role in neurotransmitter release, by interacting with syntaxin-1 to bring the SNARE complex together and bridge the vesicle and plasma membranes (Magdziarek *et al.*, 2020). *UNC13A* is also crucial to synaptic vesicle release and mice with *Munc13-1* (equivalent to *UNC13A* in humans) knockout have a 90% reduction in numbers of synaptic vesicles and a subsequent reduction in the action potential-mediated glutamate release (Augustin *et al.*, 1999).

#### 1.1.3.4.8 Other Autophagy-Associated Proteins

*GRN* encodes the protein progranulin and mutations in this gene are one of the most common causes of FTD, being responsible for up to 10% of cases (Baker *et al.*, 2006; Cruts *et al.*, 2006). Granulin is a secreted growth factor with a range of roles including neurite outgrowth with enhanced neuronal survival and inflammation (Ahmed *et al.*, 2007; Van Damme *et al.*, 2008). Almost all mutations in this gene cause loss of function with TDP-43 protein accumulation (Kumar-Singh, 2011). Further, *GRN* has been shown to be regulated by miR-659 which increased the likelihood of developing FTD (Rademakers *et al.*, 2008).

## 1.2 Autophagy

Autophagy is one of two processes utilised by cells to degrade and recycle unwanted or damaged components, to ensure cell survival. The dysfunction of autophagy is a candidate pathomechanism in ALS. Indeed, several genes crucial to autophagy are implicated in ALS and are discussed in the section 1.2.4. Proteins, organelles, pathogens and cancerous materials are all maintained by autophagy. There are three types – macroautophagy (referred to as autophagy hereafter), microautophagy and chaperone-mediated autophagy. During microautophagy, the lysosomal membrane invaginates to engulf cargo directly (Mijaljica, Prescott and Devenish, 2011). During chaperone mediated autophagy, proteins with a specific KFERQ motif are transported directly across the lysosomal membrane, into the lumen (Massey, Kiffin and Cuervo, 2004). The other cellular recycling process is the ubiquitin-dependent proteasome system which involves the degradation of specific ubiquitin labelled proteins by the proteasome (Melino, 2005). Macroautophagy, on the other hand, degrades proteins *via* the lysosome.

### 1.2.1 Molecular Mechanisms

#### 1.2.1.1 Autophagosome formation

Upon autophagy induction, there is formation of an isolation membrane or phagophore. The Unc-51 like kinase 1 and 2 (ULK1 and 2) are the main inducers of

phagophore formation and autophosphorylation of ULK1 at Thr180 is critical to autophagy induction (Bach *et al.*, 2011). Autophagy related protein 13 (ATG13) binds ULK1 and 2, enabling interactions with the focal adhesion kinase family–interacting protein of 200 kDa (FIP200), which acts as a scaffolding unit. ATG13 and FIP200 are phosphorylated by ULK1 and 2 (Jung *et al.*, 2009). This ATG13-ULK-FIP200 complex is essential for localisation to the pre-autophagosomal structure (PAS), the site of phagophore formation (K. Suzuki *et al.*, 2001). ATG101 is another component of this complex and heterodimerises with ATG13 through their HORMA domains (named after Hop1p, Rev7p and MAD2 proteins), stabilising it (Mercer, Kaliappan and Dennis, 2009; Qi *et al.*, 2015). The complex of ULK1, ATG13, FIP200 and ATG101 is often referred to as the initiation complex (Figure 6). In addition, phosphorylation of ULK1/2 increases the activity of the autophagy nucleation complex, which is described below.

ULK1 is regulated by both the energy sensing AMP-activated protein kinase (AMPK) and mammalian target of rapamycin complex 1 (mTORC1) (Chang and Neufeld, 2009). mTORC1 is formed from mTOR, regulatory associated protein of mTOR (RAPTOR), target of rapamycin complex subunit LST8 (mLST8), DEP domain containing MTOR interacting protein (DEPTOR) and proline-rich AKT substrate of 40 kDa (PRAS40) (Laplante and Sabatini, 2009; Peterson *et al.*, 2009). An inhibitor of autophagy, mTORC1 phosphorylates and inactivates ULK1 and ATG13 under nutrient-rich conditions, though upon starvation or rapamycin treatment, mTORC1 becomes inactive and ULK1 and 2 are activated and undergo autophosphorylation (Hara *et al.*, 2008; Hosokawa *et al.*, 2009; Kim *et al.*, 2011). Alternatively, AMPK stimulates autophagy in response to low energy levels and phosphorylates ULK1, where it is released from mTORC1 and relocates to the phagophore assembly site (Kim *et al.*, 2011). AMPK can phosphorylate RAPTOR, to inhibit mTORC1 and induce autophagy (Gwinn *et al.*, 2008). Additionally, mTORC1 phosphorylation of ULK1 is able to prevent the interaction of AMPK with ULK1 (Kim *et al.*, 2011).

ULK1 activates the nucleation complex, consisting of the class 3 phosphatidylinositol–3 kinase (PI(3)K), vacuolar protein sorting 34 (VPS34), Beclin-1 with its regulatory subunit vacuolar protein sorting 15 (VPS15), and ATG14L (Figure

6) (Furuya *et al.*, 2005; Lindmo *et al.*, 2008). Specifically ULK1 phosphorylates Beclin-1 on Ser-14 (Russell *et al.*, 2013). ATG14L has been shown to increase the phosphorylation of Beclin-1 by AMPK (J. Kim *et al.*, 2013). An alternative complex which contains the UV resistance association (UVRAG) protein, but not ATG14L, is involved in endosome maturation (Itakura *et al.*, 2008). Autophagy is repressed by rubicon, which binds to a subset of UVRAG complexes (Zhong *et al.*, 2009). Beclin-1 is phosphorylated by ULK1 on Ser-14 and VPS34 produces phosphatidylinositol-3-phosphate (PI(3)P) through the phosphorylation of phosphatidylinositol (R. C. Russell, Tian, Yuan, Park, Y.-Y. Chang, *et al.*, 2013). This PI3P present on the ER is recognised by WIPI proteins with FYVE domains and allows the isolation membrane to form. At the ER, this is known as an omegasome (Müller and Proikas-Cezanne, 2015).

Beclin-1 is regulated by B-cell lymphoma 2 (Bcl-2), an anti-apoptotic protein. During nutrient rich conditions, Beclin-1 is bound to Bcl-2, preventing autophagy (Pattingre *et al.*, 2005). However, proteins containing Bcl-2 homology 3 (BH3) domains are able to disrupt this interaction between Beclin-1 and Bcl-2 and result in autophagy activation (Levine, Sinha and Kroemer, 2008).

A complex of ATG12-ATG5-ATG16 as well as microtubule-associated light chain 1 (MAP1LC3) (referred to as LC3)-phosphatidylethanolamine (PE) are then recruited to the PAS. This occurs as ATG7 (an E1 enzyme) activates ATG12 which is then transferred to ATG10 (an E2 enzyme) and subsequently covalently bonded to a lysine residue of ATG5 (Mizushima *et al.*, 1998; Shintani *et al.*, 1999; Tanida *et al.*, 1999). The ATG12-5 complex binds ATG16L1 and this complex aids the formation of the covalent bond between LC3 and PE by acting as an E3 enzyme (Figure 6) (Suzuki *et al.*, 2001; Yang and Klionsky, 2010). LC3 is a ubiquitin like lipidation complex synthesised as pro-LC3 and is cleaved by ATG4, a protease, at the C-terminus to produce LC3-I, which possesses an exposed glycine (Kirisako *et al.*, 2000). This is conjugated to PE, forming LC3-II, on the inner and outer phagophore membrane by ATG7 and E2 enzyme, ATG3 (Ichimura *et al.*, 2000; Kroemer, Mariño and Levine, 2010). The ratio of LC3-II/I is therefore commonly used to monitor autophagy. An N-terminal helix of ATG3 is necessary for its function and has curvature sensing

properties. It has been suggested this might concentrate the LC3 at the growing, highly curved end of the phagophore (Kabeya *et al.*, 2004).

#### 1.2.1.2 Autophagosome Maturation

In the next stage, the double membraned phagophore expands to engulf the cargo, and upon membrane fusion and resulting autophagosome formation, segregates target proteins from the cytoplasm. The autophagosome then fuses, in a soluble N-ethylmaleimide-sensitive factor attachment protein receptor (SNARE) dependent manner, with either late endosomes to form amphisomes which are then able to fuse with lysosomes, or directly with lysosomes to form autolysosomes. Here the cargo, LC3 and the autophagy receptor, p62 (which binds LC3 and cargo), are degraded. P62 has a critical role in autophagy and is often used as a measure of autophagic activity (Mizushima and Yoshimori, 2007; Klionsky *et al.*, 2016). As noted in section 1.1.3, many ALS-associated genetic mutations result in p62 pathology and mutations in p62 have been identified in both sALS and fALS (Fecto *et al.*, 2011).

The protein FYVE and coiled-coil domain containing 1 (FYCO1) has been shown to bind LC3 *via* an LC3 interacting region (LIR), Rab7 (a GTPase) *via* its CC region and to PI3P *via* its FYVE motif. This promotes the dynein mediated retrograde transport of autophagosomes along microtubules towards the centrosomes and the perinuclear region, where lysosomes are located (Kimura, Noda and Yoshimori, 2008; Pankiv *et al.*, 2010). Recruitment of the homotypic fusion and sorting protein (HOPS) complex is essential for autophagy. It acts to tether the autophagosome and lysosome through interactions with the Q-SNARE syntaxin-17, and mediates the trans-SNARE formation to enable fusion (Jiang *et al.*, 2014). Syntaxin-17 is present only on autophagosomes, not isolation membranes, and interacts with SNAP-29 and the lysosomal SNARE, VAMP8 (Itakura, Kishi-Itakura and Mizushima, 2012). Syntaxin-17 is essential for autophagosomal-lysosome fusion since depletion of syntaxin-17 causes autophagosome accumulation (Itakura, Kishi-Itakura and Mizushima, 2012). O-GlcNAcylation of the SNAP29 SNARE protein impedes its function, though this is reversed upon starvation, showing O-GlcNAcylation of SNAP29 mediates autophagy in a nutrient dependent manner (Guo *et al.*, 2014). The HOPS complex present on

lysosomes interacts with tethering factors such as Pleckstrin homology domain-containing family M member 1 (PLEKHM1), which can bind LC3 on the autophagosome membrane, enhancing the specificity of autophagosome-lysosome fusion. Additionally, PLEKHM1 is able to tether Rab7 on lysosomes to VPS41, a subunit of the HOPS complex (McEwan *et al.*, 2015).

The cargo are degraded by hydrolases present in the lysosome which are often synthesised in the pro-form and activated by the low pH maintained within the lysosome by v-ATPases (Mindell, 2012). Lysosome-associated membrane proteins (LAMP 1 and LAMP 2) are thought to make up around half of all lysosomal membrane proteins (Hunziker, Simmen and Höning, 1996). Deficiency of LAMP-2 causes accumulation of autophagosomes in mice (Eskelinen, 2006). Further, knockout of LAMP2 results in failed maturation of autophagosomes due to impaired dynein-dynactin mediated transport along microtubules in the direction of lysosomes (Eskelinen *et al.*, 2002; Binker *et al.*, 2007). The degraded macromolecular components are released into the cytoplasm by permeases where they are recycled (Yang *et al.*, 2006).

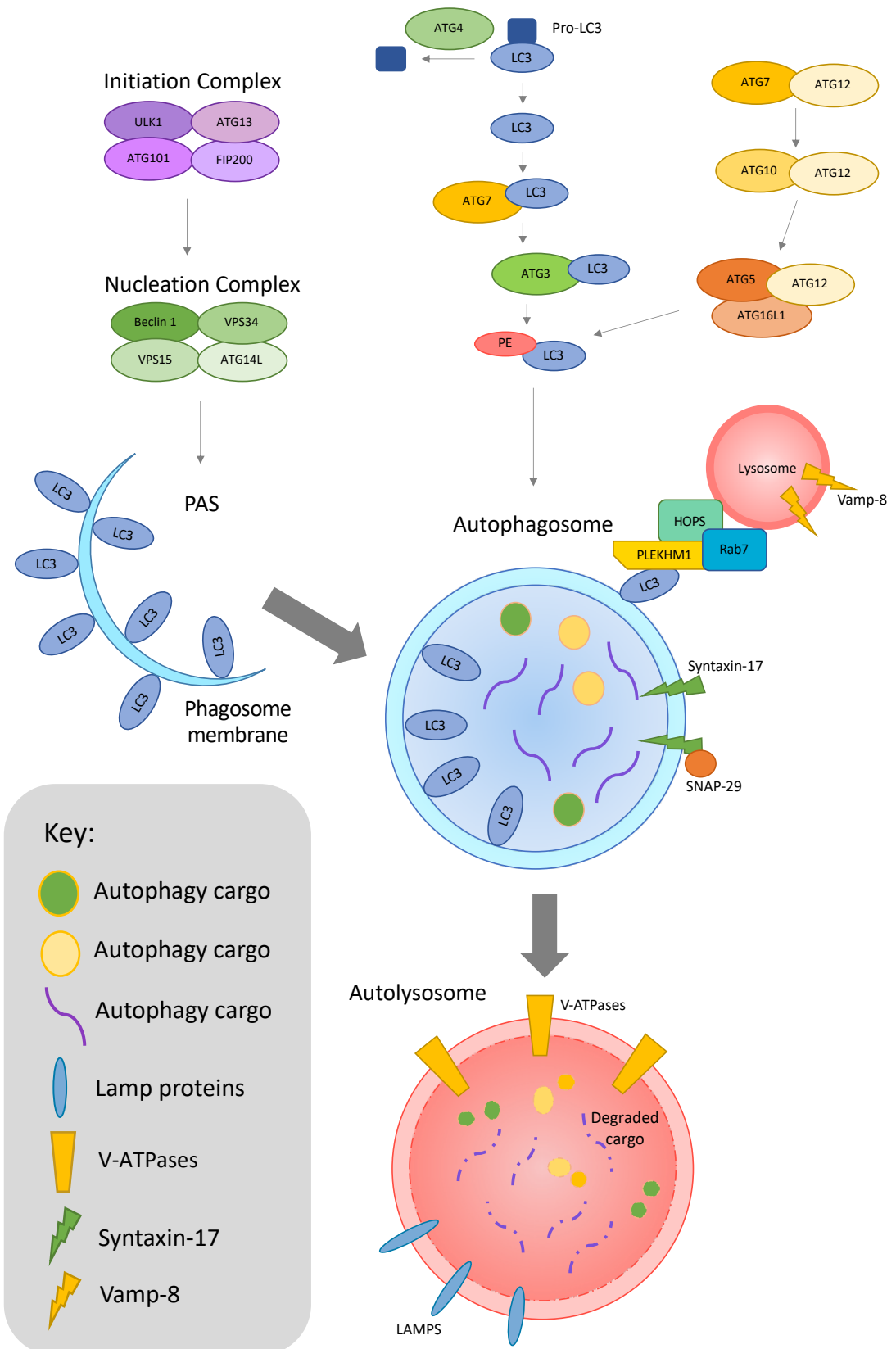


**Figure 6: Molecular mechanisms of autophagy.** The initiation complex is critical for localisation to the PAS and is formed when ULK1 is autophosphorylated and bound by ATG13, allowing the binding of FIP200. ATG101 is also part of this complex. The nucleation complex is formed from Beclin-1 which is phosphorylated by ULK1. Through its binding partner, VPS34, PI3P is made. Additionally, ATG7, an E1 enzyme, activates ATG12 which is transferred to the E2 enzyme, ATG10, and subsequently covalently bonded to ATG5. The ATG12-5 complex binds ATG16L and this complex aids formation of a covalent bond between LC3 and PE. LC3 is synthesised as pro-LC3 which is cleaved by ATG4 to form LC3-I which is conjugated to PE by ATG7 and ATG3, forming LC3-II. This is recruited to the inner and outer phagophore membrane. The HOPS complex tethers the autophagosome and lysosome through interactions with the SNARE protein, syntaxin-17. Syntaxin-17 with its partner, SNAP29, interacts with the lysosomal SNARE, VAMP8. In addition, the HOPS complex on the lysosome interacts with tethering factors such as PLEKHM1 which binds LC3 on the autophagosome membrane, increasing the specificity of the fusion. Finally, the cargo is degraded by hydrolases in the lysosome. The low pH is maintained by v-ATPases. LAMP proteins present on the lysosome membrane may prevent its own degradation by hydrolases. Drawn by author.

### 1.2.2 Selective Autophagy

Autophagy was initially considered a bulk degradative process induced by glucagon and nutrient deprivation. However, since then it has been shown that autophagy is required for normal cellular homeostasis and growing evidence suggests that even for low level, basal autophagy, specific cargo are selected for degradation. The various types of selective autophagy include mitophagy (mitochondrial degradation), xenophagy (bacteria or virus degradation), pexophagy (peroxisome degradation), reticulophagy (ER degradation), ribophagy (ribosomal degradation), nucleophagy (nuclear degradation) and aggrephagy (protein aggregate degradation) (Gatica, Lahiri and Klionsky, 2018).

For selective autophagy, the target proteins require ubiquitin tags which are recognised by autophagy receptors, including p62/sequestosome 1 (SQSTM1), optineurin (OPTN), neighbour of BRCA1 gene 1 protein (NBR1), Toll-interacting protein (TOLLIP) and calcium binding and coiled-coil domain 2 (CALCOCO2)/NDP-52 (Lamark *et al.*, 1986; Kirkin *et al.*, 2009; Wild *et al.*, 2011). These proteins act as tethers between ubiquitinated cargo and LC3 on the autophagosome membrane

(Figure 7) (Pankiv *et al.*, 2007). p62 and optineurin are both phosphorylated by TBK1 and all three proteins are highly implicated in ALS (Wild *et al.*, 2011; Pilli *et al.*, 2012).

p62 and NBR1 share similar domain architecture and bind to poly- and mono-ubiquitin on the cargo (such as damaged, aggregated protein and cytosolic bacteria) through their C-terminal ubiquitin associated (UBA) domains as well as to LC3 on the autophagosome membrane through their LC3 interacting regions (LIRs) (Lamark *et al.*, 1986; Kirkin *et al.*, 2009). However, homo-dimerisation of the UBA domain results in low affinity of p62 for ubiquitin, and may act as an auto-inhibitory mechanism (Isogai *et al.*, 2011). Phosphorylation of p62 at Ser-403 by TBK1 increases this affinity for ubiquitin (Matsumoto *et al.*, 2011; Pilli *et al.*, 2012).

As single monomers, p62 is capable of binding only one LC3 molecule and one ubiquitin molecule, though oligomerisation allows binding to multiple ubiquitin and LC3 proteins. This p62 oligomerisation increases the interaction with clustered ubiquitinated cargo and LC3 and this homo-oligomerisation is driven by its N-terminal Phox and Bem1 (PB1) domain. This in turn causes the membrane to bend around the cargo (Wurzer *et al.*, 2015). Cryo-electron microscopy has revealed p62 forms flexible polymers with the PB1 domain acting as a helical scaffold (Ciuffa *et al.*, 2015). Further, mutations in the PB1 and LIR domains of p62 demonstrated that the PB1 domain is essential for targeting to the autophagosome, whereas the LIR domains are not, meaning p62 is not targeted to the autophagosome through interactions with LC3. Instead, p62 colocalises with upstream autophagy proteins such as ULK1 (Itakura and Mizushima, 2011).

An additional regulation may be the type of ubiquitin chain, since K63 chains have been associated with autophagy, whereas K48 linked ubiquitin chains are connected with proteasomal degradation (Tan *et al.*, 2008; Komander and Rape, 2012). p62 has been shown to preferentially bind K63-linked polyubiquitin chains and monoubiquitin, over K48-linked ubiquitin chains (Seibenhener *et al.*, 2004; Long *et al.*, 2008). Interestingly, ULK1 phosphorylates p62, increasing its affinity for ubiquitin (Lim *et al.*, 2015).

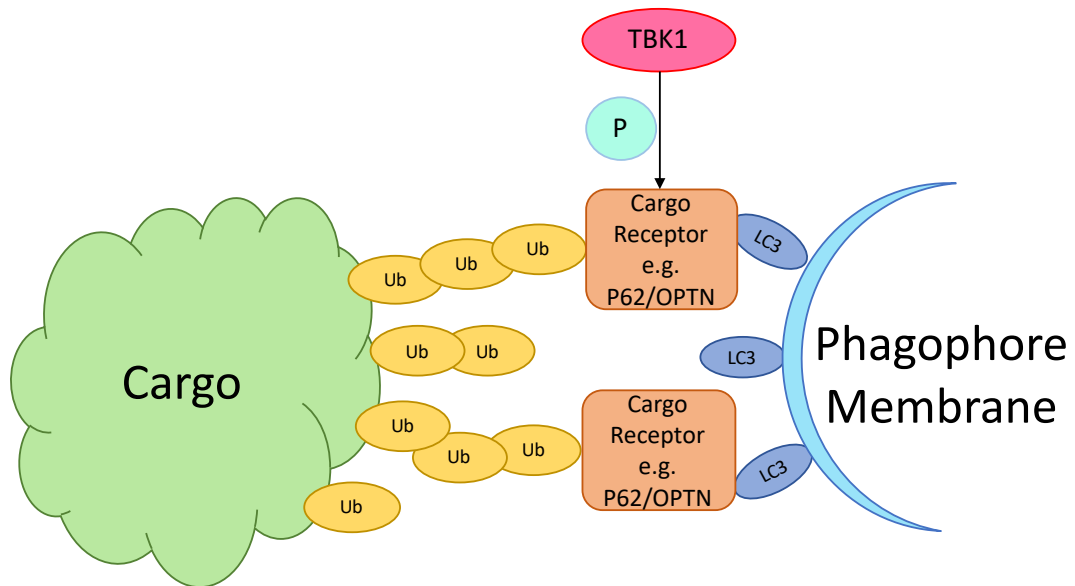


**Figure 7: Selective autophagy.** Specific ubiquitinated cargo are recognised by cargo receptors such as p62 and OPTN through their UBA domain. Similarly, the receptors recognise LC3 through their LIR domains and hence act to bridge the cargo with the phagophore membrane. Drawn by author.

### 1.2.3 Autophagy in Neurones

As previously discussed, neurones are polarised cells that consist of an axon with a cell body, termed soma, at one end, and dendrites, projections used to communicate with neighbouring cells, at the other. Autophagy in neurones is crucial to their survival which was demonstrated when neurone specific knockout of the autophagy related proteins, Atg5 or Atg7 in mice, was the single event required to induce neuronal death (Hara *et al.*, 2006; Komatsu *et al.*, 2006). Without autophagy, the distal axon becomes swollen and dies, indicating a basal level of autophagy is required for survival (Komatsu *et al.*, 2007; Nishiyama *et al.*, 2007).

In neurones, autophagosomes are formed at the distal axon and are transported in a retrograde manner along axon microtubules towards the soma (Figure 8). Membrane from the ER is donated to begin formation of the phagophore membrane, and is termed an omegasome initially. The retrograde transport of autophagosomes is dependent on the microtubule motor protein, dynein. Initially, the newly formed autophagosomes are subject to both retrograde and anterograde movement, with dynein motor protein and kinesin motor protein working in competition. The scaffold protein, JIP1, is recruited to newly formed autophagosomes and binds to both kinesin

and dynein. Binding to autophagosomes *via* LC3 blocks the interaction between JIP1 and kinesin, allowing the dynein-dependent retrograde movement of autophagosomes to dominate (Fu, Nirschl and Holzbaur, 2014). During motility towards the soma, the autophagosome may fuse with an endosome to form an amphisome, before fusing with lysosomes to form an autolysosome. Sufficient acidification of an autophagosome may require multiple lysosome fusion events. The maturation of autophagosomes into autolysosomes was demonstrated in mouse dorsal root ganglion neurones using a LC3-mCherry-GFP construct, where the authors observed reduced GFP signal towards the soma, as the acidification of autophagosomes quenched the GFP signal (Maday, Wallace and Holzbaur, 2012). The formation of amphisomes by the fusion of autophagosomes with endosomes may be necessary for transport along the axon, since the late endosomal protein SNAPIN is an adapter protein which helps attach dynein (Cheng *et al.*, 2015). It is likely that the fully acidified autolysosome contents are recycled into new proteins in the soma, the location of the majority of protein synthesis.

The process of autophagy within neurones is highly spatially controlled which may contribute to their vulnerability. It has also been suggested that neurones are unable to upregulate autophagy in response to stress, such as nutrient deprivation, as this was found to be the case in mice brains, but not in many other tissues including of the heart, liver, kidney and muscle (Mizushima *et al.*, 2003).

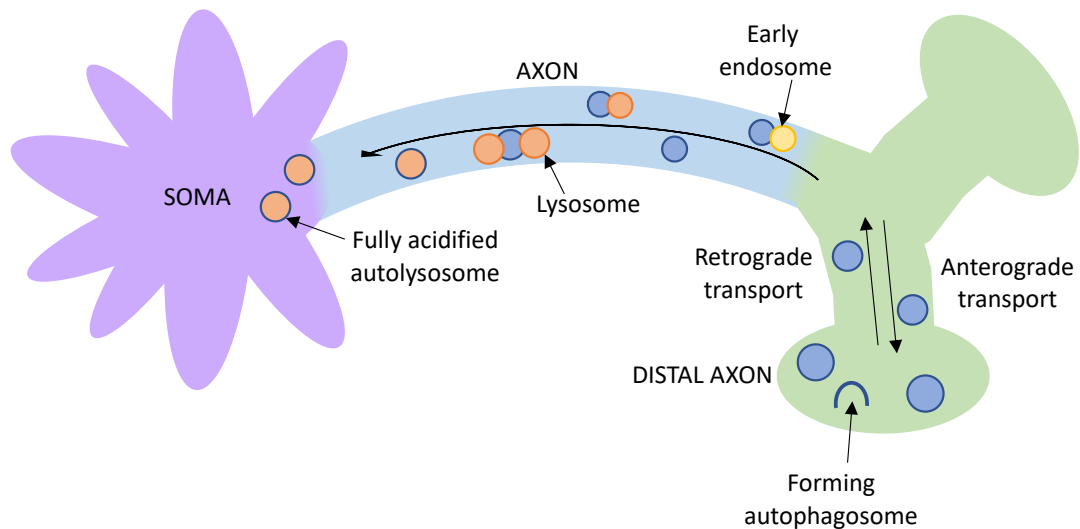


**Figure 8: Neuronal autophagy.** Autophagosomes are formed at the distal axon and undergo dynein-dependent retrograde transport along the axon to the soma. Autophagosomes fuse with early endosomes and lysosomes to become fully acidified, a process which may require multiple lysosome fusion events. The contents of the fully acidified lysosome are recycled in the soma. Drawn by author.

#### 1.2.4 Autophagic Dysregulation in Amyotrophic Lateral Sclerosis

A major hallmark of ALS is the accumulation of insoluble cytoplasmic protein aggregates and the mislocalisation of proteins in degenerating motor neurones and oligodendrocytes in the spinal cord, hippocampus, cerebellum and the frontal and temporal cortices. This implies disruption of normal protein homeostasis and implicates autophagy in ALS (Ramesh and Pandey, 2017). In motor neurones, autophagy maintains neuromuscular junction integrity at the early stage of disease, whereas at later stages, autophagy becomes detrimental and accelerates ALS progression (Rudnick *et al.*, 2017). Knockdown of the autophagy-related protein, Atg7, in the central nervous system of mice caused neuronal death and the accumulation of polyubiquitinated protein aggregates (Komatsu *et al.*, 2006). Further, autophagosomes have been shown accumulated in the spinal cords of ALS patients (Sasaki, 2011).

##### 1.2.4.1 SQSTM1/p62

The first discovered autophagy receptor, p62, binds ubiquitinated cargo for degradation by selective autophagy and variants are implicated in around 2% of ALS

cases (Pankiv *et al.*, 2007; Fecto., *et al.*, 2011). Despite this, p62 pathology is more widespread, as p62 inclusions are seen in patients with ALS-associated mutations in *C9orf72*, *PFN1*, *SOD1*, *TARDBP* and *TBK1* (Gal *et al.*, 2007; Brady *et al.*, 2011; Yang *et al.*, 2016; Sellier *et al.*, 2016). Mutations in p62 have been identified in both sALS and fALS (Fecto *et al.*, 2011). As previously mentioned, p62 has been found in ubiquitin positive inclusions in motor neurones (Gal *et al.*, 2007). It is found in similar toxic and misfolded aggregates in neurones in other neurodegenerative diseases such as Parkinson's, Alzheimer's and Huntington's disease. Mutations in both the UBA and LIR domains have been associated with ALS, though the majority occur in the UBA domain, resulting in the impairment of ubiquitin recognition (Rea *et al.*, 2013). In zebra fish, p62 knockdown resulted in shortened motor neurones, which could be improved by rapamycin, an autophagy activator. The phenotype was fully rescued with the expression of wild type human p62 but not an ALS linked mutant, p62<sup>P394L</sup> (Lattante *et al.*, 2015). The ALS associated mutation, L341V, present in the LIR domain, was shown to prevent binding of p62 to LC3-II (Goode *et al.*, 2016). Further, stress granules have been shown to be removed from cells by p62-mediated selective autophagy (Chitiprolu *et al.*, 2018).

#### 1.2.4.2 *TBK1*

Through exome sequencing of thousands of ALS patients, *TBK1* was identified as an ALS-relevant gene, in 2015 (Cirulli *et al.*, 2015; Freischmidt, Wieland, *et al.*, 2015). In addition, mutations in *TBK1* have been identified as a cause of FTD in patients with both ALS-FTD or pure FTD (Borghero *et al.*, 2015). Mutations in *TBK1* have been associated with both sALS and fALS and reside as missense, none-sense, frameshift and deletion mutants, of which the frameshift and nonsense can reduce mRNA and protein levels of *TBK1* (Cirulli *et al.*, 2015). There have been over 90 sequence variants associated with *TBK1* (Oakes, Davies and Collins, 2017). Overall, around 4% of fALS patients have loss of function *TBK1* mutations, whilst fewer than 0.1% occur in sALS patients (Nguyen, Thombre and Wang, 2019).

The first evidence of *TBK1* as a regulator of autophagy arose when it was found that the phosphorylation of the autophagy receptor, OPTN, by *TBK1* at Ser-177 increased

the affinity of OPTN for LC3 by tenfold, and promoted the degradation of *Salmonella* in HeLa cells through autophagy (Wild *et al.*, 2011). On p62, TBK1 phosphorylates Ser-403 which increases the affinity of the UBA domain of p62 for ubiquitin present on the cargo. Further, in cells with knockdown of TBK1, the autophagosome maturation to autolysosomes was inhibited (Pilli *et al.*, 2012). It has also been shown that homozygous ALS associated TBK1<sup>R228H/R228H</sup>;SOD1<sup>G93A</sup> mice with impaired kinase ability show reduced phosphorylation of p62 and OPTN, providing evidence which directly implicates ALS-relevant TBK1 mutations in autophagy (Gerbino *et al.*, 2020). Besides p62 and OPTN, TBK1 also phosphorylates the autophagy cargo adaptor protein, NDP52 (Heo *et al.*, 2015).

Recently, another role of TBK1 in the induction of autophagy was discovered. TBK1 was shown to phosphorylate syntaxin-17 at Ser-202 which then localised to the ATG13-FIP200 complex, which does not occur with unphosphorylated syntaxin-17. Knockout of TBK1 or syntaxin-17 reduced ATG13-FIP200 complexes with ULK1 (Kumar *et al.*, 2019). Interestingly, TBK1 phosphorylates the binding partner of the ALS-relevant protein C9orf72, Smith-Magenis syndrome chromosomal region candidate gene 8 protein (SMCR8), and depletion of SMCR8 caused accumulation of p62 positive aggregates through disturbed autophagy (Sellier *et al.*, 2016).

TBK1 has four domains, an N-terminal serine/threonine domain, two coiled coil domains (CCD1/2) and a ubiquitin-like domain (Larabi *et al.*, 2013). TBK1 phosphorylates p62 and OPTN, mediated by associations with its CCD2 domain, and some mutations associated with ALS cause a truncated version of TBK1, without CCD2, preventing its association with optineurin (Freischmidt, Wieland, *et al.*, 2015; Le Ber *et al.*, 2015; Richter *et al.*, 2016). Indeed, the ALS associated mutation, TBK1<sup>E696K</sup>, located in the CCD2 domain, prevents the association of TBK1 with OPTN, resulting in disrupted mitophagy (Moore and Holzbaur, 2016).

SOD1<sup>G93A</sup> mice harbouring heterozygous *TBK1* deletions or homozygous mutations resulting in reduced kinase function experience impaired motor neurone autophagy as well as accelerated neurodegeneration at early stages of disease. Respectively, the authors observed accumulated motor neurone p62 and hyperphosphorylated p62

and OPTN with increased protein aggregates (Brenner *et al.*, 2019; Gerbino *et al.*, 2020). Despite these mice displaying preponed ALS phenotypes at early stages of disease, at later stages they experienced extended survival. This suggests that TBK1 contributes opposingly to ALS progression at early and late ALS stages, hinting at the complex role of TBK1 in ALS. Further, injection with adeno-associated viral vectors encoding TBK1 into SOD1<sup>G93A</sup> mice increased their survival, without impacting disease onset (Duan *et al.*, 2019).

Additionally, TBK1 is known to have a role in neuroinflammation. Recognition and binding of ligands such as double stranded DNA to the TLR3 receptor recruits the adaptor proteins TRIF and TRAF3. This activates TBK1 in complex with its interacting proteins NAP1, SINTBAD, IKK $\epsilon$  and TANK. TBK1 goes on to phosphorylate TRF3, a transcription factor which promotes the expression of antiviral type-I and type-III IFNs (INF $\alpha$  / $\beta$ ) (Fitzgerald *et al.*, 2003; Sharma *et al.*, 2003).

#### 1.2.4.3 OPTN

*OPTN* encodes the protein optineurin. Mutations in *OPTN* account for around 3% of fALS and 1% of sALS cases (Iida *et al.*, 2012). Mutations in *OPTN* are varied, including deletion of exon 5, nonsense (Q398X and Q65X), missense (E478G) and truncation (c.1320delA) mutants (Maruyama *et al.*, 2010; Weishaupt *et al.*, 2013). Optineurin is important in aggrephagy, mitophagy and xenophagy. Its role in mitophagy is disturbed by the ubiquitin binding UBA domain mutation, E478G, and the LIR domain mutation, F178A, causing impaired ubiquitin and LC3 binding respectively (Wild *et al.*, 2011; Wong and Holzbaur, 2015). Further, the E478G mutation causes neuronal cell death in mice (Liu *et al.*, 2018). This mutant, and Q398X, are unable to bind myosin VI, which is critical for the transport of autophagosomes during autophagy (Sundaramoorthy *et al.*, 2015). Ser-177 OPTN was found colocalised with SOD1<sup>G93A</sup> mutant aggregates and TBK1 in transgenic mice, suggesting TBK1 phosphorylation of OPTN is involved in the clearance of these aggregates (Korac *et al.*, 2012). TBK1 is unable to associate with OPTN possessing the mutations E478G and R398X and causes failed mitophagy (Wong and Holzbaur, 2015; Moore and Holzbaur, 2016).

#### 1.2.4.4 *C9orf72 and Autophagy*

C9orf72 functions as a GEF for Rab GTPases which regulate autophagy and vesicle trafficking (Webster *et al.*, 2016). Further evidence supports a role of C9orf72 in vesicle trafficking and autophagy processes through the discovery that C9orf72 binds several small GTPases involved in autophagy – Rab1, Rab5, Rab7 and Rab11 (Farg *et al.*, 2014).

C9orf72 binds SMCR8 during normal functioning and it has been shown this complex localises to the lysosomal protein, LAMP1, upon amino acid starvation. Knockout of either *C9orf72* or SMCR8 impaired lysosome morphology and the ability of mTORC1 to signal in response to amino acid levels (Amick, Roczniak-Ferguson and Ferguson, 2016). One study has shown C9orf72 binds SMCR8 and WDR41 to act as a GEF for Rab8a and Rab39b. This complex weakly binds p62 and OPTN and reduction of C9orf72 caused the build-up of TDP-43 and p62 aggregates in mouse cortical neurones, mirroring the classical hallmarks of ALS (Sellier *et al.*, 2016).

It has also been shown that C9orf72 interacts with the ULK1 initiation complex which assists the formation of the autophagosome (M. Yang *et al.*, 2016; Sullivan *et al.*, 2016; Webster *et al.*, 2016). Interestingly, knockdown of *C9orf72* inhibits the initiation of autophagy in neuronal cells, despite treatment with the autophagy inducer, Torin1. In this same study it was shown that in *C9orf72* ALS/FTD patient derived differentiated induced neural progenitor cells, levels of autophagy were reduced. Further, reduction of C9orf72 in HeLa and primary cortical neurones caused an accumulation of p62 (Webster *et al.*, 2016).

#### 1.2.4.5 *TDP-43 and Autophagy*

Numerous studies have shown TDP-43 plays a significant role in the regulation of autophagy and TDP-43 aggregates can be p62 positive (Brady *et al.*, 2011). TDP-43 knockdown caused reduced Atg7 mRNA levels and disrupted autophagy in the mouse neuronal-like, Neuro2A (N2A) cells (Bose, Huang and Shen, 2011). TDP-25 and TDP-35 are caspase-cleaved forms of TDP-43 and when autophagy was inhibited with 3-Methyladenine (3-MA) treatment, they accumulated in N2A and SH-SY5Y cells.

Further, autophagy induction with rapamycin increased TDP-43, TDP-35 and TDP-25 degradation, indicating their levels are maintained by autophagic clearance (Caccamo *et al.*, 2009). Further to this, it has been demonstrated that new autophagy enhancing compounds (fluphenazine, methotrimeprazine and 10-(4'-(N-diethylamino)butyl)-2-chlorophenoxazine) increased turnover of TDP-43, and importantly, the survival of motor neurones (Barmada *et al.*, 2014).

One particular study discovered the ability of TDP-43 to bind and stabilise the mRNA of RAPTOR, an mTORC1 subunit. Silencing of TDP-43 in HeLa cells reduced RAPTOR levels and inactivated mTOR. Further consequences included reduced mTOR phosphorylation on transcription factor EB (TFEB), a master transcription factor for genes controlling lysosome biogenesis and autophagy, leading to its nuclear localisation (Sardiello *et al.*, 2009). In turn, this led to increased protein levels of TFEB target genes involved in lysosomal biogenesis and autophagy, including LAMP1, ATG5 and Beclin-1. However, the silencing of TDP-43 also impaired autophagosome-lysosome fusion (Xia *et al.*, 2016).

#### 1.2.4.6 FUS and Autophagy

Autophagy induction with rapamycin increased the rate of FUS stress granule turnover in primary neurones with mutant FUS, and further, reduced cell death in the ALS related FUS<sup>R521C</sup> mutant neurones (Ryu *et al.*, 2014). FUS stress granules were also shown to co-localise with autophagosomes (Ryu *et al.*, 2014). Mutant FUS caused reduced omegasomes and autophagosomes and accumulated p62. Additionally, LC3-positive vesicles were increased in the motor neurones of spinal cords of FUS<sup>521C</sup> ALS patients, and Rab1 overexpression rescued the autophagy inhibition by reducing LC3-positive vesicles and increasing omegasomes (Soo *et al.*, 2015). In FUS knockout Neuro2A cells, genes (and subsequently their proteins) crucial to early stages of autophagy were decreased, including ATG16L1, ATG12 and FIP200. The expression of ATG16L1 and ATG12 were rescued by re-expressing FUS, which demonstrates how FUS regulates the expression of autophagy-relevant genes (Arenas *et al.*, 2021).

#### 1.2.4.7 SOD1 and Autophagy

Many studies have implicated SOD1 pathophysiology in autophagy. Initially this link was discovered when the inhibition of autophagy caused accumulation of SOD1 insoluble aggregates in motor neurones (Kabuta, Suzuki and Wada, 2006). Interestingly, SOD1<sup>G93A</sup> mouse spinal cord motor neurones presented with p62 positive aggregates which colocalised with ubiquitin and the SOD1 mutants (Gal *et al.*, 2007). The same study found p62 selectively bound mutant SOD1 over wild type and the ubiquitin binding domain of p62 was dispensable for this (Gal *et al.*, 2009). Instead, two separate regions of p62 are required for its ALS mutant SOD1 interaction and are distinct from the interaction of p62 with LC3. These include the PB1 domain and a previously unnamed region (Gal *et al.*, 2009).

In SOD1<sup>G93A</sup> motor neurone cell cultures, there was increased LC3-I to LC3-II processing as well as increased LC3-II turnover, implying autophagy induction (Wei, 2014). Mutant SOD1 aggregates sequestered dynein and impaired axonal retrograde transport in a SOD1<sup>G93A</sup> murine model (Bilsland *et al.*, 2010). This interaction did not occur with wild type SOD1 (Zhang *et al.*, 2007).

The role of ALS relevant mutant SOD1 in autophagy appears to be complex. Indeed, when SOD1<sup>G93A</sup> mice were treated with resveratrol, an autophagy inducer, they showed reduced motor neurone loss and increased survival (Mancuso *et al.*, 2014). However, when treated with another autophagy activator, rapamycin, SOD1<sup>G93A</sup> mice experienced reduced survival and enhanced degeneration of motor neurones (Zhang *et al.*, 2011).

In SOD1 ALS patients, *BECN1*, the gene encoding Beclin-1 which is part of the autophagic nucleation complex, was downregulated. Additionally, loss of Beclin-1 in mutant SOD1 mice impaired autophagy and increased SOD1 accumulation (Tokuda *et al.*, 2016). One study crossed motor neurone *Atg7* knockout mice with SOD1<sup>G93A</sup> mutant mice and the inhibition of autophagy from lack of *Atg7* in motor neurones resulted in accelerated disease progression, suggesting autophagy protects neurones in the early stages of disease (Rudnick *et al.*, 2017).

## 1.3 MicroRNAs

MiRNAs are small, non-coding RNAs, typically 20-22 nucleotides (nt) long and are evolutionarily conserved (Lagos-Quintana *et al.*, 2001; Lee, Risom and Strauss, 2007). They act as post-transcriptional regulators of gene expression and are thought to be involved in almost all cellular processes studied to date (Krol, Loedige and Filipowicz, 2010). Around a third of human gene products are regulated by miRNAs (Hammond 2015). The first miRNA discovered was lin-4 in *C.elegans*, which, in 1993 was reported independently by both the Ambros and Ruvkun groups. They reported that lin-4 was able to regulate the gene, lin-14 through its 3'UTR, in a post-transcriptional manner (Lee, Feinbaum and Ambros, 1993; Wightman, Ha and Ruvkun, 1993). In the latest release, there are 2,654 mature human miRNAs listed on miRbase, a searchable database of published miRNAs (release 22.1: 2018) (Kozomara, Birgaoanu and Griffiths-Jones, 2019).

MiRNAs are present in both intracellular and extracellular environments, where they are highly stable (Mitchell *et al.*, 2008). Extracellular miRNAs may be protected through association with extracellular vesicles, or through complexation with AGO proteins or high density lipoproteins (Arroyo *et al.*, 2011; Turchinovich *et al.*, 2011, 2013; Vickers *et al.*, 2011). These extracellular, circulating miRNAs have been found in almost all biological fluids including cerebrospinal fluid (CSF), plasma, blood and serum (Chen *et al.*, 2008; Weber *et al.*, 2010; Sang *et al.*, 2013). MiRNAs target ALS gene products and are also regulated by ALS-associated proteins (Kawahara and Mieda-Sato, 2012). As a result, they have increasingly been considered as biomarkers of disease, including ALS (Dardiotis *et al.*, 2018).

### 1.3.1 Biogenesis and Function

MiRNAs are present in the human genome either as individual genes or within the introns of protein-coding genes (Carthew and Sontheimer, 2009). Several miRNA loci may be located in close proximity, leading to a cluster in which these miRNAs are transcribed together (Roush and Slack, 2008). These miRNAs may have similar seed sequences and are considered a family (Tanzer and Stadler, 2004). MiRNA biogenesis

occurs *via* the canonical or non-canonical pathway, with canonical being the dominant and discussed here (Figure 9).

Though most commonly transcribed by RNA polymerase II, some miRNAs are transcribed by RNA polymerase III (Lee *et al.*, 2004; Borchert, Lanier and Davidson, 2006). The primary miRNA transcripts (pri-miRNA) are processed by the microprocessor complex, in the nucleus, by the nuclear ribonuclease III, Drosha, in complex with the dimeric, double stranded RNA binding protein, DiGeorge Syndrome Critical Region 8 (DGCR8), to generate a ~70 nucleotide precursor miRNA (pre-miRNA) (Lee *et al.*, 2003; Gregory *et al.*, 2004). DGCR8 recognises particular motifs in the pri-miRNA, including an N6-methyladenylated GGAC (Alarcón *et al.*, 2015). Additional pri-miRNA identifiers include a 35 base pair stem containing a mismatched GHG motif, a basal UG motif and apical UGUG and CNNC motifs (Michlewski and Cáceres, 2019). The recognition of these motifs allows Dicer and DGCR8 to maintain the correct orientation of the pri-miRNA (Nguyen *et al.*, 2015). DGCR8 is required for the enzymatic activity of Drosha, which is the catalytic unit and cleaves the double stranded pri-miRNA (Lee *et al.*, 2003; Gregory *et al.*, 2004; Han *et al.*, 2004). It leaves a 2 nucleotide flanking region at the 3' end (Zeng, 2006). A pri-miRNA typically consists of a single stranded flanking region, a stem and a terminal loop. A terminal loop greater than 10 nucleotides is preferred by Drosha (Zhang *et al.*, 2005). The terminal loop and the sequences flanking this are critical for cleavage (Zeng and Cullen, 2003). DGCR8, but not Drosha, is able to bind the miRNA and cleavage occurs 11 base pairs from the flanking region (Han *et al.*, 2006).

Transport of the resulting pre-miRNA into the cytoplasm through nuclear pores is dependent on exportin 5 and Ran-GTP (Yi *et al.*, 2003; Lund *et al.*, 2004). GTP to GDP conversion results in the pre-miRNA's release into the cytoplasm. The pre-miRNA is then cleaved by the endoribonuclease, Dicer, near the terminal loop, to create a mature, double-stranded miRNA, 20-22 nucleotides in length (Bernstein *et al.*, 2001; Hutvagner *et al.*, 2001). Dicer recognises the 2 nucleotide 3' overhangs produced by Drosha, via the PAZ domain, and cleaves approximately 20 nucleotides away (Lingel *et al.*, 2003; Zhang *et al.*, 2004). An N-terminal helicase domain interacts with the terminal loop, enhancing the recognition of miRNAs (Tsutsumi *et al.*, 2011). It

produces miRNA constructs with a 2 nucleotide long 3' flanking region (Zhang *et al.*, 2004). During this process, Dicer is associated with transactivation response RNA-binding protein (TRBP) and protein activator of the interferon-induced protein kinase (PACT) (Kye and Gonçalves, 2014).

The 5' end of the pre-miRNA hairpin becomes the 5p miRNA, whilst the 3p miRNA is formed from the 3' end. Both strands of the miRNA can become associated with Argonaut (AGO) proteins to form an RNA induced silencing complex (RISC) (Chendrimada *et al.*, 2005). AGO is bilobal with an N-terminal PAZ lobe and C-terminal Piwi lobes (Song *et al.*, 2004). The PAZ domain recognises the 2 nucleotide 3' overhang produced by Dicer (Ma, Ye and Patel, 2004). Initially, the miRNA duplex is associated with one of the four human AGO proteins – which undergo conformational changes to accommodate the miRNA – to form the pre-RISC complex (Wang *et al.*, 2009). This conformational change is ATP dependent and mediated by Hsp90 which binds to the N-terminal of AGO2 (Iwasaki *et al.*, 2010). 182 kDa glycine-tryptophan (GW128) proteins are also associated with AGO and are critical for gene silencing (Rehwinkel *et al.*, 2005; Eulalio, Huntzinger and Izaurralde, 2008).

The mature RISC complex is formed by the removal of one strand, termed the passenger strand, which was previously denoted as miRNA\* (Lagos-Quintana *et al.*, 2001). It is now understood that either strand can be loaded preferentially into the RISC complex, and indeed both strands may have equal preference (Meijer, Smith and Bushell, 2014). Conventionally, the dominant strand and therefore the most active miRNA of the two strands is often written without its 5p or 3p status. The strand favoured for the guide strand is thought to be the one with the less stable base pairing within its 5' terminus (Schwarz *et al.*, 2003). Human miRNAs with a 5' uracil and an excess of purines are favoured for the guide strand, whilst a 5' cytosine and excess of pyrimidines favours a miRNA for the passenger strand (Hu *et al.*, 2009). The guide strand is thus part of the mature RISC complex and is more biologically active (Ha and Kim, 2014). Mismatches at the seed sequence and at positions 12-15 promote miRNA duplex unwinding within the RISC (Yoda *et al.*, 2010).

At the 5' end of the miRNA, a seed sequence at nucleotides 2-8 interacts with the 3'UTR of a target mRNA, called the miRNA response element (MRE) (He and Hannon, 2004). Perfect sequence complementarity leads to mRNA degradation through cleavage by AGO2, whereas imperfect complementarity leads to the inhibition of the mRNA's translation (Figure 9) (He and Hannon, 2004; Jo *et al.*, 2015). This occurs as GW182 is recruited, which in turn recruits poly A deadenylase complexes which promote poly-A deadenylation (Behm-Ansmant *et al.*, 2006). The mRNA is also decapped and degraded by exoribonuclease 1 (Braun *et al.*, 2012). Each miRNA may have hundreds or thousands of mRNA targets and mRNAs can contain many MREs (Paraskevopoulou *et al.*, 2013). The mechanism of miRNA induced degradation or translational inhibition of target mRNAs is not fully understood.

MiRNA biogenesis may alternatively use non-canonical pathways, as opposed to the canonical pathways detailed above. These include Drosha/DGCR8 independent pathways and Dicer independent pathways (Cheloufi, Dos Santos, Chong, & Hannon, 2010). Mirtrons, which are produced from the introns of mRNA during splicing, utilise these pathways and are able to bypass Drosha processing (Ruby, Jan, & Bartel, 2007).

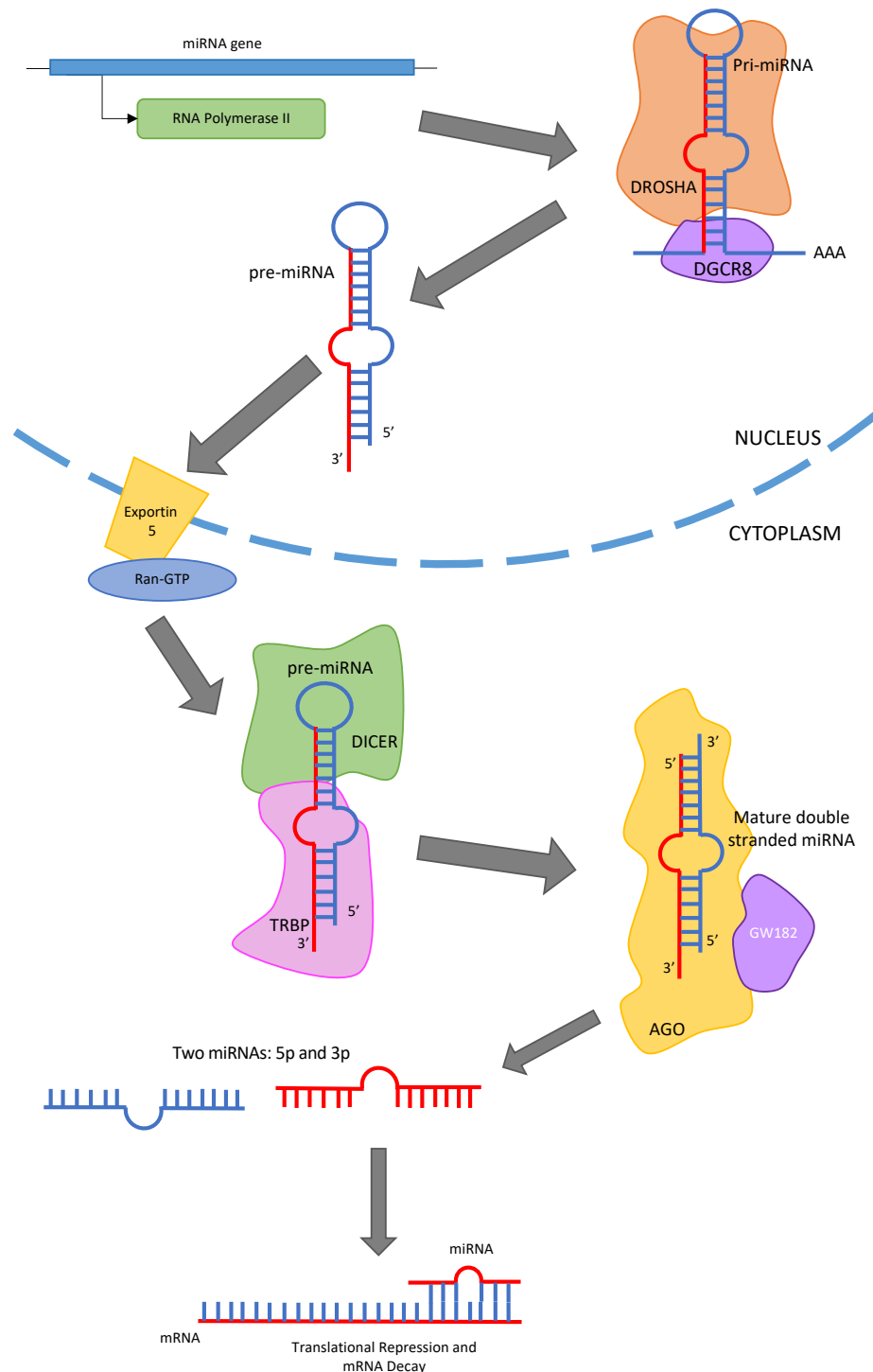


**Figure 9: The canonical miRNA biogenesis pathway.** MiRNAs are transcribed by RNA polymerase II to produce pri-miRNA. This is processed in the nucleus by Drosha/DGCR8 to produce a 70 nt pre-miRNA with 2 nt 3' overhangs. The pre-miRNA is exported into the cytoplasm via exportin 5 where it is further processed by Dicer to produce a mature 20-22 nt miRNA which also processes 2 nt 3' overhangs. Dicer is associated with other proteins including TRBP. Either strand of this resulting miRNA duplex may be incorporated into the RISC complex with AGO proteins and GW182. The single stranded miRNA targets mRNA through complementarity of the miRNA seed sequence and MREs on the mRNA. This leads to either mRNA decay or inhibition of translation. Drawn by author.

### 1.3.2 MiRNA Target Predictions

In order to predict whether specific miRNA-mRNA target interactions occur, a range of bioinformatic tools have been developed over the last 15 years. There are several web-based tools which perform these predictions and include Diana Tools, TargetScan, miRanda and PicTar (Krek *et al.*, 2005; Betel *et al.*, 2010; Agarwal *et al.*, 2015). The algorithms utilised by these software differ, though they all require the same fundamental information. For example, it is necessary to know the miRNA and mRNA sequences. Specifically, the 3'UTR of mRNA is considered to be most frequently targeted by miRNAs (Riffo-Campos, Riquelme and Brebi-Mieville, 2016). Critically, the seed region of the miRNA, at nucleotides 2-8 from the 5' to 3' direction should have perfect base complementarity to a site within the 3'UTR of the mRNA for it to be considered a target (Wightman, Ha and Ruvkun, 1993). Additionally, most web-based miRNA-mRNA prediction tools include the level of conservation of the seed sequence between differing species, as the more highly conserved, the more likely it is biologically advantageous and the more reliable the prediction is considered to be (Friedman *et al.*, 2009). The stability of the miRNA-mRNA complex is also measured by their free energy. Complexes with a lower free energy require more energy to break the bonds between them and are therefore more thermodynamically stable. This is an important consideration as these complexes are more likely to exist (Thadani and Tammi, 2006). The 3D structure of the target mRNA is also often considered by prediction software, as the MRE within must be accessible to the miRNA (Robins, Li and Padgett, 2005). Additionally, the number of MREs within a mRNA can determine the level of repression. For example, multiple MREs within 10-50 nucleotides of a mRNA target often leads to a greater level of repression, whereas multiple MREs closer together than this can lead to competitive binding of miRNAs (Grimson *et al.*, 2007).

mRNA sequences can be found in databases such as Ensemble, whilst miRNA sequences are found on databases such as miRbase (Kozomara, Birgaoanu and Griffiths-Jones, 2019). In 2007, miRbase contained 5,922 mature miRNA sequences from 58 species, whereas the latest version, released just over ten years later, in

2018, contains 48,860 mature miRNAs from 271 species (Griffiths-Jones *et al.*, 2008; Kozomara, Birgaoanu and Griffiths-Jones, 2019). This demonstrates the rapid growth in miRNA sequences added to such databases and depositories over the last decade. Further, sites such as miRTarBase provide information on the miRNA-mRNA interactions that have been experimentally validated (Chou *et al.*, 2018).

### 1.3.3 MiRNAs in Neurones

Local translation of mRNAs along axons is crucial to normal functioning of neurones, which are highly morphologically complex. For example, as axons lengthen, proteins required at the axon terminals cannot be synthesised in the soma and rapidly delivered. Local translation in neurones therefore allows specific spatiotemporal protein translation which is critical for their growth, development and maintenance (Hengst *et al.*, 2009; Gracias, Shirkey-Son and Hengst, 2014; Batista, Martínez and Hengst, 2017). Trafficking of mRNAs throughout neurones is dependent on microtubules, and the mRNAs are directed to various compartments *via* specific motifs (Kislauskis, Zhu and Singer, 1994; Bassell *et al.*, 1998). MiRNAs are also transported along axons in the precursor form and have been found differentially expressed in various neuronal compartments (Kye *et al.*, 2007; Corradi *et al.*, 2020). As known regulators of mRNA translation, their involvement in spatiotemporal regulation of mRNAs and the subsequent impacts on cellular functioning have begun to be elucidated.

For example, miR-26a was shown to target *GSK3B* and inhibition of miR-26a in the axon, but not the soma, increased GSK3B protein levels in both the axon and soma. This miR-26a inhibition also resulted in reduced axon growth. This was attributed directly to the miR-26a-inhibition mediated increase of GSK3B, with the use of a pharmacological inhibitor of GSK3B, which rescued the decreased axon length caused by miR-26a inhibition (Lucci *et al.*, 2020).

Further, overexpression of miR-9 in mouse primary neurones was found to inhibit axonal growth, whereas addition of a miR-9 inhibitor specifically to axonal compartments, not the soma, increased axon growth. The microtubule associated

protein, *Map1b* was confirmed as a target of miR-9. Its impact on axon growth was found to be mediated by Map1b through the use of a target protector, which prevented the interaction of miR-9 with the MRE within *Map1b* and increased axon length. The authors further showed that short stimulation with brain-derived neurotrophic factor (BDNF) promoted axonal growth, decreased miR-9 levels and increased Map1b levels. The increase in axonal growth was reversed with miR-9 overexpression. This suggests that short stimulation with BDNF reduced the expression of miR-9, which lead to an increase of Map1b levels and subsequently increased axon growth (Dajas-Bailador *et al.*, 2012).

Additionally, neuronal pre-miRNAs can be activated by a stimulus. For example, it was found that axonal pre-miR-181a-1 and pre-miR-181a-2 were induced into the mature miR-181a-5p/3p by Semaphorin 3A (Sema3A). A target of miR-181a-5p, Tubulin isoform beta 3 (*TUBB3*), a microtubule isoform, is translated at basal levels at growth cones and this is reduced with Sema3A exposure. Blocking the maturation of miR-181a-1 in axons or preventing its interaction with the *TUBB3* MRE, rescued the translation of *TUBB3*, providing evidence that the newly generated, mature miR-181a-5p can target *TUBB3* and reduce its expression in axons due to Sema3A exposure (Corradi *et al.*, 2020).

By trafficking pre-miRNAs to their desired neuronal location, they represent a collection of inactive miRNAs that can be activated when desired. The trafficking of miRNAs in the precursor form prevents undesirable miRNA-target interactions outside the desired final location. The polarised nature of neurones coupled with the role of miRNAs in regulating neuronal protein translation spatiotemporally, suggests that miRNA dysregulation may be of significant importance specifically in neurodegenerative diseases.

### 1.1.1 MiRNAs as Biomarkers of ALS

Whilst miRNA are produced intracellularly, they are also present at quantifiable levels in the extracellular environment. These circulating miRNAs can be within membrane-bound vesicles or bound protectively by proteins such as AGO2 and high

density lipoproteins (Valadi *et al.*, 2007; Arroyo *et al.*, 2011; Vickers *et al.*, 2011). They are unusually well preserved in a range of biological samples, including blood plasma or serum, and cerebrospinal fluid, and are measurable with greater sensitivity and stability than proteins (Chen *et al.* 2008; Weber *et al.* 2010). Over the last decade there has been a drive to identify specific miRNA biomarkers for ALS, to potentiate more rapid and accurate diagnosis, disease stratification and monitoring. Numerous studies have demonstrated deregulation of miRNAs in ALS patients, many with the specific goal of identifying clinically-relevant biomarkers (Dardiotis *et al.*, 2018). Indeed, there is growing evidence implicating miRNA dysregulation is a hallmark of ALS.

Relevant to the ALS context, miRNAs present in CSF are thought to be good representatives of CNS conditions, since the presence of a blood-CSF barrier would prevent miRNA from the CNS being diluted in the wider circulation (Rao, Benito and Fischer, 2013). However, it is also possible for miRNAs to transfer across this barrier, such that blood miRNAs may provide a window on nervous system dysfunction (Ricci, Marzocchi and Battistini, 2018). It has been demonstrated that cells can transfer functional miRNA between one another in an exosome-mediated manner (Valadi *et al.*, 2007). Since miRNAs in EVs appear to differ between healthy and pathological conditions, it has been proposed that cells can selectively load the miRNAs to be released (Sohel, 2016). Thus, EVs may reflect the cells of origin with some of these miRNAs likely mirroring the ALS pathology and physiology.

Despite recent efforts, no specific molecular biomarker has yet been identified for ALS (Otake, Kamiguchi and Hirozane, 2019). Reviews have summarised the potential role of miRNAs as biomarkers of ALS (Joilin *et al.*, 2019). Dardiotis and colleagues reviewed and collated the results of 24 studies, from 2010 to 2017, documenting those miRNAs most frequently reported, with the aim of clarifying the most appropriate biomarkers for future evaluation (Dardiotis *et al.* 2018).

### 1.3.4 MicroRNAs in Autophagy

The molecular mechanisms of autophagy are highly dynamic and require the function of numerous proteins, including some implicated in ALS. Many of these have been identified as targets of specific miRNAs which may lead to the impairment of normal autophagy. For example, the first connection between miRNAs and autophagy was the discovery that miR-30a-5p targets *Beclin-1* mRNA (Zhu *et al.*, 2009). *Beclin-1* is also regulated by miR-17-5p, miR-30d-5p, and miR-376b-3p amongst others (Korkmaz *et al.*, 2012; Yang *et al.*, 2013; Hou *et al.*, 2017). Additionally, miR-376b-3p also regulates *ATG4*, demonstrating the ability of miRNAs to target multiple genes within the same pathway (Korkmaz *et al.*, 2012).

At the early stages of autophagy, *ULK1* has been shown to be targeted by miR-20a-5p and miR-106b-5p (Wu *et al.*, 2012). MiR-30a-5p has additionally been shown to target *ATG5*, along with miR-181a, whilst miR-519a regulates *ATG10* (Huang, Guerrero-Preston and Ratovitski, 2012; Yu *et al.*, 2012; J. Yang *et al.*, 2018). Tens of miRNAs have been shown to target proteins involved in autophagy. For a full list of these miRNAs and a review of the topic, refer to Akkoc and Gozuacik (2020).

A selection of miRNAs have been linked to autophagy, though with a neurological relevance. For example miR-193-3p was downregulated in a SOD1<sup>G93A</sup> ALS mouse model and has been shown to inhibit autophagy in NSC-34, motor neurone like cells, through targeting of tuberculosis sclerosis (*TSC1*) which regulates mTORC1 (C. Li *et al.*, 2017). Further, miR-421 has been found to target *MYD88* and through its downregulation, inhibits autophagy in hippocampal neurones of epilepsy mice (Wen *et al.*, 2018). However, there is been limited systematic analysis of miRNA regulation of ALS genes.

### 1.3.5 MicroRNAs as Therapeutics

MiRNAs have been recognised for their therapeutic potential and several are in phase I or phase II clinical trials. To repress miRNAs, antisense oligonucleotides (ASOs) which are complementary to the miRNA of interest have been developed. For example, Miravirsen is an antagomiR, which represses miR-122 to control hepatitis C

viral (HCV) infections. It is currently in phase II clinical trials. The virus' replication appeared to be successfully inhibited, as patients who received Miravirsen had no detectable HCV RNA (Lindow and Kauppinen, 2012). Besides Miravirsen, the small interfering RNA (siRNA) drug, Patisiran was approved by the FDA for use to treat polyneuropathy. It binds and degrades transthyretin mRNA (Kristen *et al.*, 2019).

Another miRNA antagomiR currently in both phase I and phase II clinical trials is MRG-106, which targets miR-155 in an attempt to treat lymphoma and leukaemia (Seto *et al.*, 2018). Another antagomiR developed by the same company, MRG-107 also targets miR-155, but with the aim of treating ALS, though this is still preclinical.

Several miRNA mimics are also in phase I clinical trials, including a mimic for miR-16, which a recent phase I clinical trial evaluated by using a new technology for the delivery of miRNA drugs to patients. The method uses non-viable 'mini cells' derived from bacteria which contain the miRNA of interest and are coated in a specific antibody for specific cell type recognition. The trial, named MesomiR delivered a miR-16 mimic specifically to tumour cells *via* an epidermal growth factor receptor antibody coated on the mini cell surface. Data shows control of thoracic cancer after 6 weeks of MesomiR therapy in five of six patients undergoing the clinical trial (Reid *et al.*, 2013, 2016).

## 1.4 Summary and Thesis Aims

ALS is a complex disease resulting in the progressive loss of motor neuronal function and ultimately, death. Studies have attributed this to the disruption of several cellular and molecular mechanisms, including, but not limited to, autophagy. A growing body of evidence implicates the dysregulation of miRNAs in ALS. As regulators of protein translation, many miRNAs influence autophagy proteins, including those linked to ALS, and their dysregulation may represent a key factor which results in autophagic impairment during ALS. Crucially, miRNA mimics or antagomiRs/inhibitors represent a potential future therapy to target multiple genes of one or several pathways.

We hypothesised that ALS-dysregulated miRNAs may contribute to the dysfunction of biological pathways in ALS, such as autophagy and oxidative stress. We also hypothesised that these miRNAs contribute to ALS implicated pathway dysfunction by directly targeting proteins which influence these pathways. Therefore, to further contribute to knowledge of miRNA regulation of autophagy with relevance to ALS, the following broad aims were established:

- Collate dysregulated miRNAs in human ALS patients.
- Establish a pipeline to identify autophagy-relevant and ALS-dysregulated miRNAs and select a candidate miRNA to explore experimentally.
- Investigate the role of this miRNA in cellular autophagy and on downstream proteins of relevance to ALS.
- Identify a novel, direct target of the candidate miRNA with relevance to ALS and autophagy.
- Investigate a neuroprotective role of the candidate miRNA in human astrocytes.
- Experimentally determine the regulation of multiple ALS-relevant and autophagy-relevant genes by the candidate miRNA.
- Connect extracellular secretion of ALS-associated proteins to autophagy dysfunction.

Overall, these aims have been achieved, with highlights including:

- Identifying TBK1 as a novel direct target of miR-340.
- Demonstrating regulation of autophagy by miR-340 in live cells.
- Demonstrating that miR-340 inhibition can elevate NRF2 protein levels in human astrocytes, a potentially neuroprotective phenotype.
- Providing evidence (by RNA-Seq) that miR-340 can regulate 24/154 ALSod genes.
- Linking autophagy failure to Tbk1 secretion *via* extracellular vesicles.

## Chapter 2 - Materials and Methods

### 2.1 Identification of ALS-Associated, Patient-Relevant MiRNAs from a Systematic Literature Review

#### 2.1.1 Studies of Deregulated MicroRNAs in ALS Patients

A comprehensive literature search of PubMed using the MeSH terms 'microRNA' AND 'amyotrophic lateral sclerosis' with studies from 1/1/2013-31/12/2018 was used to identify all relevant peer-reviewed studies which recorded and compared the levels of multiple miRNAs taken directly from ALS patients and controls. If not already stated, miRNAs were assigned as 5p or 3p manually, using information available on miRbase. No duplicates were included for any individual study, and to count the total ALS dysregulated miRNA number, each miRNA was considered only once.

#### 2.1.2 Heatmaps

Heatmaps of ALS dysregulated miRNAs were made using the DIANA-Tools software, mirPath v3.0, by selecting the pathways union option and the microT-CDS prediction method for each miRNA with a threshold of 0.8. A Fisher's Exact Test was used for the pathway enrichment analysis presented on the heatmap.

#### 2.1.3 Bioinformatic MicroRNA Target Predictions of ALS Genes

Bioinformatic predictions of specific miRNAs were made using DIANA-Tools, MicroT-CDS v5.0 with a threshold of 0.7 (Paraskevopoulou *et al.*, 2013). For each miRNA, the resulting genes were cross-referenced to ALS-related genes of interest taken from ALSod.

## 2.2 Investigation of ALS-Relevant miR-340 as a regulator of Autophagy

### 2.2.1 Bioinformatic Autophagy-Targeting MicroRNA Predictions

Predictions of all human miRNAs targeting the 'regulation of autophagy' (KEGG pathway: hsa04140) pathway were made using DIANA Tools, mirPath v3.0 software, using the KEGG reverse search option and the microT-CDS v5.0 method with a threshold of 0.8 (Vlachos *et al.*, 2015). The list of miRNAs generated, along with the reported number of pathway relevant genes they were predicted to target was extracted. To identify those miRNAs predicted to target *TBK1*, DIANA-Tools, MicroT-CDS v5.0 with a threshold of 0.7 was utilised.

### 2.2.2 Cell Culture

Henrietta Lacks (HeLa) cells, Human embryonic kidney (HEK293T) cells and the proliferating mouse neuroblastoma cell line, Neuro2A (N2A) were cultured in Dulbecco's modified Eagle's medium (DMEM) (Sigma-Aldrich, D6429) with 1% (v/v) penicillin/streptomycin (Sigma-Aldrich, P0781) and 10% (v/v) FBS (Sigma-Aldrich, F9665) and incubated at 37 °C with 5% CO<sub>2</sub>.

### 2.2.3 MicroRNA Transfections

In all instances transfections of locked nucleic acid (LNA) miRNA inhibitors, mimics and respective negative controls were performed 24 hours post seeding, using Lipofectamine 2000 (Invitrogen, 11668019) and OptiMEM (Invitrogen, 31985062). All miRNAs (inhibitors, mimics, and controls) were transfected at 50 nM. The negative mimic control has no known homology to any miRNA or mRNA in human or mouse, and the negative inhibitor control shows no hits with over 70 % homology to any species in NCBI and miRbase databases. The sequences of the transfected miRNAs are given in Table 1.

The miRCURY LNA miRNA mimics used in this thesis include a guide strand identical in sequence to the miRNA of interest according to miRBase. The passenger strand is

composed of two nucleotides with complementarity to the guide strand. The fragmentation of the two passenger strands ensures only the guide strand is loading into the RISC.

miRCURY LNA miRNA inhibitors used in this thesis are antisense oligonucleotides that are of perfect sequence complementarity to the miRNA of interest. They sequester the miRNA and prevent their interactions with mRNA targets.

**Table 1: List of miRNAs used in this thesis, their nucleotide sequence and purchase information.** For the hsa-miR-340-5p mimic and negative mimic control, the sequence given is that of the guide strand.

<b>MiRNA Name</b>	<b>Sequence</b>	<b>Purchase Information</b>
Hsa-miR-340-5p Inhibitor	5' ATCAGTCTCATTGCTTTATA 3'	miRCURY LNA miRNA inhibitor cat #YI04106015
Hsa-miR-340-5p Mimic	5'UUAUAAAGCAAUGAGACUGAUU 3'	miRCURY LNA miRNA mimic cat #YM00473089
Negative control LNA miRNA mimic	5' UCACCGGGUGUAAAUCAGCUUG 3'	miRCURY LNA miRNA mimic control cat #YM00479902
Negative control LNA miRNA inhibitor	5' TAACACGTCTATACGCCCA 3'	miRCURY LNA miRNA inhibitor control cat #YI00199006

## 2.2.4 Western Blotting

### 2.2.4.1 Seeding and Transfecting Cells for Western Blotting

HeLa or N2A cells were seeded in 12 well plates at  $0.8 \times 10^5$  cells/well in 1 mL media (DMEM, 10% (v/v) FBS, 1% (v/v) Penicillin streptomycin). Transfection of miRNA inhibitors and mimics was performed 24 hours after seeding using Lipofectamine 2000 and optiMEM. All miRNAs (inhibitors, mimics, and respective controls) were transfected at 50 nM. Briefly, transfections were performed by mixing 1.5  $\mu$ L lipofectamine 2000 and 100  $\mu$ L optiMEM per well for 20 minutes. In conjunction, a second mixture of 100  $\mu$ L optiMEM and 0.75  $\mu$ L miRNA mimic or inhibitor (yielding a final concentration of 50 nM in a 1 mL volume) per dish were combined for 5 minutes. The first and second mixtures were then combined and incubated at room

temperature for 30 minutes, and 200  $\mu$ L was subsequently added dropwise to each well.

#### *2.2.4.2 Preparation of Samples for Western Blotting*

Cells were harvested in PBS 48 hours after transfection and pelleted at 4000 rpm for 10 minutes at 4 °C. The pellet was resuspended in RIPA buffer (150 mM NaCl, 1% (v/v) IGEPAL® CA-630 (Sigma-Aldrich®, I8896), 0.5% (w/v) sodium deoxycholate, 0.1% (w/v) SDS, 50 mM Tris, pH 8.0, including protease inhibitors (Sigma-Aldrich, P8340) and phosphatase inhibitors (Sigma-Aldrich, P5726) at a 1:1000 dilution). A BCA assay (Pierce) was then used to determine the protein concentration as per the manufacturer's guidelines and bovine serum albumin (BSA) was used as a standard. Briefly, cell suspensions in RIPA were subject to sonication and centrifuged at 13,000 rpm for 20 minutes at 4 °C. The resulting supernatant was removed and used for downstream analysis. Reactions were incubated at 37 °C for 40 minutes and measurements obtained using a MultiSkan FC plate reader (ThermoFisher).

#### *2.2.4.3 SDS-PAGE and Western Blotting*

Cell lysate samples were analysed via SDS PAGE and western blotting. 5-20% gradient acrylamide gels were used and the constitution is given in Table 2. From each sample, 20  $\mu$ g protein was loaded into a SDS-PAGE gel and run at 40 mAmps until completion. The gel was incubated against nitrocellulose membrane overnight in transfer buffer (25 mM Tris, 192 mM glycine and 20 % (v/v) methanol) at 40 mAmps. Membranes were blocked in blocking buffer (5% (w/v) Marvel in TBS-Tween-20 (20 mM Tris, 150 mM NaCl, pH 7.5 and 0.05% (v/v) Tween-20)) for one hour at room temperature. Primary antibodies were applied at appropriate dilutions in blocking buffer; Anti-NRF2 (Santa Cruz, cat# sc-13032) at 1:500, anti-p62 (BD Biosciences, cat# 610833) at 1:3000, anti-LC3B at 1:3000, anti-TBK1 (Cell Signalling Technology, cat# 3013) at 1:1000, anti-Ser-403 phosphorylated-p62 (MBL, cat# D343-3) at 1:1000 and anti-STING (Cell Signalling Technology, cat# D2P2F) at 1:1000 and  $\beta$ -actin (Sigma-Aldrich, cat# a1978) at 1:50,000. Anti- $\beta$ -actin was incubated for three hours at room temperature whilst antibodies against NRF2, p62, LC3B, TBK1,

Ser-403 p62 and STING primary antibodies were incubated overnight at 4 °C. Following primary antibody incubation, membranes were washed for five minutes, three times in TBS-Tween-20 and HRP conjugated secondary antibody (rabbit, mouse or rat) was applied at 1:3000 dilution in blocking buffer, matching the primary antibody species. Membranes were incubated at room temperature for one hour before washing for five minutes, three times in TBS-Tween-20. Membranes were then developed in the dark using enhanced chemiluminescence (ECL) reagents (Perkin Elmer). Imaging film (Kodak) was placed on the membrane and subject to exposures ranging from 10 seconds to 25 minutes depending on the antibody and sample. The film was then immersed in developing solution followed by fixing solution.

**Table 2: 5-20 % gel solution components.** Buffer A (1.1M Tris, 0.1% (w/v) SDS, 30% (w/v) glycerol, pH 8.8). Buffer B (1.1M Tris, 0.1% (w/v) SDS, pH8.8). Stacking buffer (0.14M Tris, 0.1% (w/v) SDS, pH6.8).

Component	5% Solution	20% Solution	Stacking Gel
Buffer A		3.33 mL	
Buffer B	3.33 mL		
Stacking Buffer			5 mL
Distilled Water	5 mL		
30% Acrylamide Bisacrylamide	1.67 mL	6.67 mL	1 mL
10 % Sodium dodecyl sulfate (SDS) (w/v)	100 µl	100 µl	
10 % Ammonium persulfate (APS) (w/v)	100 µl	100 µl	100 µl
Tetramethylethylenediamine (TEMED)	10 µl	10 µl	10 µl

#### 2.2.4.4 Analysis of Western Blots

Western blots were scanned at 600 dpi and subject to densitometry analysis using ImageJ/Fiji. Briefly, the images were converted to greyscale and the intensity of each band with a corresponding background area of the same size was measured. The net protein was calculated by subtracting the background intensity from the protein band intensity. The net protein intensity was then normalised to that of  $\beta$ -actin. Finally, protein measurements were normalised to the experimental control.

## 2.2.5 Immunocytochemistry

HeLa cells were seeded on coverslips at a density of  $2.2 \times 10^4$  cells/well in 1 mL media (DMEM, 10% (v/v) FBS, 1% (v/v) Penicillin streptomycin). After 24 hours, cells were transfected with 50 nM negative control mimic or miR-340 mimic as described in section 2.2.4.1. After 48 hours the cells were washed in PBS and fixed in 1 mL 4% paraformaldehyde (PFA) (4% (w/v) in PBS, heated to 60 °C followed by the addition of NaOH dropwise until dissolved) at 37 °C for 10 minutes. The fixed cells were washed in PBS for five minutes, three times, before permeabilization in 1 mL 0.1% (w/v) Triton-X100 in PBS for 10 minutes. The cells were then washed in PBS for five minutes, three times and blocked in 3% BSA in PBS for 1 hour at room temperature. Primary antibody was applied to coverslips at appropriate dilutions in 3% (w/v) BSA and incubated overnight at 4 °C. Anti-NRF2 was used at 1:50 dilution. The cells were then washed in PBS for five minutes, three times and incubated in secondary antibody (Alexa Fluor 488, Molecular Probes) at a dilution of 1:500 for 45 minutes at room temperature in the dark. The secondary antibody was removed and Dapi (Vectorlabs) was added to the wells at a final concentration of 300 nM in 3% BSA for 10 minutes. The cells were then washed in PBS for five minutes, three times and the coverslips mounted onto microscope slides. The slides were stored at 4 °C prior to imaging.

## 2.2.6 Analysis of Immunocytochemistry Images

Images were taken using a 20X magnification and the NRF2 fluorescence excited at 488 nm and dapi fluorescence (for nuclear detection) excited at 405 nm. A wide field fluorescence microscope (Axiovert 200M, Zeiss) coupled to a CCD camera (Photometrics CoolSnap MYO). The outline of the cell body was manually drawn around and the intensity of the resulting space was measured using ImageJ/Fiji. For each cell, three nearby background areas were also measured. The average background intensity for each cell was scaled to that of the exact area of the measured cell, using the formula  $Area \times Mean = Integrated\ Density$  and subtracted from the cell intensity. For each replicate of the experiment, the intensity

of the net protein was averaged and normalised to that of the experimental control. A minimum of 50 cells per condition were analysed.

## 2.2.7 Live Cell Autophagic Flux Assay

### 2.2.7.1 *Seeding and Transfecting Cells for the Live Cell Autophagy Assay*

HeLa or N2A cells were seeded at a density of  $0.8 \times 10^5$  cells in 2 mL media (DMEM, 10% (v/v) FBS, 1% (v/v) Penicillin streptomycin) in glass bottom dishes (WillCo dishes). Transfections were performed using Lipofectamine 2000 with 100 ng P-DEST-mCherry-EGFP-*SQSTM1*/p62 construct and 50 nM miR-340 mimic, inhibitor or respective controls. The transfection protocol used was the same as that described in section 2.2.4.1.

### 2.2.7.2 *Imaging the Live Cell Autophagy Assay*

For establishing the assay, 48 hours post transfection with P-DEST-mCherry-EGFP-*SQSTM1*/p62 construct, cells were treated with 50 nM bafilomycin using an equal volume of DMSO as a negative control and incubated at 37 °C with 5% CO<sub>2</sub>. After 16 hours cells were washed in PBS, placed in 1 mL Ringer's buffer (2 mM CaCl<sub>2</sub>, 10 mM glucose, 10 mM HEPES, 5 mM KCl, 2 mM MgCl<sub>2</sub>·6H<sub>2</sub>O, 155 mM NaCl and 2 mM NaH<sub>2</sub>PO<sub>4</sub>·H<sub>2</sub>O, pH 7.2) and imaged using the DeltaVision widefield microscope at 37 °C. For miRNA experiments, cells were transfected with 100 ng P-DEST-mCherry-EGFP-*SQSTM1*/p62 construct and 50 nM miRNA mimic, inhibitor or appropriate control. After 48 hours cells were washed in PBS and visualised in 1 mL Ringer's buffer using the DeltaVision widefield microscope. The live cell filter wheel with Quad mCh polychronic was used. The EGFP fluorescence was excited at 475 nm and measured at 525 nm and the mCherry fluorescence was excited at 575 nm and measured at 632 nm. For all live cell imaging, the images were taken sequentially, creating a Z-stack.

### 2.2.7.3 Image Analysis

Images were processed using the Hougan's Professional software. Firstly, images were deconvoluted, then analysed for their colocalization to obtain Pearson's correlation coefficient (PCC) values using the Costes method for estimating thresholds (Costes *et al.*, 2004). A minimum of 50 cells per condition were analysed.

## 2.2.8 Luciferase Reporter Assay

### 2.2.8.1 Cloning Oligonucleotides into the pmirGLO Vector

Oligonucleotides containing part of the target mRNA 3'UTR which harboured the miRNA seed sequence predicted binding site were cloned into the pmirGLO vector (Promega, E1330). Table 3 shows the oligonucleotide sequences used for cloning and significant parts of the sequences are highlighted. The oligonucleotides were designed with restriction enzyme overhangs to enable their insertion into the pmirGLO vector. A Not1-HF restriction enzyme site was included in each oligonucleotide, as the pmirGLO vector also contained a Not1-HF site. This enabled confirmation of successful ligation of the oligonucleotides into the vector, as the two fragments formed by treatment with Not1-HF could be visualised by agarose gel electrophoresis.

The pmirGLO vector was digested with the restriction enzymes, Nhe1-HF and Sal1-HF, for 15 minutes at 37 °C. To achieve this, 2 µL pmirGLO vector, 1 µL of each restriction enzyme and 5 µL cutSmart buffer (New England Biolabs) were added to a final volume of 50 µL with hyclone water. Reactions were then treated with 1% (v/v) alkaline phosphatase for one hour at 37 °C to prevent vector re-ligation.

The vector was then purified using agarose gel electrophoresis. Briefly, 1 g agarose was dissolved in 100 mL TAE buffer (40 mM Tris-acetate and 1 mM EDTA, pH 8) using gentle heating. Once cooled, 0.01% (v/v) SYPRO Orange (Invitrogen, S6650) was added to the 1% agarose solution and poured into a gel cassette. A comb was added and the gel left to set. Samples were diluted with DNA loading dye (New England Biolabs, B7024S) and run at 100 V in TAE buffer until complete. The band was excised

and the DNA purified using the QIAquick gel extraction kit (Qiagen) as per the manufacturer's instructions.

The oligonucleotides were received lyophilized and were resuspended to 1 µg/µL in hyclone water. They were annealed using oligo annealing buffer (New England Biolabs) for three minutes at 90 °C, then at 37 °C for 15 minutes. 4 ng of annealed oligonucleotide was ligated in 50 ng digested pmirGLO vector using T4 DNA ligase and T4 DNA ligase buffer for 16 hours at 16 °C.

**Table 3: Oligonucleotides used for cloning.** Significant parts of the sequence are highlighted. Pink; miRNA response element (the sequence complementary to the miRNA seed sequence). Yellow; the remaining miRNA sequence overlay. Green; Not1-HF restriction enzyme site. Red; Nhe1-HF restriction site overhang. Blue; Sal1-HF restriction enzyme overhang. The whole miRNA binding site and the predicted miRNA response elements have been shown in all sequences. F (forward sequence), R (reverse sequence).

Oligonucleotide Name	Sequence
TBK1_340-5p_F	5' CTAGCATGCGGCCGCATTTTATCTTTTAACATTATAATACACG 3'
TBK1_340-5p_R	5' TCGACGTGTATTATAAATGTTAAAAGATAAAATCGCGGCCGCATG 3'

### 2.2.8.2 Transformation into XL10 Gold Competent Cells

5 µL of the pmirGLO ligation reaction was transformed into 100 µL XL10 gold competent cells. Briefly, samples were incubated on ice for 30 minutes, heat shocked at 42 °C for 40 seconds and incubated on ice for two minutes. The reaction was made up to 1 mL with Luria broth (LB) and incubated for 1 hour at 37 °C with shaking at 200 rpm. The cells were centrifuged for 5 minutes at 2000 rpm and the cell pellet resuspended in 200 µL LB broth. Cells were plated on LB-agar ampicillin (final concentration 100 µg/mL) and incubated at 37 °C for 16 hours.

Colonies were picked and cultured in LB with ampicillin (100 µg/mL) at 37 °C for 16 hours. The cultures were miniprep using the QIAprep spin miniprep kit (Qiagen) following manufacturer's guidelines. The presence of the oligonucleotides was confirmed by Not1-HF restriction enzyme digests, as previously described, and the

presence of two separate bands was visualised by agarose gel electrophoresis. The correct sequence of the ligated oligonucleotides was confirmed by Sanger sequencing (DeepSeq Lab, University of Nottingham).

### 2.2.8.3 Site Directed Mutagenesis

Site directed mutagenesis (SDM) was used to confirm the interaction between the miRNA and the specific predicted miRNA response element present on the target 3'UTR. Mutant strands were designed so the sequence remained exactly the same as that used in section 2.2.8.1, though with four nucleotides from the specific microRNA response element mutated (Table 4).

**Table 4: Primers used for SDM.** Pink; the mutated predicted miRNA response element. Yellow; the sequence complementary to the remaining miRNA sequence.

Primer Name	Sequence
TBK1_340-5p_Mut_F	5' GCGATTTTATCTTTTAACA <b>TCCGCA</b> ATACACGTCGACCTGCAGGC 3'
TBK1_340-5p_Mut_R	5' GCCTGCAGGTCGACGTGTA <b>TGCGGA</b> <b>TGTTAAAAGATAAAA</b> TCGC 3'

Mutant strand synthesis was performed using the polymerase chain reaction (PCR) and the components of each reaction are given in Table 5. Phusion reaction buffer and Phusion HF DNA polymerase were used with 100 ng/μL of each primer and 40 mM of dNTP mix. The cycle reaction parameters were as follows: 1 cycle of 95 °C for 30 seconds; 18 cycles of 95 °C for 30 seconds, 55 °C for 1 minute, 68 °C for 1 minute/kb length (pmirGLO is 7,350 bp so 7.5 minutes was required).

A Dpn1 digestion for 1 hour at 37 °C was then performed to digest the parental, non-mutated DNA. The mutated DNA was transformed into XL10 gold cells as described in 2.2.8.2. The correct sequence of the ligated mutated oligonucleotides was confirmed by Sanger sequencing (DeepSeq Lab, University of Nottingham).

**Table 5: PCR reaction for site directed mutagenesis.**

<b>Component</b>	<b>Sample Reaction</b>	<b>Control Reaction 1</b>	<b>Control Reaction 2</b>
5x Phusion reaction buffer	10 µL	10 µL	10 µL
dsDNA template (10 ng/µL)	5 µL	5 µL	5 µL
Forward primer (100 ng/µL)	1.25 µL	1.25 µL	0 µL
Reverse primer (100 ng/µL)	1.25 µL	1.25 µL	0 µL
40 mM dNTP mix	1 µL	1 µL	1 µL
DMSO (100%)	0.5 µL	0.5 µL	0.5 µL
Phusion HF DNA Polymerase (2 Units/µL)	0.5 µL	0 µL	0.5 µL
Hyclone Water	30.5 µL	31 µL	33 µL

#### **2.2.8.4 Seeding and Transfection of HEK293T Cells for Luciferase Assay**

HEK293T cells were seeded in 24 well plates at a density of  $0.6 \times 10^5$  cells/well in 1 mL media (DMEM, 10% (v/v) FBS, 1% (v/v) Penicillin streptomycin). After 24 hours the cells were transfected in triplicate using the protocol described in section 2.2.4.1. Each well received 200 ng ligated vector DNA with 50 nM negative control mimic or miR-340-5p mimic. Following a 48-hour incubation, media was removed and the cells washed in PBS. The cells were lysed in 100 µL passive lysis buffer (Promega) for 30 minutes at room temperature.

#### **2.2.8.5 Dual Luciferase Reporter Assay**

The dual luciferase assay system was supplied by Promega and the LAR II and Stop and Glo® reagent was made according to manufacturer's guidelines. 10 µL of each lysis sample was added to a 96 well plate in triplicate. Per well, 25 µL each of the LAR II and Stop and Glo® reagents were added using a GloMax navigator microplate luminometer (Promega) which measured the luminescence. A reduction in the activity of the reporter gene, Firefly luciferase, indicated the miRNA bound the cloned miRNA response element. The control gene, Renilla luciferase, was also measured and the Firefly luciferase signal was normalised to the Renilla luciferase

signal of each well. The triplicate values were averaged and expressed as a percentage of the negative mimic control values.

## 2.2.9 HeLa Cell Treatment with BX-795

HeLa cells were seeded at a density of  $0.8 \times 10^5$  cells/well in 1 mL media (DMEM, 10% FBS, 1% Penicillin streptomycin). After 48 hours, cells were treated with 1  $\mu$ M BX-795 using an equal volume of DMSO as a control. After 16 hours the cells were harvested in PBS, centrifuged at 4000 rpm for 10 minutes and stored at -20 °C. Cells were prepared for western blotting as described in section 2.2.4.2 and western blotting using BX-795 treated samples was performed as described in section 2.2.4.3.

## 2.3 Investigation of miR-340 Function in Human Astrocytes

### 2.3.1 Seeding and Treatment of Cells for RNA Extraction

HeLa cells were seeded at  $0.8 \times 10^5$  cells/well in 12 well plates and human primary astrocyte cells (ScienCell, #SC-1800) were seeded at  $7 \times 10^4$  cells/well in 6 well plates. HeLa cells were transfected with 50 nM miRNA mimics or inhibitors 24 hours after seeding as described in section 2.2.4.1 and incubated at 37 °C with 5% CO<sub>2</sub> for 48 hours. Human primary astrocyte cells were treated with 100 nM cell permeable miR-340 inhibitor or cell permeable negative control inhibitor 24 hours after seeding and incubated at 37 °C with 5% CO<sub>2</sub> for 48 hours. Table 6 shows the miRNA inhibitors used in Chapter 5, their sequence and purchase information.

**Table 6: : List of cell permeable miRNA inhibitors used in Chapter 5, their nucleotide sequence and purchase information.**

MiRNA Name	Sequence	Catalogue Number
hsa-miR-340-5p Power Inhibitor	5' ATCAGTCTCATTGCTTTATA 3'	# 339131
Negative Control Power Inhibitor	5' TAACACGTCTATACGCCCA 3'	# 339136

### 2.3.2 TRIZOL Extraction of RNA

Cells were lysed in 200  $\mu$ L of TRIzol<sup>®</sup> Reagent per well for 12 well plates and 500  $\mu$ L per well for 6 well plates. The homogenised samples were incubated at room temperature for 5 minutes in RNase free, low-bind epindorpha. The samples were pooled into one epindorph per condition. 100% chloroform was then added at one fifth the TRIzol volume and incubated at room temperature for 2-3 minutes before centrifugation at 12,000 x g for 15 minutes at 4 °C. The upper aqueous phase was removed and placed in a clean RNase free low-bind epindorph. 100% isopropanol was then added at half the TRIzol volume and incubated at room temperature for 10 minutes before centrifugation at 12,000 x g for 10 minutes at 4 °C. The supernatant was removed and the RNA pellet washed in 75% ethanol at an equal volume to that of TRIzol used. The RNA pellet was vortexed and centrifuged at 7,500 x g for 5 minutes at 4 °C and the wash discarded. The RNA pellet was then air dried for 5-10 minutes and the transparent, gel-like pellet was resuspended in 20  $\mu$ L RNase free water and incubated at 55 °C for 10-15 minutes. The RNA concentration and purity was assessed using a 2000c UV/IV Spectrophotometer (Nanodrop).

### 2.3.3 mRNA Sequencing

In house analysis of mRNA quality was assessed, generating RNA integrity numbers (RIN) as a stringent indicator of RNA quality (University of Nottingham, DeepSeq). A minimum of 200 ng RNA was analysed by mRNA sequencing at 20 million reads per sample by Novogene, Cambridge.

### 2.3.4 Bioinformatics to Determine Direct and Indirect mRNA Targets of miR-340

The list of mRNAs found with altered expression in HeLa cells with miR-340 overexpression were cross-referenced with DIANA-T-CDS predicted targets of miR-340 with a threshold set at 0.2 as well as TargetScan predicted targets of miR-340. This low threshold with DIANA-T-CDS was set to include any mRNA with a possible MRE to miR-340. Those mRNAs which were predicted to target miR-340 were classed

as 'direct' targets of miR-340, whereas those without a prediction to be targeted by miR-340 were classed as 'indirect' targets of miR-340.

## 2.4 Investigation of Autophagy Failure – Impact on Extracellular Vesicle Proteomes

### 2.4.1 Cell Culture for Exosome Purification

N2A cells were seeded at equal densities into T75 cell culture flasks in 12 mL media (DMEM, 10% (v/v) FBS, 1% (v/v) Penicillin streptomycin). After 48 hours, media was removed and cells washed in PBS. 20 mL serum free media (DMEM and 1% Penicillin streptomycin, no FBS) was added and the cells grown for 24 hours before harvesting the media for exosome purification. Cells were harvested in PBS, centrifuged at 4,000 rpm at 4 °C and stored at -20 °C. For initial characterisation of exosomes, a total of 40 mL media from two T75 flasks were used.

### 2.4.2 Bafilomycin Treatment of N2A cells Cultured for Exosome Purification

N2As were seeded at equal densities in T75 cell culture flasks, in 12 mL DMEM (10% FBS, 1% Penicillin streptomycin). After 48 hours, media was removed and cells washed in PBS. 8 mL serum free media (DMEM and 1% Penicillin streptomycin, no FBS) containing 50 nM Bafilomycin A1 was added to one T75 flask. A T75 flask with 8 mL media (DMEM and 1% Penicillin streptomycin, no FBS) with DMSO at an equal volume to Bafilomycin A1 was used as a control. The media was harvested for size exclusion chromatography (SEC) 16 hours later.

### 2.4.3 Purification of Exosomes using Size Exclusion Chromatography

The FBS free media from N2A cells was collected after 16 or 24 hours depending on the experiment (as described in sections 2.4.1 and 2.4.2) and centrifuged at 1,500 rpm for 5 minutes at room temperature to pellet any cell debris and the supernatant was placed in a 10 kDa molecular weight concentrator and centrifuged at 4,000 x g

at room temperature for approximately 30 minutes until 500  $\mu$ L of sample remained in the concentrator.

Exosomes were purified using size exclusion chromatography columns (Izon, qEVoriginal/70nm) using manufacturer's guidelines. The SEC column storage buffer, sodium azide was removed and stored at 4 °C. The column was then washed with 30 mL PBS (sterile filtered using 0.2  $\mu$ m filter to remove larger particles capable of blocking the column). The 500  $\mu$ L media remaining in the concentrator was then added to the SEC column and fractions immediately collected. Throughout the process the column was prevented from drying using PBS washes. The first three fractions, each 1 mL in volume, contained only PBS or sodium azide. The following three fractions, each 500  $\mu$ L in volume, contained exosomes, and the final three fractions, each 1 mL in volume, contained protein. The SEC columns were then flushed with 30 mL PBS, stored in sodium azide at 4 °C and reused up to five times.

#### 2.4.4 Preparation of Exosome Samples for Western Blotting and Mass Spectrometry

For western blotting analysis, a 40  $\mu$ L sample of each of the three 500  $\mu$ L exosome fractions was combined with 15  $\mu$ L gel loading buffer and loaded into a 5-20% SDS-PAGE gel which was run to completion at 45 mAmps. The exosome fractions were too dilute for accurate quantification of total protein by BCA assay. Where cell lysate samples were used for western blotting, a BCA assay was performed and 20  $\mu$ g protein loaded into the gel. Western blotting was then performed as described in section 2.2.4.3. Primary antibodies were used at the following dilutions: Alix at 1:1,000 and Flotillin-1 at 1:500.

For mass spectrometry analysis, a 40  $\mu$ L sample of the second EV fraction was combined with 15  $\mu$ L gel loading buffer and loaded into a 5-20% SDS-PAGE gel. The sample was run through the entire stacking gel into the start of the resolving gel. The gel was Coomassie stained (50% (v/v) methanol, 20% (v/v) glacial acetic acid, 1.12% (w/v) Coomassie Brilliant Blue) for 1 hour at room temperature and de-stained overnight. The bands were cut out of the start of the resolving gel. Mass

spectrometry (LC/MS/MS) was performed by the Cambridge Centre for Proteomics, Cambridge, with a one hour liquid chromatography run.

#### 2.4.5 Treatment and Western Blotting of N2A Cells

N2A cells were seeded at  $0.8 \times 10^5$  cells/well in a 12-well plate in 1 mL media (DMEM, 10% FBS, 1% Penicillin streptomycin) and incubated at 37 °C with 5% CO<sub>2</sub> for 48 hours. Cells were treated with 50 nM bafilomycin and an equal volume of DMSO was used as a control. After 16 hours, cells were washed in PBS, harvested and stored at -20 °C. Samples were prepared for western blotting as described in section 2.2.4.2 and western blotting was performed as described in section 2.2.4.3.

### 2.5 Statistical Analysis

All data were analysed using Graphpad Prism 9. Unless otherwise stated, data were subject to normalisation tests and statistical analysis was performed using two-tailed students T-test. Statistical significance was attributed at  $p < 0.05$  (\*),  $p < 0.005$  (\*\*) and  $p < 0.001$  (\*\*\*). Unless otherwise stated, data are shown as mean +/- SEM from a minimum of three independent experiments.

## Chapter 3 - Identification of ALS-Associated miRNAs from a Systematic Literature Review

### 3.1 Introduction

A growing body of evidence suggests miRNA dysregulation is a hallmark of ALS. This evidence includes the expanding number of studies which profile collections of miRNAs found dysregulated in various ALS patient clinical samples compared to controls, though there have been few attempts to organise these miRNAs into a single data set. Indeed, to date, no analysis or evaluation of all known ALS dysregulated miRNAs has been performed. In this chapter we address this need by performing a systematic literature review to identify all ALS patient dysregulated miRNAs in studies published from 2013-2018 with the aim of providing a comprehensive list of those most frequently found dysregulated in ALS. The relationship between ALS dysregulated miRNAs and their ALS-relevant mRNA target predictions has also not been fully investigated. We hypothesised that those miRNAs most frequently reported as dysregulated in ALS would have a greater number of predicted ALS-relevant gene targets. To address this, we use bioinformatic software to determine whether miRNAs found to be dysregulated most often in ALS patients are predicted to target more ALS-associated genes than miRNAs found less frequently dysregulated in ALS patients. This work also helps highlight candidate miRNAs to explore future functional analyses.

#### 3.1.1 Experimental Aims

The overall aim of the work in this chapter was to determine the total set of published ALS patient dysregulated miRNAs to highlight a subset of candidate miRNAs for potential further investigation. We also aimed to identify a candidate ALS-patient dysregulated miRNA with relevance to the biochemical pathway, autophagy, implicated in ALS. To achieve this, the following objectives were applied:

- Perform a systematic literature review to collate all miRNAs reported as dysregulated between ALS patients and controls and subsequently identify miRNAs most frequently found dysregulated in ALS.
- Correlate the ALS patient dysregulated (or otherwise) miRNAs with ALS-relevant predicted mRNA targets to determine any correlation between numbers of predicted targets and frequency of ALS dysregulation.
- To distinguish the tissue sources the ALS patient dysregulated miRNAs were extracted from to determine miRNAs found dysregulated in tissues of specific interest such as neuronal tissue and cerebrospinal fluid (CSF).
- Through re-analysis of ALS patient-dysregulated miRNAs with a focus on those with relevance to the autophagy pathway, determine a candidate miRNA for experimental evaluation.

## 3.2 Results and Discussion

### 3.2.1 Review of Studies of miRNA Expression in ALS Patients

To identify miRNAs with potential functional relevance to ALS, a robust literature search of PubMed using the MeSH terms ‘microRNA’ AND ‘amyotrophic lateral sclerosis’ with studies from 1/1/2013-31/12/18 was conducted. This identified 27 peer-reviewed studies which specifically included those recording and comparing levels of multiple miRNAs directly from ALS patients and controls (Appendix I) (Foggin *et al.*, 2019). At the time of analysis, no specific miRNA had been identified as a biomarker of ALS, though many studies have attempted to identify one. Previously, Dardiotis and colleagues reviewed 15 of the same studies included here, whilst Joilin and colleagues reviewed 11 (Dardiotis *et al.*, 2018; Joilin *et al.*, 2019). Our approach identified a total of 727 patient deregulated miRNAs across the 27 peer-reviewed studies. Several papers reported miRNAs no longer accepted as valid, and these were manually removed. Other studies denoted the passenger strand with an asterisk (\*), and in these cases, either a 3p or 5p was manually added to the miRNA name as appropriate. A list of the dysregulated miRNAs from each study is given in Appendix 2.

The studies were highly varied, extracting miRNAs from patient whole blood, serum, plasma, CSF, spinal cord and muscle. They also varied in the numbers of ALS patients and controls involved in the study. Additionally, some studies included a variety of clinical characteristics of ALS participants, including sALS, fALS and PLS (primary lateral sclerosis). Some studies included both healthy and alternative disease control participants. Further, the studies varied in the methods used for sample preparation, profiling of individual miRNAs, the interpretation and analysis of data. For example, methods used to isolate and quantify miRNAs included next generation sequencing (NGS), RT-PCR and RNA sequencing from whole transcriptomes. Several studies attempted to address the functional implications of their observed miRNA expression changes, utilising a range of bioinformatic resources such as TargetScan, Pictar, miRanda, DIANA-Tarbase and miRtarbase to identify potential mRNA targets, enriched biological themes, protein interaction networks, gene ontology and

pathway analysis (Campos-Melo *et al.*, 2013; Wakabayashi *et al.*, 2014; Freischmidt *et al.*, 2014; Raman *et al.*, 2015; Chen *et al.*, 2016; Figueroa-Romero *et al.*, 2016; Waller *et al.*, 2017a; D'Erchia *et al.*, 2017a; Taguchi and Wang, 2018; De Felice *et al.*, 2018; Kovanda *et al.*, 2018; Liguori *et al.*, 2018; Saucier *et al.*, 2018). A summary of the participants, tissue source and main methods are given for each study in Appendix 1.

### 3.2.2 ALS Patient-Deregulated MicroRNAs

To identify those miRNAs with potential pathological relevance, we ranked the identified 727 patient-dysregulated miRNAs by the number of different studies reporting their dysregulation. Table 7 shows the 24 mature miRNAs found dysregulated in five or more different studies out of a maximum of 27. All miRNAs dysregulated in six or more studies were found both up and downregulated between ALS patients and controls which could be due to the variation of methods for miRNA extraction and quantification or the profiling technique. Alternatively, the direction of the miRNA expression change may be irrelevant, since the dysregulation of a specific miRNA, in either direction, could have deleterious effects on targeted pathways. Further, the large number of miRNAs found dysregulated could reflect the broad RNA dysfunction, where a vast array of miRNAs may be dysregulated.

**Table 7: Mature miRNAs found dysregulated in five or more different studies reporting altered miRNA levels in ALS patients compared to controls out of a maximum of 27.**

MiRNA Name	Number of Studies Dysregulated (Total of 27)	MiRNA Name	Number of Studies Dysregulated (Total of 27)
hsa-miR-133a-3p	9	hsa-miR-100-5p	5
hsa-let-7a-5p	7	hsa-miR-106a-5p	5
hsa-let-7f-5p	6	hsa-miR-142-5p	5
hsa-miR-124-3p	6	hsa-miR-151a-5p	5
hsa-miR-127-3p	6	hsa-miR-17-5p	5
hsa-miR-155-5p	6	hsa-miR-221-3p	5
hsa-miR-183-5p	6	hsa-miR-23a-3p	5
hsa-miR-206-3p	6	hsa-miR-26a-5p	5
hsa-miR-455-3p	6	hsa-miR-28-3p	5
hsa-let-7b-5p	5	hsa-miR-338-3p	5
hsa-let-7d-5p	5	hsa-miR-584-5p	5
hsa-miR-1-3p	5	hsa-miR-9-5p	5

It is important to note that the following review and contextualisation of the literature was performed in 2019, at the time of the systematic literature review. A more up to date consideration of miRNAs implicated in ALS is provided in Chapter 7. Of the most frequently reported miRNAs, hsa-miR-133a-3p was found deregulated in 9/27 studies. Interestingly, hsa-miR-133a-3p is a known myomiR, enriched in muscle tissue (Siracusa et al., 2018). Of the 27 studies reported for ALS, several measured the expression levels of myomiRs alone, potentially introducing a tissue bias (Jensen et al., 2016; Pegoraro et al., 2017; Di Pietro et al., 2017; Russell et al., 2013; Tasca et al., 2016) (Appendix I). However despite its description as a myomiR, hsa-miR-133a-3p has also been suggested as a motor neurone enriched miRNA since it was found enriched almost three fold in brainstem or spinal cord motor neurones compared to other CNS neurones (Mariah L Hoyer *et al.*, 2017). MiR-133a-3p is also an established tumour suppressor in gastric cancer, prostate cancer and bladder cancer (Uchida *et al.*, 2013; Ji *et al.*, 2016; Dong *et al.*, 2018). Further, overexpression

of miR-133a-3p was found to inhibit autophagy in gastric cancer cell lines, whilst the reverse occurred through inhibition of miR-133a-3p. In the same study, GABARAPL1, belonging to the same family as LC3B (the human ATG8 family) and with a role in autophagy that involves interacting with ULK1, was identified as a direct target of miR-133a-3p using the dual luciferase assay (Alemu *et al.*, 2012; X. Zhang *et al.*, 2018). This supports evidence that ALS dysregulated miRNAs may functionally impact autophagy.

Using the mirPath v3.0 software of DIANA-Tools, the relationship between these miRNAs report as dysregulated in five or more of the 27 studies was shown through a cluster dendrogram (Figure 10). Additionally, the pathways predicted to be associated with these miRNAs (using pathways union option within the mirPath v3.0 software of DIANA-Tools) were identified (Figure 10).

Interestingly, the “prion diseases pathway” had the third most significant p value from this analysis ( $p < 3.4e^{-8}$ ) and the prion like nature of SOD1 in ALS has been suggested. For example, the overexpression of ALS-associated mutant misfolded SOD1<sup>G127X</sup> and SOD1<sup>G85R</sup> has been shown to cause misfolding of wild type SOD1 in human cell lines, including the neuroblastoma cell line, SH-SY5Y. Further, a tryptophan residue was demonstrated to enable this, which is human specific and no effect on wild type SOD1 was observed when the experiment was performed in the mouse motor neurone like cell line, N2A (Grad *et al.*, 2011).

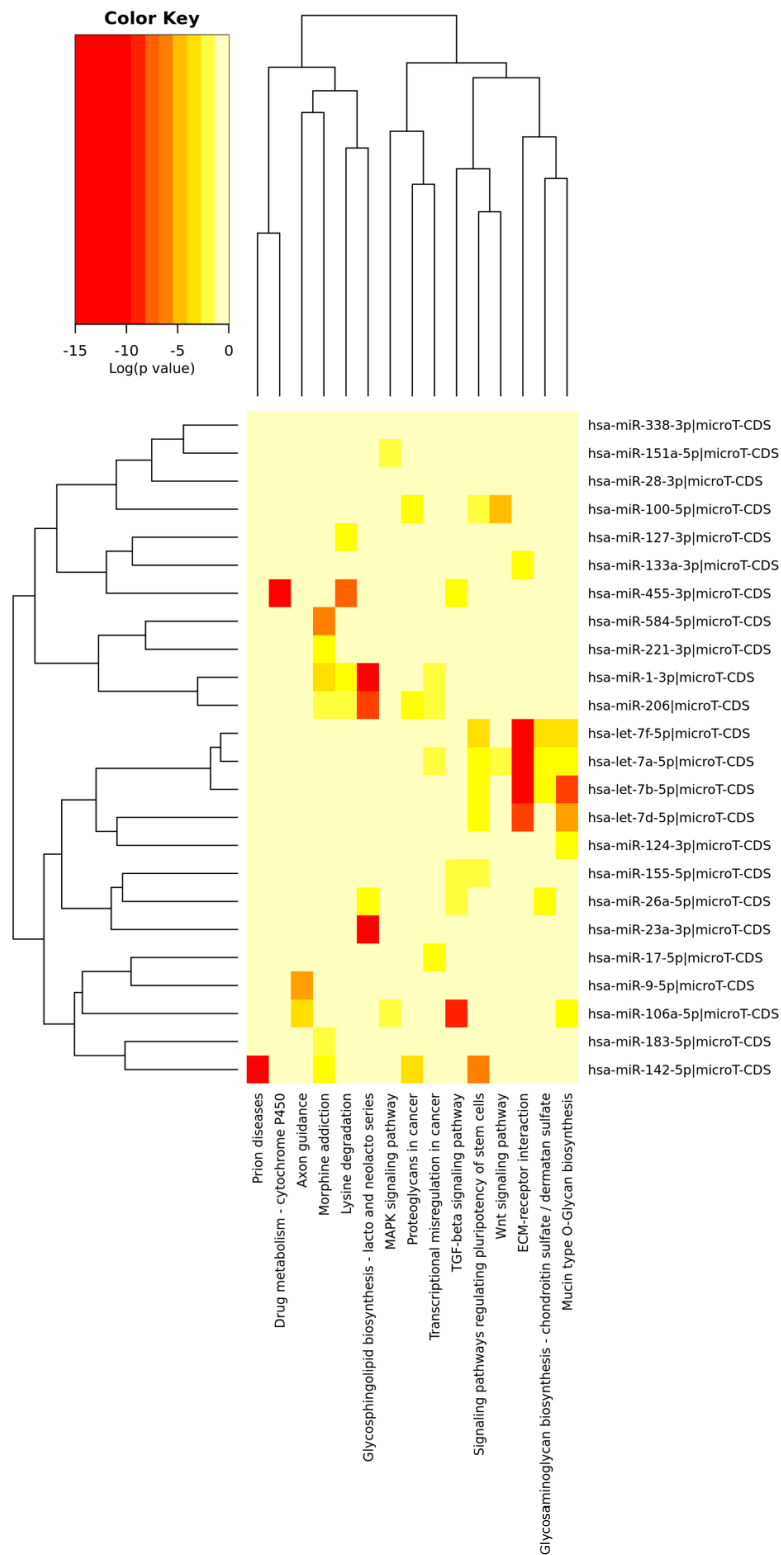


**Figure 10: Heatmap of miRNAs most frequently reported as dysregulated in ALS.** The relationship between miRNAs is shown with a cluster dendrogram on the left hand side. The predicted related pathways are shown underneath and their relationship is shown with a cluster dendrogram above. Generated using DIANA mirPath v3.0 with a MicroT threshold of 8.0. Pathways union selected with Fisher's exact test enrichment analysis method used.

TDP-43 is also considered to behave in a prion-like manner. Indeed, its C-terminal presents a prion-like structure which is prone to aggregation (Fuentelba *et al.*, 2010). Injections of patient FTD-TDP-43 into mouse brains lead to the formation of TDP-43 inclusions and this pathology spread throughout the brain in a time-dependent manner (Porta *et al.*, 2018). Further, insoluble TDP-43 from sALS or FTD patients was introduced into SH-SY5Y cells and induced TDP-43 aggregation (Nonaka *et al.*, 2013).

Further, axon guidance was also amongst the most significantly associated pathways, and the mRNA of an axon guidance protein, Sema3A, was found increased in terminal Schwann cells within muscle of SOD1<sup>G93A</sup> mice and could result in de-adhesion of motor neurones from the neuromuscular junction (De Winter *et al.*, 2006; Schmidt, Pasterkamp and van den Berg, 2009).

### 3.2.3 Correlating Deregulated MicroRNAs with Target Gene Predictions

#### 3.2.3.1 Frequently Deregulated microRNAs and Target Prediction of ALS Genes

Next, we sought to determine whether *in silico* methods predict these deregulated miRNAs to target known ALS-related genes using a database of collated ALS associated genes, called ALSod (<http://alsod.ac.uk>). The ALS genes considered total 154 (last updated 2021), which includes both causative and known disease modifier genes. If a correlation was to be observed between those most frequently reported ALS dysregulated miRNAs and the number of ALS relevant genes they were predicted to target, it would establish a method to identify potential miRNA biomarkers of disease, provided the disease linked genes are known. It would also suggest that miRNA dysregulation may not simply be a consequence of ALS progression, but may drive the development of disease.

For the prediction analysis we used DIANA-microT-CDS v5.0 (Paraskevopoulou *et al.*, 2013; Reczko *et al.*, 2012). As reviewed by Riffo-Campos *et al.* (2016), TargetScan was shown as the most precise of the sequence-based tools, but this was impacted by a high false negative rate that leads to low sensitivity. By contrast, miRanda has greater sensitivity, but a higher false-positive rate. Instead, the DIANA-microT attempts to

apply a more balanced predictive approach and displays comparisons to TargetScan in its analysis.

From the *in silico* analysis, 8/9 of the most frequently dysregulated miRNAs, reported in six or more studies, were predicted to target at least one of these 154 ALS/D genes (Table 8A), with hsa-let-7f-5p predicted to target 16/154 of the genes. There appeared to be no obvious relationship between the total number of ALS genes that the individual miRNAs were predicted to target and the number of studies reporting these miRNAs to be dysregulated. The most frequently predicted ALS targeted genes were those encoding the single stranded DNA/RNA binding protein, *RBMS1*, and the E3 ubiquitin ligase, *RNF19A* (4/9 most frequently dysregulated miRNAs). The total count of predicted ALS target genes for the combined nine miRNAs was 71, and overall, 46/154 ALS genes were predicted to be targeted by at least one of the nine miRNAs.

### *3.2.3.2 Less Frequently Deregulated microRNAs and Target Prediction of ALS Genes*

We next performed the same analysis with nine randomly selected miRNAs that although reported to be dysregulated in the 27 ALS studies, appeared in fewer than 6 reports. Randomisation was achieved by selecting from all deregulated miRNAs, with all duplicates removed, using a Microsoft Excel randomisation function. The results of this analysis are shown in Table 8B. Of the nine miRNAs, dysregulation was reported in between one to five of the 27 studies. 8/9 of these randomly selected miRNAs were predicted to target at least one of the ALS genes. Further, one of the miRNAs, hsa-miR-302a-5p (dysregulated in 1/27 studies) was predicted to target 11/154 ALS genes. The most frequently predicted ALS targeted genes were *ERBB4* and *SOD2* (4/9 miRNAs). The total count of predicted ALS target genes for the combined nine miRNAs was 67, comparable to the total count for the nine most commonly dysregulated miRNAs – 71 (Table 8A). Overall, 40/154 ALS genes were predicted to be targeted by at least one of the nine miRNAs.

### 3.2.3.3 Analysis of Randomly Selected and Non-Deregulated microRNAs

To investigate if predicted gene targets for dysregulated ALS miRNAs reflected an enrichment compared to non-dysregulated miRNAs, we randomly selected nine mature miRNAs not reported as dysregulated in any of the 27 studies and performed the same analysis (Table 8C). We selected from all *Homo sapien* mature miRNA sequences recorded on miRBase release 22.1: October 2018 (Kozomara and Griffiths-Jones, 2014). One of the random miRNAs, hsa-miR-603-3p, was predicted to target 16/154 of the ALS genes. The major ALS gene, *TARDBP*, was predicted most frequently, along with *SOD2* and *ALAD* (3/9 miRNAs).

Compared to the nine most frequently reported (Table 8A) or the dysregulated but less frequently reported miRNAs (Table 8B), this random selection of miRNAs gave a total count of 50 predicted ALS target genes (Table 8C), representing only 34/154 of the ALS genes. However, similar to those in Table 8A and 8B, 8/9 of these random miRNAs were predicted to target at least one of the 154 ALS genes. Further randomisations with additional sets of nine random miRNAs were also performed (not shown). Statistical analysis (binomial test, Graphpad Prism 9) indicates dysregulated miRNAs from ALS patient studies do not appear to more frequently target ALS genes than randomly selected miRNAs do, at least based on *in silico* predictions. This could also suggest that at present, the number of genes linked to ALS do not provide a sufficiently high number of targets for specific selectivity of miRNA networks. Conversely, current ALS genes might represent widely distributed signalling networks, and more specific pathways may be required for target enrichment. In summary, at present, our *in silico* analysis did not support a clear link between dysregulated miRNAs and ALS pathological processes, at least at the level of predicted disease-associated target genes.

**Table 8: ALS dysregulated and non-dysregulated miRNAs and ALS gene target predictions.** The ALS genes predicted by DIANA-microT-CDS v5.0 to be targets of (A) the nine most frequently reported miRNAs from the studies, (B) nine dysregulated miRNAs randomly selected from all ALS studies and (C) nine randomly selected miRNAs not reported to be dysregulated in the ALS studies. Note that we report mature miRNAs; where specific miRNAs were not reported we considered dominant strands as reported on miRBase release 22.1: October 2018. For (A), all miRNAs dysregulated in at least six studies were considered. For (B) nine miRNAs were randomly selected from those reported as dysregulated by less than 6 of the 27 studies. For (C) miRNAs not reported as dysregulated in any of the 27 studies were randomly chosen. MiRNAs in bold have confirmed interactions with the target experimentally, using miRTarBase v7.0 (Chou et al., 2018).

	miRNAs	Number of Studies Deregulated (out of 27)	Direction of Deregulation (Up/Down/ Both)	ALS Genes Predicted by DIANA-T-CDS	
<b>A</b>	hsa-miR-133a-3p	9	Both	<i>CSNK1G3, EFEMP1, RBMS1, RNF19A, SCN7A, SYT9, TUBA4A, UNC13A, VAPB, VPS54</i>	MicroRNA hits (8/9)  Genes (46/154)
	hsa-let-7a-5p	7	Both	<i>ARHGEF28, DIAPH3, EPHA4, HFE, NIPA1, RBMS1, ZNF512B</i>	
	hsa-let-7f-5p	6	Both	<i>BCL6, C1ORF72, CHMP2B, CSNK1G3, EPHA4, ERBB4, HNRNPA2B1, NIPA1, RNF19A, SETX, SLC1A2, SOD2, SOX5, SPAST, UBQLN2, VPS54</i>	
	hsa-miR-124-3p	6	Both	<i>B4GALT6, BCL11B, BCL6, CHMP2B, ELP3, HNRNPA2B1, NIPA3, PSEN1, RBMS1, SEMA6A, SIGMAR1, SOD2, SQSTM1</i>	
	hsa-miR-127-3p	6	Both		
	hsa-miR-155-5p	6	Both	<i>LOX, RNF19A, TBK1, UBQLN2</i>	
	hsa-miR-183-5p	6	Both	<i>BCL11B, EPHA4, LOX, RBMS1, SARM1, TUBA4A, VAPB</i>	
	hsa-miR-206-3p	6	Both	<i>ATXN2, CNTN6, CRIM1, HNRNPA1, LOX, MATR3, RNF19A, SLC1A2, SUSD1, VEGFA</i>	
	hsa-miR-455-3p	6	Both	<i>CDH13, ITPR2, SLC1A2, TARDBP</i>	
<b>B</b>	hsa-let-7b-5p	5	Down	<i>ARHGEF28, DIAPH3, EPHA4, HFE, NIPA1, RBMS1, ZNF512B</i>	MicroRNA hits (8/9)  Genes (40/154)
	hsa-let-7c-5p	4	Down	<i>ARHGEF28, DIAPH3, EPHA4, HFE, NIPA1, RBMS1, ZNF512B</i>	
	hsa-miR-154-5p	3	Down		
	hsa-miR-212-3p	2	Down	<i>B4GALT6, C9orf72, ERBB4, FIG4, SOD2, SOX5, SPAST</i>	
	hsa-miR-329-3p	2	Down	<i>C1orf27, CSNK1G3, EPHA4, ERBB4, MAPT, OPTN, RNF19A, SOX5, TARDBP, VAPB</i>	
	hsa-miR-766-3p	2	Both	<i>DAO, DCTN1, DYNC1H1, ELP3, SARM1, SIGMAR1, SLC1A2, UNC13A, VAPB</i>	
	hsa-miR-204-3p	1	Down	<i>CNTN6, ERBB4, SOD2, SOX5, VAPB, VDR, ZFP64, ZNF512B</i>	
	hsa-miR-302a-5p	1	Down	<i>ARHGEF28, BCL11B, CSNK1G3, ERBB4, EWSR1, HNRNPA2B1, LMNB1, SCN7A, SLC1A2, SOD2, SPAST</i>	
hsa-miR-876-3p	1	Down	<i>ALS2, CNTN6, DPP6, ELP3, FIG4, PON2, SIGMAR1, SOD2</i>		
<b>C</b>	hsa-miR-3168-5p			<i>ALAD, CST3, TARDBP</i>	MicroRNA hits (8/9)  Genes (34/154)
	hsa-miR-875-5p			<i>SCN7A, VPS54</i>	
	hsa-miR-611-5p				
	hsa-miR-603-3p			<i>ATXN2, BCL6, CRIM1, CSNK1G3, EPHA4, ERBB4, FUS, HNRNPA2B1, MAPT, MATR3, OPTN, RNF19A, SOD2, TARDBP, VAPB, ZNF746</i>	
	hsa-miR-500b-3p			<i>ALAD, DCTN1, ERBB4, HNRNPA2B1, SOD2, ZNF746</i>	
	hsa-miR-325-5p			<i>HNRNPA1</i>	
	hsa-miR-764-5p			<i>AGT, PVR, SARM1, SOX5, SPG7, VDR</i>	
	hsa-miR-665-3p			<i>BCL6, CRIM1, DCTN1, DIAPH3, HEXA, KDR, LOX, SLC1A2, SOD2, VDR</i>	
hsa-miR-4277-5p			<i>ALAD, DAO, EPHA4, RNF19A, TARDBP, VAPB</i>		



We noted considerable overlap between miRNAs extracted from plasma/blood/serum with those from CSF (total of 18 of the 22 miRNAs within the CSF group), supporting the notion that circulating miRNAs can provide a window into CSF changes (Ricci, Marzocchi and Battistini, 2018). MiRNAs in the CSF in turn reflect pathological and physiological conditions within the wider CNS, suggesting CNS reflective miRNAs could be measured from the blood/plasma/serum, resulting in a non-invasive procedure to identify biomarkers in ALS patients (Rao, Benito and Fischer, 2013).

Since ALS is a neurodegenerative disorder, those miRNAs dysregulated in patient CSF and spinal cord/nervous tissue were considered of particular interest. Of these 22 miRNAs, miR-125b-2-3p is exclusive to only these two sources. Notably, of the 24 miRNAs found dysregulated in 5 or more of the 27 studies (Table 7), eight overlapped with these 22 CSF-spinal cord/nervous tissue extracted miRNAs. These miRNAs were let-7a-5p, let-7b-5p, let-7f-5p, miR-124-3p, miR-127-3p, miR-28-3p, miR-142-5p and miR-9-5p.

Hsa-miR-124-3p was reported as down-regulated in ALS patients in five studies (Campos-Melo, et al., 2013; Y. Chen et al., 2016; D'Erchia et al., 2017; De Felice et al., 2018b; Emde et al., 2015), with only one study finding it upregulated (Waller, et al., 2017). Despite the caveats to the predictive approach highlighted above, it is notable that this miRNA is predicted to target 13 ALS-relevant targets. MiR-124-3p has also been shown to be deregulated in the spinal cord and brainstem of SOD1 transgenic mice and has been linked to astrocyte differentiation and neurogenesis in the mouse brain (Cheng, et al., 2009; Zhou et al., 2018). Further, hsa-miR-124-3p is found almost exclusively in the brain, spinal cord and associated tissues (Ludwig *et al.*, 2016). In one study, miR-124-3p was shown to directly target *SQSTM1*, promoting autophagy in BV2 cells and reduce apoptosis of neuroblastoma SH-SY5Y cells (Yao *et al.*, 2019). Another study identified increased miR-124-3p expression in NSC-34 cells and their derived exosomes when transfected with SOD1<sup>G93A</sup> mutant compared to wild type SOD1. (Pinto *et al.*, 2017).

Hsa-miR-127-3p was not predicted to target any of the ALS genes and was found almost consistently down-regulated in ALS patients (De Felice *et al.*, 2012; Campos-Melo *et al.*, 2013; Figueroa-Romero *et al.*, 2016; D'Erchia *et al.*, 2017b; Saucier *et al.*, 2018) with only one study reporting its upregulation (Waller, *et al.*, 2017). MiR-127-3p has been shown to cause neuronal loss, neurodegeneration and apoptosis in primary spinal neuronal cells potentially by targeting mitoNEET, a mitochondrial membrane protein (He *et al.*, 2016). Whilst little is reported in relation to ALS, hsa-miR-127-3p has been found deregulated in frontotemporal dementia (FTD) patients compared to control groups and Alzheimer's disease patients (Piscopo *et al.*, 2018). This suggests it may be an FTD-ALS specific miRNA, rather than a general indicator of neurodegeneration. This result is also consistent with a miRNA tissue atlas, which found hsa-miR-127-3p predominantly expressed in brain tissue (Ludwig *et al.*, 2016).

Hsa-let-7a-5p was found downregulated in seven of the ALS patient studies, making it the second most deregulated ALS miRNA (Table 7). It is predicted to target seven of the 154 ALS associated genes, (Table 8). Let-7a-5p has been found downregulated in the plasma of Parkinson's disease patients compared to healthy controls, showing it may not be useful as an ALS specific biomarker (Chen *et al.*, 2018). This same study also found let-7f-5p and miR-142-3p downregulated in the Parkinson's disease samples. These were both miRNAs found in the CNS-spinal cord/nervous tissue crossover that were among the most frequently deregulated miRNAs (Table 7).

The single miRNA unique to the CSF and spinal cord/nervous tissue overlapping group was hsa-miR-125b-2-3p. This miRNA was not one of the top 24 ALS deregulated miRNAs and was found deregulated in three studies (Figueroa-Romero *et al.*, 2016; Waller, Wyles, *et al.*, 2017; De Felice *et al.*, 2018). It was found downregulated by De Felice and colleagues (2018) and Figueroa-Romero and colleagues (2016) whilst Waller and colleagues (2017) found it upregulated in ALS patients compared to controls. This miRNA has been found significantly downregulated in ischaemic stroke patients compared to controls, with high diagnostic accuracy (D.-B. Li *et al.*, 2017).

The only miRNA found deregulated from all four ALS patient source groups was hsa-miR-28-3p. It was one of the top 24 deregulated miRNAs (Table 7), found deregulated in five studies (Campos-Melo *et al.*, 2013; Waller, Wyles, *et al.*, 2017; De Felice *et al.*, 2018; Kovanda *et al.*, 2018; Liguori *et al.*, 2018). All but one study found it downregulated in ALS patients compared to controls (Campos-Melo *et al.*, 2013). It has also been found upregulated in Alzheimer's disease patients and this study also found hsa-let-7a-5p and hsa-let-7f-5p downregulated in Alzheimer's disease patients which suggests that several of these miRNAs may not be ALS specific (Sato, Kino and Niida, 2015).

### 3.2.5 Analysis of Deregulated MiRNAs with Relevance to Autophagy

In the above sections we highlighted specific miRNAs found dysregulated in ALS patient blood/plasma/serum, CSF and spinal cord/nervous tissue which we suggested as appropriate candidates for further study. The 727 miRNAs found dysregulated in ALS patient tissue could also be interpreted by their relevance to biochemical pathways associated with ALS, such as autophagy.

There has been increasing interest in identifying miRNAs with the ability to (dys)regulate autophagy in the context of neurodegenerative disease, in part due to their ability to target multiple genes in a single pathway. Recently, miR-335-5p was reported downregulated in ALS patient serum and its inhibition (effective down-regulation) in SH-SY5Y human neuroblastoma cells lead to abnormal mitophagy (De Luna *et al.*, 2020). Separately, miR-193-3p was found downregulated in a SOD1<sup>G93A</sup> ALS mouse model and by western blotting and microscopy for autophagy markers, its overexpression was shown to inhibit autophagy in NSC-34, motor neurone-like cells with increased p62 levels and decreased LC3-II/I ratio. The authors used the luciferase assay to show miR-193-3p directly targets tuberculosis sclerosis (TSC1) a regulator of mTORC1 (C. Li *et al.*, 2017), which inhibits autophagy during nutrient rich conditions (Kim *et al.*, 2011).

We sought to determine an ALS-patient dysregulated miRNA implicated in autophagy. Firstly, to predict autophagy relevant miRNAs with the aim of cross-

referencing to ALS-relevant miRNAs of interest, the mirPath (v3.0) function of DIANA-Tools (Paraskevoudoulou *et al.*, 2013) was utilised. Using the KEGG reverse search ability, all miRNAs involved in the 'regulation of autophagy' pathway in humans (KEGG pathway: hsa04140) were predicted, with a miTG score threshold set at 0.8. This generated a total of 1017 miRNAs, ordered by the number of autophagy-relevant genes they were predicted to target, with 12 target genes being the highest for a single miRNA.

Next, those miRNAs predicted to target 'regulation of autophagy' relevant genes that were also found deregulated in ALS patients from the 27 studies previously collated, described in section 3.2.1, were determined. These overlapping miRNAs numbered 253 in total (Figure 12A). Overall, one ALS-relevant miRNA was predicted to target seven autophagy relevant genes, six miRNAs were predicted to target six autophagy relevant genes and five miRNAs were predicted to target five autophagy relevant genes (Figure 12B).

Taken together, of the 253 miRNAs that were predicted to target 'regulation of autophagy' relevant genes and were deregulated in ALS patient studies, miR-340-5p was amongst those predicted to target five human autophagy relevant genes – *PIK3C3*, *PRKAA2*, *ATG4C*, *PRKAA1* and *IFNG*. This means that of those 253 miRNAs, only seven miRNAs were predicted to target more autophagy genes than hsa-miR-340-5p (hereafter referred to as miR-340), with four other miRNAs also predicted to target five autophagy genes (Figure 12A). Overall, miR-340 was amongst the top 12 miRNAs predicted to target autophagy genes that was also found dysregulated in ALS patients (Figure 12B).

In addition, we performed further bioinformatic predictions of the gene targets of miR-340, cross-referencing with the 154 ALS related genes obtained from ALSOD as mentioned previously (list obtained 2020). MiR-340 was predicted to target 37/154 ALS related genes, including *TBK1*, which plays a significant role in autophagy through phosphorylating cargo receptors such as p62 (see section 1.2.3). Whilst the 'regulation of autophagy' KEGG pathway includes *TBK1*, the miTG predictive score for miR-340-*TBK1* interaction is below the miTG threshold of mirPath, which was set

to 0.8. Therefore *TBK1* is not included as one of the five autophagy relevant genes predicted to be targeted by miR-340 in this instance. Of the other 252 miRNAs implicated in the 'regulation of autophagy' and dysregulated in ALS patients, an additional 66 were predicted to target *TBK1* (Figure 12A and C). Of these 66, no other miRNA found deregulated in ALS patients was predicted to target more autophagy-relevant genes than miR-340.

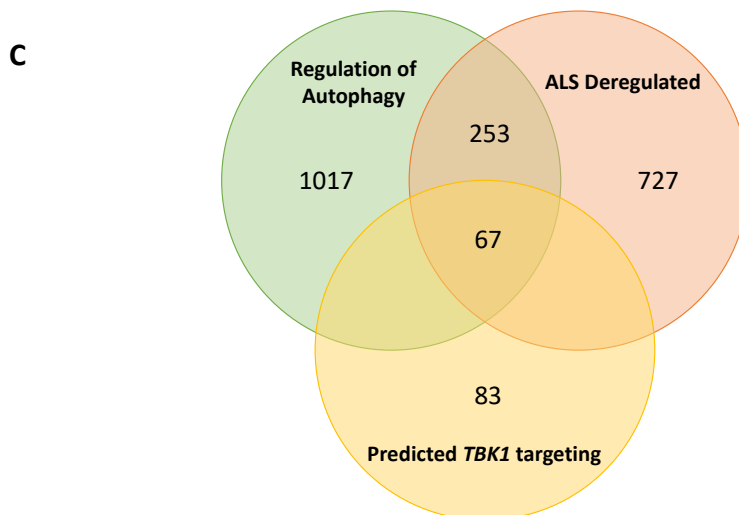
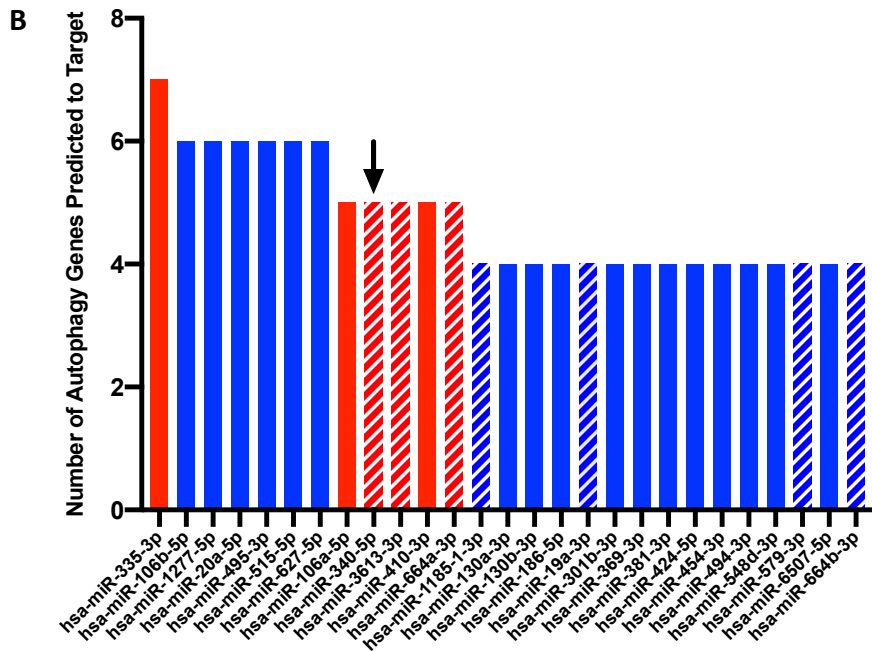
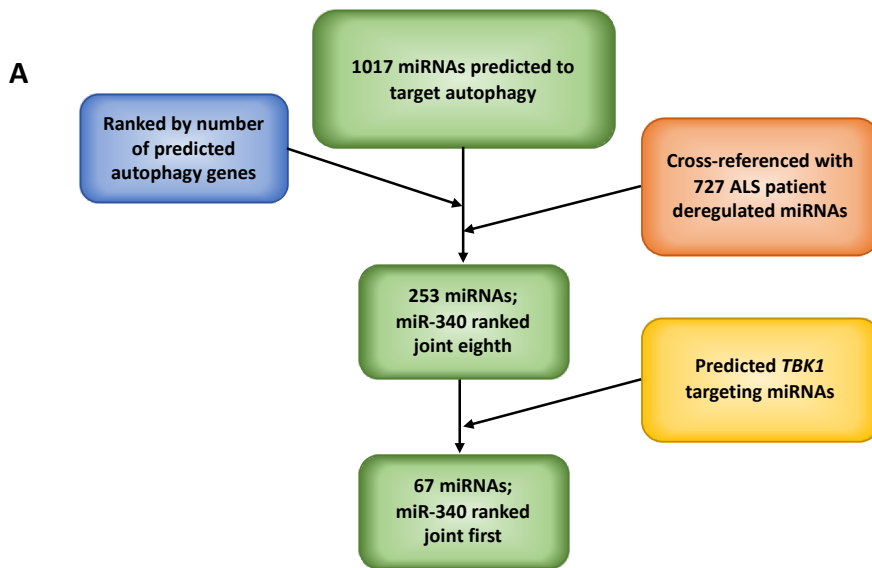


**Figure 12: Bioinformatic processes identified miR-340 as a candidate TBK1-targeting miRNA.** A) Using the mirPath function of DIANA Tools, 1017 miRNAs were predicted to target the autophagy pathway (KEGG pathway: hsa04140) which were ranked by the number of autophagy genes predicted to target, from highest to lowest. Cross-referencing with ALS patient deregulated miRNAs obtained from our previous systematic review (orange box) (Chapter 3) generated 253 miRNAs. The miRNAs were ordered by the total number of autophagy genes each was predicted to target. Of these ordered 253 miRNAs, miR-340 was in joint eighth place. Of those 253 miRNAs, 67 were predicted to target TBK1 with miR-340 ranked joint first (based on numbers of autophagy gene targets). B) After cross-referencing ALS dysregulated miRNAs with those predicted to target autophagy and ordering by the number of autophagy genes predicted to be targeted, miR-340 was in joint eighth place. MiR-340 was predicted to target five autophagy genes, along with four other miRNAs. Only 7/253 miRNAs were predicted to target more. Those miRNAs predicted to target four autophagy genes are also shown, but not those predicted to target three or less. MiRNAs predicted to target TBK1 are shown with dashed bars. C) Venn diagram showing crossover of miRNAs predicted to target the 'regulation of autophagy' pathway with those found dysregulated in ALS patients and those predicted to target TBK1.

MiR-340 was detected as deregulated between healthy controls and ALS patients in three of the studies discussed in section 3.2.1 (Campos-Melo *et al.*, 2013; De Felice *et al.*, 2018; Raheja *et al.*, 2018). Raheja *et al.* (2018) found it downregulated in ALS patient blood serum vs healthy controls. Campos-Melo *et al.* (2013) also found it downregulated though in ALS patient spinal cords. In contrast, De Felice *et al.* (2018) found it upregulated in ALS neuromuscular junction compared to healthy control blood. The identification of miR-340 dysregulation in patient blood samples could allow easy and non-invasive sample collection and monitoring from ALS patients.

In addition, miR-340 has also previously been shown to target *NFE2L2*, the gene encoding NRF2, a protein strongly implicated in ALS pathogenesis, and functions within the same pathway as TBK1, which is discussed in section 4.1.4.2. This gene is not included in the 'regulation of autophagy' pathway and the miTG score generated by DIANA Tools is below that considered as strongly predictive of gene targeting (0.7), though does not discount biological relevance (Table 9). Further, miR-340 was one of only three miRNAs showing altered expression between neuronal axon and soma compartments in both a TDP-43<sup>A315T</sup> and SOD1<sup>G93A</sup> ALS mouse model (Rotem *et al.*, 2017). Recent quantitative small non-coding RNA sequencing of whole cell,

axon and exosomes of rat primary neurones also revealed miR-340 was consistently one of the most abundant 80 miRNAs detected (Mesquita-Ribeiro *et al.*, 2021). Only four other miRNAs are predicted to target both *NFE2L2* and *TBK1* that were also found dysregulated in ALS patients in our systematic literature review (section 3.2). These are miR-16-1-3p, miR-369-3p, miR-33a-3p and miR-770-5p.

**Table 9: MiTG scores (predicted likelihood of gene targeting) of *TBK1* and *NFE2L2*.** Scores generated from DIANA Tools, with a threshold of >0.70 considered to be strongly predictive of gene targeting, although lower scores may still be biologically relevant (e.g., *NFE2L2* is an experimentally verified target of miR-340 with predicted score only 0.66). Number of studies out of 27 relates to the number of different ALS biomarker analyses (from a total of 27) considered that reported expression changes in the given miR-340 in the ALS patient cohort compared to controls.

miRNA	Number of Studies out of 27	<i>TBK1</i> miTG Score	<i>NFE2L2</i> miTG Score
hsa-miR-340-5p	3	0.79	0.66

The role of miR-340 in a further neuronal context has previously been investigated. For example, overexpression of miR-340 in a rat model of sciatic nerve crush injury resulted in reduced Schwann cell migration ability and decreased axonal growth. These effects were a result of the direct targeting of tissue plasminogen activator by miR-340 (S. Li *et al.*, 2017). Further, in a model of Alzheimer’s disease (whereby SH-SY5Y human neuroblastoma cells were transfected with a mutant form of amyloid precursor protein), miR-340 was found to reduce the accumulation of amyloid  $\beta$  through targeting  $\beta$ -site amyloid precursor protein cleaving enzyme 1 (BACE1) (Tan *et al.*, 2020). These studies add confidence that miR-340 functions with neuronal relevance and support our selection of miR-340 as an ALS-relevant candidate suitable for further analysis.

### 3.3 Conclusions and Future Directions

We have shown that miRNAs found dysregulated in published studies investigating ALS patients have limited overlap, with 727 found dysregulated in ALS patients compared to controls. This is likely due to the wide variation in tissue extraction and miRNA detection methods used. Future emphasis should centre on standardising tissue extraction and miRNA profiling methods.

However, we identified 24 miRNAs reported as dysregulated in at least 5 of the 27 studies. Despite the top nine deregulated miRNAs being commonly predicted to target ALS-associated genes, a group of randomly selected miRNAs not found dysregulated in ALS patients, showed similar enrichments. However, those in the latter group were still predicted to target 34 ALS-associated genes compared to 46 in the former group, out of a possible 154 genes. As such, our *in silico* analysis did not demonstrate a clear correlation between deregulated miRNAs and ALS-relevant genes reported on ALSOD. This indicates that though predicting thousands of candidate genes with *in silico* methods is informative, they should be used alongside experimental functional testing. Our observations may also be explained by limitations of the available bioinformatics approach.

We have additionally shown that, since only one dysregulated miRNA appeared in all tissue sources analysed (miR-28-3p), the patient tissue source has a significant impact on the miRNAs detected and demonstrates that miRNAs are not ubiquitously expressed. Importantly, we have shown that many of the miRNAs most frequently reported as dysregulated appear in CSF, spinal cord/nervous tissue and blood/plasma/serum. This suggests miRNAs can transfer between CSF and blood, and the latter may provide a clinically accessible source which may mirror ALS pathology in the CNS. We therefore identified miRNAs such as let-7a-5p, let-7b-5p, let-7f-5p, miR-124-3p, miR-127-3p, miR-28-3p, miR-142-5p and miR-9-5p as good candidates for further study. Alternatively, the 727 miRNAs found dysregulated in ALS patient tissue could also be interpreted by their relevance to biochemical pathways associated with ALS, such as autophagy.

We next presented a stringent bioinformatic approach to refine the 727 miRNAs dysregulated in ALS patients, to determine a subset with additional relevance to autophagy. Finally, we selected miR-340 as a candidate miRNA for functional testing, due to its *TBK1* target prediction. We noted that miR-340 is additionally known to target NRF2, a protein which functions in the same pathway as TBK1 and is also implicated in ALS pathogenesis.

Overall, we have demonstrated the need for a broad approach, which utilises patient data and bioinformatic predictions. Most critically, the approach should contain experimental follow-up, to resolve the significance of these ALS– implicated miRNAs. In Chapter 4, we functionally assess the impact of miR-340 on autophagy and on autophagy-relevant downstream pathways and proteins.

# Chapter 4 - Investigation of ALS-Relevant miR-340 as a Regulator of Autophagy

## 4.1 Introduction

In Chapter 3, 727 miRNAs were collated that were found either over or under-expressed across 27 different biomarker studies of ALS patient samples compared to controls. Bioinformatic approaches were applied to prioritise one of these 727 miRNAs, miR-340, as a candidate of interest with respect to (de)regulation of autophagy.

In the following chapter an experimental investigation of its role in this pathway of relevance to ALS is conducted. We identify potential new gene targets through which miR-340 might exert its biological effects, with emphasis on ALS and autophagy-relevant downstream impacts of this miRNA.

### 4.1.1 The miR-340 Gene

MicroRNA-340 was first identified in rat primary cortical neurons in 2004, where isolation and sequencing of RNAs 20-25 nucleotides in size, identified 40 previously unreported miRNAs (Kim *et al.*, 2004). The human miR-340 gene is located within the second intron of the *RNF130* gene, located on chromosome 5q:35.3 and consistent with its intronic localisation, the expression of miR-340 correlates with that of *RNF130*, an E3 ubiquitin ligase. MiR-340 is largely conserved amongst mammals (Figure 13). The predominant mature miRNA is the 5' version and the mature hsa-miR-340 sequence is shown in red in Figure 13.

Capra	GTT-TGTACCTGGTGTGATTATAAAGCAATGAGACTGATTGTCATGTGTC
Equus	GG-----TTATAAAGCAATGAGACTGATTGTCATGTGTC
Homo	TT---GTACCTGGTGTGATTATAAAGCAATGAGACTGATTGTCATATGTC
Macaca	TT---GTACCTGGTGTGATTATAAAGCAATGAGACTGATTGTCATATGTT
Mus	CAATTGTACTTGGTGTGATTATAAAGCAATGAGACTGATTGTCATATGTC
Oryctolagus	TT-----ATAAAGCAATGAGACTGATTGTCATATGTT
Rattus	CACTTGTACTCGGTGTGATTATAAAGCAATGAGACTGATTGTCATGTGTC
	***** **
Capra	GTTTGTGGGATCCGTCTCAGTTACTTTATAGCCATACCTGGTATCTTATA
Equus	GCTTGTGGGATCCGTCTCAGTTACTTTATAGC-----
Homo	GTTTGTGGGATCCGTCTCAGTTACTTTATAGCCATACCTGGTATCTT---
Macaca	GTTTGTGGGATCCGTCTCAGTTACTTTATAGCCATACCTGGTATCTT---
Mus	GTTTGTGGGATCCGTCTCAGTTACTTTATAGCCATACCTGGTATCTT---
Oryctolagus	GTTTGTGGGATCCGTCTCAGTTACTTTATAGC-----
Rattus	GTTTGTGGGATCCGTCTCAGTTACTTTATAGCCATACCTGGTATCTT---
	* * *****
Capra	CCACAGA
Equus	-----C
Homo	-----A
Macaca	-----A
Mus	-----A
Oryctolagus	-----C
Rattus	-----A

**Figure 13: T-coffee alignment showing conservation of mammalian miR-340-5p gene sequences.** Species include *Homo sapiens* (human), *Mus musculus* (mouse), *Ratus norvegicus* (rat), *Macaca mulatta* (Rhesus monkey), *Capra hircus* (goat), *Oryctolagus cuniculus* (rabbit) and *Equus caballus* (horse). Asterisk indicates nucleotides conserved among all species shown. In red and underlined is the mature human *hsa-miR-340-5p* sequence. All sequences are shown 5'-3'.

#### 4.1.2 Established Gene Targets of hsa-miR-340

According to miRTarBase (release 8.0), over 470 target genes of miR-340 have been identified. Table 10 contains a list of those functionally confirmed using luciferase reporter assays, qRT-PCR, immunohistochemistry, immunocytochemistry and/or western blotting taken from miRTarBase (release 8.0) (Chou *et al.*, 2018). Targets experimentally validated using photoactivatable ribonucleoside-enhanced crosslinking and immunoprecipitation (PAR-CLIP), high-throughput sequencing of RNA isolated by crosslinking immunoprecipitation (HITS-CLIP) or sequencing alone have not been included in Table 10. Of genes targets of miR-340 included in Table 10, *HNRNPA2B1* is associated with ALS (Kim *et al.*, 2013).

**Table 10: Known targets of hsa-miR-340-5p. A) Targets confirmed using at least one of the following methods: luciferase reporter assay, qRT-PCR, immunohistochemistry, immunocytochemistry and western blotting. Information obtained from MiRTarBase (release 8.0). All targets shown are Homo sapien. B) Known targets of miR-340 not reported on MiRTarBase for unknown reasons, confirmed with same criteria as (A).**

Target	Method	Function	Target	Method	Function
AKT1	Immunohistochemistry, Luciferase reporter assay, qRT-PCR, Western blot	Encodes the serine-threonine protein kinase B-1. Is a known oncogene. Regulates proliferation, angiogenesis and cell survival.	PUM1	Luciferase reporter assay, qRT-PCR, Western blot	Encodes an RNA binding protein that adds to the 3'UTR of mRNAs to regulate their translation. May have a role in cell development and differentiation.
CCND1	qRT-PCR, Western blot	Encodes cyclin D1, one of three homologues of cyclin D, which regulates cyclin dependent kinases. It has a crucial role in the G1/S transition of the cell cycle.	PUM2	Immunoprecipitation, Luciferase reporter assay	Encodes an RNA binding protein that adds to the 3'UTR of mRNAs to regulate their translation. Aids miRNA translational repression
CCND2	qRT-PCR, Western blot	Encodes cyclin D2, one of three homologues of cyclin D, which regulates cyclin dependent kinases. It has a crucial role in the G1/S transition of the cell cycle.	RHOA	Luciferase reporter assay, qRT-PCR, Western blot	Encodes Rho GTPase and facilitates cytoskeletal reorganisation to regulate cell shape and motility.
CCNG2	Luciferase reporter assay, qRT-PCR, Western blot	Encodes cyclin G2 which is involved in regulation of the cell cycle.	ROCK1	Immunohistochemistry, Luciferase reporter assay, qRT-PCR, Western blot	Encodes Rho associated coiled-coil associated protein kinase 1. Involved in regulating actin cytoskeleton and smooth muscle contraction.
CDK6	Luciferase reporter assay, qRT-PCR, Western blot	A catalytic unit of a complex formed with cyclin proteins to regulate the G1/S transition of the cell cycle.	SKP2	Western blot	Encodes a subunit of the E3 ubiquitin ligase complex, SKP-cullin-F-box, which mediates ubiquitination of proteins and their subsequent degradation.
HNRNPA2B1	Luciferase reporter assay, qRT-PCR, Western blot	Has a role in miRNA biogenesis and the packing and transport of mRNA. hnRNP A1 is involved in the recognition of splice sites on mRNA .	SOX2	Luciferase reporter assay, qRT-PCR, Western blot	Encodes SRY-box transcription factor 2. Crucial for embryonic development, including embryonic stem cell pluripotency
IL4	Luciferase reporter assay, qRT-PCR, Western blot	Encodes interleukin 4, a cytokine produced by activated T-cells. This protein mediates a variety of human host responses including acute inflammation and allergic reactions.	STAT3	Luciferase reporter assay, qRT-PCR, Western blot	Encodes signal transducer and activator of transcription 3. It is activated by JAK phosphorylation in response to a range of cytokines growth factors and mediates expression of an array of genes.
KRAS	Luciferase reporter assay, qRT-PCR, Western blot	Encodes an oncogenic small GTPase. A single amino acid missense mutation is responsible for its activation and it silences tumour suppressor genes.	NFE2L2	Luciferase reporter assay, qRT-PCR, Western blot	Encodes NRF2 which regulates the expression of antioxidant response element genes during exposure to oxidants.
MDM2	Luciferase reporter assay, qRT-PCR, Western blot, Microarray	Encodes a nuclear E3 ubiquitin ligase which can target tumour suppressor proteins such as p53 for proteasomal degradation, thus promoting tumour formation.	NFkB1	Luciferase reporter assay, Western blot	Encodes the Nfkb1 105 kDa subunit which can be processed into a 50 kDa subunit by the proteasome. Nfkb1 is a transcription factor activated by numerous signals such as cytokines and viral products. It upregulates over 200 genes and dysfunction is associated with inflammatory diseases.
MECP2	Luciferase reporter assay, qRT-PCR, Western blot	Encodes methyl CpG binding protein 2 which can bind methylated DNA and repress transcription	FHL2	qRT-PCR	Encodes four and a half LIM domains 2 and may function in the assembly of plasma membranes and contribute to cell growth.
MET	Luciferase reporter assay, qRT-PCR, Western blot	Receptor binding activates several pathways including the STAT and NOTCH pathways.	ANXA3	Luciferase reporter assay, qRT-PCR and Western blot	Encodes a member of the annexin family which inhibits phospholipase 2 and is involved in anti-coagulation.
MITF	Luciferase reporter assay, qRT-PCR, Western blot	Encodes a transcription factor that is involved in melanocyte development.	c-Met	Luciferase reporter assay, qRT-PCR and Western blot	Encodes the tyrosine-kinase receptor, MET. Receptor binding activates several pathways including the STAT and NOTCH pathways.
PTBP1	Luciferase reporter assay, qRT-PCR, Western blot	Is a heterogenous nuclear ribonucleoprotein which bind RNA and has a role in pre-mRNA splicing.	PDCD4	Luciferase reporter assay	Encodes programmed cell death protein 4 (PDCD4). Functions as a tumour suppressor which prevents translation initiation and cap-dependent translation. May function by inhibiting the interaction between EIF4A1 and EIF4G.

### 4.1.3 Known functions of miR-340

The majority of current research related to miR-340 (as for many miRNAs) relates to cancer biology. For example, miR-340 was found decreased in ovarian cancer cell lines and its overexpression inhibited cell proliferation and invasion and induced apoptosis in two ovarian cancer cell lines. The authors demonstrated that these effects were mediated through direct targeting of miR-340 with *NFκB1* with overexpression of this transcription factor overcoming the inhibitory effect of miR-340 on proliferation and invasion (Liu, Li and Sun, 2016).

In another study focussed on ovarian cancer, miR-340 was also found downregulated and to target *FHL2*. At low levels of miR-340, a subsequent increase in FHL2 (four and a half LIM domains 2) protein was found to be associated with lower patient survival (Huang *et al.*, 2019). Overexpression of miR-340 was then found to reduce FHL2 protein and decrease colon cancer cell migration and invasion (Algaber *et al.*, 2021). The effect of miR-340 on cell survival was also observed in a study on colorectal cancer, where patients with lower levels of miR-340 had lower predicted overall survival and were associated with lymph node metastasis and histological grade. Overexpression of miR-340 levels inhibited colorectal cancer cell proliferation and migration through directly targeting *ANXA3* (L. Yang *et al.*, 2018).

miR-340 has also been found to target oncogenes such as *ROCK1*. Here, the authors observed downregulation of miR-340 in patients with glioblastoma multiforme and restoration of miR-340 levels inhibited glioma cell proliferation. The authors identified *ROCK1* as a target of miR-340 and found silencing of *ROCK1* mirrored the protective effects of miR-340 overexpression (Huang *et al.*, 2015).

Further, miR-340 was found significantly reduced in breast cancer tissues compared with benign disease tissues and miR-340 overexpression suppressed breast cancer MCF-7 cell migration and invasion, whilst miR-340 inhibition reversed these effects (Wu *et al.*, 2011). The authors subsequently showed, using western blotting and the luciferase assay, that miR-340 directly targets the oncoprotein c-Met, which is often overexpressed in cancer (Kong *et al.*, 2009; Wu *et al.*, 2011). Further, the authors

found that reduction of miR-340 was correlated with lymph node metastasis and that patient's whose tumours expressed miR-340 experienced longer overall survival than patients whose tumours did not (Wu *et al.*, 2011).

Reduced expression of miR-340 has been linked to worsened severity of osteoporosis. The authors found miR-340 was downregulated during osteoclast formation and this was confirmed in a mouse model of osteoporosis. Importantly, miR-340 was found further decreased in older mice, indicating the decrease of miR-340 was linked to osteoporosis progression (Ma *et al.*, 2016).

More recent work of relevance to this thesis, has identified a potential neuroprotective effect of miR-340 in a rat model of ischemia stroke/reperfusion injury using oxygen glucose deprivation/reoxygenation. The authors observed reduced expression of miR-340 in neurones following injury and a decreased cell viability. Conversely, overexpression of miR-340 rescued cell viability whilst inhibition of miR-340 reduced cell viability further. The authors used the dual luciferase assay to find miR-340 directly targeted *PDCD4*, which was increased during ischemia injury and was able to reverse the neuroprotective effect of miR-340 (Zheng *et al.*, 2020). It has similarly been observed that in a rat model of spinal cord injury, miR-340 was found reduced and overexpression of miR-340 reduced microglia inflammation by targeting the gene, *MAPK14*, which encodes p38 (Qian *et al.*, 2020).

Taken together these studies indicate that in instances of cancer, as well as other disease models such as osteoporosis and ischemic stroke, overexpression of miR-340 can provide cellular protection.

In contrast, Zhu and colleagues identified miR-340 as the most upregulated miRNA in myocardial biopsy samples from patients with end stage heart failure compared to healthy controls (Zhu *et al.*, 2013). Subsequently, miR-340 inhibition was shown to reduce signs of hypertrophy. MiR-340 was found to target *DMD*, a gene encoding a structural protein present in cardiomyocytes which protects cells from shearing during contraction (Zhou *et al.*, 2015).

Overexpression of miR-340 has also been observed in thyroid cancer, and cells with higher pathological grade exhibited higher miR-340 expression. Indeed, inhibition of miR-340 reversed this effect and inhibited tumour growth in a xenograph mouse model of thyroid cancer (Zhao *et al.*, 2018).

These contrasting results demonstrate a negative role of miR-340 in health and disease and indicate that whilst miR-340 appears to be protective (largely in the cancer context), in other diseases and health conditions, it is often associated with poorer health.

#### 4.1.4 NRF2

Nuclear factor erythroid 2-related factor 2 (NRF2) is a member of the cap and collar transcription factor family with basic region leucine zipper factor family (cnc-bZip). It is ubiquitously expressed and redox sensitive and has been implicated in both autophagy and ALS. The major roles of NRF2 include defence against oxidative stress whereby it activates anti-oxidant genes through the NRF2-ARE pathway, in particular in astrocytes, protecting against neurodegeneration. NRF2 is encoded by the gene *NFE2L2*. This gene is a known target of miR-340, first confirmed in a human cell line in 2014 (Shi *et al.*, 2014).

##### 4.1.4.1 NRF2 Signalling

The NRF2 protein is functionally classified into seven ECH (erythroid cell derived protein with CNC homology with chicken nrf2) homology domains, Neh1 – Neh7. During basal conditions, two molecules of Kelch ECH associating protein (KEAP1) form a homodimer and bind NRF2 within its Neh2 domain, at the low affinity DLG and high affinity ETGE motifs (Zipper and Timothy Mulcahy, 2002; Furukawa and Xiong, 2005; Tong *et al.*, 2006, 2007). Through its BTB domain, KEAP1 can also bind the ubiquitin ligase, Cullin-3 (Cul-3) which ubiquitinates lysine residues within NRF2 and targets it for proteasomal degradation (Zhang and Hannink, 2003; Furukawa and Xiong, 2005). During these conditions, NRF2 has a half-life of just 20-30 minutes, ensuring relatively low cellular levels of NRF2 (Kobayashi *et al.*, 2004).

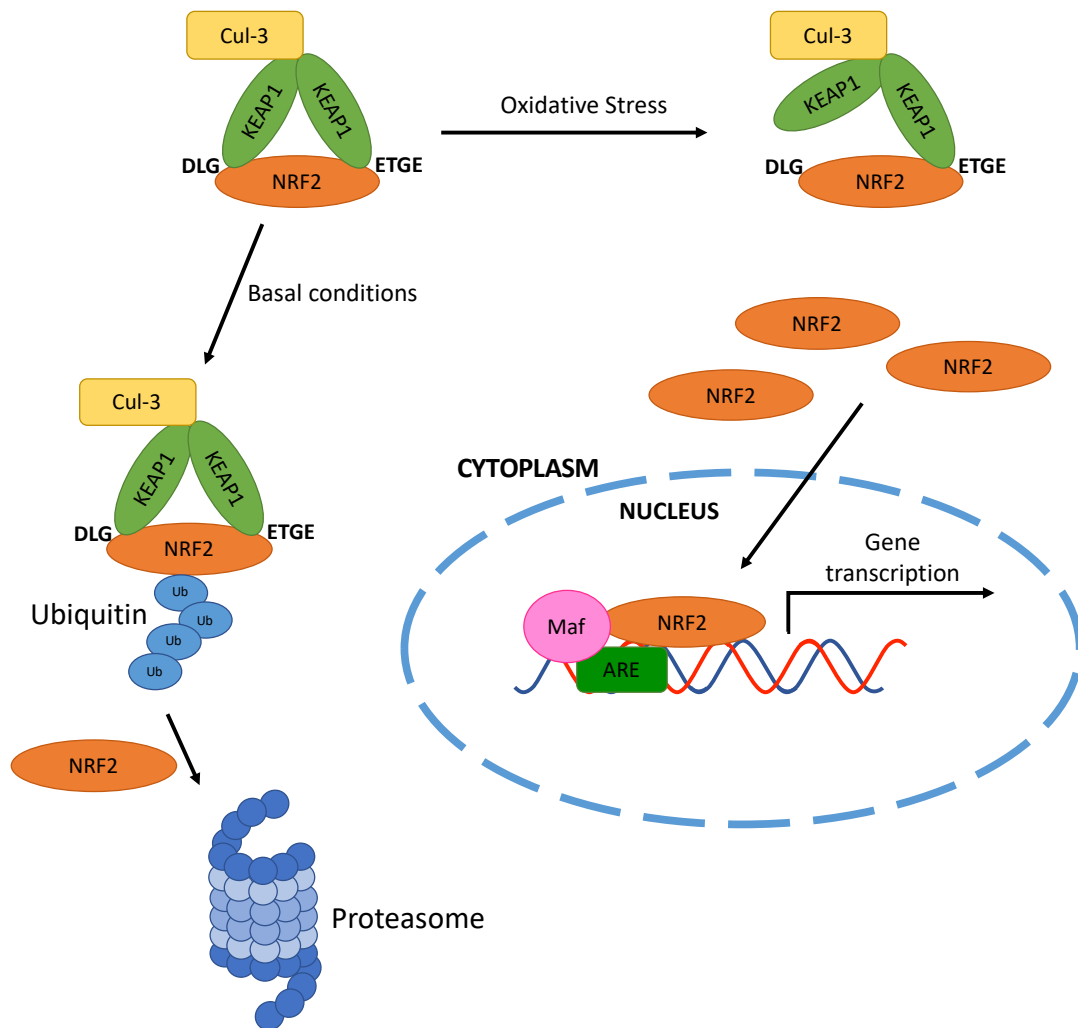


**Figure 14: Diagrammatic representation of the KEAP1:NRF2 pathway.** A KEAP1 homodimer binds NRF2 at the DLG and ETGE domains as well as to Cul-3 ubiquitin ligase. During basal conditions, Cul-3 ubiquitinates NRF2 and targets it for proteasomal degradation. During oxidative stress, the weaker interaction between KEAP1 and NRF2 at the DLG site is disrupted by a conformational change and NRF2 is no longer ubiquitinated and degraded by the proteasome. Instead, NRF2 is free to translocate to the nucleus where it binds Maf proteins and to ARE and induces transcription of ARE target genes. Drawn by author.

KEAP1 is composed of five regions and through oxidation of cysteine residues within its intervening domain (IVR), KEAP1 is a sensor of electrophiles and oxidative stress (Sekhar, Rachakonda and Freeman, 2010). This oxidation causes KEAP1 to undergo a conformational change which disrupts the KEAP1-NRF2 interaction at the weaker DLG binding site and stabilises the NRF2 protein. This prevents ubiquitination and proteasomal degradation of NRF2 and facilitates active NRF2 translocation to the nucleus (Tong *et al.*, 2007). Here, it binds to small musculoaponeurotic fibrosarcoma

(Maf) proteins and then to the antioxidant response element (ARE) within various gene targets. This promotes transcription of oxidation and reduction factors, conjugation enzymes and efflux transporters, antioxidants such as glutathione, phase II detoxifying enzymes and anti-inflammatory molecules (Itoh *et al.*, 1997) (Figure 14). The ARE nucleotide sequence is 5'-(G/A)TGA(G/C)XXXGC(G/A)-3' where X is any nucleotide. As expected, KEAP1 knockout mice exhibit Nrf2 accumulation in the nucleus and increased expression of phase II detoxifying enzymes (Wakabayashi *et al.*, 2003). Interestingly, human *NFE2L2* contains two ARE-like sequences in its promoter, allowing NRF2 to induce its own expression and autoregulate itself (Kwak *et al.*, 2002).

#### 4.1.4.2 Pathway Overlap of NRF2 and TBK1

Phosphorylation of p62 at Ser-403 by the ALS-associated kinase TBK1 results in its translocation and binding to ubiquitinated cargo. Here, phosphorylation by mTORC1 at Ser-349 occurs, and this phosphorylated p62 competes for the interaction with KEAP1 and leads to autophagic degradation of KEAP1 and the activation of NRF2 (Figure 15) (Copple *et al.*, 2010; Komatsu *et al.*, 2010; Ichimura *et al.*, 2013; Ishimura, Tanaka and Komatsu, 2014). Additionally, TBK1 has also been shown to phosphorylate p62 at Ser-349, implicating TBK1 directly in the regulation of NRF2 activation (Foster *et al.*, 2020).

NRF2 is also able to activate the expression of several autophagy related genes including those which encode ULK1, ATG2B, ATG4D, ATG5, ATG7, ATG10, ATG16L1, GABARAPL1, NDP52 and p62 (Jain *et al.*, 2010; Pajares *et al.*, 2016). The autophagy receptor, NDP52, was shown to recruit TBK1 during autophagy, which indicates a potential positive feedback loop between NRF2-mediated increased expression of p62 and NDP52, to promote continued NRF2 activation (Thurston, 2009).

ALS-relevant TBK1 mutations (R47H, R357Q and M559R) have been shown to reduce Ser-403 phosphorylation of p62, whilst mutations in the CCD2 domain of TBK1 did not impede p62 phosphorylation (Deng *et al.*, 2019). Additionally, ALS-relevant p62 mutations (G427R, P348L and G351A) have been shown to reduce the activation of

NRF2 (Goode, Rea, *et al.*, 2016; Deng *et al.*, 2019). Collectively, this evidence suggests aberrant TBK1 function may contribute to ALS pathogenesis through reduced phosphorylation of p62 and subsequent disruption in NRF2 signalling.

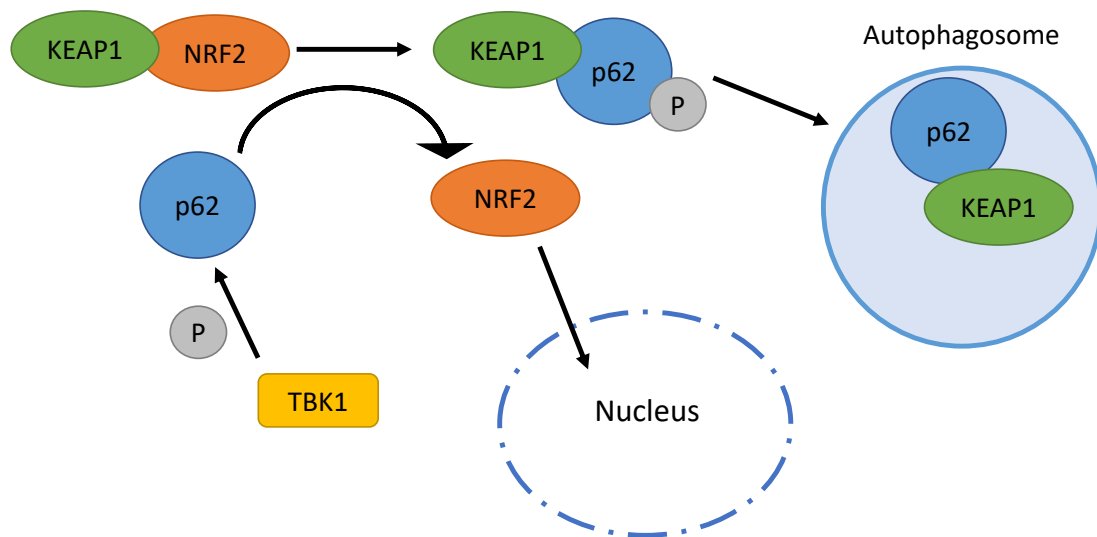


**Figure 15: Diagrammatic representation of the relationship between TBK1 and NRF2 signalling.** TBK1 phosphorylates p62 at Ser-403 which results in the competition of p62 for the interaction with KEAP1 and causes autophagic degradation of phosphorylated p62 and KEAP1, whilst NRF2 is activated. P= phosphorylation event. Drawn by author.

#### 4.1.4.3 NRF2 and ALS

In the 1990s it was observed that sporadic ALS patients exhibited significantly greater levels of protein carbonyl groups (an indication of oxidative damage) within their lumbar spinal cords than controls (Shaw *et al.*, 1995). Oxidative stress is now considered a hallmark of ALS, though it is unclear whether oxidative stress is a cause or consequence of the disease. In 2008 it was reported that NRF2 mRNA and protein levels were reduced in post mortem ALS patient spinal cord and brain (Sarlette *et al.*, 2008). Further, NRF2 overexpression in ALS mutant hSOD1<sup>G93A</sup> mouse astrocytes increased mice survival and delayed disease onset, and the NRF2 overexpression in hSOD1<sup>G93A</sup> expressing astrocytes was found to protect cocultured motor neurons from the toxicity of hSOD1 (Vargas *et al.*, 2008). Survival of hSOD1<sup>G93A</sup> mice was not affected by overexpression of NRF2 in neurones and muscle suggesting the protective role of NRF2 is astrocyte specific (Vargas *et al.*, 2013). Further, knockout

of NRF2 in hSOD1<sup>G93A</sup> mice resulted in earlier disease onset and increased astrocyte proliferation (Guo *et al.*, 2013).

NRF2 is a prominent regulator of antioxidants such as glutathione (GSH), which it regulates by controlling the expression of the two enzymes which synthesise it - glutathione synthetase and glutamate-cysteine ligase (Moinova and Mulcahy, 1999; Wild, Moinova and Mulcahy, 1999). Further, the transcription of other ROS detoxifying genes is controlled by NRF2, including glutathione peroxidase 2, which enables glutathione to donate electrons to reactive oxygen species (Singh *et al.*, 2006). SOD1<sup>G93A</sup> astrocytes treated with the NRF2 inducer, tBHQ, increased the production and release of glutathione and prevented motor neurones from undergoing apoptosis. This protective effect was abolished when glutathione synthesis and release by astrocytes was inhibited (Vargas *et al.*, 2006). In addition, nitro fatty acids were shown to prevent SOD1<sup>G93A</sup> astrocyte toxicity to motor neurons and depended on NRF2 (Diaz-Amarilla *et al.*, 2016). Further, prevention of nuclear import of NRF2 increases cell vulnerability to ROS in ALS, since the RNA-binding protein 45 (RBM45) translocates to the cytoplasm during oxidative stress and stabilises KEAP1, leading to a reduction of active NRF2, resulting in reduced production of antioxidants (Bakkar *et al.*, 2015). The ALS relevant p62<sup>G427R</sup> mutation was shown to reduce NRF2 signalling and extended to increase TDP-43 stress granule formation and impair dendrite complexity in neurones (Deng *et al.*, 2020).

Activation of NRF2 is believed to be part of the mechanism of action of Edaravone, an FDA approved ALS drug (though not approved for use in the UK) (D. Zhang *et al.*, 2018; Y *et al.*, 2019). Indeed, there are a variety of NRF2 activators with clinical trials currently underway for a range of diseases besides ALS, such as prostate cancer, psoriasis and the neurodegenerative disease, multiple sclerosis. The NRF2 activators in clinical trials include electrophilic compounds, cyanoenone triterpenoids, fumaric acid esters, hydroxylamine, nitro fatty acids, sulforaphane, and p62 activators, recently reviewed by Bono and colleagues (Bono, Feligioni and Corbo, 2021). Cyanoenone triterpenoids and fumaric acid esters function by reacting with C515 in KEAP1, disrupting the KEAP1-Cul-3 interaction and subsequently reducing the

ubiquitination and proteasomal degradation of NRF2. One particular fumaric acid ester, DMF, was FDA approved in 2014 for the treatment of multiple sclerosis.

#### 4.1.5 STING Signalling

Recently, it was discovered the cyclic GMP-AMP synthase (cGAS)-STING (stimulator of interferon genes) pathway is also implicated in ALS (Yu *et al.*, 2020). cGAS is a DNA sensor, crucial to the response against bacterial and viral infections and binds cytoplasmic DNA (such as viral or mitochondrial), which activates the second messenger cGAMP (Sun *et al.*, 2013; Wu *et al.*, 2013). cGAMP binds dimers of the ER transmembrane STING, leading to its activation (Zhang *et al.*, 2013). STING then binds TBK1 and the transcription factor IRF3, by first trafficking from the ER to the ER-Golgi intermediate compartment (ERGIC) where it oligomerises with TBK1 and causes TBK1 phosphorylation and activation (Ishikawa, Ma and Barber, 2009; Tanaka and Chen, 2012). In this conformation, TBK1 phosphorylates neighbouring STING proteins and IRF3, to induce the transcription of type 1 interferons (Figure 16) (Liu *et al.*, 2015; C. Zhang *et al.*, 2019).

In addition, NRF2 has been identified as a repressor of STING, by decreasing STING mRNA stability, leading to reduced protein levels. As a result of this, in response to cytosolic DNA, silencing NRF2 with siRNA caused an increase in phosphorylated TBK1 levels, as NRF2 repression of STING was abolished (Figure 16) (Olagnier *et al.*, 2018).

Further, stimulation of STING by cytosolic DNA induced autophagy, by increasing the conversion of LC3-I to LC3-II, measured by western blotting. Inhibition of autophagy also prevented degradation of STING, suggesting STING degradation occurs *via* autophagy, since inhibition of the proteasome afforded no impact on STING levels (Figure 16). The authors of this study also observed p62 colocalised with STING and that in cells without p62, STING was unable to traffic to autolysosomes. STING was also not degraded in cells deficient of TBK1. Taken with the finding that stimulation with DNA increased TBK1 phosphorylation of p62 at Ser-403, but not in TBK1 knockout cells, the data strongly suggest that TBK1 phosphorylation of p62 is necessary for autophagic degradation of STING upon cytosolic DNA stimulation (Prabakaran *et al.*, 2018).

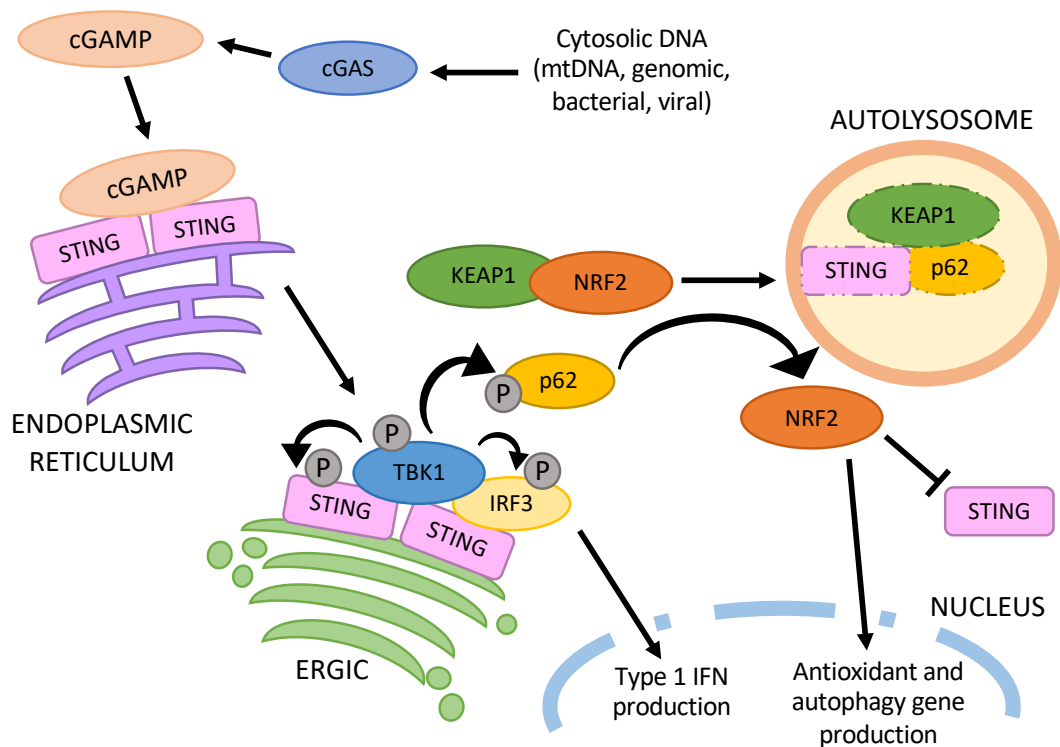


**Figure 16: Diagrammatic representation of the STING pathway.** cGAS is stimulated by cytosolic DNA and synthesises the second messenger, cGAMP. cGAMP binds two molecules of STING present on the ER and results in the translocation of STING to the ERGIC. Here, TBK1 is recruited and activated and binds STING and IRF3, phosphorylating both. Active IRF3 increases the production of type 1 IFNs. TBK1 also phosphorylates p62 which leads to the release of active NRF2 which increases the expression of antioxidant and autophagy genes and reduces the protein levels of STING. p62, STING and KEAP1 are degraded by autophagy. Drawn by author.

#### 4.1.5.1 *STING and ALS*

Recently, a study by Yu and colleagues placed STING among those proteins implicated in ALS (Yu *et al.*, 2020). In response to overexpression of ALS associated mutant TDP-43 (A315T or Q331K), mitochondrial DNA (mtDNA) was released into the cytoplasm, and the DNA sensing cGAS became active and bound this mtDNA and activated STING (Wang *et al.*, 2016; Yu *et al.*, 2020). The heterozygous ALS mutant TDP-43<sup>A315T</sup> mice deficient for STING experienced a 40% extended life time compared to ALS mutant TDP-43 mice possessing both STING alleles. Interestingly, deletion of a single allele of STING still extended their life span though not to the same extent as double allele deletion mice. This is potentially due to the reduction in TBK1 activated by STING and therefore a reduction in type 1 IFNs and neuroinflammation. Indeed, the double STING deletion mice exhibited reduced neurodegeneration and neuroinflammation, measured by inflammatory type 1 INF and *NFκB* levels in ALS patient iPSC-derived motor neurones (Yu *et al.*, 2020). Critically, the authors used a STING inhibitor molecule, H-151 which reduced motor neurone death of iPSCs and appeared to prolong disease progression in mutant TDP-43 mice.

#### 4.1.6 Experimental Aims

In Chapter 3 we reported hundreds of miRNAs previously found dysregulated in ALS patients, and these miRNAs can be further grouped based on their implication in pathways of relevance to ALS, such as autophagy. We previously selected miR-340 as a candidate for experimental evaluation based in its dysregulation in ALS patients and implication in the autophagy pathway. We hypothesised that miR-340 would directly target TBK1, a protein crucial to autophagic function and that overexpression of miR-340 would therefore impair autophagic flux. We also hypothesised that miR-340 overexpression could affect protein levels downstream of TBK1 function.

The overall aim of the work presented in this chapter was to elucidate the potential involvement of miR-340 in autophagy and its impact on proteins of relevance to this pathway, through which it might impact ALS pathogenesis. To achieve this, a set of objectives were determined:

- Determine the impact of manipulation of miR-340 on autophagy in a live-cell assay.
- Determine potential targets of miR-340, implicated in both ALS and autophagy, which may affect its role in autophagy.
- Investigate the downstream impacts of expression changes of miR-340 on pathways and proteins of relevance to ALS.

## 4.2 Results and Discussion

### 4.2.1 MiR-340 Overexpression Reduces NRF2 Protein Levels

As noted previously, miR-340 was shown to target the NRF2 gene, *NFE2L2*, in human hepatocellular carcinoma cells resistant to the chemotherapy drug, cisplatin (Shi *et al.*, 2014). NRF2 is a neuroprotective transcription factor implicated in autophagy, and is downstream of TBK1 signalling. As discussed in section 4.1.4.1, in this pathway, KEAP1 binds NRF2, rendering it inactive and targeted for proteasomal degradation and thereby prevents its translocation to the nucleus. Interestingly, phosphorylated p62 competes for the interaction with KEAP1 and results in autophagic degradation of KEAP1 and the release of active NRF2 (Komatsu *et al.*, 2010; Copple *et al.*, 2010). Released NRF2 is able to activate the expression of a range of autophagy-related genes including *SQSTM1* which indicates a potential positive feedback loop between activated NRF2 and p62 expression to promote continued NRF2 activation (Pajares *et al.*, 2016).

To first confirm miR-340 can target endogenous NRF2, HeLa cells were analysed (Figure 17A). Cells were transfected with 50 nM miR-340 mimic (which simulate miRNAs and in this instance, increased the cellular miR-340 levels) or negative control mimic, and harvested after 48 hours. MiR-340 overexpression resulted in significantly reduced protein levels of NRF2 in HeLa cells by western blot ( $p < 0.05$ ) (Figure 17B). In parallel, immunocytochemistry (ICC) of HeLa cells was performed, which were transfected with 50 nM negative mimic control or miR-340 mimic for 48 hours, and fixed in 4% PFA (Figure 17C). The same NRF2 antibody as for western blotting was used, with DAPI for identification of the nucleus, with NRF2 staining predominantly nuclear as expected. Here a statistically significant reduction of nuclear and cytoplasmic NRF2 protein levels in HeLa cells transfected with miR-340 mimic compared to negative control mimic was also observed ( $p < 0.005$  and  $p < 0.05$  respectively) (Figures 17D and E). Collectively, these findings are consistent with the targeting of *NFE2L2* by miR-340, as previously reported (Shi *et al.*, 2014).

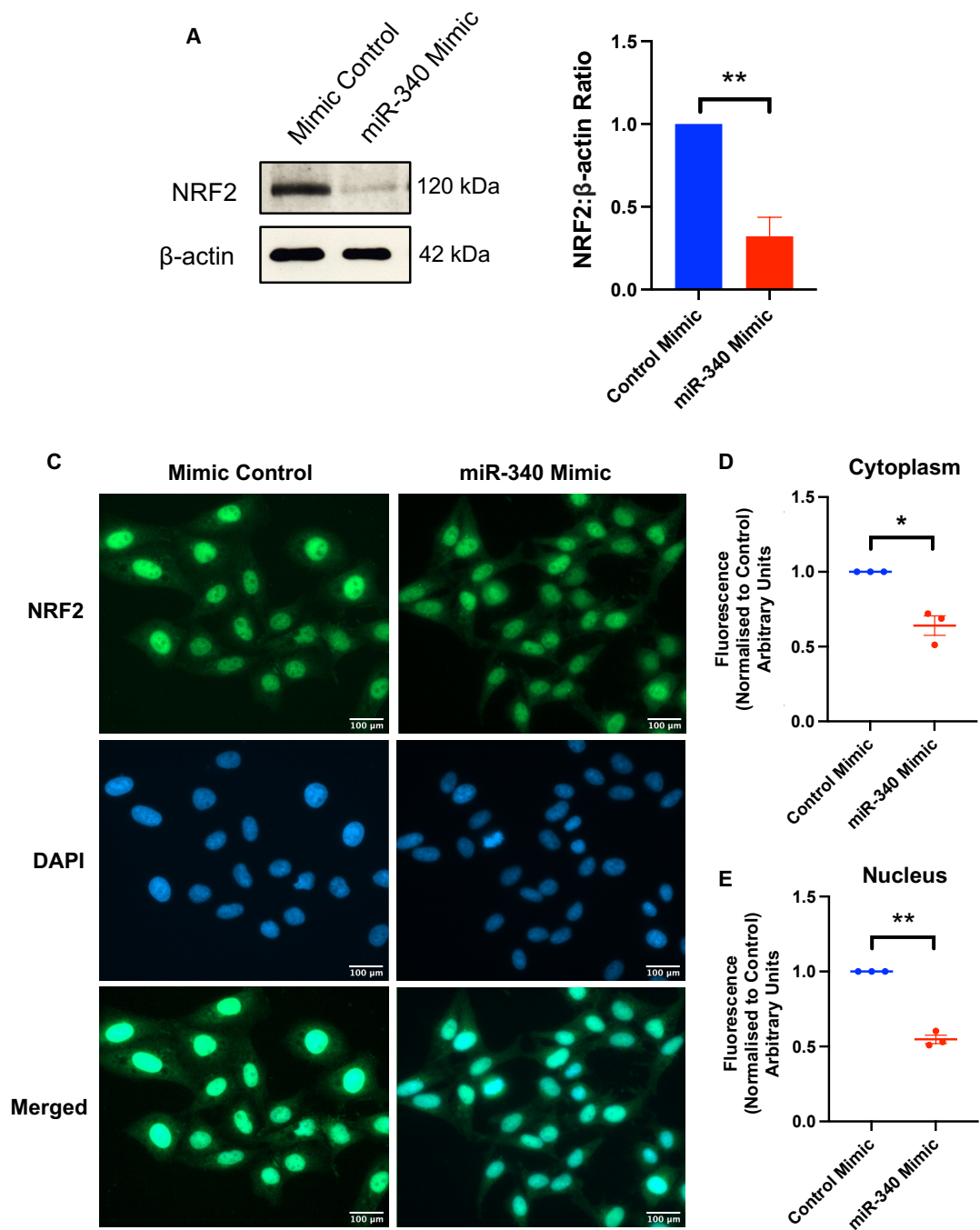


**Figure 17: miR-340 reduces NRF2 protein levels in HeLa cells.** A) Representative western blot showing endogenous protein levels of NRF2 when HeLa cells were transfected with 50 nM miR-340 mimic or control for 48 hours. B) Densitometry analysis of western blots. C) Representative images of NRF2 protein and DAPI when HeLa cells were transfected with 50 nM miR-340 mimic or negative control. D) Fluorescence analysis of cytoplasmic NRF2 from ICC images. E) Fluorescence analysis of nuclear NRF2 from ICC images. Scale bar shows 100  $\mu$ m. All data is shown as mean  $\pm$  SEM from three independent experiments with a minimum of 50 cells analysed per condition.

#### 4.2.2 Impact of miR-340 on Autophagy in a Live-Cell Model

As miR-340 was selected for further analysis largely due to predictions that it would target a high number of autophagy relevant genes, an investigation of the impact of miR-340 on autophagic activity in living cells was performed. To achieve this, a double tagged GFP-mCherry-*SQSTM1*/p62 autophagy reporter was transfected into HeLa cells, allowing the visualisation of this ectopic reporter of autophagic flux by widefield microscopy (with p62 itself also consumed as part of the autophagic process). In principle, GFP becomes quenched by the acidic environment within lysosomes, revealing only mCherry fluorescence. A distinction can therefore be made between cells trafficking autophagosomes containing p62 and cargo to lysosomes normally, and those with inhibited fusion of autophagosomes to lysosomes. The latter would prevent the degradation of p62 and cargo, so both GFP and mCherry fluorescence is observed which presents as yellow puncta when merged.

Firstly, to calibrate the assay, HeLa cells were treated with DMSO control or bafilomycin A1, a well characterised inhibitor of V-ATPases present on the lysosomal membrane which control the acidic pH within lysosomes. HeLa cells transfected with reporter and treated with bafilomycin A1 displayed visibly more yellow puncta when mCherry and GFP images were merged than those treated with DMSO, which resulted in increased Pearson's correlation coefficient (PCC) values compared to the DMSO control (Figure 18A and B). This is consistent with a previous study (from the laboratory) using NSC-34 cells transfected with the GFP-mCherry-*SQSTM1*/p62 construct and treated with bafilomycin A1 (Goode *et al.*, 2016).

Next, 50 nM miR-340 mimic was co-transfected into HeLa cells with the GFP-mCherry-*SQSTM1*/p62 construct and visualised by widefield microscopy after 48 hours (Figure 18A). It is important to note the GFP-mCherry-*SQSTM1*/p62 reporter does not contain UTRs which could be targeted by miR-340. As with bafilomycin A1 treatment, the miR-340 mimic also resulted in a significant increase in PCC values ( $p=0.001$ ) compared to the negative control mimic, suggesting miR-340 overexpression can inhibit autophagic flux (Figure 18C).

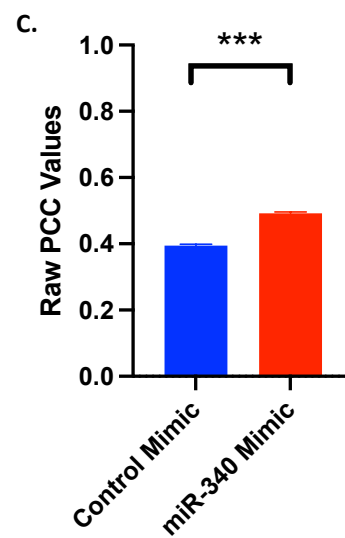
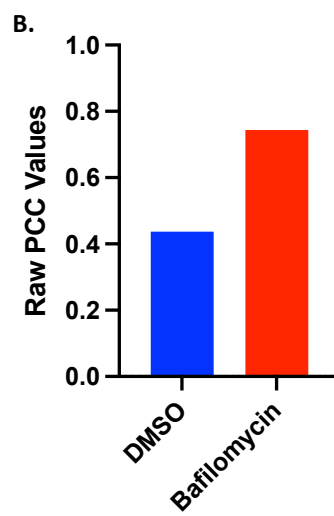
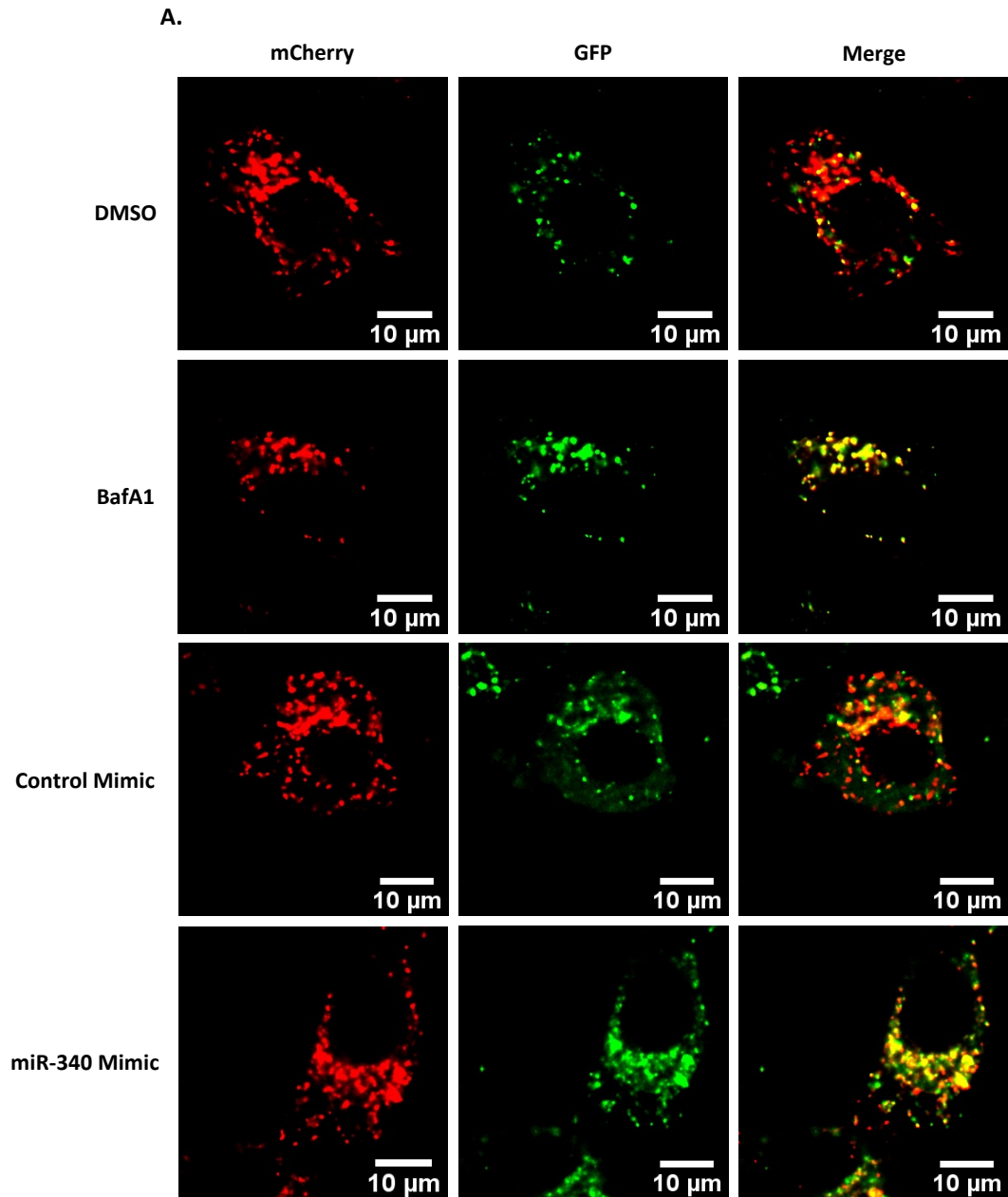


**Figure 18: Live HeLa cells transfected with miR-340 show inhibited autophagic flux that phenocopies pharmacological inhibition of autophagy.** A) Representative images of HeLa cells treated with DMSO or bafilomycin A1 and transfected with 50 nM control mimic or miR-340 mimic taken on the DeltaVision Microscope. Images show mCherry, GFP and merged channels. B) PCC values for the DMSO and bafilomycin A1 treated cells shows bafilomycin A1 significantly inhibited autophagy. Data show raw PCC values (arbitrary units) and is from a single experiment with a minimum of 20 cells analysed per condition. C) PCC values for the control mimic and miR-340 mimic transfected cells show the miR-340 mimic significantly inhibited autophagy ( $p=0.001$ ). Data show raw PCC values (arbitrary units) +/-SEM from three independent experiments with a minimum of 50 cells analysed per condition.

To determine whether miR-340 impacted on endogenous autophagy markers, p62 and LC3B-I and II, HeLa cells were transfected with 50 nM miR-340 mimic or negative control mimic for 48 hours. Western blotting was used to measure the levels of endogenous p62 and LC3B-I and II (Figure 19A).

The miR-340 mimic appeared to have no impact on the levels of endogenous p62 protein (Figure 19B), despite the impact on autophagy revealed in the live-cell assay. Of note, *SQSTM1* is predicted to be insensitive to targeting by miR-340, with a very low predictive miTG score of 0.38. Any changes observed in p62 protein levels would therefore be unlikely due to direct miR-340-*SQSTM1* interaction. In instances of autophagy inhibition, an accumulation of p62 would rationally be anticipated, as the degradation of p62 following the fusion of autophagosomes with lysosomes would be inhibited (Mizushima and Yoshimori, 2007). During autophagy progression, LC3-I is converted to LC3-II, meaning a reduction in LC3-II/LC3-I ratio was expected for inhibited autophagy. However, there was no apparent change in this ratio between the control and miR-340 mimic (Figure 19C). We rationalise that western blotting may not be sensitive enough to detect miR-340 exerts on autophagic function which do not present in these crude autophagy marker assays.

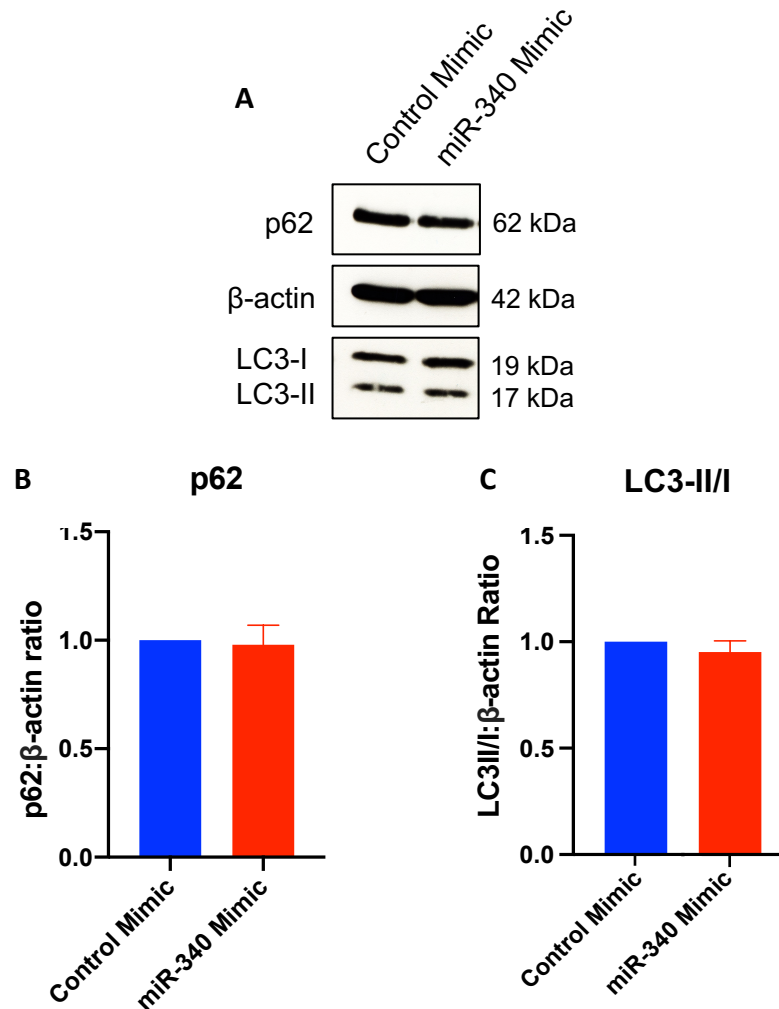


**Figure 19: Western blotting for endogenous autophagy markers with miR-340 mimic in HeLa cells.**  
 A) Representative western blot showing endogenous protein levels of the key autophagy protein markers p62 and LC3B when HeLa cells were transfected with 50 nM miRNA mimic and negative controls for 48 hours. B, C) Densitometry analysis of western blots. Data shown as mean  $\pm$  SEM from three independent experiments.

In contrast to our findings, some studies have shown that miR-340 overexpression induces autophagy in different cell types. For example, in a study which observed a correlation between higher levels of miR-340 and glioblastoma multiforme patient survival, overexpression of miR-340 in human primary glioblastoma cells reduced p62 protein levels and accumulated LC3-II levels, indicative of induced autophagy (Huang et al., 2015). Further, treatment of MG63 osteosarcoma cells with the tumour suppressor, lentinan (LNT), increased miR-340 expression and autophagy. The

authors established that the increase in autophagy was mediated by miR-340, since inhibition of miR-340 prevented the autophagy increase (H.-L. Xu *et al.*, 2018).

Despite these findings, it should be noted that very few studies have investigated a role of miR-340 in autophagy. The varied effects of miR-340 expression across different diseases is considered in section 4.1.3. Coupling previous knowledge of the role of miR-340 in autophagy with our work demonstrates that the effect of miR-340 on cellular pathways such as autophagy may vary depending on the model used.

#### 4.2.3 *TBK1* is a Direct Target of miR-340

In order to rationalise the observed effects of miR-340 on autophagy in our live-cell assay at the molecular level, further potential gene targets were explored. Since miR-340 was predicted to target *TBK1*, a critical regulator of autophagy, as discussed in section 3.2.5, whether miR-340 directly bound a predicted target site within the 3'UTR of *TBK1* using the dual luciferase reporter assay was investigated (Figure 20A). Oligonucleotides containing a predicted miR-340-*TBK1* MRE were cloned into the pmirGLO vector (Table 4 and Figure 20A). The luciferase signal of the vector containing the predicted miR-340-*TBK1* binding site was reduced by 22% when transfected alongside the miR-340 mimic compared to the negative control mimic, and this was statistically significant ( $p < 0.005$ ). When the predicted MRE was mutated by changing four nucleotides, the luciferase signal was completely rescued, despite transfection of the miR-340 mimic. These observations indicate miR-340 can bind specifically to a predicted MRE in *TBK1* when cloned into the pmirGlo vector (Figure 20B).

The luciferase assay demonstrates the ability of miR-340 to bind a MRE within the 3'UTR of *TBK1*, but it does not demonstrate this happens *in cellulo*. Therefore, attempts were made to validate this functional interaction using western blotting of HeLa transfected with 50 nM miR-340 mimic or negative control mimic for 48 hours (Figure 20C). Consistent with the results of the dual luciferase reporter assay, the

miR-340 mimic significantly reduced endogenous TBK1 protein levels compared to the control ( $p < 0.05$ ), validating *TBK1* as a direct target of miR-340 in HeLa (Figure 20D).

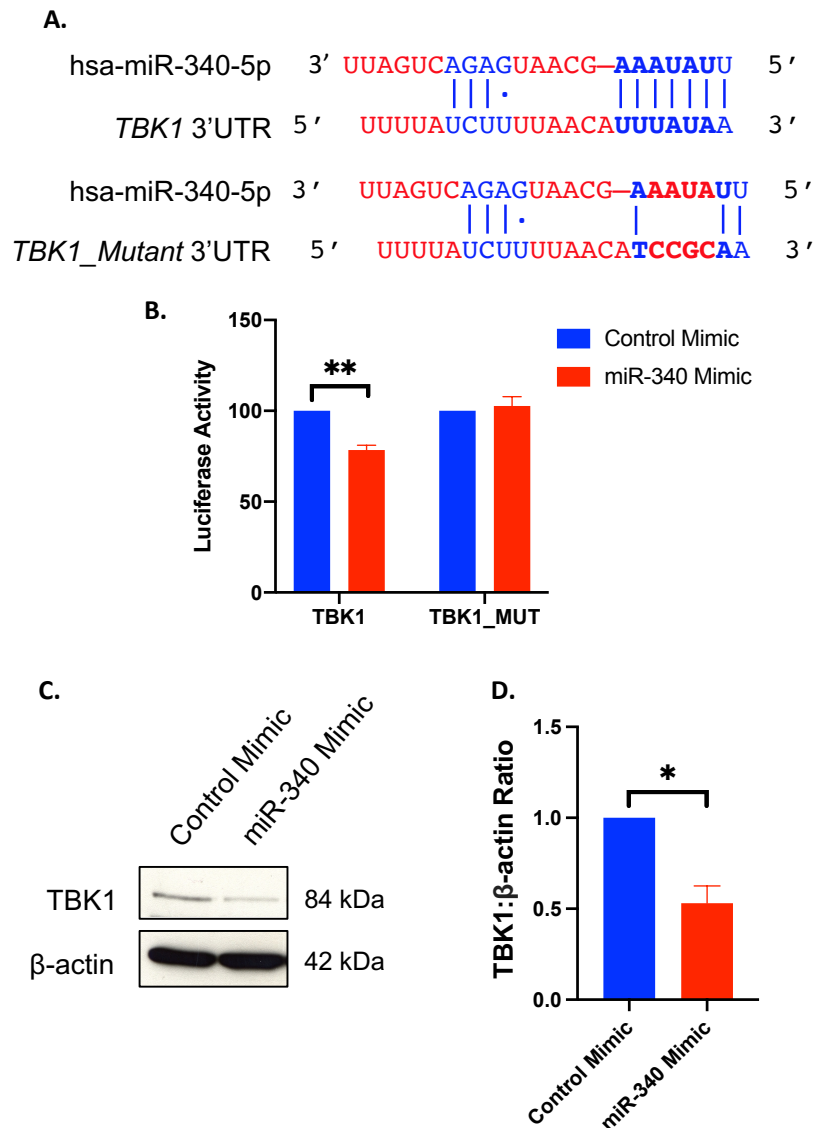


**Figure 20: Dual luciferase reporter assay shows miR-340 can directly target *TBK1*.** A) A predicted miR-340 binding site within the 3' UTR of *TBK1* and the mutated version of the site. Complementary nucleotides between the miR-340 and *TBK1* mRNA are shown in blue whilst non-complementary nucleotides are shown in red. The seed sequence of miR-340 and the miRNA response element within *TBK1* mRNA are shown in bold text. B) The luciferase activity was significantly decreased by 22% upon addition of miR-340 mimic to reporter constructs with cloned *TBK1*-miR-340 predicted response element ( $p < 0.005$ ). When this specific site was mutated, the luciferase signal was recovered. C) Representative western blot showing endogenous *TBK1* levels when HeLa cells were transfected with 50 nM miR-340 mimic or control. D) Densitometry analysis of western blots. Data shown as mean  $\pm$  SEM from three independent experiments.

Our observations that reduction of TBK1 protein by miR-340 may be linked to impaired autophagy observed in the live-cell assay is consistent with a study by Pilli and colleagues who found TBK1 knockdown suppressed maturation of autophagosomes into autolysosomes (Pilli *et al.*, 2012). Also, in agreement with our findings, a more recent study utilised TBK1-mutant iPSCs which resulted in reduced cellular TBK1 levels. As a consequence of this, the authors observed an accumulation of p62 positive phagophores, due to a slow-down of autophagic flux (Catanese *et al.*, 2019). Both studies strongly connect TBK1 reduction with impaired autophagy, and indicate miR-340 overexpression may be capable of causing these insults by decreasing TBK1 protein levels.

Since the miR-340 MRE within *TBK1*, which we identified as a direct target of miR-340 in human HeLa cells, is not conserved in mice, western blotting for TBK1 in mouse N2A cells transfected with 50 nM miR-340 mimic or control for 48 hours was performed as a negative control (Figure 21A). No change in the TBK1 protein levels in mouse N2A cells was observed, consistent with the lack of miR-340 MRE (Figure 21B). This highlights the decrease in TBK1 protein observed with overexpression of miR-340 in HeLa cells could be due to the direct interaction between miR-340 and *TBK1*.

We also performed the live cell autophagy experiment as described in section 4.2.2 using N2A cells, and this did not produce a statistically significant result either (Appendix 3). This again suggests the inhibition of autophagy by miR-340 is mediated (at least in part) by its suppression of TBK1.

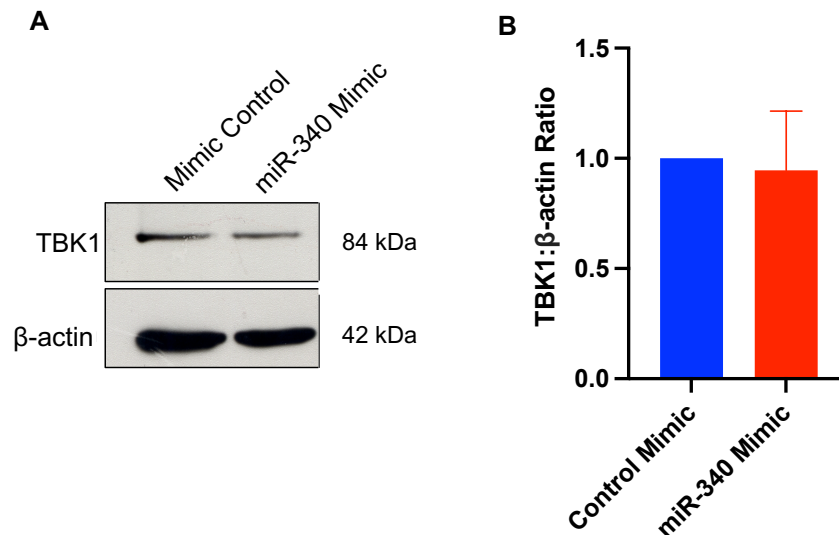


**Figure 21: Western blotting for TBK1 in mouse N2A cells with miR-340 mimic and control.** A) A representative western blot of N2A cells transfected with 50 nM miR-340 mimic negative control for 48 hours. B) Densitometry analysis of western blots of N2A cells transfected with miR-340 mimic or negative control. Data shows mean  $\pm$  SEM and is from three independent experiments.

The reduction of TBK1, a protein implicated in the release and activation of NRF2 from KEAP1, by miR-340, taken with the knowledge that miR-340 is capable of directly targeting NRF2, lead us to rationalise that the reduction of NRF2 protein levels upon transfection of the miR-340 mimic could be due to a combination of these direct and indirect effects.

Besides miR-340, other miRNAs have been shown to target *TBK1*. For example, miR-155-5p, dysregulated in six ALS patient studies (from Chapter 3), was shown to directly target *TBK1* using the luciferase reporter assay (Zhao *et al.*, 2019). Additionally, miR-199a, a miRNA found upregulated in ALS patient extracellular vesicles, was also shown to directly target *TBK1* using the luciferase reporter assay (Wang *et al.*, 2018). However, no published work appears to show the targeting of *TBK1* by a miRNA to result in changes in autophagic function. Coupling our findings with the results of other studies which show the targeting of *TBK1* by other miRNAs, suggests multiple miRNAs may physiologically target *TBK1* with the potential to regulate autophagy.

Although mutations in *TBK1* are a known cause of ALS, neither heterozygous *Tbk1* deletion, conditional motor neurone *Tbk1* knockout nor ALS-associated *Tbk1* missense mutations (resulting in reduction of kinase function and autophosphorylation) cause neurodegeneration in mice. However, *SOD1*<sup>G93A</sup> transgenic mice harbouring these *Tbk1* genetic abnormalities experience earlier, accelerated neurodegeneration and disease onset than control *SOD1*<sup>G93A</sup> mice (Brenner *et al.*, 2019; Gerbino *et al.*, 2020). This implies loss of TBK1, coupled with a 'second hit', could induce ALS phenotypes. We speculate the second hit may take the form, not only of the *SOD1*<sup>G93A</sup> mutation, but of NRF2 signalling failure. Reduced NRF2 mRNA and protein levels were found in ALS patients and we have shown miR-340 is able to reduce the protein levels of both NRF2 and TBK1 proteins in human cells (Sarlette *et al.*, 2008). When taken with the knowledge that overexpression of astrocytic NRF2 afforded protection to cocultured motor neurones from mutant *SOD1* toxicity (Vargas *et al.*, 2008), the use of miRNAs to target multiple genes, or miRNA inhibitors to increase gene and therefore protein expression, is attractive as a therapeutic.

In summary, we have shown overexpression of miR-340 impairs autophagic flux, which is potentially a result of the simultaneous reduction of TBK1 protein by this miRNA. Further, recent work has highlighted the important role of TBK1 in autophagic function during ALS progression. Both heterozygous *Tbk1*<sup>+/-</sup>;*SOD1*<sup>G93A</sup> mice and homozygous *Tbk1*<sup>R228H/R228H</sup>;*SOD1*<sup>G93A</sup> mice with impaired kinase function showed perturbed motor neurone autophagy and neurodegeneration at early stages of disease (Brenner *et al.*, 2019; Gerbino *et al.*, 2020). These mice, along with conditional motor neurone *Tbk1* knockout *SOD1*<sup>G93A</sup> mice, also experience extended survival, despite early disease onset. Despite the role of *Tbk1* in autophagy, the dysfunction of *Tbk1* at later stages may impact more greatly on another pathway, such as neuroinflammation. A miR-340 mimic could therefore be used to increase survival at later disease stages, despite its role in inhibiting autophagy.

In keeping with TBK1 dysfunction acting to promote ALS phenotypes when in synergy with a 'second hit', another study has found hemizygous *Tbk1* expression is sufficient to promote key hallmarks of ALS such as neuroinflammation, TDP-43 aggregation and

neuronal loss when expression of Tak1 is reduced to 50% in mice. Further, both TBK1 and TAK1 can phosphorylate and inhibit RIPK1, and the authors show that inhibition of RIPK1 rescues the ALS phenotypes seen during reduced expression of Tbk1 and Tak1. It is interesting to note the authors also identified TAK1 becomes reduced in normal human brains over 60 years old. Thus, we could speculate that underlying *TBK1* mutations come into effect when aging brains possess reduced TAK1 levels, allowing the unimpeded activity of RIPK1 to cause ALS phenotypes (D. Xu *et al.*, 2018).

The findings discussed here, which strongly implicate TBK1 in ALS progression when in conjunction with a second abnormality, provide a strong rationale behind further investigating the impact of miRNAs which impact both *TBK1* and *NRF2* expression, such as miR-340.

#### 4.2.4 Impact of miR-340 on Targets Downstream of TBK1 Signalling

TBK1 phosphorylates the autophagy receptor, p62 at Ser-403 and this has been shown to increase the levels of active NRF2, as phosphorylated p62 enhances its interaction with KEAP1, resulting in the subsequent release of NRF2 (Komatsu *et al.*, 2010; Hashimoto *et al.*, 2016). Although several ALS associated TBK1 mutations have been shown to reduce Ser-403 phosphorylation of p62, and ALS relevant *SQSTM1/p62* mutations have been shown to reduce activation of NRF2, it is not known whether ALS-relevant *TBK1* mutations impact NRF2 activation (Goode, Rea, *et al.*, 2016; Deng *et al.*, 2019). In addition, the protein, STING, which becomes activated upon cytoplasmic DNA detection, has recently been connected with ALS (Yu *et al.*, 2020). Data suggests STING activates TBK1, whilst NRF2 reduces STING mRNA and protein levels (Figure 16) (Ishikawa, Ma and Barber, 2009; Tanaka and Chen, 2012; Olganier *et al.*, 2018). Therefore, an investigation of the impact of miR-340 expression or TBK1 disturbance on downstream signalling, including Ser-403 p62 phosphorylation, NRF2 activation and STING protein levels, was performed.

#### 4.2.4.1 Phosphorylated p62

To establish whether transfection with miR-340 mimic (associated with TBK1 reduction) would lead to a reduction in Ser-403 phosphorylation of p62 (as opposed to total p62 levels (Figure 19)), as a downstream target of TBK1, HeLa cells were transfected with 50 nM miR-340 mimic or negative control mimic and western blotted for Ser-403 phosphorylated p62 after 48 hours (Figure 22A).

The miR-340 mimic significantly reduced the levels of Ser-403 phosphorylated p62 ( $p < 0.05$ ) (Figure 22B). It was previously noted the miR-340 mimic does not alter the levels of total p62, implying the reduction in phosphorylated p62 seen here is not due to a prior reduction of total p62 (Figure 19B). This suggests that the reduction of TBK1 protein by miR-340 extends to reduce the TBK1-mediated Ser-403 phosphorylation of p62.

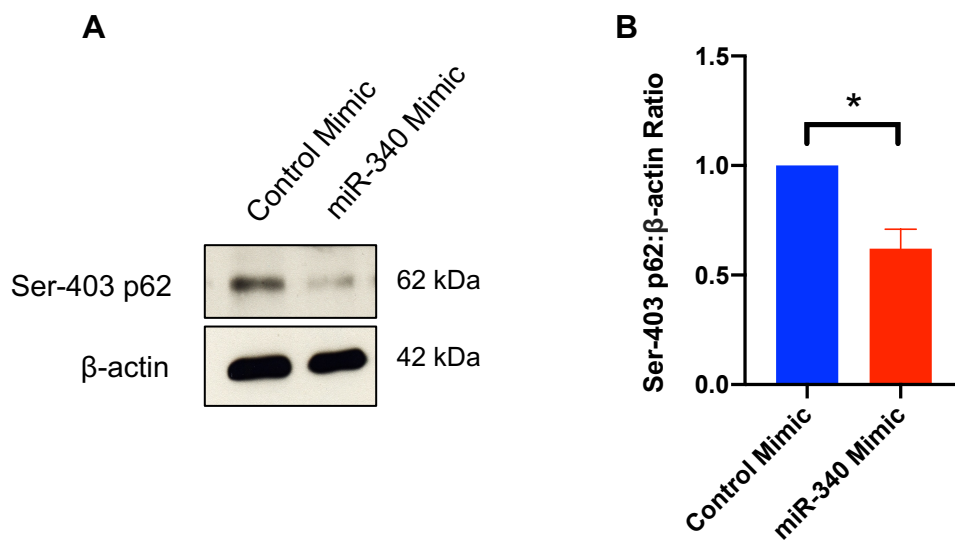


**Figure 22: Western blotting for Ser-403 phosphorylated p62.** A) Representative western blot showing endogenous levels of Ser-403 phosphorylated p62 in HeLa cells transfected with 50 nM miR-340 mimic or control for 48 hours. B) Densitometry analysis western blots. Data is shown as mean  $\pm$  SEM from four independent experiments.

#### 4.2.4.2 NRF2

Given that TBK1-mediated Ser-403 phosphorylation of p62 can regulate NRF2 activation (Copples *et al.*, 2010; Komatsu *et al.*, 2010; Ichimura *et al.*, 2013; Ishimura,

Tanaka and Komatsu, 2014), we considered whether miR-340 may exert its effects on NRF2 levels (Figure 17) *via* an indirect TBK1/Ser-403 phosphorylated p62-mediated mechanism, in addition to direct targeting of *NRF2* by miR-340 (Figure 23). To explore the contribution of TBK1 to NRF2 proteostasis, pharmacological inhibition of TBK1 was achieved using the compound BX-795, a known TBK1 inhibitor which blocks autophosphorylation at Ser-172 and activation (Clark *et al.*, 2009).

HeLa cells were treated with 1  $\mu$ M BX-795 and DMSO control for 16 hours and western blotting performed for NRF2 (Figure 24A). BX-795 significantly reduced the protein levels of NRF2 ( $p < 0.05$ ) (Figure 24B). This supports the notion that impacting TBK1 activity can result in reduced NRF2 protein levels. Considering that a direct consequence of reduced TBK1 protein by miR-340 would be the reduction of autophosphorylated TBK1, as for treatment with BX-795, we can speculate that the reduction of TBK1 by miR-340 (as well as the direct targeting of NRF2 by miR-340), may also contribute to our observed reduction of NRF2 (Figure 17).

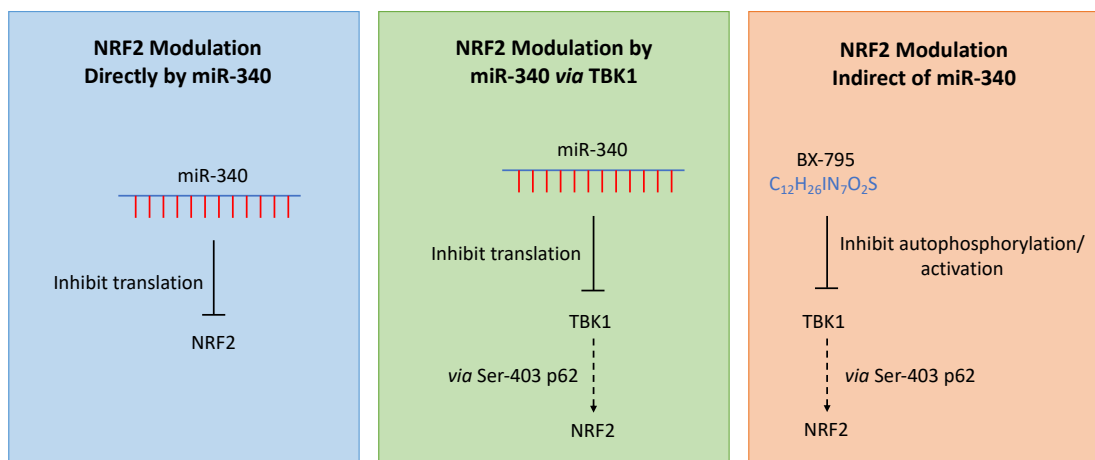


**Figure 23: Direct vs indirect modulation of NRF2 by miR-340.** MiR-340 directly binds NRF2 mRNA and results in reduced NRF2 protein levels. MiR-340 directly reduces active NRF2, potentially through TBK1 and Ser-403 phosphorylated p62. BX-795 may impact active NRF2 independently of miR-340, by inhibiting the activation of TBK1.

Notably, although this work shows that inhibiting TBK1 activity with BX-795 results in a decrease of active NRF2 protein, it has recently been reported that TBK1 acts as a suppressor of NRF2 signalling, and a kinase deficient mutant form of TBK1 lacks this suppression, suggesting a critical role of TBK1 kinase function for inhibiting NRF2 (Foster *et al.*, 2020). However, since our results clearly show inhibiting TBK1 activity results in decreased NRF2 protein levels in HeLa cells, more work should be done to elucidate the relationship between TBK1 dysfunction or reduction and NRF2 activation.

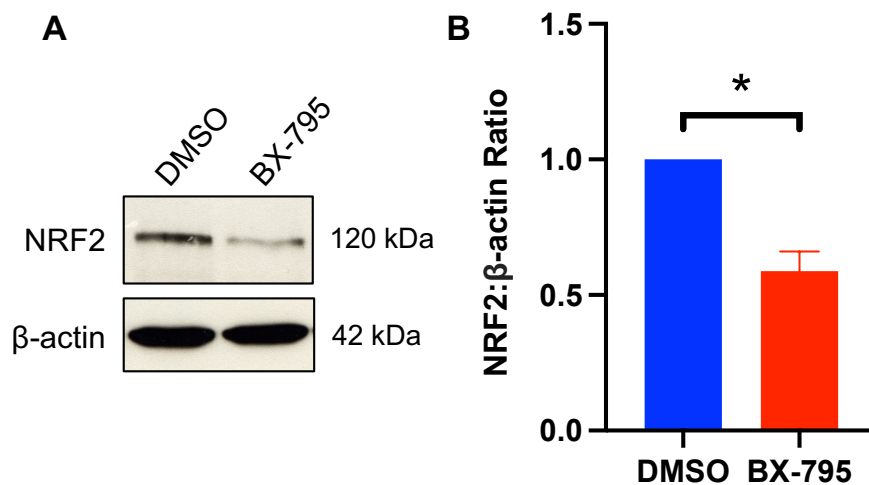


**Figure 24: TBK1 inhibition with BX-795 decreases NRF2 protein levels.** A) Representative western blot showing endogenous levels of NRF2 when HeLa cells were treated with DMSO control or 1  $\mu$ M BX-795. B) Densitometry analysis of western blots. Data is shown as mean  $\pm$  SEM from three independent experiments.

As presented, miR-340 overexpression does not appear to reduce the TBK1 protein levels in mouse N2A cells, consistent with the lack of a miR-340 MRE in TBK1 in mice (Figure 21). We also performed additional western blotting with N2A cells transfected with 50 nM miR-340 mimic and negative control mimic and showed there was no impact on NRF2 protein levels after 48 hours with western blotting (Appendix 4). This implies the observed decrease in NRF2 due to miR-340 overexpression may be specific to human cells and provides greater evidence that reduction in NRF2 levels upon transfection with miR-340 is at least in part contributed by a decrease in TBK1 levels. However, miR-340 has previously been shown to reduce the protein levels of NRF2 in a mouse myoblast cell line, though did not impact on the levels of

NRF2 mRNA (Mei *et al.*, 2019). These differences could be due to the differing cell types or could be impacted by the low levels of endogenous NRF2 we detected in the N2A cells.

#### 4.2.4.3 STING

Due to the relevance of STING signalling to the autophagy pathway, its implications in ALS, and especially due to its direct interaction with TBK1 as discussed in section 4.1.5, we next sought to determine the downstream impact of miR-340 on protein levels of STING. We performed western blotting with the miR-340 mimic and negative control and observed significantly decreased levels of STING protein in HeLa cells transfected with 50 nM miR-340 mimic (Figure 25A and B). STING is not a predicted target of miR-340, which indicates the reduction of STING observed with the miR-340 mimic is an indirect effect, mediated at least in part by the reduction of TBK1 protein.

As described in section 4.1.5, ALS-relevant mutant TDP-43 mice, deficient of STING, experienced a 40% extended life span compared with mutant TDP-43 mice with both STING alleles, which demonstrates how miRNA mimics, such as miR-340, could be used as therapeutics to target STING and other ALS relevant genes (Yu *et al.*, 2020). This is especially relevant given a molecular inhibitor of STING (H-151) prolonged survival in ALS mutant TDP-43 mice (Yu *et al.*, 2020).

With the impact of STING deficiency on life span in mind, we would also anticipate the life span of *Tbk1* deficient mice would increase, due to reduced TBK1 activation of type 1 IFN production and neuroinflammation. Indeed, Gerbino and colleagues showed that homozygous *SOD1*<sup>G93A</sup> mice also carrying the ALS-relevant TBK1 mutation, R228H, displayed reduced IFN production in spinal cord astrocytes and microglia, reduced motor neurone loss and exhibited a slower disease progression with an extended life span (Gerbino *et al.*, 2020).

The decrease in STING by overexpression of miR-340 implies STING is directly targeted by miR-340, since the decrease in TBK1 would be expected to decrease the active, phosphorylated form of STING, rather than total STING levels. Further work

could measure phosphorylated STING in response to miR-340 overexpression. In these experiments we did not stimulate the STING pathway with exogenous DNA, which could be performed in the future using commercially available dsDNA or cGAMP (Prabakaran *et al.*, 2018).

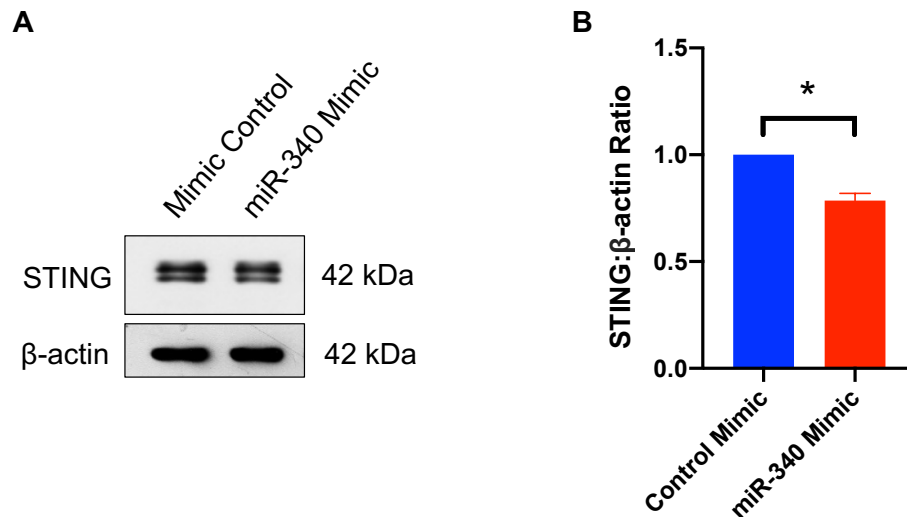


**Figure 25: Western blotting for STING in HeLa cells.** A) Representative western blot showing endogenous STING levels in HeLa cells transfected with miR-340 mimic and negative control mimic. B) Densitometry analysis of western blots. Data is shown as mean  $\pm$  SEM from three independent experiments.

#### 4.2.5 The miR-340 Inhibitor Has Minimal Effects On Autophagy and Proteins of Interest in HeLa Cells

Transfection of cells with a miRNA mimic (above) resembles overexpression of the particular miRNA, whilst a miRNA inhibitor is used to observe the effects of repressed activity of the endogenous miRNA of interest. As such, the effects of a miRNA mimic are logically expected to oppose those of a miRNA inhibitor. The relative expression level of the endogenous miRNA in a given cell type is a confounder, however.

Whilst our use of 50 nM of the miR-340 mimic in HeLa cells produced a statistically significant change in the protein levels of NRF2, TBK1, Ser-403 phosphorylated p62, and STING, and also resulted in autophagy inhibition in a live cell assay, use of 50 nM

miR-340 inhibitor had, in almost all instances, no statistically significant impact (anticipated in the opposite directions) on any of these readouts (Table 11).

The miR-340 mimic significantly reduced the NRF2 protein levels in HeLa cells (Figure 17), and we therefore anticipated the miR-340 inhibitor may induce a significant increase in NRF2 protein levels. However, we observed no significant change in the NRF2 levels compared to the negative inhibitor control upon western blotting for NRF2 in HeLa cells transfected with 50 nM miR-340 inhibitor or negative control inhibitor (Figure 26A and B). This contrasts to previous observations of significantly increased NRF2 protein in a mouse myoblast cell line transfected with a miR-340 inhibitor (Mei *et al.*, 2019).

The live cell autophagic flux assay in HeLa cells (Figure 18) showed significantly increased PCC values, indicative of inhibited autophagy with the miR-340 mimic, however, when the experiment was conducted using the miR-340 inhibitor, no difference in PCC values was found compared to the negative inhibitor control (Figure 26C). To function opposingly to the miR-340 mimic, we expected the miR-340 inhibitor may stimulate autophagy, and result in decreased PCC values, although this was not observed. We did not measure a known autophagy stimulator in our assay (as we did a known inhibitor, bafilomycin A1), however previous use of the same double tagged GFP-mCherry-*SQSTM1*/p62 construct transfected alongside treatment with a known autophagy inducer, rapamycin, did not produce a statistically significant decrease in PCC values in live NSC-34 cells (Goode, Butler, *et al.*, 2016). This suggests the live cell autophagy assay is not as sensitive to autophagy stimulation as it is to inhibition.

The miR-340 mimic did not produce a statistically significant change in endogenous p62 or LC3 levels or ratios (Figure 19), which act as indicators or markers of autophagy. Similarly, with the miR-340 inhibitor, there was no change in the p62 levels compared to the negative inhibitor control when western blotting for p62 and LC3 in HeLa cells transfected with 50 nM miR-340 inhibitor or negative control (Figure 26D, E). However, there was a significant decrease in the LC3-II/LC3-I ratio, implying some reduction in the conversion of LC3-I to LC3-II, suggesting potential inhibition of

autophagy (Figure 26F). This observation was expected for autophagy inhibition with the miR-340 mimic, and implies there is a complex mechanism of action concerning miR-340 and the autophagy pathway.

We observed a significant reduction of TBK1 protein upon transfection with miR-340 mimic (Figure 20D). We therefore expected the miR-340 inhibitor would allow protein levels of TBK1, no longer reduced by endogenous miR-340, to increase. Unexpectedly, transfection of HeLa cells with 50 nM of the miR-340 inhibitor reduced TBK1 protein levels compared to the negative inhibitor control, and this was almost significant ( $p=0.071$ ) (Figure 26G and H). Although not statistically significant, this trend is consistent with the results in section 4.2.2 which show the miR-340 inhibitor significantly reduced the LC3-II/I ratio and confirms the likelihood of complex mechanistic control of autophagy by miR-340.

We found the miR-340 mimic extended its effects to significantly reduce the Ser-403 phosphorylated p62 levels in HeLa cells (Figure 22). We therefore expected the miR-340 inhibitor to increase these levels, though there was no significant change (Figure 26I and J). However, as the miR-340 inhibitor did not significantly change the TBK1 levels, the lack of a change in phosphorylated p62 levels by the miR-340 inhibitor provides confidence that the reduction in Ser-403 p62 observed with the miR-340 mimic is mediated by its reduction of TBK1.

Finally, we observed a significant decrease in STING protein levels with the miR-340 mimic (Figure 25) and though we had expected the opposite result upon transfection with the miR-340 inhibitor, there was no alteration (Figure 26K and L). However, this is in keeping with the pathway in which TBK1 protein levels remain unchanged by miR-340 inhibition, resulting in normal activation of STING.

**Table 11: Summary of findings of miR-340 mimic and inhibitor.**

<b>Assay</b>	<b>miR-340 Mimic</b>	<b>miR-340 Inhibitor</b>
WB of HeLa cells for NRF2	Decreased NRF2	No significant change
HeLa cell live cell autophagy assay	Increased PCC values	No significant change
WB of HeLa cells for p62	No significant change	No significant change
WB of HeLa cells for LC3-II/I	No significant change	Decreased LC3-II/I
WB of HeLa cells for TBK1	Decreased TBK1	No significant change
WB of HeLa cells for Ser-403 p62	Decreased Ser-403 p62	No significant change
WB of HeLa cells for STING	Decreased STING	No significant change

A recently updated miRNA expression atlas from six humans indicates miR-340 is highly expressed in the brain, including in the frontal, temporal and occipital lobes (Keller *et al.*, 2021). We therefore rationalise observations whereby miR-340 inhibition in HeLa cells did not reflect our expectations is due to potentially low levels of endogenous miR-340 compared to other cell types, such as those from the brain. In cells with naturally low levels of endogenous miR-340, a miR-340 inhibitor would be unable to exert a strong functional impact. In cells with greater endogenous miR-340 expression, however, whereby its effects on protein levels are potent, the transfection of a miR-340 inhibitor would be expected to produce more profound changes on protein levels (Figure 27). To validate this, qPCR could be used to measure the miR-340 levels in HeLa cells and cells types such as neurones or astrocytes.

A database of miRNA tissue expression suggests miR-340 is expressed in low levels in HeLa cells (Panwar, Omenn and Guan, 2017). We averaged the expression in reads per million of each miRNA detected in HeLa cells across multiple studies. We then expressed the average reads per million value of each miRNA as a percentage of the total reads per million of all miRNAs. This showed that the miRNA with the highest reads per million value, miR-20a-3p, accounted for 13.3% of all reads. MiR-340-5p accounted for just 0.07% of all reads, indicating its expression is low in HeLa cells.

90% of the total reads were accounted for by 87 miRNAs, suggesting a dominance of these miRNAs over the remaining 2,567 (miR-340 among these).

Overexpression of miR-340 has increased senescence in WI-38 human diploid fibroblasts from foetal lung (Herman *et al.*, 2021). It is important to note that our treatment of cells with miR-340 mimic or inhibitor did not visually alter cell morphology compared to controls, and BCA protein quantification assays consistently demonstrated very similar total protein concentrations between treatments. The manufacturer (Qiagen) recommends miRNA mimics are used in concentrations up to 50 nM, which we used here in Chapter 4. The manufacturer also recommends the use of miRNA inhibitors up to 100 nM, and here we used 50 nM, though warns that when used over 50 nM, they can become toxic.

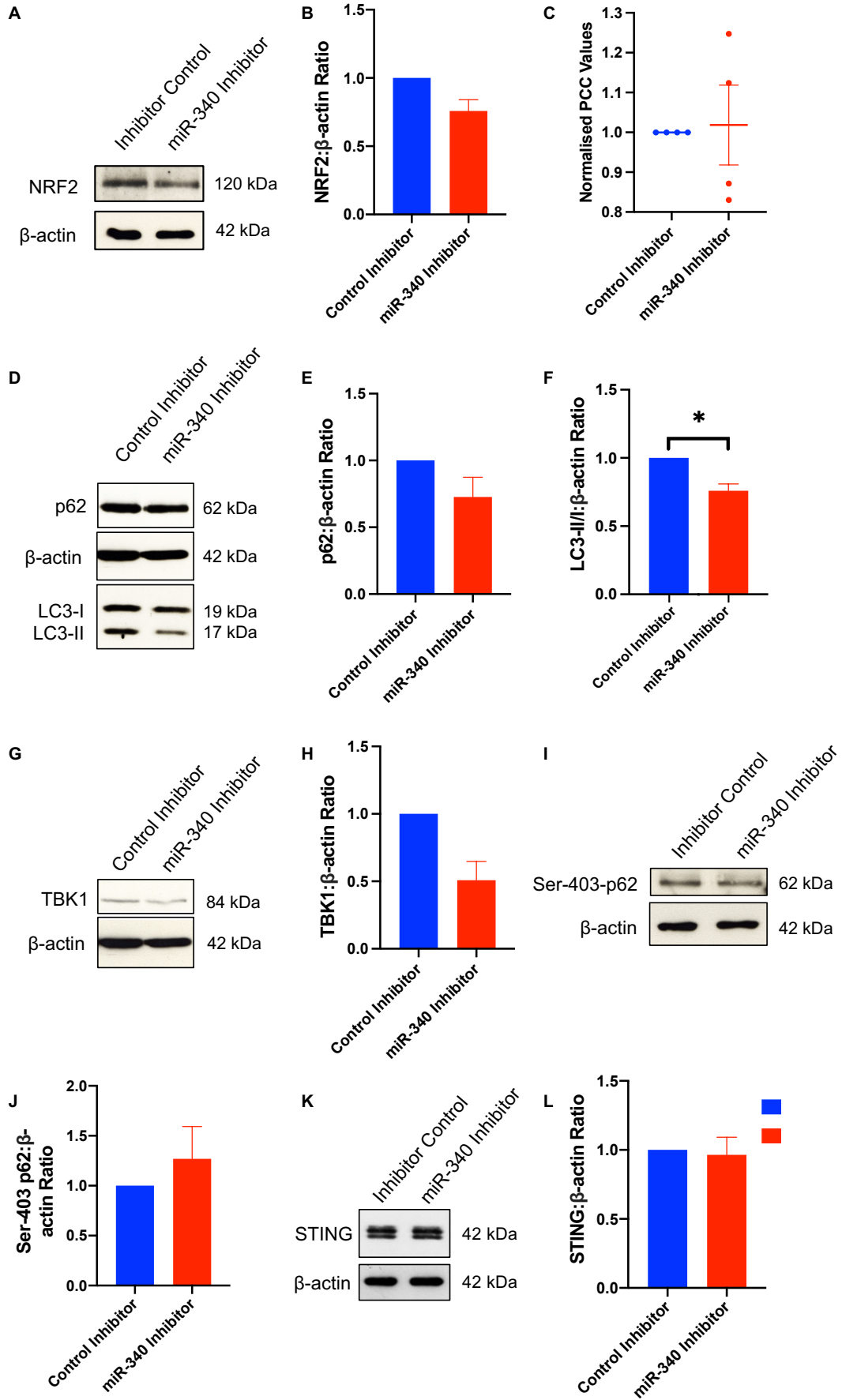


**Figure 26: Use of the miR-340 inhibitor in HeLa cells.** A) Western blotting for NRF2 in HeLa cells transfected with 50 nM miR-340 inhibitor or negative inhibitor control for 48 hours. B) Densitometry analysis of NRF2 protein levels. C) PCC values for HeLa cells treated with a double tagged GFP-mCherry-SQSTM1/p62 construct and transfected with 50 nM miR-340 inhibitor for 48 hours. A minimum of 50 cells were analysed per condition. D) Western blotting for SQSTM1/p62, LC3-I and LC3-II in HeLa cells transfected with 50 nM miR-340 inhibitor or negative inhibitor control for 48 hours. E and F) Densitometry analysis of SQSTM1/p62 protein levels and the LC3-II/I ratio respectively. G) Western blotting for TBK1 in HeLa cells transfected with 50 nM miR-340 inhibitor or negative inhibitor control for 48 hours. H) Densitometry analysis of TBK1 protein levels. I) Western blotting for Ser-403 p62 in HeLa cells transfected with 50 nM miR-340 inhibitor or negative inhibitor control for 48 hours. J) Densitometry analysis of Ser-403 p62 protein levels. K) Western blotting for STING in HeLa cells transfected with 50 nM miR-340 inhibitor or negative inhibitor control for 48 hours. L) Densitometry analysis of STING protein levels. Data is shown as mean +/- SEM from a minimum of three independent experiments.

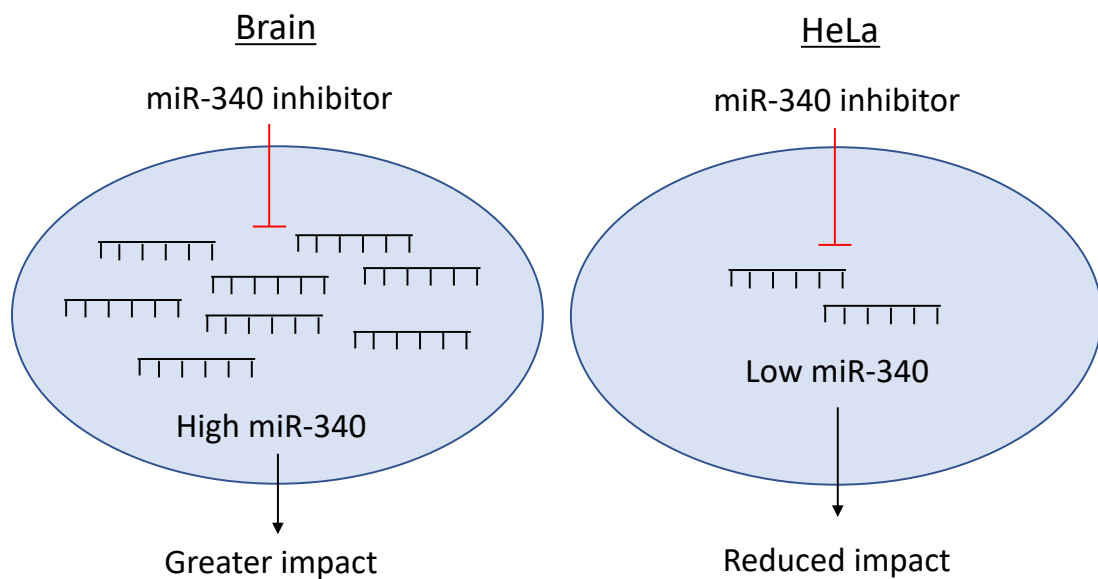


**Figure 27: Impact of miR-340 inhibition in cells with high endogenous levels of miR-340 compared to low.** miR-340 inhibition likely has a greater impact in cells with higher endogenous miR-340 expression, such as in areas of the brain, than in cells with lower miR-340 expression.

### 4.3 Conclusions and Future Directions

Here, we performed experimental evaluation of miR-340, an ALS-dysregulated miRNA implicated in autophagy. We noted that an established target of miR-340 was *NFE2L2*, the gene encoding NRF2, a protein strongly relevant to antioxidant signalling in ALS, and we confirmed the decrease of NRF2 in HeLa cells transfected with miR-340 mimic.

We next investigated the impact of miR-340 on autophagy in live HeLa cells and demonstrated that its overexpression inhibited cellular autophagic flux. This was realised by the reduced incorporation of a transfected p62 reporter into acidic vesicles in miR-340 mimic transfected cells compared to those transfected with control mimic. Despite this, western blotting for the endogenous autophagy markers p62 and LC3 with HeLa cells transfected with miR-340 mimic or control, revealed no change in p62 levels. Although we anticipated an increase in p62 levels in cells transfected with miR-340 mimic, we rationalised that western blotting may not be sensitive enough to observe these subtle changes.

We subsequently showed miR-340 was capable of directly targeting a specific nucleotide sequence within the 3' UTR of human *TBK1* using the dual luciferase assay. This adds gravity to both the ALS and autophagy relevance of miR-340, since TBK1 is a key component of autophagy and a known ALS-causative gene. We then validated this interaction in HeLa cells where the effect of the miR-340 mimic extended to significantly reduce the protein levels of TBK1. We further observed that TBK1 was unaffected by miR-340 overexpression in a mouse neuronal cell line, N2A, where the *TBK1*-miR-340 binding site is not conserved. Therefore, the N2A cell line (or other mouse cell lines) could be used as a control for off-target effects that are not a direct consequence of the TBK1 reduction by miR-340 overexpression.

We then investigated the impact of miR-340 on proteins downstream of TBK1 signalling. Interestingly, miR-340 overexpression reduced the protein levels of Ser-403 phosphorylated p62, which suggests miR-340's suppression of TBK1 protein

levels extended to reduce the amount of TBK1-mediated Ser-403 p62 phosphorylation.

We also demonstrated that NRF2 protein levels were decreased by a TBK1 pharmacological inhibitor, BX-795, suggesting a dependence upon TBK1 kinase activity for activation of NRF2. Western blotting for NRF2 in N2A cells transfected with miR-340 mimic or control did not reveal a change in NRF2 protein levels, suggesting the reduction of TBK1 by miR-340 may contribute to the reduction of NRF2 in HeLa cells.

Western blotting for STING, a protein recently connected to ALS progression and which is phosphorylated by TBK1, revealed a significant decrease in protein when HeLa cells were transfected with the miR-340 mimic. This indicates STING is a direct target of miR-340, though it is not a predicted target of miR-340. Further work could validate this with qPCR. To determine the effect of reduced TBK1 by miR-340 overexpression, the TBK1 mediated phosphorylation of STING could be measured in future experiments.

Finally, we showed that whilst western blotting for NRF2, TBK1, Ser-403 phosphorylated p62 and STING in HeLa cells transfected with miR-340 mimic produced significant reductions in protein levels, similar transfections using a miR-340 inhibitor (to impede endogenous miR-340), did not have a significant impact. We rationalised this was due to the relatively low absolute levels of miR-340 present in HeLa cells, and speculated that an effect would more likely be observed with the use of a miR-340 inhibitor in neuronal or glial cells. Although the miR-340 inhibitor was unable to promote autophagy in our live cell autophagic flux assay, western blotting for LC3-I and LC3-II revealed miR-340 inhibition significantly reduced the LC3-II/I ratio. This is consistent with autophagy inhibition, which we also observed using the miR-340 mimic and demonstrates the complexity regarding the role of miR-340 in the regulation of autophagy, which could be investigated further.

Overall, the work in this chapter has provided a new and potentially important connection between an ALS dysregulated miRNA, miR-340, and an ALS and

autophagy relevant protein, TBK1. We have provided novel insight into the functional mechanisms by which miR-340 may influence the dysfunction of autophagy during ALS, and our work contributes to growing knowledge of the pathomechanisms of ALS.

# Chapter 5 - Investigation of miR-340 Function in Human Astrocytes

## 5.1 Introduction

In Chapter 4, HeLa cells were used as a vehicle to study human miR-340-target gene interactions. As previously noted, the species of cells utilised is crucial for determining whether specific miRNAs target mRNAs, as these interactions are not always conserved. However, apart from being a model of the human cellular environment, HeLa cells have limited physiological relevance to studies of ALS pathomechanisms. Due to their relevance to ALS pathology and the neuroprotection provided by astrocytic NRF2 (a miR-340 target), commercially sourced human primary astrocyte cells, isolated from the cerebral cortex of human foetal brains were used, to further investigate the impact of miR-340 on ALS pathways of relevance.

As noted earlier, antioxidant signalling involving NRF2 is highly relevant in astrocytes. Its overexpression in SOD1<sup>G93A</sup> mouse astrocytes delayed ALS onset and increased mouse survival whereas survival was unaffected by NRF2 overexpression in neurones or muscle (Vargas *et al.*, 2008, 2013). NRF2 overexpression in SOD1<sup>G93A</sup> astrocytes also protected cocultured motor neurones from SOD1 toxicity (Vargas *et al.*, 2008). We compared potential miR-340-targeted genes using mRNA sequencing of both HeLa and human astrocytic cells, to determine the total whole cell mRNA affected by miR-340 dysregulation. By cross-referencing subsequently over or under-expressed genes after miR-340 overexpression (HeLa) or inhibition (astrocytes) with known ALS and autophagy-relevant genes, we aimed to elucidate potential broader mechanisms of miR-340-mediated target suppression.

### 5.1.1 Astrocytes

Astrocytes represent the most common cell type in the CNS and are considered to be 10-50 times more abundant than neurones. They are responsible for supporting neuronal (including motor neurone) function and maintaining their environment by performing a range of roles, including the synthesis and secretion of cytokines and

neurotrophic factors, maintenance of the blood brain barrier, regulation of intracellular calcium levels and participation in glucose metabolism (Dehouck *et al.*, 1990; Sang *et al.*, 2007). They also have a role in axon regeneration and aid axonal migration as well as regulating synapse function (Perea and Araque, 2005; Anderson *et al.*, 2016). They are involved in neurotransmitter recycling and play a crucial role in antioxidant defences (Deitmer, Bröer and Bröer, 2003; Dringen, Pawlowski and Hirrlinger, 2005). When triggered by injury or stress within the CNS, astrocytes transform into a reactive state. The remodelling of astrocyte biology to adopt this reactive phenotype is coined astrogliosis.

#### 5.1.1.1 Astrocytes and ALS

In ALS, astrocytes respond to neurodegeneration by entering a reactive state, which is often referred to as astrogliosis. Astrocytes become reactive in response to a change in brain homeostasis, though the precise molecular mechanisms which trigger the initial reactivity are unknown. Astrocytes likely detect the presence of misfolded proteins or altered neurotransmission and release growth factors, cytokines and purines which bind astrocyte receptors to activate downstream signalling pathways and establish a reactive state (Gong *et al.*, 2000; Abbracchio and Ceruti, 2006). Indeed, the presence of mutant SOD1 in mouse astrocytes induced their reactivity (Gong *et al.*, 2000). During astrogliosis, astrocytes upregulate glial fibrillary acidic protein (GFAP), vimentin and reduce levels of nestin.

Importantly, post-mortem patient-derived astrocytes from both sporadic and familial cases of ALS have been found to be toxic to cocultured motor neurones (Haidet-Phillips *et al.*, 2011). Early studies found human or mice embryonic stem cell derived astrocytes expressing human ALS mutants SOD1<sup>G37R</sup> or SOD1<sup>G93A</sup> respectively, decreased motor neurone numbers (Nagai *et al.*, 2007; C.N. Marchetto *et al.*, 2008). This extends to *in vivo*, where human ALS SOD1<sup>D90A</sup> patient iPSC derived astrocytes transplanted into mice spinal cords reduced the numbers of motor neurones by 40% (Chen *et al.*, 2015). Further, healthy rats treated with conditioned media from astrocytes expressing hSOD1<sup>G93A</sup> experienced motor dysfunction and loss of motor neurones from the ventral horn (Ramírez-Jarquín *et al.*, 2017).

Astrocyte toxicity to motor neurones may be mediated *via* secreted factors, since conditioned media from ALS mutant SOD1<sup>G93A</sup> expressing astrocytes was fatal to motor neurones (Nagai *et al.*, 2007). Interestingly, astrocytes expressing hSOD1<sup>G93A</sup> secrete 37% more protein (measured with BCA assay) through exosomal release than wild type SOD1 astrocytes, and exosomes secreted by SOD1<sup>G93A</sup> astrocytes reduced motor neurone survival, suggesting the toxic secreted factors could be transmitted by exosomes (Basso *et al.*, 2013).

The relevance of TBK1 function in astrocytes is largely unknown, though mice with *Tbk1* knockout presented abnormally shaped astrocytes among other abnormalities including p62 and ubiquitin aggregation (Duan *et al.*, 2019). Further, astrocytes immunopositive for TBK1 were identified in human post-mortem brains of patients with multiple system atrophy (Inoue *et al.*, 2021).

#### ***5.1.1.2 Astrocyte Mediated Motor Neurone Toxicity***

Astrocytes take up the neurotransmitter, glutamate, released into the synaptic cleft, through sodium-dependent excitatory amino acid transporters (EAAT1/GLAST and (EAAT2/GLT1). EAAT2 is most prevalent at astrocytic processes (Roberts, Roche and McCullumsmith, 2014). Excess glutamate which is not cleared leads to sustained activation of the neuronal glutamate receptors, alpha-amino-3-hydroxy-5-methyl-4-isoxazole propionic acid (AMPA) and N-methyl-D-aspartate (NMDA), leading to prolonged intracellular calcium ion accumulation and toxicity (Figure 28). Indeed, loss of EAAT2/GLT1 from astrocytes has been reported in ALS patient brains and spinal cords (Rothstein *et al.*, 1995). Further, glutamate levels have been found increased in ALS patient CSF (Spreux-Varoquaux *et al.*, 2002). The ALS approved drug, Riluzole, was also found to increase the uptake of glutamate by astrocytes, through increased expression of EAAT2/GLT1 (Frizzo *et al.*, 2004; Fumagalli *et al.*, 2008).

Neuronal calcium ion influx is modulated by AMPA receptors, tetramers composed of different combinations of subunits GluA1-4. They rely on the presence of glutamate receptor 2 (GluA2) subunit to prevent calcium entrance (Jonas *et al.*, 1994; Geiger *et al.*, 1995). Astrocytes regulate the expression of GluA2, and the ALS

associated SOD1<sup>G93A</sup> mutation abolishes the ability of astrocytes to control GluA2 expression. This results in a decrease of GluA2 and subsequent uncontrolled increase of calcium ions inside neurones, which can cause mitochondrial dysfunction leading to disruption of the respiratory chain and increased ROS production, resulting in glutamate excitotoxicity (Carriedo *et al.*, 2000; Van Damme *et al.*, 2007). Additionally, the GluA2 subunit undergoes RNA editing to convert a glutamine (Q) to an arginine (R), which is responsible for the impermeability of the AMPA receptor to calcium ions (Figure 28) (Sommer *et al.*, 1991; Takuma *et al.*, 1999). One study observed AMPA receptors lacking this amino acid change were present in all sALS patient motor neurones analysed, whereas all control subject motor neurones exhibited a higher proportion of editing of Q to R (Hideyama *et al.*, 2012). This RNA editing is mediated by adenosine deaminase acting on RNA 2 (ADAR2) which was found downregulated in ALS patient motor neurones (Melcher *et al.*, 1996; Hideyama *et al.*, 2012). Patient motor neurones without ADAR2 also exhibit TDP-43 mislocalisation, immunostaining positive for cytoplasmic phosphorylated TDP-43, whilst lacking unphosphorylated nuclear TDP-43 (Aizawa *et al.*, 2010). Further, the AMPA antagonist, Perampanel, ameliorates motor neurone degeneration in mice with conditional motor neurone *Adar2* knockout, suggesting that specifically targeting astrocytes is a viable approach for future drugs against ALS (Akamatsu *et al.*, 2016).

In addition, mitochondrial dysfunction and disruption of the respiratory chain in astrocytes can lead to an increase in production of ROS such as peroxynitrate, which can diffuse into neighbouring motor neurones, and lead to cell death (Radi, 2013). The increase in ROS would cause the release of active NRF2 from KEAP1 and the increase in transcription of antioxidant genes (Figure 28) (Wang *et al.*, 2019).

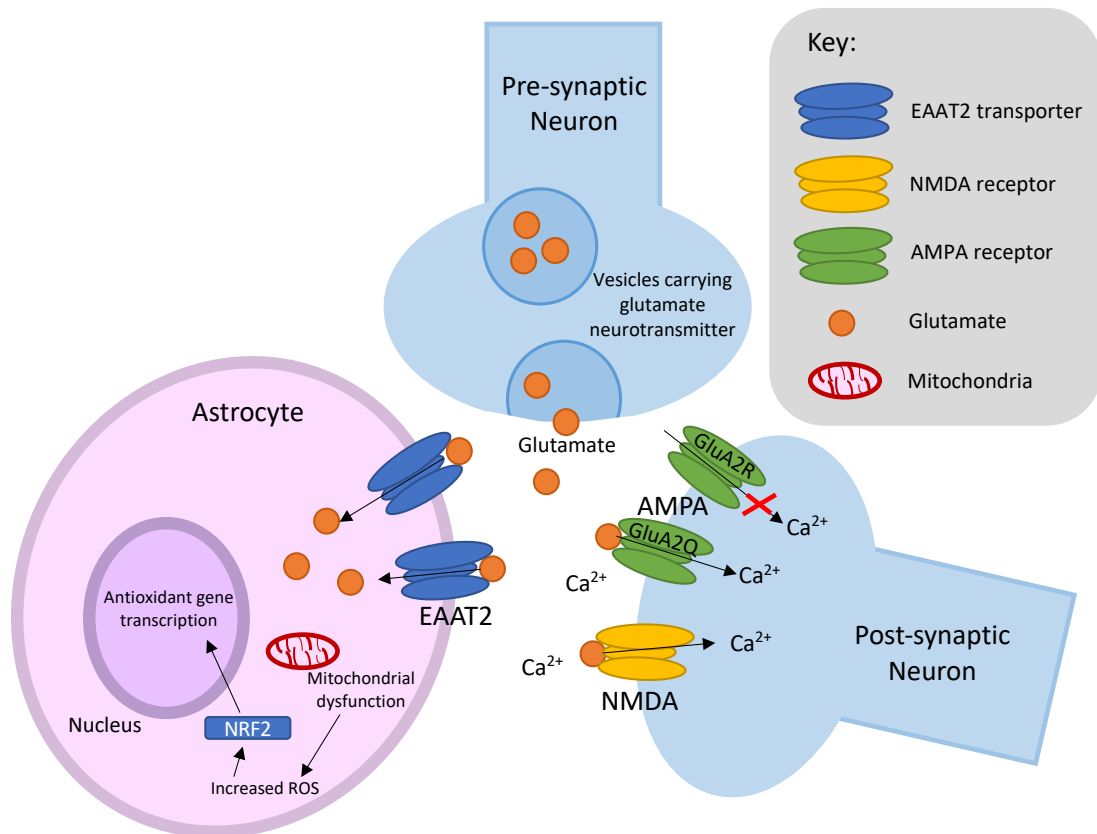


**Figure 28: Astrocytic neuroprotection.** Excitotoxicity is caused by an excess of glutamate in the synapse, delivered by the pre-synaptic neuron. The astrocytic glutamate transporter, EAAT2, clears excess glutamate from the synapse, but has been found decreased in ALS patient brain and spinal cord. The surplus glutamate causes excessive stimulation of neuronal glutamate receptors, AMPA and NMDA, leading to a large influx of Ca<sup>2+</sup>. Mitochondrial dysfunction can and lead to ROS production, activating NRF2 which translocates to the nucleus where it transcribes a variety of antioxidant genes. Normally, AMPA receptors undergo RNA editing to change a glutamine (Q) to an arginine (R), rendering the receptor impermeable to Ca<sup>2+</sup>, though lack of editing has been observed in sALS patients, contributing to the increased Ca<sup>2+</sup> influx, resulting in excitotoxicity. Drawn by author.

### 5.1.1.3 Astrocytic miRNAs in ALS

The motor neurone ‘specific’ miR-218 is expressed at low levels in astrocytes of both healthy and ALS mice and could be expressed at 150-fold higher levels in motor neurones than astrocytes (Hoye *et al.*, 2018). In rats, dying and dysfunctional motor neurones release miR-218 extracellularly, bound by proteins, and this miRNA was found to be taken up by neighbouring astrocytes (Mariah L. Hoye *et al.*, 2017; Hoye

*et al.*, 2018). Importantly, once in astrocytes, miR-218 repressed the protein expression of EAAT2. Further, the inhibition of miR-218 in SOD1<sup>G93A</sup> mice rescued the EAAT2 levels (Hoye *et al.*, 2018). In addition, the authors also observed inhibition of motor neurone-derived miR-218 mitigated astrogliosis, measured by a reduction in GFAP levels. This indicates miR-218 released from dying motor neurones triggers astrogliosis.

More recently, miR-146a expression was reduced in SOD1<sup>G93A</sup> astrocytes and their secreted extracellular vesicles (Gomes *et al.*, 2019, 2020). Over expression of miR-146a in mouse SOD1 astrocytes by transfection with pre-miR-146a rescued some ALS phenotypic abnormalities (Barbosa *et al.*, 2021).

### 5.1.2 Experimental Aims

Notwithstanding the known miR-340 and *NRF2* relationship, the implications of this interaction in human astrocytes has not been investigated, in spite of the crucial role of astrocytes in ALS progression. We hypothesised that miR-340 inhibition in human astrocyte cells would lead to an increase in *NRF2* and *TBK1* and affect the RNA of ALS-relevant and autophagy-relevant genes. To further explore the contribution of miR-340 to the regulation of specific ALS-relevant protein expression, we established the following goals:

- Determine the impact of endogenous miR-340 inhibition on *NRF2* and *TBK1* protein levels in human primary astrocytes.
- Explore whole cell mRNA expression in response to miR-340 overexpression or inhibition.
- Establish a pipeline to distinguish potential miR-340 ‘direct’ and ‘indirect’ targets to provide further insight into the mechanism of action of miR-340 using a workflow which could be applied to other miRNAs and data sets.

## 5.2 Results and Discussion

### 5.2.1 Impact of miR-340 on NRF2 and TBK1 in Astrocytes

As previously discussed, the survival of hSOD1<sup>G93A</sup> mice was increased by overexpression of Nrf2 in astrocytes, but was not affected by overexpression of Nrf2 in neurones and muscle, suggesting the protective role of NRF2 is astrocyte specific (Vargas *et al.*, 2013). Additionally, NRF2 overexpression in astrocytes increased survival of neighbouring motor neurones in hSOD1<sup>G93A</sup> mice, extended life-span and delayed disease onset (Vargas *et al.*, 2008). Taking this into consideration, regulatory mechanisms *via* miRNAs that could increase protein levels of astrocytic NRF2 may promote neuroprotection and enhance survival, and could be used as a potential therapeutic.

We first investigated the effect of miR-340 dysregulation on the protein levels of TBK1 and NRF2, by performing western blotting with human primary astrocyte cells. In Chapter 4, transient transfection of miRNA mimics or inhibitors were used to manipulate miR-340 levels and functional mechanisms in HeLa cells. However, preliminary experiments (not shown) were performed whereby astrocytes were transfected with P-DEST-mCherry-EGFP-*SQSTM1*/p62 construct and monitored for fluorescence. This exposed the low-level transfection efficiency in the primary astrocyte cells and led to the use of cell-permeable miRNA inhibitors instead, which possess a complementary sequence to the miRNA of interest and repress the endogenous miRNA activity. The addition of a phosphorothioate backbone makes these miRNA ‘power inhibitors’ resistant to enzymatic degradation. They are taken up into cells through a process known as gymnosis, without the need for transfection reagents such as lipofectamine (Stein *et al.*, 2010; Soifer *et al.*, 2012). No equivalent cell permeable miRNA mimic is currently available.

Commercially available human primary astrocyte cells (passaged a maximum of six times) were treated with 100 nM cell permeable miR-340 inhibitor and negative control 24 hours after seeding, and harvested for western blotting 48 hours post treatment (Figure 29A). The reduction in endogenous miR-340 function following

addition of the specific inhibitor was associated with a significant increase in NRF2 protein but, conversely, a significant decrease in TBK1 protein in human astrocytes (Figure 29B and C). The increase in NRF2 is consistent with our previous observations in HeLa cells, of decreased NRF2 protein following miR-340 overexpression. However, an increase in TBK1 was also expected due to our previous observations in HeLa cells, of decreased TBK1 protein following miR-340 overexpression.

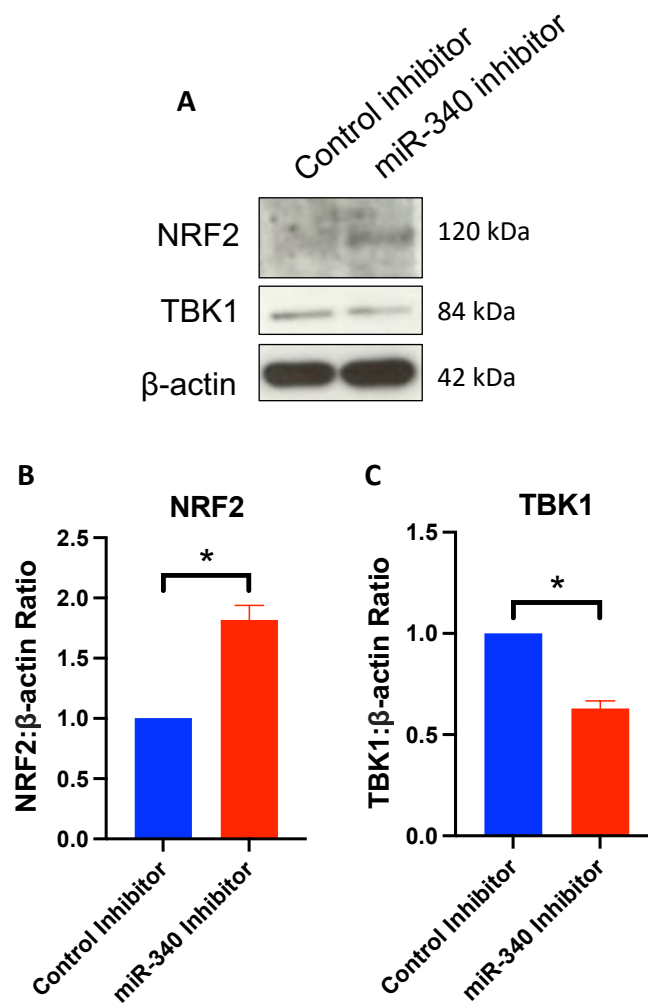


**Figure 29: Western blotting for NRF2 and TBK1 protein in human primary astrocytes.** A) Representative western blot showing NRF2 and TBK1 levels in human astrocyte cells treated with 100 nM miR-340 cell permeable inhibitor or negative control. B) Densitometry analysis of NRF2 protein levels. C) Densitometry analysis of TBK1 protein levels. Data is shown as mean +/- SEM from three independent experiments.

The manufacturer recommends the use of cell permeable inhibitors at a minimum concentration of 100 nM, which we used here in Chapter 5, and concentrations up to 5  $\mu$ M should have no impact on cell viability or morphology.

Integrating our findings that both miR-340 overexpression (Section 4.2.3) and inhibition decreased TBK1 protein levels (in HeLa and human primary astrocyte cells respectively) hints at the complexity of the mechanisms underlying miR-340 regulation of TBK1. When using a transfectable miR-340 inhibitor in HeLa cells in section 4.2.5, we also observed a reduction in TBK1 protein levels by western blotting. Whilst not significant, this data generated a p value of 0.07, very close to statistical significance. This supports our observation of significantly decreased TBK1 protein in human primary astrocytes following miR-340 inhibition. We speculate that despite *TBK1* being a direct target gene, the observed decrease in TBK1 levels in astrocytes following miR-340 inhibition are due to other targets of miR-340 (possibly in the same pathway(s)) as TBK1, which may combine function to ultimately reduce total TBK1 levels. Upon miR-340 inhibition, these yet unknown targets would become upregulated, resulting in the net reduction of TBK1 protein. Although the outcome observed would be due to indirect regulation of TBK1 by miR-340, this is potentially a real effect of miR-340 which could be further explored. For example, miR-340 is predicted to target Dual specificity tyrosine phosphorylation regulated kinase 2 (DYRK2), with a high predictive miTG score of 0.95 (Kishore *et al.*, 2011). DYRK2 targets TBK1 for proteasomal degradation by phosphorylating TBK1 at Ser-527 (An *et al.*, 2015). Therefore, under endogenous miR-340 inhibition, DYRK2 levels may increase, resulting in proteasomal degradation and reduction of TBK1. Additionally, the E3 ubiquitin ligase, DTX4, is recruited to TBK1 for K48 polyubiquitination, which leads to the proteasomal degradation of TBK1. Knockdown of DTX4 was shown to reduce the degradation of TBK1 (Cui *et al.*, 2012). DTX4 is also a predicted target of miR-340, though with a low predictive miTG score of 0.42. Upon endogenous miR-340 inhibition, the levels of DTX4 may rise, resulting in a subsequent decrease of TBK1 due to its increased proteasomal degradation. The impact of DYRK2 and DTX4 on TBK1 levels may out way the resulting increase of TBK1 induced by miR-340 inhibition (Figure 30). Future work could perform qPCR or western blotting to

measure the levels of DYRK2 and DTX4 mRNA and protein levels in response to miR-340 inhibition.

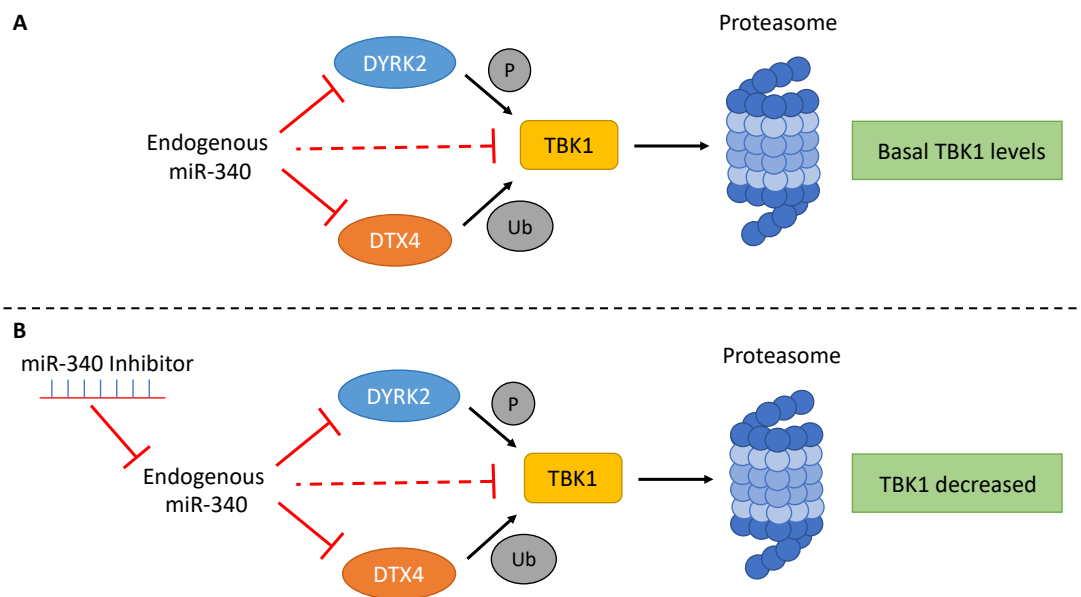


**Figure 30: Diagrammatic model of regulation of TBK1 levels under normal conditions or endogenous miR-340 inhibition.** A) Under normal conditions, DYRK2 and DTX4 target TBK1 for proteasomal degradation via phosphorylation at Ser-527 or K48 linked polyubiquitination, and endogenous miR-340 may influence DYRK2 and DTX4 levels as well as directly targeting TBK1. B) Upon treatment with a miR-340 inhibitor, endogenous miR-340 is repressed and any influence on DYRK2 or DTX4 is diminished, allowing greater levels of TBK1 degradation by the proteasome. This effect may out way the resulting increase of TBK1 induced by miR-340 inhibition. Drawn by author.

Immunohistochemical analysis using post-mortem brain tissue of patients with the neurodegenerative disorder, multiple system atrophy, revealed an increase in the number of TBK1 and STING positive astrocytes compared to controls. In addition, the number of STING and TBK1 positive astrocytes correlated with the number of GFAP positive cells, indicating STING and TBK1 could be overexpressed as part of the biochemical changes accompanying astrogliosis and may contribute to the pathogenesis of the disease. Overexpression of miR-340 could be used to manipulate both STING and TBK1 protein levels in astrocytes, which demonstrates how miRNAs have potential not only as biomarkers of disease, but also as therapies (Inoue *et al.*, 2021). Similarly, the opportunity to simultaneously raise NRF2 and reduce TBK1 is attractive as a potential therapy. Whilst miRNAs define the targets of interest, ASOs

complementary to these target mRNAs can be developed to inhibit translation. Indeed ASOs to target mRNAs have been used successfully in some ALS animal models and clinical trials (Evers, Toonen and van Roon-Mom, 2015).

To our knowledge, no work investigating miR-340 function with astrocytes has been published to date (Feb 2022). Our observations regarding miR-340 modulation of ALS and/or autophagy-relevant proteins in astrocytes highlights miR-340 as a potential novel therapeutic target which could be further explored.

Finally, we sought to determine whether the increase in NRF2 by miR-340 inhibition in human primary astrocytes would lead to a subsequent decrease in ROS caused by the increase in expression of NRF2 mediated antioxidant genes. We used 2',7'-Dichlorodihydrofluorescein diacetate (H2DCFDA), a ROS indicator which is converted to the highly fluorescent DSF upon recognition of ROS. We treated astrocytes with H<sub>2</sub>O<sub>2</sub> with H2DCFDA as a positive control and miR-340 inhibitor with H2DCFDA or control inhibitor with H2DCFDA. Unexpectedly, we observed that as the H<sub>2</sub>O<sub>2</sub> concentration was increased, the fluorescence signal was reduced using flow cytometry. Unfortunately, despite attempts to overcome this, including the use of other positive controls such as tBHQ, we were unable to successfully show a fluorescence increase with ROS increase. As an alternative, future experiments could use RT-qPCR to determine the levels of specific antioxidant genes whose expression is increased by NRF2.

### 5.2.2 Exploration of Human miR-340 Targets *In Cellulo*

To more broadly determine potential mRNA targets of miR-340 whilst also providing a possible rationale for observed effects of miR-340 manipulation throughout this thesis, RNA-sequencing was utilised. Initially, three independent preparations of human primary astrocyte cells were treated with 100 nM cell permeable control or cell permeable miR-340 inhibitor and total RNA was extracted after 48 hours. RNA quality/integrity was assessed *in house* (DeepSeq, University of Nottingham) and samples with an RIN of 10.0 were submitted for RNA sequencing to Novogene.

Overall, 29,051 RNAs were detected across all six samples (three inhibitor controls and three miR-340 inhibitor), though only 73 had statistically significant differential expression between cells subject to miR-340 inhibition and control inhibition. Of these, 29 (0.1%) were found upregulated and 44 (0.15%) downregulated (Figure 31). Figure 30B shows all detected RNAs, plotted with their  $-\log_{10}(\text{p-value})$  and  $\log_2\text{FoldChange}$ . Of the significantly differentially expressed, the  $\log_2\text{FoldChange}$  ranged from -4.944 to 4.148. The 30 most significantly deregulated RNAs as well as the most upregulated and downregulated genes are given in Table 10. A minimum number of one read from one condition resulted in the inclusion of the RNA in the analysis.

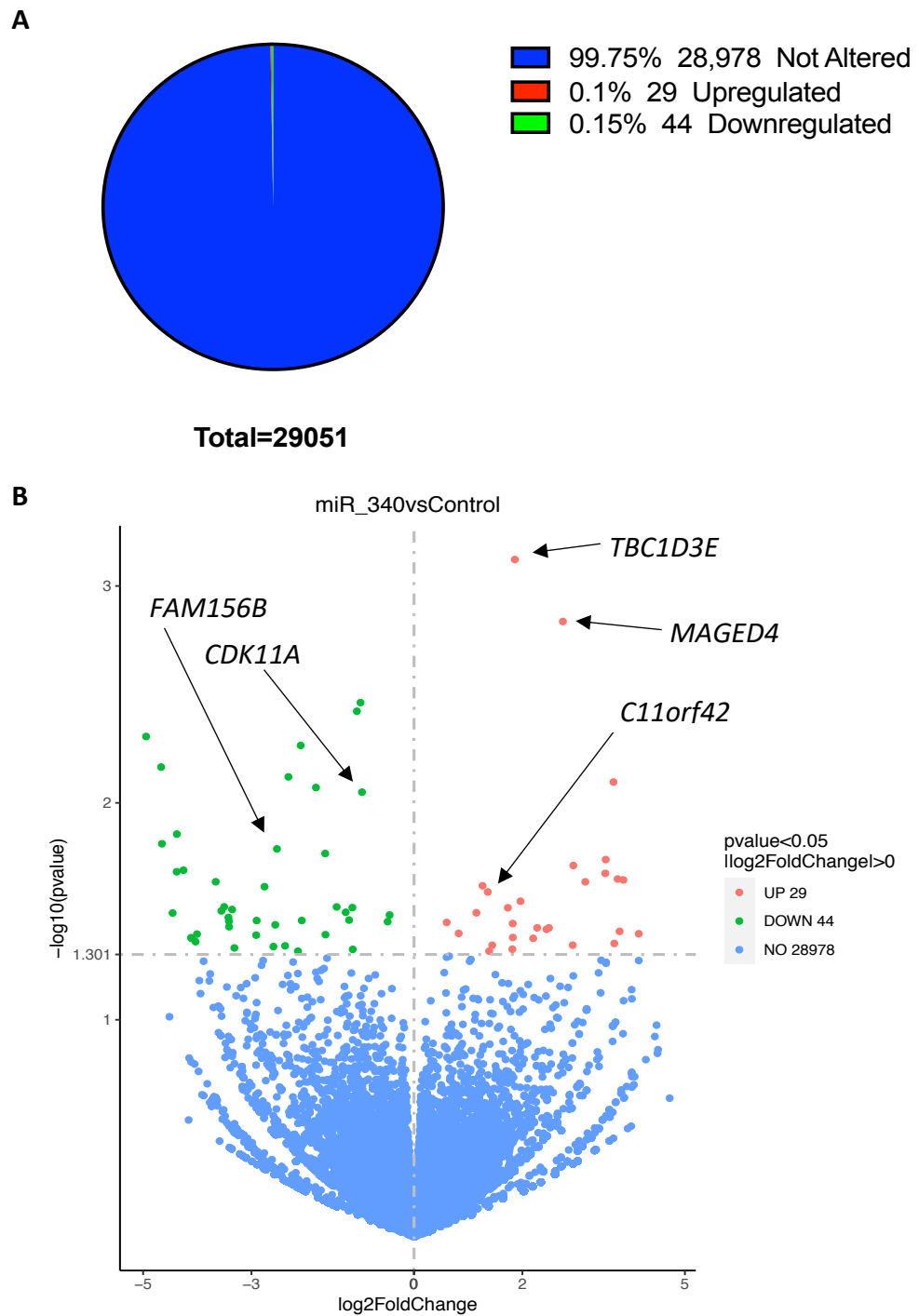


**Figure 31: Summary of gene expression distribution from human primary astrocytes treated with miR-340 inhibitor or control inhibitor.** A) The total RNA detected categorised into genes found not differentially expressed, significantly upregulated and significantly downregulated between miR-340 treated cells and controls. Values from left to right show the percentage of the total mRNAs each group accounts for and the total number of mRNAs in each group. B) Each detected mRNA is plotted with its  $\log_2\text{FoldChange}$  value against its  $p$ -value. Those upregulated (UP), downregulated (DOWN) or not differentially expressed (NO) are shown. The protein coding genes are labelled.

Among the mRNAs found most significantly deregulated, a range of gene biotypes were present. Of these 30 mRNAs, only six were categorised as protein coding (labelled in Figure 30B and shown with a red asterisk (\*) in Table 12). Other gene biotypes detected included antisense strands and long intergenic non-coding RNA. Both *TBK1* and *NFE2L2* genes were detected though neither showed a significant expression change upon miR-340 inhibition. However, we did observe significant changes in their protein levels in corresponding western blots (Figure 29). Of those showing significant expression changes, there was no overlap to known autophagy genes or ALS-related genes (from ALSod, obtained in 2022).

**Table 12: Noteworthy mRNAs from sequencing of human primary astrocytes treated with miR-340 inhibitor or control inhibitor.** Columns from left to right display the 30 most statistically significant mRNAs according to p-values, the most upregulated mRNAs and the most downregulated mRNAs according to log2FoldChange values. Protein coding genes are shown with a red asterisk.

Most significant		Most Upregulated		Most Downregulated	
Gene Name	p-value	Gene Name	log2FoldChange	Gene Name	log2FoldChange
* TBC1D3E	0.001	AC109454.1	4.148	IGKV1OR9-2	-4.944
* MAGED4	0.001	AL139398.1	3.864	MIR4256	-4.667
HIST2H2BD	0.003	AC010342.1	3.795	AC062015.1	-4.652
SPCS2P4	0.004	PSG8-AS1	3.758	Z82217.1	-4.456
IGKV1OR9-2	0.005	LIMS4	3.696	MFSD13B	-4.380
AP001783.1	0.005	DOCK9-DT	3.681	AC090186.1	-4.377
MIR4256	0.007	AC087289.5	3.539	AL050341.1	-4.255
AC008443.4	0.008	AC007923.4	3.530	AC120024.1	-4.115
DOCK9-DT	0.008	TAGLN2P1	3.161	AC009159.2	-4.102
AC084024.4	0.008	MYH16	2.941	RNA5SP155	-4.102
* CDK11A	0.009	BGLAP	2.929	AL391832.3	-4.032
AC090186.1	0.014	MAGED4	2.748	AL110118.2	-4.005
AC062015.1	0.015	UBA52P6	2.490	AC138409.1	-3.660
* FAM156B	0.016	EXOC5P1	2.446	AC048380.2	-3.555
AC105277.1	0.017	PCBP2-OT1	2.273	AC020916.2	-3.504
AC087289.5	0.018	DENND5B-AS1	2.199	AC090579.1	-3.425
MYH16	0.019	AC004832.5	1.965	OTUD4P1	-3.416
AL050341.1	0.020	TBC1D3E	1.862	NFE4	-3.413
MFSD13B	0.021	AC245595.1	1.824	NPIP10P	-3.358
AC007923.4	0.021	AL136985.3	1.822	SNORD1B	-3.316
PSG8-AS1	0.022	MAGED4B	1.815	AL049874.3	-2.913
AL139398.1	0.023	MKX	1.733	AC091729.1	-2.905
AC138409.1	0.023	GRHL3	1.443	AC103739.1	-2.759
TAGLN2P1	0.023	SNHG9	1.387	LINC01473	-2.595
ZGLP1	0.024	C11orf42	1.362	GCOM2	-2.561
AC103739.1	0.024	ZGLP1	1.265	FAM156B	-2.529
* C11orf42	0.026	SRRM3	1.151	ZBTB40-IT1	-2.379
AC004832.5	0.028	PHOSPHO2	0.825	AC008443.4	-2.318
AC020916.2	0.030	GCSHP5	0.603	AC012358.3	-2.142
AC109460.3	0.030			AP001783.1	-2.091

MiRNA inhibitors function by binding to, and preventing the activity of endogenous target miRNAs. With the use of a miR-340 inhibitor we therefore expected to observe a greater number of upregulated genes (29), which were no longer repressed by endogenous miR-340. There occurred a larger number of significantly downregulated genes (44), which we suggest is due to indirect effects of miR-340 inhibition. These effects could be the result of an increase in proteins normally repressed by endogenous miR-340 that functionally repress translation activators or transcription factors that would normally result in the increased expression of other genes (as described above for the case of TBK1 (Figure 30)).

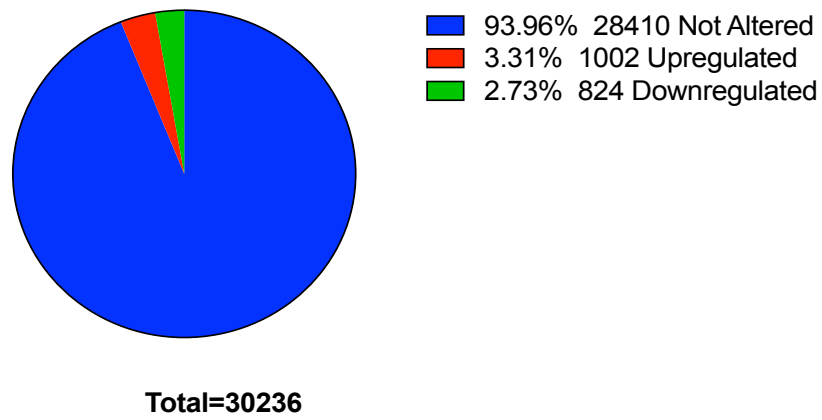
By comparing the results of this quantitative mRNA sequencing with protein quantification, the mechanism of a miRNA in regulating its target can be inferred. For example, should a mRNA target be reduced by a miRNA at both the mRNA and protein level, it implies the miRNA targets the mRNA for degradation. Alternatively, should a mRNA target not be reduced by a miRNA, but its protein is, this implies the miRNA targets the mRNA for translational inhibition. Therefore, a limitation of quantitative mRNA sequencing is that without combining with protein quantification data, it is unknown whether mRNAs without altered expression are possible targets of a miRNA.

The lack of protein coding genes among those significantly deregulated in astrocytes with miR-340 inhibition prompted us to compare RNA changes in HeLa cells, which were used extensively throughout Chapter 4. In this case, we used a miR-340 mimic rather than an inhibitor, since previous work in this thesis with HeLa cells was most successful with the use of a miR-340 mimic. Cells were transfected with 50 nM control mimic or miR-340 mimic on three independent occasions and samples with an RINe value of 10.0 (as determined by *in house* services – DeepSeq, University of Nottingham) were submitted for sequencing at 20 million reads per sample, to Novogene.

Overall, 30,236 mRNAs across the six samples (three mimic controls and three miR-340 mimic treated) were detected, whilst 1,826 showed a statistically significant expression change, with 1,002 significantly upregulated with miR-340

overexpression, and 824 significantly downregulated (Figure 32A). Combined, miR-340 significantly altered the expression of almost 6% of detected mRNAs in HeLa cells. Figure 32B shows all detected mRNAs, plotted with their  $-\log_{10}(\text{padj})$  (adjusted p value) and  $\log_2\text{FoldChange}$ . The  $\log_2\text{FoldChange}$  of mRNAs with significantly altered expression ranged from -3.027 to 2.538. The 30 most statistically significantly altered mRNAs as well as the 30 most upregulated and downregulated genes are given in Table 13. Genes of interest which are discussed in this thesis are indicated by a red asterisk (\*). Of the 1,826 mRNAs with significantly altered expression, 1,722 (94%) were protein coding.

A



B

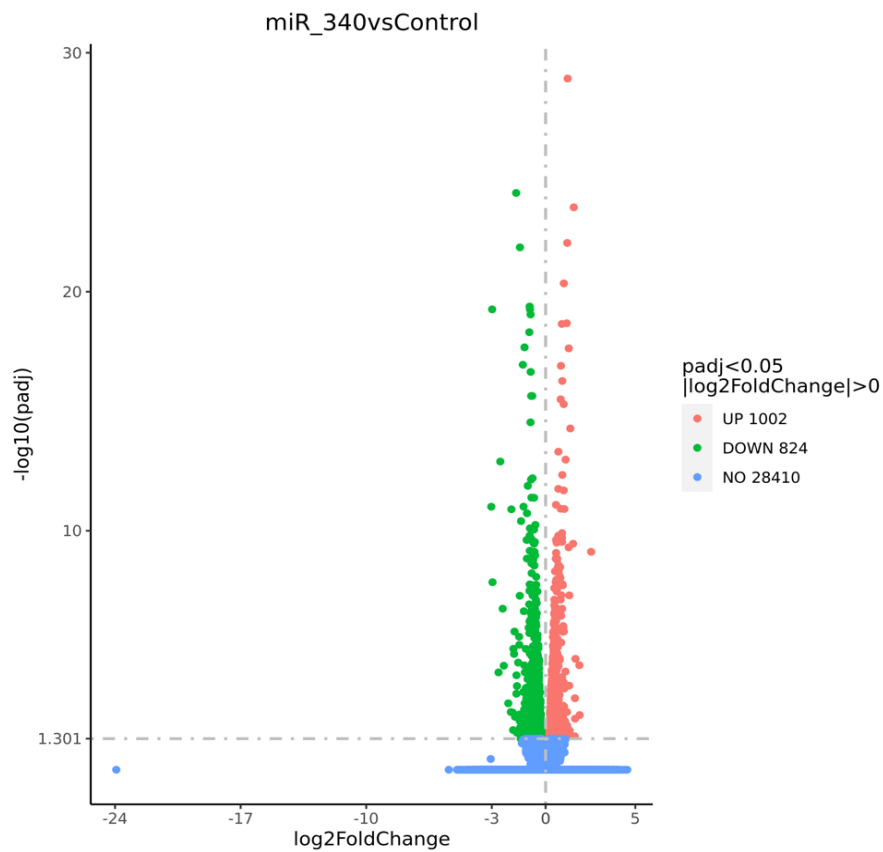


**Figure 32: Summary of gene expression distribution from HeLa cells transfected with miR-340 mimic or control.** A) The total mRNA detected categorised into those found without altered expression, those found significantly upregulated and significantly downregulated between miR-340 treated cells and controls. The percentage of the total mRNAs each group accounted for and the total number of mRNAs in each group. B) Each detected mRNA is plotted with its  $\log_2\text{FoldChange}$  value against its  $\text{padj}$ . Those upregulated (UP), downregulated (DOWN) or without altered expression (NO) are shown.

**Table 13: Noteworthy mRNAs from sequencing of miR-340 mimic or control transfected HeLa cells.**

Columns from left to right display the 30 most statistically significant mRNAs according to padj values, the 30 most upregulated mRNAs and the 30 most downregulated RNAs according to log2FoldChange values. Genes of interest are shown with a red asterisk.

Most Significant		Most Upregulated		Most Downregulated	
Gene Name	Padj	Gene Name	log2FoldChange	Gene Name	log2FoldChange
HYOU1	1.20E-29	TMEM151A	2.538	CYP4F11	-3.027
AKR1C2	7.35E-25	KANK4	1.897	HIST2H4A	-2.980
* UNC13A	2.94E-24	PIWIL3	1.882	F2RL2	-2.960
FOXM1	9.08E-23	STMN3	1.664	SLC7A11	-2.525
ITGAV	1.39E-22	CCL21	1.642	RAPSN	-2.332
LITAF	4.46E-21	DHRS2	1.635	FBXW10	-2.081
NEK7	4.15E-20	PYGM	1.622	NMRAL2P	-1.936
HIST2H4A	5.46E-20	* UNC13A	1.568	MAP2	-1.908
DCUN1D1	5.46E-20	NEURL1B	1.531	ZFHX2	-1.831
UHMK1	8.96E-20	FAM234A	1.377	RSPO3	-1.810
B4GALT1	2.08E-19	CPLX1	1.320	GCNT3	-1.795
POLR2A	2.22E-19	PDIA6	1.314	PATL2	-1.758
* NFE2L2	4.94E-19	RMND5A	1.291	CD22	-1.734
TTC8	2.12E-18	MAPK8IP2	1.284	SLC7A4	-1.700
RMND5A	2.34E-18	TMEM145	1.257	AKR1C2	-1.642
TRIM16L	1.13E-17	HYOU1	1.229	NECAB2	-1.628
CPT1A	1.26E-17	FOXM1	1.207	KIAA0319	-1.595
UGDH	2.26E-17	FES	1.199	AKR1C1	-1.529
SPG21	5.41E-17	FGF18	1.187	SAMD9L	-1.465
LIMS1	2.29E-16	B4GALT1	1.176	ITGAV	-1.431
API5	2.29E-16	CKAP4	1.115	TSNAXIP1	-1.416
ROR2	3.17E-16	ADCY10P1	1.103	CCDC30	-1.416
CBX6	5.07E-16	GALNTL6	1.100	MRPS30-DT	-1.389
ROCK1	2.92E-15	MUC5AC	1.094	CLIP4	-1.369
FAM234A	5.26E-15	BANCR	1.074	CDH23	-1.282
NR4A1	4.92E-14	TP53I3	1.044	TRIM16L	-1.269
CKAP4	1.05E-13	RASGRP2	1.036	C3orf35	-1.259
SLC7A11	1.27E-13	PPIB	1.028	HIST1H2AI	-1.240
DSP	4.63E-13	CARMIL3	1.022	RPL12P14	-1.236
MYL12A	6.34E-13	RASL10B	1.016	ADAM21	-1.236

MiRNA mimics function to promote the degradation of, or inhibit the translation of target mRNAs, resulting in a reduction of the target mRNA and/or protein levels. Here, despite the transfection of HeLa cells with a miRNA mimic, a greater number of mRNAs with significantly altered expression were found to be upregulated (1,002) than downregulated (824). The resulting overexpressed mRNAs are likely a result of

miR-340 indirect effects, whereby miR-340 overexpression indirectly causes mRNAs to become increased upon suppression of a direct mRNA target.

It would be interesting to compare the list of these mRNAs with altered expression with proteins found deregulated by miR-340 overexpression in HeLa cells, using quantitative mass spectrometry. This would reveal whether protein expression changes mirror the direction of their equivalent genes, revealing whether the impact of a miRNA on protein levels is reflective of its impact on mRNA levels. Further, information about the potential mechanism of action of a miRNA can be inferred when both mRNA and protein expression data is known. For example, if no statistically significant change in the expression of a particular mRNA is observed, but a reduction in its protein levels are, it suggests the miRNA acts to reduce translation rather than degrade the mRNA. Additionally, a significant reduction in both a mRNA and its protein would indicate the miRNA acts by degrading the mRNA rather than inhibiting its translation into a protein.

From the quantitative mRNA sequencing experiment, the levels of *TBK1* mRNA were not altered by the miR-340 mimic in HeLa cells, though our western blot analysis demonstrated the miR-340 mimic reduced TBK1 protein levels compared to the control in HeLa cells. This suggests miR-340 acts to reduce the translation of *TBK1* mRNA, rather than degradation of its mRNA. The proteins DYRK2 and DTX4 were discussed in section 5.2.1 as potential miR-340 targets which result in the reduction of TBK1 protein when miR-340 is inhibited. The mRNAs DTX4 and DYRK2 were not significantly altered by miR-340 overexpression, although without proteomic data to compare, whether miR-340 targets these mRNAs for translational inhibition, or does not target them, is unclear. Although this is indirect miR-340-TBK1 regulation, during miR-340 inhibition, the MRE is less relevant than during its overexpression.

On the other hand, the levels of *NFE2L2* mRNA were significantly decreased (with a log<sub>2</sub>foldchange of -0.910) by the miR-340 mimic in HeLa cells in the quantitative mRNA sequencing experiment, and we showed by western blotting that the NRF2 protein was also decreased by miR-340 mimic in HeLa cells. It is noteworthy that

*NFE2L2*, was also among those most significantly altered by miR-340 overexpression, consistent with our and others' findings (Table 13).

Further, in Chapter 4, we showed miR-340 overexpression did not impact the levels of p62 protein compared to the control, although the levels of *SQSTM1* gene were statistically significantly reduced by miR-340 overexpression (adjusted p value=  $2.8 \times 10^{-5}$ ) with a log2foldchange of -0.56. This suggests miRNA-mediated reductions of mRNA do not always result in subsequent reductions of protein at least within specific timeframes. STING protein levels were also reduced upon miR-340 overexpression (section 4.2.4.3), although the STING gene, *TMEM173*, did not have statistically significantly altered expression. This implies miR-340 acts to inhibit translation of the mRNA, rather than promote its degradation in this instance. These results demonstrate how comparisons of protein and mRNA levels from the same cell line transfected with a miRNA mimic, help rationalise the mechanism of action of the miRNA. Broadly, whether the miRNA primarily inhibits translation of the mRNA or promotes its degradation can be deduced. Table 14 summarises the impact of miR-340 overexpression on protein and mRNA levels of TBK1, NRF2, p62 and STING and the potential miR-340 mechanism of action that can be inferred from this.

**Table 14: Impact of miR-340 overexpression on protein and mRNA levels of TBK1, NRF2, p62 and STING in HeLa cells. The potential mechanism of action of miR-340 on each mRNA is also shown.**

	Impact of miR-340 Overexpression		Potential miR-340 mechanism of Action
	Protein	mRNA	
<b>TBK1/TBK1</b>	Decreased	Not Altered	Translational Inhibition
<b>NRF2/NFE2L2</b>	Decreased	Decreased	mRNA Degradation
<b>p62/SQSTM1</b>	Not Altered	Decreased	NA
<b>STING/TMEM173</b>	Decreased	Not Altered	Translational Inhibition

The third most significantly altered mRNA induced by miR-340 overexpression was *UNC13A*, which was also within the top ten upregulated mRNAs upon miR-340

overexpression and is highlighted with a red asterisk in Table 13. *UNC13A* was first associated with ALS in 2009, through a genome-wide association study (Van Es *et al.*, 2009). It has been shown to modify survival and susceptibility to ALS (Diekstra *et al.*, 2012). A major role of TDP-43 is to prevent cryptic exon inclusion during RNA splicing and was shown to repress a cryptic exon splicing event in *UNC13A* (Ling *et al.*, 2015; Ma *et al.*, 2022). Reduction of TDP-43 from the nucleus of human brains and neuronal cell lines resulted in the inclusion of the cryptic exon in this gene and was recently found to lead to *UNC13A* protein loss. Further, knockdown of TDP-43 promoted the inclusion of this cryptic exon. Two polymorphisms associated with ALS and FTD in *UNC13A* also overlap with TDP-43 binding sites (Brown *et al.*, 2022). ALS risk-associated single nucleotide polymorphisms (SNPs) in *UNC13A* are located in the intron containing the cryptic exon and they promote the inclusion of this exon (Ma *et al.*, 2022). The presence of TDP-43 mislocalisation from the nucleus to the cytoplasm to form aggregates in 97% of ALS cases implicates the subsequent deregulation of *UNC13A* protein in almost all ALS cases (Neumann *et al.*, 2006).

*UNC13A* has a role in neurotransmitter release, by interacting with syntaxin-1 to bring the SNARE complex together and bridge the vesicle membrane with the plasma membrane (Magdziarek *et al.*, 2020). *UNC13A* is also crucial to synaptic vesicle release and mice with *Munc13-1* (equivalent to *UNC13A* in humans) knockout have a 90% reduction in the amount of synaptic vesicles and therefore a reduction in the action potential-mediated glutamate release (Augustin *et al.*, 1999).

The upregulation of *UNC13A* by log2FoldChange of 1.568 upon miR-340 overexpression suggests miR-340 as a potential therapy to promote increased *UNC13A* protein, which could rescue reductions in neurotransmitter release and increase survival of ALS patients. We attempted to validate the *UNC13A* protein levels in astrocytes by western blotting, but failed to observe any antibody signal. Future work could validate the increase of *UNC13A* RNA levels by qPCR.

A comparison of the mRNAs with changed expression upon miR-340 mimic transfection, with 154 known ALS relevant genes reported on ALSod (updated in 2020), revealed 24 ALS relevant genes (15.6% of ALS relevant genes) were among

those statistically significantly altered by miR-340 overexpression. 11 of these genes were upregulated, whilst 13 were downregulated by miR-340 in HeLa cells (Table 15). Of all 1,826 mRNAs with significantly altered expression induced by miR-340 overexpression, notably *UNC13A* was the third most deregulated with an adjusted p value of  $2.94 \times 10^{-24}$  and log2Foldchange of 1.568 (Table 10) and was both the most significantly altered mRNA and the mRNA with the greatest fold change of the ALS-associated mRNAs with altered expression upon miR-340 overexpression.

**Table 15: ALS-relevant mRNAs with altered expression induced by miR-340 overexpression in HeLa cells.** The 24 ALS-relevant genes from ALSod also significantly deregulated upon miR-340 overexpression with their log2FoldChange. Genes are ordered by their adjusted p value (Padj). Genes of interest are shown with a red asterisk.

Gene Name	Log2FoldChange	Padj
* UNC13A	1.568	2.937E-24
ERLIN1	-0.545	7.639E-08
VPS54	-0.459	1.816E-05
* SQSTM1	-0.559	2.758E-05
ZNF512B	0.464	7.775E-05
CCNF	0.586	0.0001
MAOB	0.375	0.0011
LMNB1	0.331	0.0023
LIF	-0.368	0.0041
CAV2	-0.439	0.0044
DNMT3B	0.397	0.0049
TUBA4A	-0.312	0.0081
GARS	0.286	0.0086
ANXA11	0.280	0.0092
SOD2	-0.246	0.0153
NEK1	-0.363	0.0218
ARHGEF28	-0.415	0.0246
AR	-0.276	0.0281
LUM	0.355	0.0314
ALS2	-0.278	0.0331
MAPT	-0.701	0.0345
EWSR1	0.194	0.0364
DNMT3A	0.288	0.0371
B4GALT6	-0.308	0.0458

We also compared the mRNAs altered by miR-340 overexpression in HeLa cells with a list of 781 known autophagy genes (taken from Human Autophagy Database) and found an overlap of 85 genes. The 30 most significantly deregulated are given in Table 16. Overall, 15 autophagy related genes were found upregulated and 15 were downregulated. It is noteworthy that *NFE2L2*, the gene for NRF2 was the most statistically significantly altered by miR-340 overexpression, with a log2FoldChange of -0.910, consistent with our and others' findings and is indicated with a red asterisk in Table 16.

**Table 16: Autophagy-relevant mRNAs with altered expression induced by miR-340 overexpression in HeLa cells. The 30 most significant autophagy-relevant genes deregulated upon miR-340 overexpression with their log2FoldChange. Genes are ordered by their adjusted p value (Padj)**

Gene Name	log2FoldChange	padj
* NFE2L2	-0.910	4.94E-19
SLC7A11	-2.525	1.27E-13
CAPN7	-0.790	4.10E-12
SMPD1	0.840	1.20E-11
MAPK8IP2	1.284	4.94E-10
ACBD5	-0.786	2.30E-09
E2F2	0.615	2.17E-07
PPP2R1B	-0.493	2.85E-07
SESN1	-0.632	2.37E-06
SEC24D	0.503	7.45E-06
CAPN10	-0.644	1.36E-05
PREX1	0.410	2.35E-05
SQSTM1	-0.559	2.76E-05
MTMR2	-0.364	3.02E-05
SEC23A	-0.448	3.33E-05
MAPKAP1	0.452	3.76E-05
PRKAA2	-0.438	5.60E-05
SEC16A	0.335	7.06E-05
VPS41	-0.428	8.42E-05
GBF1	0.388	8.82E-05
TBC1D5	-0.422	9.24E-05
PPP2R5C	0.356	0.00019
AP3B2	0.587	0.00030
KLHL13	0.382	0.00037
MYLK3	0.555	0.00038
AURKA	0.372	0.00051
PLD1	-0.316	0.00059
TNS3	0.354	0.00068
MARK3	0.370	0.00084
KLHL3	-0.908	0.00095

Next, mRNAs significantly deregulated by miR-340 overexpression were compared with both ALS and autophagy genes. This revealed two genes were among all three groups - *SQSTM1* and *SOD2* (Figure 33).

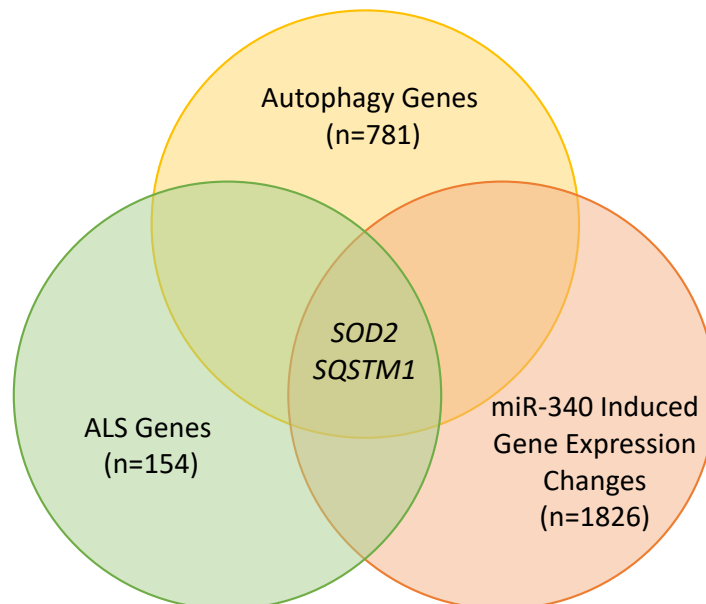


**Figure 33: Comparison of mRNAs with significantly altered expression upon miR-340 overexpression in HeLa cells, with known ALS and autophagy genes. *SOD2* and *SQSTM1* are the two genes common to all three groups.**

The protein p62 (encoded by *SQSTM1*) is extensively implicated in ALS and its role in the disease is discussed in section 1.2.4.1. MiR-340 overexpression was associated with the significant downregulation of *SQSTM1* at the mRNA level ( $\log_2\text{FoldChange} = 0.56$ ,  $p = 2.8 \times 10^{-5}$ ) which adds confidence to the role of miR-340 in ALS. Whilst *SOD1* mutations account for around 20% of fALS cases, the link between *SOD2* and ALS is tenuous. Whilst *SOD1* is localised largely to the cytoplasm, *SOD2* resides within the mitochondrial matrix in both mouse lung and liver tissue and human cell lines, where it functions as an antioxidant enzyme (Weisiger and Fridovich, 1973). Here it is in close proximity to the electron transport chain where the inevitable production of reactive oxygen species as a by-product of oxidative phosphorylation occurs, including superoxide free radicals ( $\text{O}_2^-$ ). *SOD2* catalyses superoxide species into

hydrogen peroxide which is further converted to water and oxygen molecules by catalase (Cadenas and Davies, 2000).

#### 5.2.2.1 A Pipeline for Distinguishing Potential Direct and Indirect Targets of miR-340

We next attempted to develop a pipeline to determine potential direct and indirect targets of miR-340, using miRNA-target prediction software (Figure 35A). Firstly, a comparison of the mRNAs with altered expression resulting from miR-340 overexpression in HeLa cells was made with the predicted human target genes of hsa-miR-340. To establish a robust list of predicted targets of miR-340, the results of DIANA-Tools v5.0 and Target Scan v8.0 were combined, which generated a list of 2,085 human mRNAs predicted to be directly targeted by hsa-miR-340. Although by default the threshold of DIANA-Tools miRNA-target predictions is set at 0.8 for miTG scores, here the threshold was set at 0.2 to encompass all mRNAs with potential MREs for miR-340. Cross-referencing with mRNAs with altered expression induced by miR-340 in HeLa cells, revealed that 1,016 of these 1,826 mRNAs with altered expression were also predicted to be targeted by miR-340. It is likely that miR-340 **directly** binds these mRNAs through one or more of their predicted MREs to result in the deregulation of this mRNA. The remaining 44% (810) of the mRNAs with altered expression which were not predicted as miR-340 targets, lack any clear MREs which would have otherwise determined the mRNA as a predicted target of miR-340 by the bioinformatic miRNA-target predictions. Broadly, the result is a group of mRNAs which may not be directly targeted by miR-340, but whose altered expression is **indirect** of miR-340 (Figure 34A).

To these miR-340 'directly' and 'indirectly' deregulated mRNAs their fold change (given as log<sub>2</sub>FoldChange) was then considered. This enabled mRNAs with altered expression to be represented by both their fold change and their status as a predicted target of miR-340 (either yes or no) (Figure 34B).

We considered those direct mRNA targets (i.e., those predicted as miR-340 targets) with a negative fold change from mRNA sequencing, expected of mRNAs targeted by

miR-340 upon overexpression of miR-340. These mRNAs likely possess MREs through which they directly interact with miR-340, causing degradation of their mRNA and resulting in their downregulation. The genes are depicted in the bottom left quadrant of Figure 34B. They number 547 and account for 30% of mRNAs with expression altered by miR-340.

mRNAs depicted in the top left quadrant of Figure 34B are also predicted to be targeted by miR-340, though experimentally were observed to be upregulated upon miR-340 overexpression. These genes could perhaps represent the false positive rate of miRNA target prediction software, (which has been estimated is as high as 50%) but could also be examples of mRNAs to which miR-340 directly binds and results in their upregulation, rather than downregulation (Pinzón *et al.*, 2017). This phenomenon of upregulation of a mRNA by a miRNA has been shown to occur in specific conditions such as quiescent cells and cells in cell cycle arrest (Truesdell *et al.*, 2012).

We next considered those indirect mRNA targets (i.e. those not predicted as miR-340 target mRNAs which do not contain clear MREs through which to bind miR-340). The mRNAs depicted within the top right quadrant of Figure 34B were experimentally observed to be increased when miR-340 was overexpressed, the opposite direction of regulation to that expected for miR-340 regulation. This group numbers 533 genes and accounts for 29% of deregulated genes. The genes depicted within the bottom right quadrant were downregulated in response to miR-340 overexpression, the expected direction of change for mRNAs targeted by miR-340, although this is likely not the result of direct miR-340 binding. They number 277 genes, accounting for 15% of deregulated genes.

Recently, the importance of distinguishing between mRNAs directly or indirectly targeted by a miRNA has been highlighted by Amin and colleagues, who recognised that whilst mRNAs classed as *direct* miRNA targets exhibited an inversely proportional relationship with miR-218 (an ALS-associated miRNA) dose in a mouse model, mRNAs the authors classed as *indirect* targets displayed a directly proportional one (Amin *et al.*, 2021). Briefly, as miR-218 genetic expression within

mice decreased, the expression of *directly* targeted mRNAs increased, whilst the expression of *indirectly* targeted mRNAs decreased in a dose-sensitive manner. The authors suggested that genes may contribute distinctly to motor neurone function depending on whether miR-218 *directly* or *indirectly* regulated them.

We observed both *NFE2L2* (the gene encoding NRF2) and *SQSTM1* (the gene encoding p62) were among those mRNAs predicted to be targeted by miR-340 and were downregulated (bottom left quadrant). It therefore seems likely these genes are direct targets of miR-340. However, it should be noted that HeLa cells in this instance were transfected with a constant concentration of miR-340, whereas Amin and colleagues utilised mice which together harnessed a titration of miR-218 (Figure 35). Some subtlety in the classification of direct or indirect targets of miR-340 will be missed without observing the impact on mRNA with changing miR-340 concentration. Of the ALS-relevant genes whose mRNA expression was altered by miR-340 overexpression in HeLa cells, those classified as direct (expected or unexpected) or indirect targets of miR-340 are shown in Table 17. Most were classed as 'direct' and expected (42%), which is greater than the portion of mRNAs classed as 'direct' and unexpected (25%). In total 67% were classed as 'direct' targets whilst 33% were classed as 'indirect'.

**Table 17: ALS-relevant genes with altered expression in HeLa cells with overexpressed miR-340 classed as 'direct' or 'indirect' targets of miR-340.** Those with decreased expression and with DIANA-Tools microT-CDS (threshold 0.2) or TargetScan miR-340 target predictions were classed as direct and expected targets of miR-340. Those upregulated with miR-340 target predictions were classed as direct and unexpected targets of miR-340 and those without miR-340 target predictions were classed as indirect targets of miR-340.

<b>Direct + Expect</b>	<b>Direct + Unexpected</b>	<b>Indirect</b>
ERLIN1	ZNF512B	CCNF
ALS2	DNMT3A	ANXA11
AR	DNMT3B	GARS
ARHGEF28	EWSR1	MAOB
B4GALT6	LMNB1	MAPT
CAV2	LUM	TUBA4A
LIF		UNC13A
NEK1		
SOD2		
SQSTM1		
VPS54		

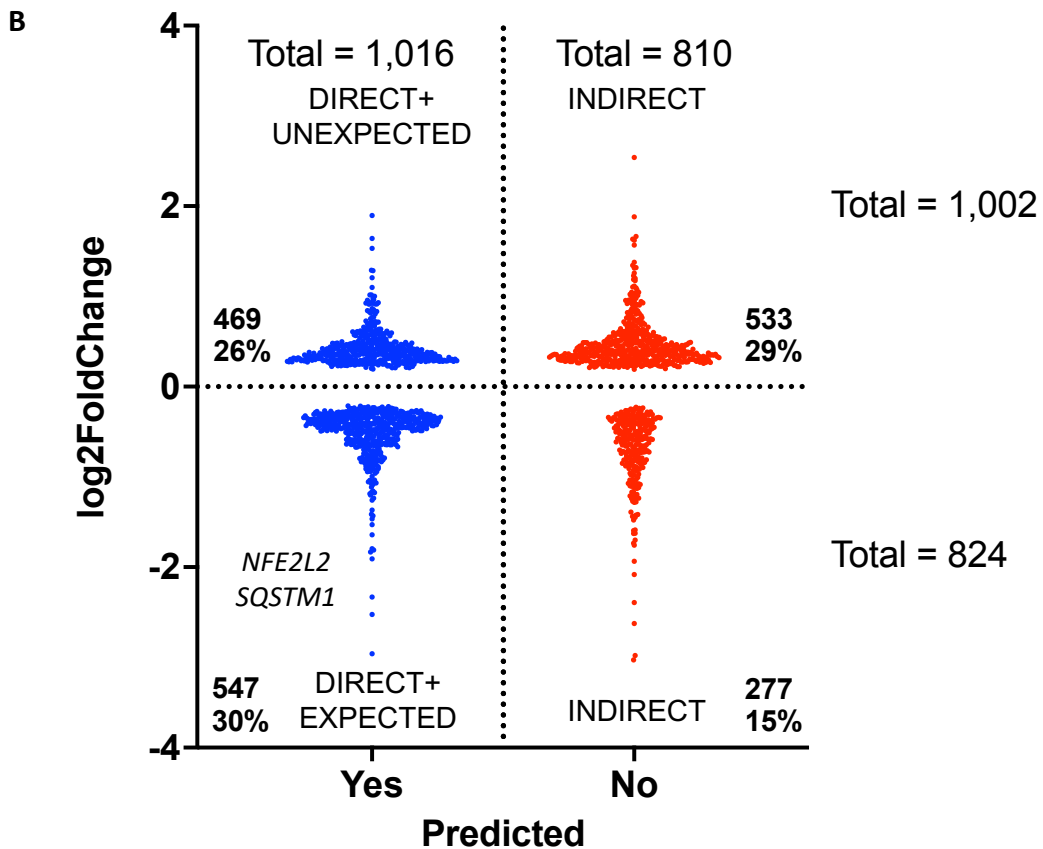
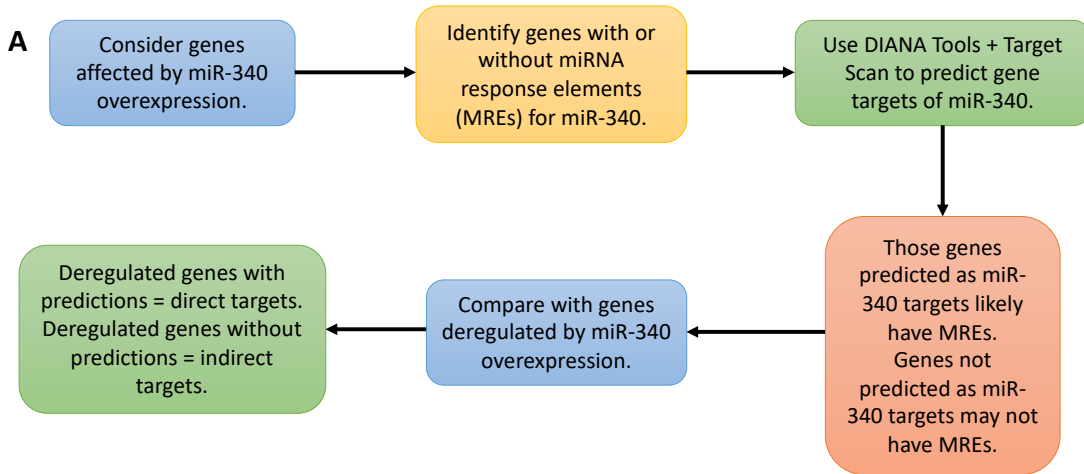


**Figure 34: Identifying potential miR-340 direct and indirect gene targets.** A) Diagrammatic representation of the methodology behind assigning mRNAs with altered expression upon miR-340 overexpression in HeLa cells, as direct or indirect targets. B) mRNAs with altered expression induced by miR-340 were ordered by their log<sub>2</sub>FoldChange and then categorised on whether they appeared as a predicted target of miR-340-5p based on DIANA-Tools v3.0 and TargetScan v8.0. The numbers in the corner of each quadrant depict the total genes in that quadrant. The number of genes in each quadrant is given as a percentage of the total number of deregulated genes (1,826).

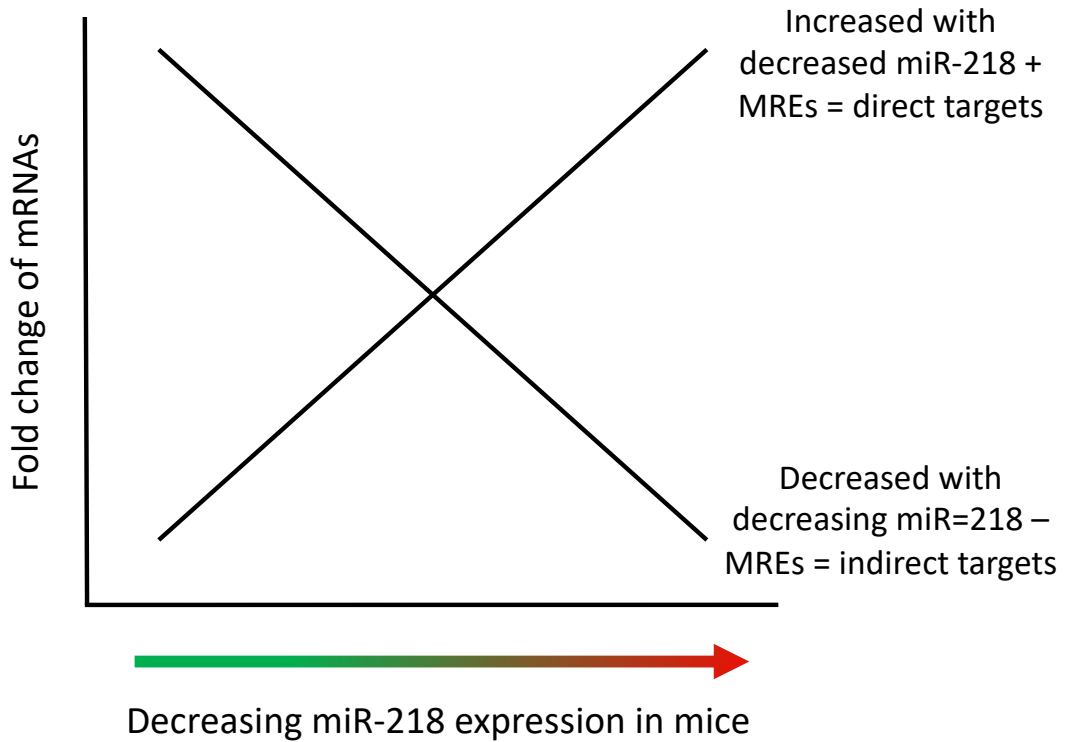


**Figure 35: Representation of Amin and colleagues' findings in mice with decreasing miR-218 expression.** As the expression of miR-218 in mice decreases, some mRNAs were increased and possess MREs and are classed as direct targets. Some mRNAs were decreased and do not possess MREs and are classed as indirect targets.

Here we have shown that by combining mRNA sequencing data of genes influenced by overexpression of a miRNA with bioinformatic miRNA target predictions, potential mechanistic insight can be explored. Since the work by Amin and colleagues (as discussed above) has highlighted the functional importance of distinguishing directly and indirectly miR-218 regulated genes, future work could test the expression of potential directly and indirectly targeted genes in response to gradual increases or decreases of miR-340, as opposed to a single concentration of miR-340 overexpression (Amin *et al.*, 2021).

### 5.3 Conclusions and Future Directions

Here we selected a human primary astrocyte cell line with relevance to ALS, and found that upon inhibition of endogenous miR-340, the levels of NRF2 protein were increased compared to control, consistent with an NRF2 decrease in HeLa cells transfected with a miR-340 mimic. Overexpression of NRF2, specifically in astrocytes, has been shown to protect neurones from hSOD1<sup>G93A</sup> toxicity, and a miR-340 inhibitor could be used as a therapeutic, elevating NRF2 levels in ALS patients and provide support to neurones (Vargas *et al.*, 2008, 2013). To this end, future work could determine the impact of miR-340 inhibition on subsequent antioxidant gene production since their increase would be expected to coincide with increased NRF2 expression.

Interestingly, we found TBK1 protein levels were significantly reduced when human primary astrocytes were treated with a miR-340 inhibitor, though rationally an increase in TBK1 levels were expected. We speculate this was caused indirectly by miR-340, specifically, that miR-340 inhibition triggered the upregulation of genes which encode proteins that normally function to target TBK1 for degradation such as *DYRK2* and *DTX4* (Cui *et al.*, 2012; An *et al.*, 2015). Further work is needed to determine whether *DYRK2* and *DTX4* are direct targets of miR-340 using the luciferase assay and western blotting. However, if this is found to be true, it would be difficult to increase the TBK1 levels by miR-340, since the inhibition of highly expressed miR-340 leads to a decrease in TBK1 levels, as does the overexpression of miR-340 in HeLa cells.

We then sought to explore the broader impact of miR-340 on human genes by performing mRNA sequencing of human primary astrocyte cells treated with a cell permeable miR-340 inhibitor. This revealed 73 mRNAs were significantly altered compared to control, though there was no overlap with known autophagy or ALS genes and of the 30 most significantly deregulated, only six were protein coding. To extend this work, we performed mRNA sequencing of HeLa cells transfected with a miR-340 mimic or control. This resulted in the dysregulation of 1,826 mRNAs compared to the control and 94% represented protein coding genes. These mRNAs

included 24 or 15.6% of known ALS genes according to ALSod, including *UNC13A*, which was the mRNA with the third most statistically significant expression change and was among the top ten most upregulated mRNAs of all 1,826. This is of particular importance as recent connections between TDP-43 dysregulation and *UNC13A* protein reduction have been made, which demonstrates *UNC13A* is a potential therapeutic target for 97% of ALS cases (Brown *et al.*, 2022; Ma *et al.*, 2022). Additionally, autophagy-relevant genes were dysregulated by miR-340 overexpression, including *NFE2L2*, the gene encoding NRF2, which was among the overall most significantly deregulated and was downregulated, consistent with ours' and others' findings.

We proposed that using RNA sequencing data alongside proteomics data, from either quantitative mass spectrometry or western blotting could provide insight into the possible mechanism of a miRNA's mode of mRNA repression, whether inhibition of translation or mRNA decay.

Next, by cross-referencing mRNAs with altered expression by miR-340 overexpression with mRNAs predicted to be targets of miR-340, we classified miR-340 deregulated mRNAs as 'direct' targets or 'indirect' targets of miR-340. We generalised that mRNAs predicted to be targeted by miR-340 (by DIANA-Tools and TargetScan) likely possessed MREs for miR-340 and would therefore be directly bound by the miRNA.

mRNAs classed as 'direct' targets were predicted to be targeted by miR-340. Of the 'direct' targets, those downregulated by miR-340 overexpression – the expected direction of mRNAs targeted by miR-340 – accounted for 30% of deregulated genes and were the true direct targets. Those upregulated by miR-340 overexpression accounted for 26% of mRNAs with expression changes and may give an indication of the false positive rate of miRNA-target prediction software. Alternatively, it has been shown on some occasions, such as in cell cycle arrest, that miRNAs directly bind mRNAs and cause their protein upregulation, rather than downregulation (Truesdell *et al.*, 2012).

Those classed as 'indirect' targets were not predicted to be targeted by miR-340. Those upregulated by miR-340 overexpression – the opposite direction expected for mRNAs targeted by a miRNA – accounted for 29% of mRNAs with altered expression. Those downregulated by miR-340 overexpression accounted for 15% of mRNAs with altered expression, though it is unlikely they are downregulated by direct binding of miR-340.

Determining direct and indirect gene targets of disease relevant miRNAs has been shown to have functional importance, as in a mouse model where miR-218 expression decreases, direct gene targets were shown to increase in a dose dependent manner, whilst indirect gene targets were shown to decrease in a dose dependent manner. These two groups may contribute distinctly to the function of motor neurones (Amin *et al.*, 2021). This form of analysis could be routinely performed to identify potential mechanisms of action of miRNAs and may contribute to our understanding of miRNA-induced functional changes in ALS models.

# Chapter 6 - Investigation of Autophagy Failure – Impact on Extracellular Vesicle Proteomes

## 6.1 Introduction

In Chapter 4 we provided evidence that overexpression of miR-340, a miRNA found dysregulated in ALS patients, inhibited autophagic flux in HeLa cells using a live cell autophagy assay. This potentially occurred by direct targeting of *TBK1* (an ALS relevant gene), with a subsequent decrease in TBK1 protein levels. This impacted on events downstream of TBK1, such as in the reduction of Ser-403 phosphorylated p62. Here, in an exploratory study, we modelled another downstream consequence of autophagy failure, specifically, the impact on exosome biology and their protein composition. We hypothesised that inhibition of autophagy will alter the exosomal protein content, including ALS and autophagy-relevant proteins.

### 6.1.1 Extracellular Vesicles

Almost all eukaryotic cell types release extracellular vesicles containing a range of biologically active cytosolic components such as proteins, DNA and RNA into the surrounding body fluid (Y. Zhang *et al.*, 2019). There are three types of extracellular vesicle; ectosomes (also known as microvesicles), exosomes and apoptotic bodies. Vesicles formed from budding of the plasma membrane are classed as ectosomes, whilst exosomes are formed from multivesicular bodies (MVBs) or endosomes. On the other hand, apoptotic bodies are released from dying cells undergoing apoptosis (Cocucci and Meldolesi, 2015).

#### 6.1.1.1 Exosomes

All cell types secrete exosomes and they have been identified in a wide range of biological fluids (L. M. Doyle and Wang, 2019). Exosomes are smaller than ectosomes, with a diameter within the range of 30-200 nm compared to 200-500 nm (Cocucci and Meldolesi, 2015). Originally, exosomes were considered cellular waste, but more

recently, it has been discovered they carry specific cargo which can be transmitted to target cells, to participate in short and long-range intercellular communication.

#### 6.1.1.2 Exosome Biogenesis

Exosome biogenesis begins when early endosomes mature into late endosomes (Meldolesi, 2018). Invagination of the endosomal membrane forms intraluminal vesicles (ILVs) within the late endosomes themselves, which are now termed multivesicular bodies (MVBs) (Figure 36) (Huotari and Helenius, 2011). Ubiquitinated cargo proteins are recognised by the endosomal sorting complex required for transport (ESCRT) machinery, specifically by ESCRT-0 which is comprised of two ubiquitin binding subunits, enabling its affinity to endosomes enriched with ubiquitinated substrate (Henne, Buchkovich and Emr, 2011). The proteins are sequestered to the endosomal membrane where they become the cargo of ILVs (Clague, 2002; Villarroya-Beltri *et al.*, 2014). ESCRT-0 sequesters ESCRT-I which recognises ubiquitinated cargo and aids their sorting into the MVBs (Katzmann, Babst and Emr, 2001). Together they interact with ESCRT-II and form a complex with ESCRT-III, which initiates budding of the endosomal membrane. ESCRT-III is also involved in the deubiquitination of proteins and allows the budding membrane to close into ILVs (Henne, Buchkovich and Emr, 2011). The ESCRT complex then dissociates from the MVB using energy driven by the AAA-type ATPase, VPS4 (Babst *et al.*, 1997). An alternate molecular mechanism of exosome biogenesis has been proposed, which occurs without ESCRT machinery, since silencing of subunits from all four ESCRT complexes (ESCRT-0-III) still allowed the formation of ILVs within MVBs (Stuffers *et al.*, 2009). This was proposed to occur through neutral sphingomyelinase 2 (nSMase2), since inhibition of this enzyme with the drug, GW4869, in an oligodendroglial cell line, reduced exosome release (Trajkovic *et al.*, 2008). The dependence on nSMase2 in exosome release may be cell dependent, since inhibition of Smase2 in PC-3 cells did not reduce exosome release (Phuyal *et al.*, 2014).

MVBs are directed to the plasma membrane through interactions with the actin and microtubule cytoskeleton (Villarroya-Beltri *et al.*, 2014). Rab GTPases play a critical role in the transport of MVBs to the plasma membrane. For example Rab27a and

Rab27b convey MVBs rich in cholesterol to the plasma membrane (Möbius *et al.*, 2002). Knockdown of either reduces the MVBs docking to the plasma membrane and inhibits exosome release (Ostrowski *et al.*, 2010). Rab11 and Rab35 have also been shown to have roles in the docking and fusion of MVBs with the plasma membrane (Wilcke *et al.*, 2000; Hsu *et al.*, 2010). The fusion of MVB membranes to the plasma membrane is enabled by SNARE and Rab proteins, though the exact mechanisms are not fully understood. The R-SNARE, VAMP7, has been shown to be necessary for exosome release in the human cell line, K562 (Fader *et al.*, 2009). The ILVs are secreted extracellularly as exosomes upon fusion of the MVB membrane with the plasma membrane (Figure 36) (Pan *et al.*, 1985).

### 6.1.1.3 Autophagy and Exosome Biogenesis

Within the endolysosomal pathway, autophagy and exosome biogenesis overlap. Rather than fuse with the plasma membrane, MVBs containing ILVs from the endosomal pathway may fuse with autophagosomes from the autophagy pathway (Pan *et al.*, 1985; Berg *et al.*, 1998). This forms hybrid like intermediates called amphisomes which may go on to fuse with lysosomes where their cargo is degraded (Figure 36). MVBs may also directly fuse with lysosomes (Futter *et al.*, 1996).

Critically, it has been shown that induction of autophagy can inhibit exosome release, indicating MVBs become directed to autophagosomes for lysosomal degradation rather than the plasma membrane for exosome release (Fader *et al.*, 2007). Further, the autophagy related proteins ATG5, ATG16L1 and the ATG12-ATG3 complex have been implicated in exosome biogenesis and release. Knockout of ATG5 or ATG16L1 reduced exosomal release, whilst loss of the ATG12-ATG3 complex changed MVB morphology and reduced exosome biogenesis (Guo *et al.*, 2017; Murrow *et al.*, 2015). The LC3-conjugation pathway mediates the packaging and secretion of a range of RNA binding proteins and small non-coding RNAs in EVs (Leidal *et al.*, 2020).

Unconventional protein secretion (UPS) is an alternate pathway with similarities to both autophagy and exosome biogenesis. Here, cytosolic proteins which lack signal peptides that would otherwise direct them to the (ER) for trafficking to the golgi and

plasma membrane, are secreted into the extracellular space. This can occur through secretory autophagy, so called because the autophagy machinery is involved in this process. Rather than degradative autophagy or the release of exosomes, autophagosomes may fuse directly with the plasma membrane to release peptides into the extracellular space (Jiang *et al.*, 2013; Kimura *et al.*, 2017).

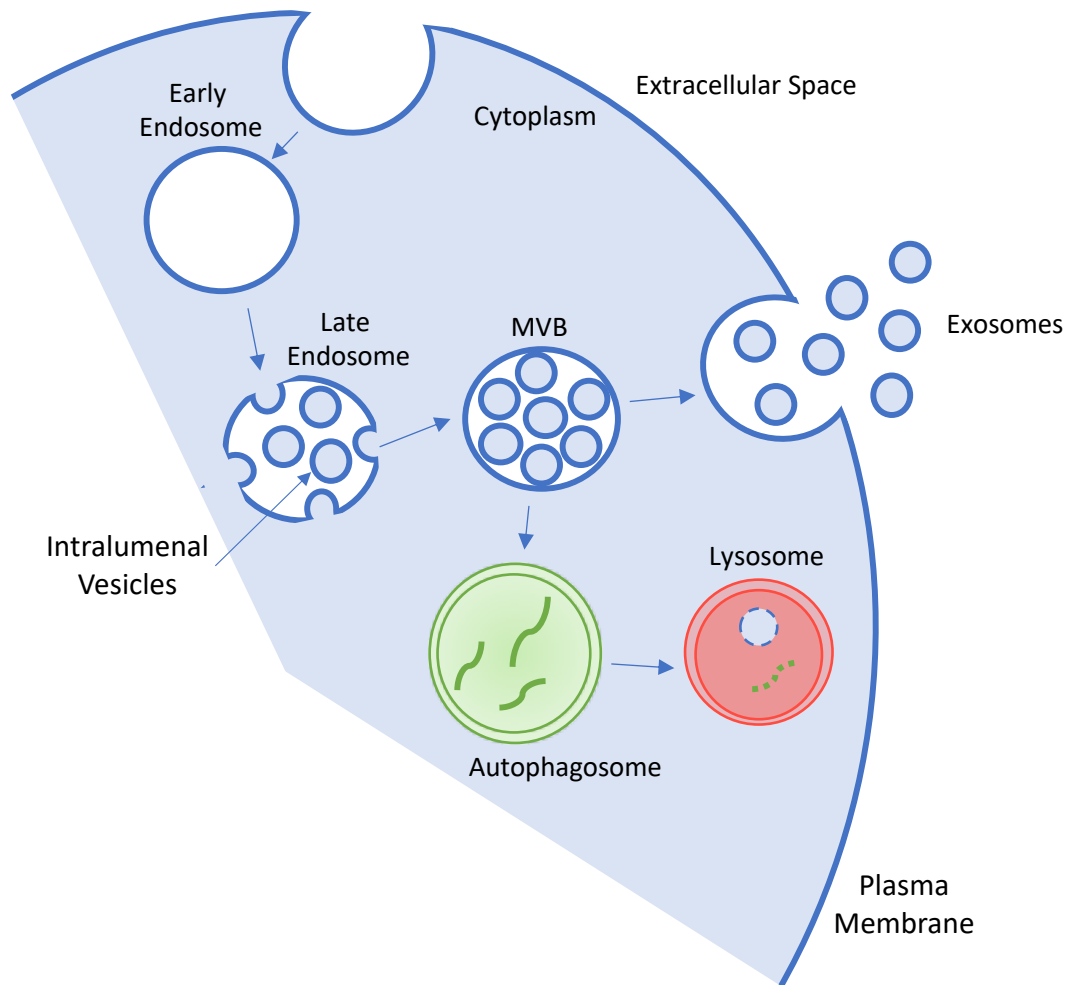


**Figure 36: Exosome biogenesis and overlap with the autophagy pathway.** The early endosome matures into the late endosome and invagination of the membrane creates intraluminal vesicles within the multivesicular body (MVB). Upon fusion with the plasma membrane these intraluminal vesicles are released into the cytoplasm as exosomes. Alternatively, the MVBs can fuse with autophagosomes and the contents are degraded in lysosomes. Drawn by author.

#### 6.1.1.4 Exosomal Contents

Exosomes contain all molecular constituents of cells, including DNA, RNA, proteins, lipids and metabolites, which are selectively loaded into exosomes depending on post-translational modifications or specific motifs (Clague, 2002; Villarroya-Beltri *et al.*, 2013a, 2014). Several proteins which are enriched in exosomes are often used as exosome markers. For example, ALIX is an ESCRT accessory protein expected to belong in exosomes and commonly used as an exosomal marker (Morita *et al.*, 2007). TSG101 is an ESCRT-1 subunit and is also commonly used as a marker for exosomes (Yoshioka *et al.*, 2013). CD9, CD63 and CD81 belong to the tetraspanin family, which are transmembrane proteins often found in exosomes and considered exosomal markers (L. Doyle and Wang, 2019). Of these, CD81 is the most exosome enriched, whereas CD63 is the least (Escola *et al.*, 1998). Tetraspanins are also involved in ESCRT-independent release of exosomes (Escola *et al.*, 1998). Flotillin-1 associates with lipid domains in the membrane of exosomes making it a common cargo that is also often used as an exosome marker (De Gassart *et al.*, 2003). Knockout of CD9 and CD63 have been shown to reduce the release of exosomes (Chairoungdua *et al.*, 2010; Hurwitz *et al.*, 2016).

Lipids are essential to vesicular transport and play a crucial role in membrane curvature (McMahon and Boucrot, 2015). Lipid anchored proteins are also present on the exosomal membrane, including CD39 and CD73 (Clayton *et al.*, 2011). nSMase2 converts sphingomyelin to ceramide and is a lipid modifying enzyme, demonstrating the crucial involvement of lipids in the release of exosomes. Ceramide was identified as enriched in exosomes in a mouse oligodendroglial cell line, Oli-neu (Trajkovic *et al.*, 2008).

Since exosomes harbour molecular contents from both healthy and diseased cells, the composition of their cargo is of great interest and is reported on databases such as ExoCarta (<http://www.exocarta.org>) and Vesiclepedia (<http://microvesicles.org>), online collections of exosomal proteins, RNA and lipids from various species. In the case of Vesiclepedia, data is collected regarding all types of EV, whereas ExoCarta is specific for exosomes (Keerthikumar *et al.*, 2016; Pathan *et al.*, 2019).

#### 6.1.1.5 *MicroRNAs as Exosomal Cargo*

Exosomes have been shown to contain 'active' miRNA, which can regulate mRNA targets in recipient cells (Valadi *et al.*, 2007; Montecalvo *et al.*, 2012). For example, treatment of endothelial cells with exosomes derived from the breast cancer cell line, MDA-MB-231, with high miR-105, was found to reduce the expression of the tight junction protein, ZO-1, an effect abolished upon transfection with a miR-105 inhibitor (Zhou *et al.*, 2014). Indeed, a subset of miRNAs, including miR-142-3p and miR-150-5p, were found to be preferentially incorporated into exosomes secreted from HEK293T cells, suggesting a mechanism of active sorting of specific miRNAs into exosomes is utilised (Guduric-Fuchs *et al.*, 2012). Further, it is likely that nSMase2 is involved in active miRNA sorting into exosomes, since its inhibition with GW4869 reduced the number of extracellular miRNAs detected (Kosaka *et al.*, 2010). Interestingly, the RNA binding and ALS-associated protein, hnRNPA2B1, has been shown to bind the 3' end of miRNA sequences at a GGAG motif and cause specific miRNA loading into exosomes (Villarroya-Beltri *et al.*, 2013b). Similarly, in several mouse cell lines, Fus has also been shown to increase loading of miRNAs with a CGGGAG motif into exosomes. Further, this resulted in downregulation of these miRNA's targets (Garcia-Martin *et al.*, 2021). The RISC has also been implicated in the active sorting of miRNAs into exosomes, since it was found localised to MVBs. MiRNAs and mRNAs (which could be potential miRNA targets) were also enriched at these sites (Gibbings *et al.*, 2009). Additionally, it has been found that the 3' end-rich poly (A) miRNAs are more abundant in B-cells, whilst the 3' end-rich poly (U) miRNAs are more abundant in B-cell derived exosomes, suggesting this acts as a mechanism of specific miRNA sorting into exosomes (Koppers-Lalic *et al.*, 2014).

Over the past decade, studies have sought to determine miRNAs differentially expressed in ALS patient-derived exosomes compared to healthy controls. Table 18 shows a comprehensive list of the differentially expressed ALS patient-derived exosomal miRNAs. This table was adapted from Chen and colleagues (Chen *et al.*, 2021).

Next generation sequencing of 14 Primary ALS patient (PALS) plasma EVs identified 27 differentially expressed miRNAs compared to healthy controls, highlighting their potential as biomarkers of ALS (Saucier *et al.*, 2019). Another study identified 30 neurone-derived exosomal miRNAs differentially expressed between ALS patients and healthy controls (Katsu *et al.*, 2019). However, there was no overlap in the differentially expressed miRNAs between these studies, potentially due to the difference in body tissues used in the two studies which emphasises the need for standardised methods of exosomal isolation, as the former study used a synthetic peptide known as Vn96 which has high affinity for heat shock proteins on the surface of EVs, whereas the latter used immunopurification with an anti-CD171 antibody.

Of the miRNAs shown in Table 18, six overlapped with the miRNAs found in 5 or more studies of our systematic literature review, shown in Table 7, section 3.2.2. These miRNAs were miR-124-3p, miR-127-3p, miR-183-5p, miR-338-3p, miR-100-5p and miR-151a-5p. They are shown with a red asterisk (\*) in Table 18.

**Table 18: Differentially expressed miRNAs found in ALS patient-derived exosomes.** The miRNA name, expression level and sample type are given. Table adapted from Chen et al., 2020. MiRNAs also found most frequently dysregulated in our systematic literature review in section 3.2.2 are shown with a red asterisk (\*).

Exosomal miRNA	Expression Level	Sample Type	Exosomal miRNA	Expression Level	Sample Type
miR-124	Up	NSC-34 Cells	miR-199a-2-3p	Up	Plasma
miR-124a	Up	Astrocyte	miR-199a-1-3p	Up	Plasma
* miR-124-3p	Up	CSF	miR-27a-3p	Down	Plasma
miR-4736	Up	Plasma	miR-1268a	Down	Plasma
miR-4700-5p	Up	Plasma	miR-2861	Down	Plasma
miR-1207-5p	Up	Plasma	miR-4508	Down	Plasma
miR-4739	Up	Plasma	miR-4507	Down	Plasma
miR-4505	Up	Plasma	miR-3176	Down	Plasma
miR-24-3p	Up	Plasma	miR-4745-5p	Down	Plasma
miR-149-3p	Up	Plasma	miR-3911	Down	Plasma
miR-4484	Up	Plasma	miR-3605-5p	Down	Plasma
miR-4688	Up	Plasma	miR-150-3p	Down	Plasma
miR-4298	Up	Plasma	miR-3940-3p	Down	Plasma
miR-939-5p	Up	Plasma	miR-4646-5p	Down	Plasma
miR-371a-5p	Up	Plasma	miR4687-5p	Down	Plasma
miR-3619-3p	Up	Plasma	miR-4788	Down	Plasma
miR-4454	Up	Plasma	miR-4674	Down	Plasma
miR-9-1-5p	Up	Plasma	miR-1913	Down	Plasma
miR-9-3-5p	Up	Plasma	miR-634	Down	Plasma
* miR-338-3p	Up	Plasma	miR-3177-3p	Down	Plasma
miR-9-2-5p	Up	Plasma	miR-532-3p	Down	Plasma
* miR-100-5p	Up	Plasma	miR-144-3p	Down	Plasma
miR-7977	Up	Plasma	miR-15a-5p	Down	Plasma
miR-1246	Up	Plasma	miR-363-3p	Down	Plasma
miR-664a-5p	Up	Plasma	* miR-183-5p	Down	Plasma
miR-7641-1	Up	Plasma	miR-146a-5p	Up	Plasma
miR-1290	Up	Plasma	miR-199a-3p	Up	Plasma
miR-4286	Up	Plasma	miR-4454	Down	Plasma
miR-181b-1-5p	Up	Plasma	miR-10b-5p	Down	Plasma
miR-1260b	Up	Plasma	miR-29b-3p	Down	Plasma
miR-181b-2-5p	Up	Plasma	miR-151a-3p	Up	Plasma
* miR-127-3p	Up	Plasma	* miR-151a-5p	Up	Plasma
miR-181a-2-5p	Up	Plasma	miR-199a-5p	Up	Plasma
miR-181a-1-5p	Up	Plasma			

One study analysed the miRNA content of mouse astrocytes and their secreted exosomes, and found 54 miRNAs were expressed by at least two fold in the astrocyte secreted exosomes than in the astrocytes themselves, or were only detected in the exosomes (Jovičić and Gitler, 2017). Of these miRNAs, 27 were found with over 1,000-fold enrichment in exosomes. This further suggests specific miRNAs are

selectively loaded into exosomes and indicates exosomal miRNAs could be useful as biomarkers of disease. When exosomal miRNAs of wild type SOD1 astrocytes were compared to ALS-relevant SOD1<sup>G93A</sup> astrocytes, no miRNA expression changes were observed, though the media from SOD1<sup>G93A</sup> astrocytes was significantly more toxic to motor neurons than wild type SOD1 media. This indicates the toxicity may not be mediated by exosomal miRNAs. It should be noted however, that the study investigated expression changes of only the 752 miRNAs commercially available for TaqMan arrays so it cannot be excluded that astrocytic toxicity is mediated by exosomal miRNAs (Jovičić and Gitler, 2017). In contrast, other evidence suggests astrocyte-derived exosomal miRNAs could be fundamental to motor neurone survival. For example, downregulation of miR-494-3p, which modulates *SEMA3A* expression, was observed in *C9orf72* iAstrocyte derived exosomes. The upregulation of *SEMA3A* is associated with ALS. When mouse motor neurones were subject to the conditioned medium of *C9orf72* iAstrocytes treated with miR-494-3p mimic or negative control, the motor neuronal *Sema3A* expression was reduced and survival of motor neurones increased with miR-494-3p treatment (Varcianna *et al.*, 2019).

#### **6.1.1.6 Exosome Functions**

Whilst originally thought to be carriers of cell secreted waste, understanding of the role of exosomes has developed, and it is now understood they have a variety of physiological roles, including in immune regulation, tissue repair and cell maintenance (Robbins and Morelli, 2014; Takahashi *et al.*, 2017; Hettich *et al.*, 2020).

For example, exosomes secreted from antigen presenting cells can also present antigens, participating in the immune response (Zitvogel *et al.*, 1998). Additionally, cells release exosomes which contain biologically active proteins and nucleic acids which contribute to intercellular communication (Zaborowski *et al.*, 2015). This is mediated through exosomal cargo internalisation by a recipient cell through endocytosis, phagocytosis, macropinocytosis or by exosome interactions with extracellular receptors on recipient cells (Jan *et al.*, 2017). Once inside the recipient cell, the exosomes fuse with endosomes. To directly fuse with the plasma membrane and release their contents into the recipient cell cytoplasm, exosomes possess cell

adhesion molecules such as integrins on their surface to mediate membrane fusion (Mulcahy, Pink and Carter, 2014). This fusion is likely mediated by SNARE and Rab proteins (Jahn and Südhof, 2003). Endocytosis of exosomes can be clathrin-mediated, lipid raft-mediated or caveolin-mediated (Kiss and Botos, 2009; Valapala and Vishwanatha, 2011; Tian *et al.*, 2014). Macropinocytosis occurs when the cell membrane extends protrusions, which may join at the tips to form an enclosure around the extracellular exosomes to engulf them into an intracellular compartment termed a macropinosome (Costa Verdera *et al.*, 2017). Exosomes are released from both healthy and diseased cells, indicating they participate in normal cellular functions as well as the progression of disease (Fevrier *et al.*, 2004).

#### **6.1.1.7 Exosomes in ALS**

Exosomes are increasingly considered to play a role in the progression of neurodegenerative diseases. Cells of the CNS such as neurones, astrocytes, microglia, and oligodendrocytes are reported to secrete exosomes, though exosomes from each of these cell types contain different proteins either displayed on their external surface or within the lumen (Jan *et al.*, 2017). Further, astrocyte derived exosomes can promote neurone survival and neurite outgrowth (Wang *et al.*, 2011; Guitart *et al.*, 2016).

We identified that of the 154 known ALS genes from ALSod, 92 of their corresponding proteins were reported on ExoCarta as being detected in human-derived exosomes as of April 2022. Of these, VCP, PFN1 and ANXA11 were among the top 100 proteins reported in exosomes on ExoCarta (Figure 37). This implies exosomal pathways are relevant to ALS pathogenesis. Indeed, overwhelming evidence implicates exosomes in the spread of ALS pathology.

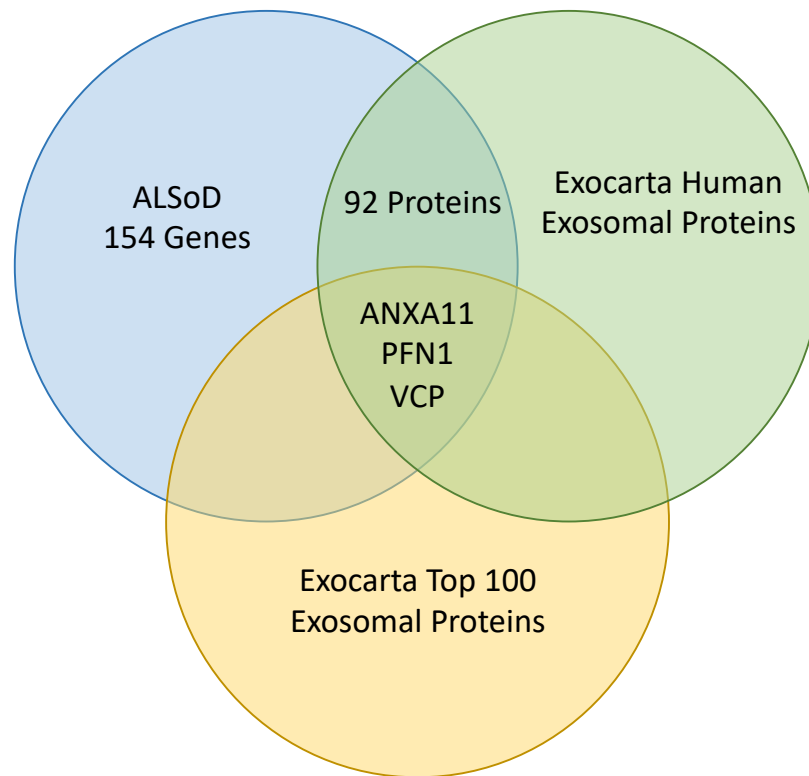


**Figure 37: Venn diagram showing the overlap between ALSod genes, the detected human exosomal proteins reported on Exocarta and the top 100 exosomal proteins reported on Exocarta.**

The ALS associated proteins SOD1, TDP-43 and *C9orf72* have each previously been implicated in the pathogenic spread of ALS *via* exosomes. TDP-43 was detected in EVs derived from N2A cells, though not microglia or astrocytes (Iguchi *et al.*, 2016). It was found enriched in exosomes from the CSF of ALS patients (Ding *et al.*, 2015). Further, TDP-43 positive aggregates were shown to be exported from cells within exosomes, preferentially taken up by neurones into the soma, and critically, were more toxic to the recipient cell than free TDP-43 (Feiler *et al.*, 2015). Exposure of glioma, U251 cells, to the CSF from ALS-FTD patients increased cellular mislocalisation and aggregation of TDP-43 C-terminal fragments after 21 days. Conversely, CSF from ALS patients alone did not produce the same effect (Ding *et al.*, 2015). Further, inhibiting exosome release in N2A cells using the nSMase2 inhibitor, GW4869, or by silencing Rab27A increased the amount of intracellular aggregated TDP-43, suggesting that exosomes are crucial to the cellular clearance of aggregated, misfolded and toxic TDP-43 (Iguchi *et al.*, 2016). Additionally, and of particular relevance to this thesis, autophagy inhibition with bafilomycin A1 caused an increase

of TDP-43 in exosomes suggesting TDP-43 that would otherwise have been degraded through autophagy, was now secreted from cells *via* exosomes (Iguchi *et al.*, 2016).

SOD1 was first detected in exosomes secreted from mouse NSC-34 cells overexpressing wild-type and mutant SOD1<sup>G93A</sup> (Gomes *et al.*, 2007). Critically, mutant SOD1 secreted by neurones transmitted ALS like traits to neighbouring neurones such as misfolding of SOD1 and indicates a prion-like role of SOD1 (Gomes *et al.*, 2007). Basso and colleagues exposed spinal neurones to astrocyte 'secretomes' containing fractions of purified or depleted exosomes. It was shown that SOD1 was only transferred to neurones when the secretome contained fractions of purified exosomes, demonstrating that SOD1 was likely transferred to motor neurones *via* exosomes. Motor neurones were also exposed to exosomes containing mutant SOD1<sup>G93A</sup> and this induced their death, whereas motor neurone cell viability was not effected by exosomes containing wild type SOD1 (Basso *et al.*, 2013). Similarly, conditioned media from HEK293 cells overexpressing ALS-relevant mutant SOD1<sup>G127X</sup> was applied to recipient HEK293 cells. This resulted in the recipient cells displaying intracellular mutant SOD1 accumulation (Grad *et al.*, 2014). The authors also found that the majority of the mutant SOD1 present in the conditioned media was present after centrifugation at 100,000 x g, consistent with its presence in exosomes. More recently, exosomes isolated from the brain and spinal cord of transgenic SOD1<sup>G93A</sup> mice as well as from human SOD1 ALS patient spinal cord tissues were found to be enriched in misfolded SOD1 compared to controls using immunoprecipitation with SOD1 misfolded antibodies (Silverman *et al.*, 2019).

The presence of the ALS associated hexanucleotide expansion in *C9orf72* prevents the interaction between *C9orf72* and Rab7L1, which regulates the transport of vesicles from MVBs to the plasma membrane. This lead to a reduction in the number of exosomes released from *C9orf72* ALS patient fibroblasts and iPSCs (Farg *et al.*, 2014; Aoki *et al.*, 2017). Additionally, DRPs from *C9orf72* expansions were released in the exosomes of iPSCs differentiated into spinal motor neurones from *C9orf72* ALS-FTD patients. These DRPs were transmitted from NSC-34 cells to primary cortical neurons (Westergard *et al.*, 2016).

FUS pull downs using GST-FUS constructs in HEK293 cells and subsequent gene ontology analysis identified that 42 of its protein partners were associated with exosomes. FUS was detected in the exosomes from N2A and SH-SY5Y cells overexpressing wild type FUS and the ALS-relevant mutants FUS<sup>R521G</sup> FUS<sup>R495X</sup>. The FUS<sup>R495X</sup> mutation was enriched in exosomes compared to the wild type and FUS<sup>R521G</sup> mutant (Kamelgarn *et al.*, 2016).

Additionally, null mutations in *GRN*, a major cause of FTD, resulted in a reduction in the number of released exosomes in human fibroblasts (Benussi *et al.*, 2016). Further, in FTD patient iPSC-derived neural stem cells, the N279K mutation in the ALS-associated gene, *MAPT*, impaired intracellular vesicle trafficking and caused a build-up of exosomes and also reduced the number of lysosomes (Wren *et al.*, 2015).

Recently, it has been suggested that NRF2 is involved in regulating the antioxidant properties of exosomes derived from human mesenchymal stem cells, which were used to treat oxidative damage in H<sub>2</sub>O<sub>2</sub>-stimulated epidermal keratinocytes (Wang *et al.*, 2020). Of particular relevance to ALS, the authors showed that in exosome recipient cells, the superoxide dismutase activities increased. Knockdown of NRF2 reduced the antioxidant capacity of the mesenchymal stem cell derived-exosomes, implicating NRF2 in the control of antioxidant properties of exosomes secreted from mesenchymal stem cells. Similarly, treatment of primary astrocytes with LPS initiated reactive astrogliosis, impaired calcium signalling and mitochondrial function and these effects were reduced upon treatment with mesenchymal stem cell-derived exosomes. Importantly, NRF2 knockdown decreased the protective effect of these exosomes (Xian *et al.*, 2019).

The participation of TBK1 in the regulation of exosomes is relatively unreported. Recently, overactivation of TBK1 was found to increase exosome release in Chinese hamster ovary cells, measured by levels of CD63 (Zhang *et al.*, 2021).

In summary, exosomes may contain all cellular molecular components including proteins and RNA, which may be selectively packaged into and exported *via* exosomes. Indeed, several miRNAs were shown to be preferentially incorporated

into exosomes and many have been found dysregulated in ALS patient exosomes. Evidence suggests astrocyte-derived exosomal miRNAs are also involved in promoting survival of motor neurones. Exosomes are thought to contribute to ALS progression. The ALS-related proteins SOD1, TDP-43 and *C9orf72* have all been implicated in the pathogenic spread of ALS *via* exosomes. Exosomal and autophagy pathways also share a number of key regulators and converge when MVBs fuse with lysosomes. Further, manipulation of autophagy has been shown to impact exosome release.

### 6.1.2 Experimental Aims

The overall aim of this chapter was to investigate the consequence of autophagy dysfunction on exosome protein content, given the close relationship of the two pathways. We have shown miR-340 overexpression inhibits autophagic flux in HeLa cells, targets TBK1 and impacts ALS-relevant proteins downstream of TBK1. Coupling this with the knowledge that several ALS-related proteins have been implicated in the pathogenic spread of ALS *via* exosomes, characterising the protein content of exosomes secreted under conditions of dysfunctional autophagy may help elucidate further proteins and mechanisms involved in the pathogenic spread of ALS. We hypothesised that inhibition of autophagy will alter the exosomal protein content, including ALS and autophagy-relevant proteins. This could be extended to any miRNA implicated in the control of autophagy regulation. The following exploratory aims were therefore established:

- Isolate and characterise exosomes secreted from living N2A cells.
- Determine and evaluate ALS and autophagy relevant protein changes in exosomes isolated from cells with impaired autophagy.

## 6.2 Results and Discussion

### 6.2.1 Isolation of Exosomes from N2A Cells

The dysfunction of autophagy is well documented as a key hallmark of ALS, and growing evidence implicates exosomes in the pathogenic spread of the disease (Komatsu *et al.*, 2006, 2007; Neumann *et al.*, 2006; Basso *et al.*, 2013; Iguchi *et al.*, 2016). Indeed, in Chapter 4, we demonstrated miR-340 mediated autophagy failure, and the pathomechanisms of autophagy and exosomal release are known to converge. Further, exosomal TDP-43, SOD1 and *C9orf72* have all been implicated in the pathogenic spread of ALS. Researching the components of exosomes released from cells with abnormal autophagy is therefore of pathological importance. Hence, we sought firstly to isolate exosomes from cultured cells, and secondly to determine the impact of dysfunctional autophagy, modelled by pharmacological inhibition with bafilomycin, on exosomal protein content.

Work to establish exosome isolations in the Layfield lab was performed previously using N2A cells. To maintain group consistency, we continued to use N2A cells for the following exosomal work. Exosomes were isolated from mouse N2A cells (without any autophagy interference) using size exclusion chromatography (SEC), as described in section 2.4. Briefly, the cells were grown in DMEM at 37 °C (with 10% (v/v) FBS and 1% (v/v) PS) for 48 hours before being grown in EV-free media (DMEM with 1% (v/v) PS) for the required duration. The conditioned media was then extracted and subjected to SEC for exosome isolation, in a method based on that by Böing and colleagues (Böing *et al.*, 2014). Briefly, this obtained 3 ml 'void' fractions followed by three exosome-containing fractions (500 µL each) and subsequently three protein fractions (1 ml each). Previously, our work investigating the impact of miR-340 on ALS-relevant proteins and pathways was performed in HeLa cells and human astrocytes. A limitation of the following work is therefore the uncertainty surrounding the impact of miR-340 in N2A cells.

The resulting isolated exosomes were characterised by western blotting for the exosomal markers Alix (also known as PDCD6IP) and Flotillin-1 (Figure 38A).

Exosomes were collected in three 500  $\mu$ L fractions (F1 – F3) and western blotting demonstrated the presence of Alix and Flotillin-1, especially in fraction 2 (F2). A BCA protein quantification assay revealed the exosome fractions were too dilute for accurate measurement of total protein, and instead, an equal volume of each fraction (40  $\mu$ L) was loaded into the gel. Transmission electron microscopy (TEM) of the second exosomal fraction also confirmed the presence of membrane bound vesicles with a diameter between that expected for exosomes (30-200 nm) which displayed typical exosome morphologies such as a central depression or 'cup shape' (Figures 38B and 38C) (Wu, Deng and Klinke, 2015).

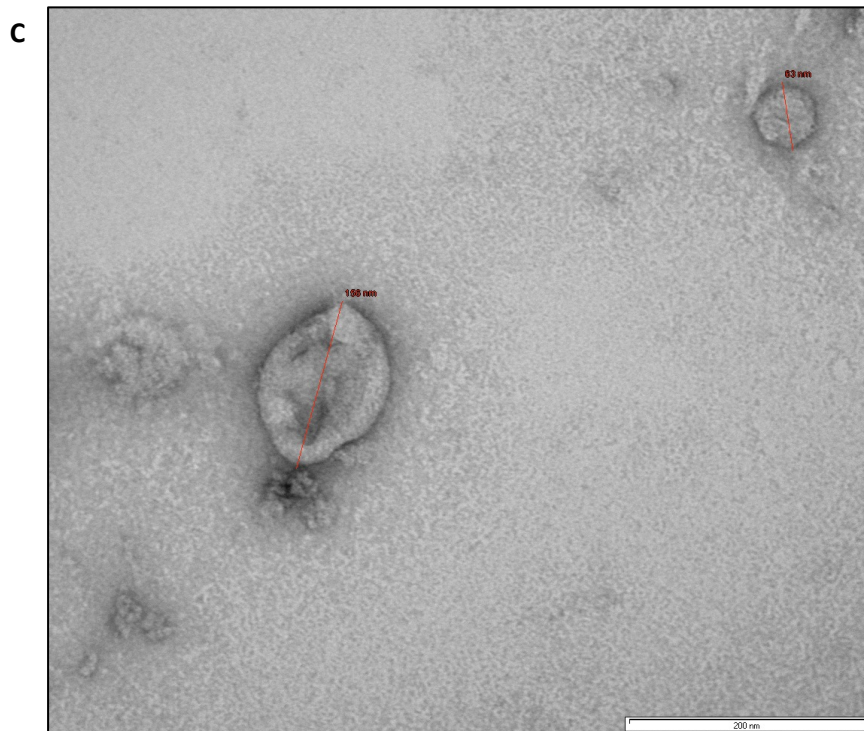
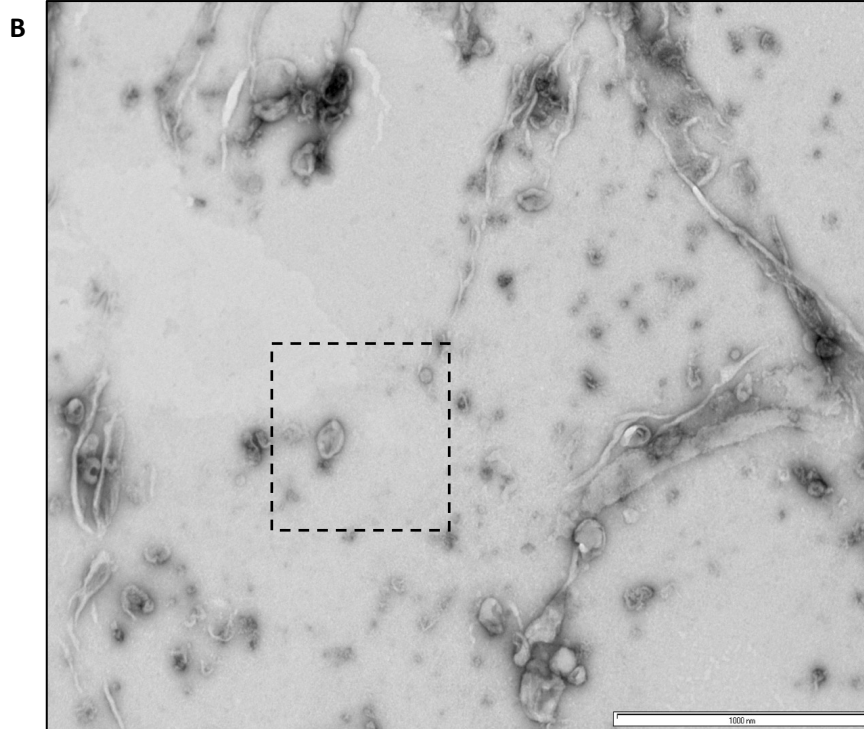
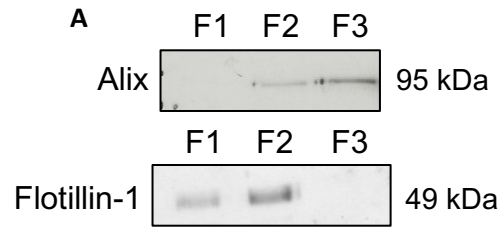


**Figure 38: Characterisation of purified exosomes from N2A cells.** A) Western blotting for endogenous levels of the exosomal markers Alix and Flotillin-1 of three exosomal fractions (F1, F2 and F3) from N2A cells. 40  $\mu$ L of each fraction was loaded into the gel (from 500  $\mu$ L fractions) prepared from a total of 40 mL media collected from two T75 flasks of N2A cells. B) TEM image of vesicles with the diameter range expected for exosomes. Scale bar shows 1000 nm. C) A magnified area of B (magnified area indicated by dashed black box). Scale bar shows 200 nm and the two exosome diameters in red from left to right are 156 nm and 63 nm.

## 6.2.2 Impact of Dysfunctional Autophagy on Exosomal Protein Content

We previously showed miR-340 inhibits autophagy in a human (HeLa) live cell model (section 4.2.2) although not in mouse N2A cells (Appendix 3). Additionally, the novel finding that *TBK1* is a direct target of miR-340 was suggested as a possible mechanism through which this autophagy inhibition occurred (section 4.2.3). However, the interaction between miR-340 and *Tbk1* in mouse N2A cells is absent, as described in section 4.2.3. Therefore, to model the impact of dysfunctional autophagy on exosomal proteins independently of the miR-340-*Tbk1* interaction, N2A cells were treated with a known autophagy inhibitor, bafilomycin A1, and their resulting exosomal protein contents analysed by mass spectrometry. This essentially models the autophagy dysfunction that may arise from various insults, including, we reason, miR-340 overexpression.

N2A cells were treated with 50 nM bafilomycin A1 or an equal volume of DMSO control for 16 hours in FBS free media, at which point the media was extracted and SEC performed. Previously, exosomes had been isolated from a total of 40 mL media, though for this experiment, exosomes were isolated from a total of 8 mL media per condition, to reduce the volume of bafilomycin needed. The three exosomal fractions (F1 – F3), plus the cell lysate and first protein fraction (which elutes from the SEC immediately after the third exosomal fraction) underwent western blotting to confirm the presence of the exosomal markers Alix and Flotillin-1, as in section 6.3.1 (Figure 39).

Exosome isolations from N2A cells treated with bafilomycin A1 or DMSO were performed on three independent occasions and in each instance the second exosome fraction (F2) from both DMSO and bafilomycin A1 treated cells were analysed by protein mass spectrometry (LC/MS/MS), resulting in a total of six samples. This second fraction visually contained consistently the most flotillin-1 and Alix by western blotting (Figure 39). Further, the first exosomal fraction (F1) likely contained some overlap with the 'void' fractions and the third exosomal fraction (F3) likely included some overlap with the first protein fraction. The second fraction however, was expected to contain a higher exosome concentration and less protein contamination.

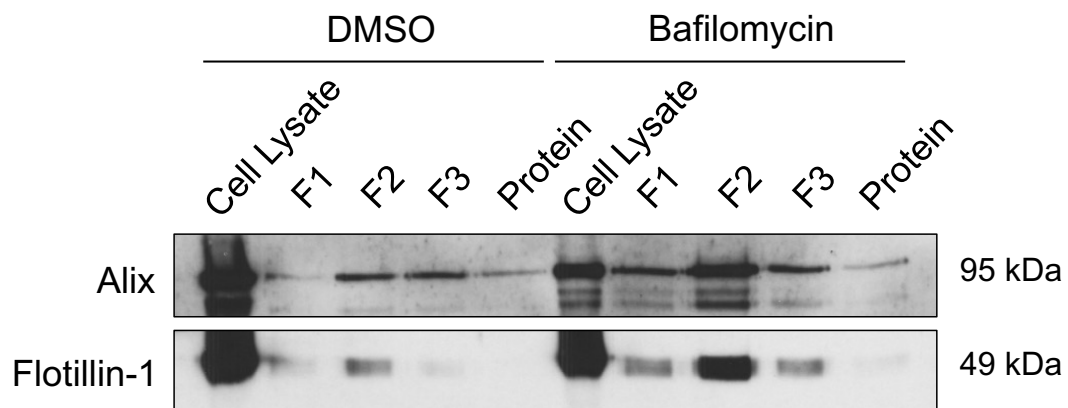


**Figure 39: Western blotting for exosomal markers from N2A derived exosomes or N2A cell lysate.** Representative western blot showing endogenous levels of the exosomal markers, Alix and Flotillin-1 of exosomes derived from N2A cells treated with 50 nM bafilomycin A1 or DMSO control. 20  $\mu$ g of cell lysate and 40  $\mu$ L of each of the exosome fractions (F1-3) (from 500  $\mu$ L fractions) and the protein fraction (from a 1 mL fraction) prepared from 8 mL total media from one T75 flask were loaded into the gel.

The mass spectrometry detected a total of 572 unique proteins across all six samples (from a minimum of two peptide sequences with a protein threshold of 99% and a FDR (false positive discovery rate) of 7.8%). 324 proteins were detected in at least one sample of the DMSO treated N2A-derived exosomes and 562 proteins in at least one sample of the bafilomycin A1 treated N2A-derived exosomes (Table 19). Additionally, the number of proteins detected in all DMSO replicates was 63 whilst in all bafilomycin replicates was 323. 54 proteins were present in all replicates of both DMSO treated N2A-derived exosomes and bafilomycin treated N2A-derived

exosomes, meaning the number of proteins unique to all DMSO or bafilomycin treated N2A-derived exosome samples was 9 and 269 respectively (Figure 40). Detection of a protein in this LC/MS/MS experiment is simply a broad indication of protein quantity. Failure to detect a protein indicates the absence of the protein or its presence in quantities below the detection limit.

**Table 19: Number of proteins detected across all six samples of N2A-derived exosomes, present in at least one DMSO repeat and at least one bafilomycin repeat.**

Total Unique Proteins	Proteins in $\geq 1$ DMSO Exosome Replicate	Proteins in $\geq 1$ Baf Exosomes Replicate
572	324	562

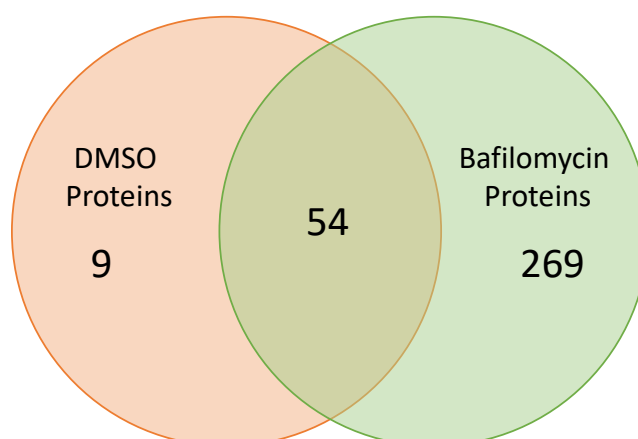


**Figure 40: Number of proteins detected from N2A-derived exosomes in all replicates of DMSO or all replicates of bafilomycin treated cells.** 63 proteins were detected in all replicates of DMSO treated cell-derived exosomes and 323 proteins were detected in all replicates of bafilomycin treated cell-derived exosomes. 54 proteins were detected in all DMSO and all bafilomycin replicates. Therefore, 9 proteins were unique to all DMSO treated cell-derived exosomes, whilst 269 proteins were unique to all bafilomycin treated cell-derived exosomes.

The proteins detected in exosomes from bafilomycin and DMSO control treatments were compared, and for the next stage of analysis, only those proteins present exclusively in at least one of the three biological replicates from bafilomycin treatment were considered, removing proteins detected in at least one biological

replicate from DMSO treatment. This analysis revealed that 248 proteins were unique to bafilomycin treatment, accounting for 44% of the proteins (562) identified from at least one of the three samples of exosomes from bafilomycin treated N2As. This is likely to show the most significantly enriched proteins in the bafilomycin exosomes compared to controls.

We then sought to determine the autophagy and ALS-related proteins detected in this group of 248 exosomal proteins unique to bafilomycin treatment. Since there were three independent replicates of this experiment, we identified the autophagy and ALS-related proteins present in only one biological replicate of bafilomycin treatment, in two replicates of bafilomycin treatment and in all three replicates of bafilomycin treatment (n=1, 2, 3), but never in control. The results of this analysis are shown in Table 20 and Table 21.

We also determined the autophagy and ALS-related proteins unique to DMSO treatment (therefore potentially downregulated in exosomes following bafilomycin treatment) as well as the proteins detected in both bafilomycin and DMSO control exosome samples (Tables 22 and 23).

A limitation of this experiment was the undetermined number or concentration of exosomes in bafilomycin treated exosomes or DMSO treated exosomes. Therefore, following initial analysis, we also attempted to normalise known exosomal markers by western blotting of bafilomycin treated exosomes to DMSO treated exosomes using equal volumes of exosome samples.

**Table 20: Mass spectrometry analysis of exosomal autophagy proteins unique to bafilomycin A1 treated N2As.** The autophagy-related proteins detected in one, two or three of the three total bafilomycin treated N2A replicates are shown. Proteins discussed in the text are highlighted, underlined and in bold.

<b>Exosome Proteins Unique to Bafilomycin Treatment</b>															
Autophagy proteins in 1/3 Baf only samples	HARS2	KRT73	KRT84	VAMP7											
Autophagy proteins in 2/3 Baf only samples	ACTR3B	AP1B1	AP2B1	EIF2S1	LAMP1	PPP2R1B	PRKACA	RAB9	RHEB	SNX1	SNX2	STX8	<b>TBK1</b>	UBE2D3	VDAC1
Autophagy proteins in 3/3 Baf only samples	ACTR2	ACTR3	AP1G1	BAG3	GABARAPL2	<b>KEAP1</b>	NBR1	PA2G4	PPP1CA	PPP2CB	RAB8A	VTI1B			

**Table 21: Mass spectrometry analysis of exosomal ALS-related proteins unique to bafilomycin A1 treated N2As.** The ALS-related proteins detected in one, two or three of the three total bafilomycin treated N2A replicates are shown. Proteins discussed in the text are highlighted, underlined and in bold.

<b>Exosome Proteins Unique to Bafilomycin Treatment</b>															
ALS proteins in 1/3 Baf only samples	ALAD	OPTN	PRPH												
ALS proteins in 2/3 Baf only samples	DCTN1	DNAJC7	DYNC1H1	<b>TBK1</b>											
ALS proteins in 3/3 Baf only samples	UBQLN1														

**Table 22: Mass spectrometry analysis of exosomal autophagy proteins detected in at least one replicate of bafilomycin treated exosomes or at least one replicate of DMSO treated exosomes.** Proteins discussed in the text are highlighted, underlined and in bold.

<b>DMSO or Bafilomycin detected Exosomal Proteins</b>															
Autophagy proteins unique to DMSO treatment	KRT4	RALB													
Autophagy proteins in at least one repeat of both Baf and DMSO	SOD1	ACTC1	ARF6	CAPN5	CAPN6	CDK1	CLTC	EEF1A1	EEF1A2	FYN	GAPDH	HSPA1L	HSPA5	HSPA8	
	KRAS	KRT5	KRT6A	KRT6B	KRT75	KRT76	KRT8	KRT90	NRAS	PPP2R1A	PRMT1	RAB10	RAB1B	RAB5A	
	RAB5B	RAB5C	RALA	RET	SLC1A4	SLC1A5	SLC3A2	SLC7A5	SMPDL3B	<b>SQSTM1</b>	STXBP1	UBE2N	VAMP3	VCP	
	VIM														

**Table 23: Mass spectrometry analysis of exosomal ALS-related proteins detected in at least one replicate of bafilomycin treated exosomes or at least one replicate of DMSO treated exosomes. Proteins discussed in the text are highlighted, underlined and in bold.**

<b>DMSO or Bafilomycin detected Exosomal Proteins</b>														
ALS proteins unique to DMSO treatment														
ALS proteins in at least one repeat of both Baf and DMSO	SOD1	GARS	PARK7	PFN1	RFTN1	<b><u>SQSTM1</u></b>	UBQLN2	VCP						

Of interest, TBK1 was detected only in exosomes derived from N2As treated with bafilomycin, indicating the loading of TBK1 into exosomes may be increased during autophagy inhibition (Tables 20 and 21). Similarly, SQSTM1 (p62) was detected in all three replicates of bafilomycin treated N2A-derived exosomes, and only one DMSO treated N2A derived exosome replicate (Tables 22 and 23).

Bafilomycin treatment has been shown to increase the release of exosomes. For example, in AD-293 cells (a derivative of HEK293 cells), bafilomycin treatment increased their release of exosomes, measured by the levels of exosomal markers (Miao *et al.*, 2015; Oshima *et al.*, 2019). It is possible therefore, that the apparent increase of TBK1 loading into exosomes after bafilomycin treatment is instead the result of an increase in the number of exosomes secreted from the cells. The levels of exosomal TBK1 from DMSO treated cells may be below the threshold for detection by mass spectrometry, potentially due to lower exosomal numbers. In our data, TBK1 was identified in two of the three bafilomycin treatment exosome replicates, though western blotting of the same samples confirmed the presence of TBK1 protein in all three (Table 20, 21 and Figure 41). This suggests the mass spectrometry performed was not sensitive enough to detect TBK1 present in the third replicate of exosomes derived from N2As treated with bafilomycin, despite our ability to visualise it by western blotting. No exosomal TBK1 was detected in any DMSO treated N2A-derived exosome replicate by mass spectrometry, and the lack of TBK1 in these samples was confirmed by western blotting (Figure 41). Thus, TBK1 was detected exclusively and in all bafilomycin treated N2A-derived exosome samples.

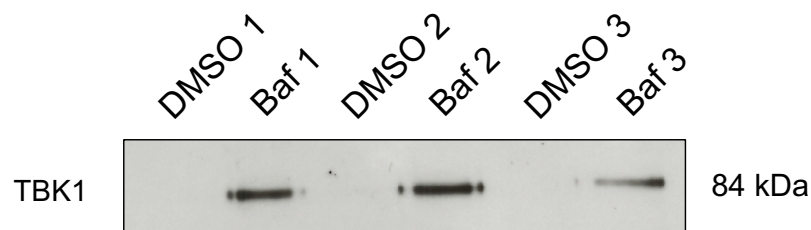


**Figure 41: Western blotting for TBK1 to validate mass spectrometry results of TBK1 in exosome samples from N2A cells treated with bafilomycin or DMSO control.** *Tbk1 was detected in all replicates of exosomes from bafilomycin treated N2As, but not in any replicates of exosomes from DMSO treated N2A control. All three replicates of the second exosome fraction are shown. The samples were the same as those sent for mass spectrometry analysis, which identified the presence of Tbk1 in bafilomycin replicates 1 and 2, but not 3. 40 ul of each sample was loaded into the wells.*

To address the issue of the anticipated increase in the number of exosomes secreted from cells treated with bafilomycin compared to DMSO, densitometry analysis of western blots of Alix and Flotillin-1 from the second exosome fraction (F2) of all three replicates was performed, as an indirect measure of total EV number. A representative western blot of Alix and Flotillin-1 for all exosome fractions, cell lysate and protein fraction is given in Figure 39. Next, normalisation of the bafilomycin-derived exosomes to the DMSO-derived exosomes was performed by calculating the fold change of Alix and Flotillin-1 for bafilomycin exosomes compared to DMSO exosomes (Figure 42). This was performed only for the second exosome fraction (F2) of each replicate, which was that used for mass spectrometry analysis. This revealed that in all cases, bafilomycin treatment led to a varied increase in the exosomal Alix and Flotillin-1, suggesting TBK1 may not be increased in the bafilomycin influenced exosomes, but rather a greater number of exosomes (containing TBK1) were present. Therefore, due to the low exosome count, detection of TBK1 in DMSO treated exosomes was not possible by mass spectrometry or western blotting. Despite this, we observed an average fold change of Alix and Flotillin-1 of 3.3 for the second replicate of bafilomycin treated exosomes (Figure 42). Were the TBK1 levels 3-fold lower in the DMSO treated exosomes in this instance, they would likely be visible by western blotting, implying TBK1 loading into exosomes may in fact be increased by bafilomycin treatment. However, to more accurately determine whether bafilomycin

treatment increased the loading of TBK1 into exosomes, analysis could be performed to quantify the concentration of exosomes per sample. For example, Nanoparticle Tracking Analysis (NTA) provides information on the particle size and concentration of nanoparticles, from 10 nm to 1000 nm.

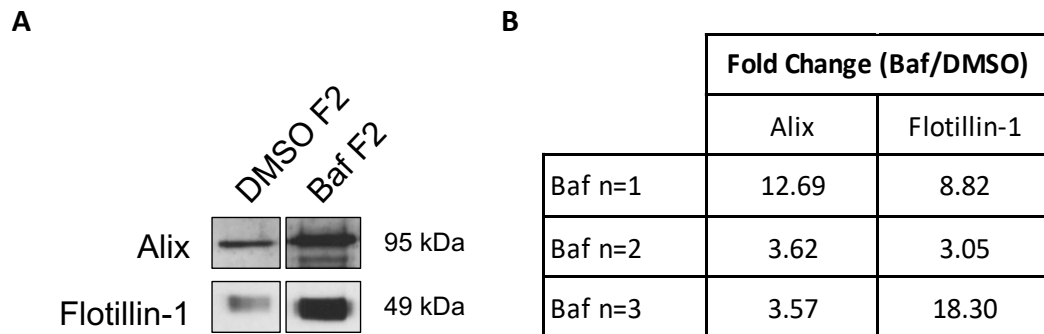


**Figure 42: Fold change of Alix and Flotillin-1 for DMSO or bafilomycin treated exosomes (second exosome fraction (F2) only) for each of the three biological replicates.** A) Representative western blot for Alix and Flotillin-1 of the second exosome fraction (F2) from N2A cells treated with bafilomycin or DMSO control. B) Densitometry analysis of western blots of Alix and Flotillin-1 for all three replicates of exosome fraction 2 (F2) was performed to calculate the fold change of Alix and Flotillin-1 from bafilomycin influenced exosomes compared to DMSO influenced exosomes.

Additionally, it was previously shown that proteasomal inhibition with MG132 in NSC-34 cells did not affect the protein levels of TBK1, whereas bafilomycin treatment resulted in an increase of TBK1 protein. This indicates TBK1 can be degraded *via* autophagy (Duan *et al.*, 2019). We repeated this experiment by treating N2A cells with 50 nM bafilomycin or an equal volume of DMSO control and western blotted for TBK1 within the cell lysate. In contrast to observations by Duan and colleagues, we observed that N2A cells treated with bafilomycin showed a trend for decreased cellular TBK1 compared to the DMSO control, though this was not significant (Figure 43). The concentration of bafilomycin used by Duan and colleagues was 20 nM, whereas N2A cells were treated with 50 nM in the current experiment. The authors also treated with bafilomycin for just six hours, whereas the N2A cells in the current experiment were treated for 16 hours, as were N2A cells prior to exosome isolation. This could imply cellular TBK1 levels fluctuate temporally in response to bafilomycin. Alternatively, the levels of TBK1 in response to bafilomycin could be cell type specific,

and differ between NSC-34 cells (used by Duan and colleagues) and N2A cells used in the current experiment.

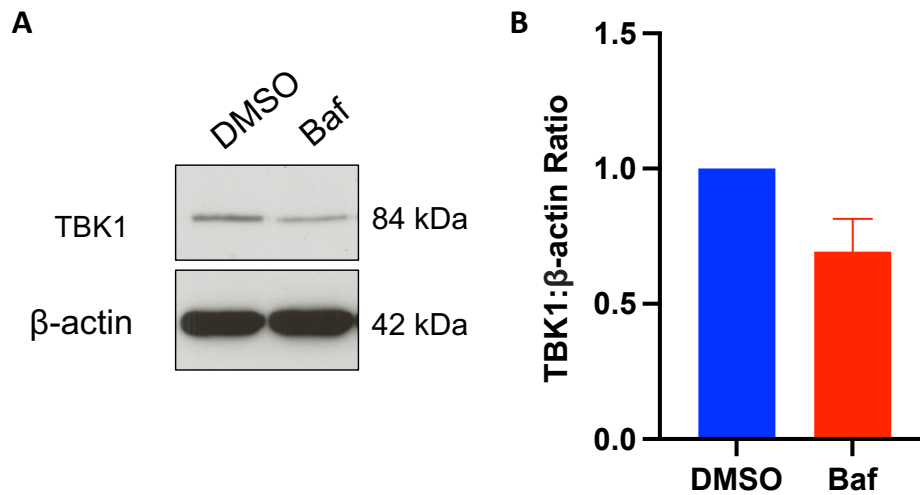


**Figure 43: Western blotting for TBK1 in N2A cells treated with DMSO and bafilomycin.** A) Representative western blot showing endogenous TBK1 levels when N2A cells were treated with 50 nM bafilomycin or DMSO control for 16 hours. B) Densitometry analysis of western blots. Data is shown as mean  $\pm$  SEM from three independent experiments.

Additionally, our observations of increased exosome number and potentially increased levels of TBK1 in exosomes from N2A cells treated with bafilomycin, combined with our observations of decreased TBK1 (though not significant) in response to bafilomycin after 16 hours, may therefore be explained by exosome release compensating for autophagy inhibition. For example, it was previously shown that the extracellular alpha-synuclein released in exosomes was increased when human neuroglioma, H4 cells, were treated with bafilomycin (Minakaki *et al.*, 2018). Upon bafilomycin treatment, of NSC-34 or N2A cells, the autophagic degradation of TBK1 may decrease, resulting in increased cellular TBK1 at earlier time points (6 hours), as identified by Duan and colleagues. However, at later time points, such as that in our experiment (16 hours), this increase in cellular TBK1 may be compensated for by its increased loading into exosomes.

Another protein detected in all bafilomycin samples by mass spectrometry, though no DMSO samples, was KEAP1 (Table 20), which as previously discussed in section

4.1.4.1, binds the antioxidant transcription factor NRF2, and targets it for proteasomal degradation. During autophagy inhibition, phosphorylated p62 can accumulate (due to its prevented degradation by lysosomes) and may sequester KEAP1, activating NRF2 (Matsumoto *et al.*, 2011). During bafilomycin treatment, the accumulated phosphorylated p62 may result in increased levels of p62-KEAP1 complexes, which would normally undergo degradation by autophagy (Jain *et al.*, 2010). Instead, KEAP1 may be removed from cells through increased loading into exosomes (Minakaki *et al.*, 2018). Also, in support of this, p62 (Sqstm1) was detected in all three bafilomycin treated exosome replicates by mass spectrometry, though was detected in one DMSO treated exosome replicate (Tables 22 and 23), and it would be interesting to determine whether exosomal p62 and KEAP1 are in complex.

A model of spinal cord injury whereby oxidative stress was triggered in mouse endothelial cells by treatment with H<sub>2</sub>O<sub>2</sub> was used to investigate the effects of microglial-derived exosomes on the NRF2/KEAP1 pathway. The authors showed that H<sub>2</sub>O<sub>2</sub> treated endothelial cells subjected to microglial-derived exosomes presented higher NRF2 protein levels and lower Keap1 levels, and increased downstream antioxidant genes (such as *Nqo1* which encodes the protein, NADH) compared to those not treated with exosomes (Peng *et al.*, 2021). These exosomes also increased the endothelial cell proliferation at the site of spinal cord injury. This implicates exosomes as a potential therapy to combat oxidative stress through the NRF2 signalling pathway.

### 6.3 Conclusions and Future Directions

Dysfunctional autophagy is a hallmark of ALS and evidence implicates exosomes in the pathogenic spread of the disease. Hence, the protein content of exosomes resulting from cellular dysfunctional autophagy is of pathological interest. We therefore aimed to investigate the impact of dysfunctional cellular autophagy on the protein contents of subsequently secreted exosomes. We successfully isolated exosomes from N2A cells, confirming the presence of exosomal markers Alix and Flotillin-1 as well as observing vesicles of the correct size and with typical 'cup shape' morphology using TEM.

We next treated N2A cells with 50 nM bafilomycin or DMSO control for 16 hours in EV-free media (FBS free media) and performed mass spectrometry (LC/MS/MS) of the second exosome fraction for both bafilomycin and DMSO treatment from three independent experiments. We subsequently determined the autophagy and ALS-relevant proteins unique to purified exosomes resulting from bafilomycin treatment and observed TBK1 was among those detected in two of the three biological replicates. To confirm the presence of TBK1 in these exosome samples, western blotting of all six samples was performed, and TBK1 was identified in all three biological replicates of bafilomycin treatment, though not in any DMSO replicate.

It has previously been shown that bafilomycin treatment can increase the release of exosomes, which may explain the visible increase in TBK1 in these samples, though we were unable to quantify the exosome number in this study. In an attempt to overcome this limitation, we attempted to normalise the bafilomycin exosome levels to the DMSO exosome levels and analysed the density of Alix and Flotillin-1 bands from western blots of equal volumes of all six exosome samples. This assumes the Alix and Flotillin-1 levels to be a crude measure of EV number. The average fold change of Alix and Flotillin-1 from DMSO to bafilomycin treatment for replicate two was three-fold (the fold change for replicates one and three were larger). We rationalise that if TBK1 was three-fold reduced in DMSO treatment from replicate two, a band corresponding to TBK1 would still be visible by western blot. This provides evidence for increased loading of TBK1 into bafilomycin treated N2A-

derived exosomes, which may compensate for increased cellular TBK1 at earlier timepoints (6 hours), though determining exosome concentration with NTA prior to mass spectrometry would aid in elucidating whether this is the case.

We also determined the autophagy and ALS-relevant proteins unique to exosomes resulting from DMSO treatment as well as proteins identified in exosomes from both bafilomycin and DMSO treatment. KEAP1 was detected in all bafilomycin treated exosome samples and no DMSO treated exosome sample by mass spectrometry, and the increase in KEAP1-p62 complexes (which would normally undergo degradation by autophagy) upon bafilomycin treatment could be removed from the cell *via* exosomes instead, since exosomes have been shown to compensate for impaired autophagy. SQSTM1 (p62) was detected in all bafilomycin exosome samples and one DMSO exosome sample, which also supports this hypothesis and it would be interesting to determine whether exosomal KEAP1 and p62 are in complex.

We also performed western blotting with N2A cell lysate after 16-hour treatment with 50 nM bafilomycin or DMSO control and observed a trend for decreased TBK1 in cells treated with bafilomycin. Previously, bafilomycin treatment has been shown to increase the cellular TBK1 protein levels, though after only 6 hours treatment. We rationalise that at 6 hours of bafilomycin treatment, the cellular TBK1 is increased since its degradation by autophagy is reduced. After 16 hours of treatment however, the increase in TBK1 may be compensated for by its increased loading into exosomes.

The work presented in this chapter has connected cellular dysfunctional autophagy with exosome protein content, identifying autophagy and ALS-relevant proteins which appear unique to exosomes from cells subjected to bafilomycin treatment. We hypothesise that TBK1 may be released in exosomes to compensate for inhibited autophagy where it is normally degraded. Future work could determine the impact on the exosome proteome following miR-340 manipulation.

## Chapter 7 - Final Discussion and Conclusions

Growing evidence implicates miRNA dysregulation as a hallmark of ALS. To date, no specific miRNA biomarker signature of ALS is clinically available, although recent work suggests this could soon be a possibility (Joilin *et al.*, 2020; Kmetzsch *et al.*, 2021). Despite extensive reviews regarding dysregulated miRNAs in ALS, only some studies have reviewed and collated the total ALS patient dysregulated miRNAs, regardless of the patient tissue source used for miRNA extraction and without any bias towards potential miRNA targets. In Chapter 3 we addressed this need by systematically reviewing all literature reporting miRNA dysregulation between ALS patients and controls from 2013-2018, which encompassed 27 separate studies.

We presented those miRNAs found most frequently dysregulated in ALS patients and sought to determine correlations between those frequently dysregulated miRNAs and the number of ALS-relevant mRNAs they were predicted to target. Our analysis showed miRNAs found frequently dysregulated in ALS did not appear to more frequently target ALS genes than random miRNAs.

Since our review of the literature in 2019, further studies have measured and reported dysregulated miRNAs between ALS patients and controls (Akbari Dilmaghani *et al.*, 2021). Many report dysregulated miRNAs from specific ALS patient tissue sources, such as extracellular vesicles. Indeed, several studies have determined the miRNAs dysregulated in extracellular vesicles of ALS patients, though we did not consider these in our systematic review. A discussion of extracellular vesicle dysregulated miRNAs in ALS is given in Section 6.1.1.5.

More recently, by measuring the expression levels of miRNAs in *C9orf72* ALS patients and controls, miR-34a-5p, miR-345-5p, miR-200c-3p and miR-10a-3p were found dysregulated. Interestingly, miR-34a-5p was also dysregulated in presymptomatic *C9orf72* mutation carrying patients (Kmetzsch *et al.*, 2021). When identifying potential miRNA biomarkers of ALS, it should be considered that these dysregulated miRNAs may not simply be consequences of disease, but may drive the initiation and

progression of disease, by regulating gene targets. Therefore, these miRNAs are also potential therapeutic targets.

Recently, miR-181 (a combined reference to miR-181a-5p and miR-181b-5p) has been suggested as a possible biomarker of ALS. In this study, miR-181 was found stable in plasma of ALS patients through the course of disease, allowing its detection in patients with both early and late stages of ALS (Magen *et al.*, 2021). Higher miR-181 levels were correlated with lower survival and this was verified in a separate cohort of ALS patients. Additionally, high plasma NFL levels are associated with lower survival and the authors observed that when combined, the levels of miR-181 and NFL were superior in accuracy of predicting patient survival (Lu *et al.*, 2015). In our review, miR-181a-5p was found dysregulated in ALS patients in four studies whilst miR-181b-5p was found dysregulated in one (Magen *et al.*, 2021). Combined (as in the above discussed study), miR-181 was dysregulated in five ALS patient studies and would have been among our most frequently reported as dysregulated in ALS patients (Table 7). MiR-181a-5p has also been shown to target autophagy-related proteins including p62 and ATG5 (J. Yang *et al.*, 2018; Goljanek-whysall *et al.*, 2020).

A recent longitudinal study collected serum from ALS patients and controls every three months for up to 30 months, to identify potential circulating miRNA biomarkers of disease (Dobrowolny *et al.*, 2021). This identified 152 miRNAs significantly downregulated in ALS patients compared to controls. The authors validated miR-151a-5p, miR-199a-5p and miR-423-3p by qPCR. The ALS patients were divided into categories based on disease progression, from mild through to terminal. The myomiR (muscle specific miRNA) miR-206 was found significantly increased at moderate disease stages, whilst the myomiR-133a-3p was downregulated at all disease stages. Of the three validated miRNAs, miR-199a-5p and miR-423-3p were significantly downregulated at mild stages of disease, and miR-199a-5p was also significantly downregulated at terminal stages. Conversely, miR-151a-5p was significantly upregulated at moderate and severe stages (Dobrowolny *et al.*, 2021). In our systematic review, miR-133-3p, miR-206-3p and miR-151a-5p were among the top dysregulated miRNAs, dysregulated in nine, six and five studies out of 27, respectively. MiR-133a-3p was the most frequently reported as dysregulated miRNA,

highlighting the potential of this particular myomiR as a biomarker of ALS. Of particular relevance to this thesis, a predicted target of miR-133a-3p is *UNC13A*.

MiR-9 and miR-105 were also shown to be downregulated in sALS. In a human neuroblastoma cell line, miR-9 was shown to target *NEFL* and reduce its mRNA levels in a more classical model of miRNA-mRNA interaction, whilst miR-105 was shown to bind and increase the mRNA of *NEFL*, indicating it acts as a *NEFL* stabiliser (Hawley, Campos-Melo and Strong, 2019). In our systematic review, miR-9 was among the most frequently reported as dysregulated miRNAs, reported in five of 27 studies.

In Chapter 3, we also analysed the patient tissue origin of extracted miRNAs and observed high overlap between miRNAs extracted from blood/plasma/serum with those extracted from the CSF, which allows a potentially clinically accessible source of miRNAs reflecting pathological changes in the CNS. Further, several miRNAs most frequently dysregulated in ALS patients were detected in the CSF and were suggested as candidates for further investigation.

ALS patient dysregulated miRNAs can also be grouped based on their implication in other pathways of relevance to ALS, such as autophagy and vesicle trafficking; RNA regulation and DNA damage control; oxidative stress and mitochondrial dysfunction; and glutamate toxicity. The process of autophagy has been strongly implicated in ALS and dysfunction causes death of neurones (Komatsu *et al.*, 2006, 2007; Neumann *et al.*, 2006). We therefore sought to determine a miRNA which our review highlighted as dysregulated in ALS patients and which was implicated in the autophagy pathway.

We applied a pipeline to filter ALS patient dysregulated miRNAs based on the number of autophagy genes they were predicted to target and those which were specifically predicted to target *TBK1* (section 3.2.5). MiR-340 was predicted to target five autophagy relevant genes (not including *TBK1*) and was dysregulated in three ALS patient studies in our review (Campos-Melo *et al.*, 2013; De Felice *et al.*, 2018; Raheja *et al.*, 2018). MiR-340 was subsequently identified as an appropriate miRNA candidate, known to target a protein relevant to ALS pathways, NRF2 (section 3.2.5), and was shown to inhibit autophagy when overexpressed in living HeLa cells. Despite

this, miR-340 overexpression did not alter protein levels of endogenous p62 or LC3-II/I which we speculate is due to insensitivity of western blotting for small protein changes (section 4.2.2). Instead, RT-qPCR could be used to measure the mRNA levels of p62 or LC3 and quantitative mass spectrometry could be used to measure their protein levels.

The protein, TBK1, is known to be crucial for normal autophagic function and we considered miR-340 may exert its inhibition of autophagic flux through targeting *TBK1* (Pilli *et al.*, 2012). *TBK1* was identified as a direct target of miR-340 which reduced TBK1 protein levels in HeLa cells when overexpressed (section 4.2.3). The presence of *Tbk1* mutations or hemizyosity in SOD1<sup>G93A</sup> mice resulted in impaired autophagy at early stages of disease, with extended survival at later stages, implicating miR-340 mimic use as a therapeutic at later stages of disease to extend survival (Brenner *et al.*, 2019; Gerbino *et al.*, 2020). Despite the critical role of TBK1 in autophagy, the dysfunction of TBK1 at later stages of disease may impact more profoundly on another ALS-associated pathway, such as neuroinflammation. A miR-340 mimic could therefore be used to increase survival at later disease stages, despite its role in inhibiting autophagy. It is unclear whether overexpression or inhibition of miR-340 would be most beneficial as a potential therapy in ALS, but potentially manipulating the miRNA in different directions at different stages of disease may be most beneficial.

Subsequent downstream protein consequences were evaluated with miR-340 overexpression including reduced protein levels of Ser-403 phosphorylated p62 and STING, whilst pharmacological inhibition of TBK1 also reduced NRF2 protein levels (section 4.2.4). Coupling this with the absence of a *Tbk1*-miR-340 interaction in mice N2A cells and the lack of an effect of miR-340 overexpression on autophagic flux in these cells, we proposed the reduction of NRF2 seen in human HeLa cells upon miR-340 overexpression was contributed to by the reduction of TBK1 by miR-340. The reduction of STING by miR-340 overexpression fits with a pathway whereby TBK1 activates STING. In mice with mutant TDP-43, a reduction in STING levels also extended survival, implicating the miR-340 mimic again as a therapeutic to increase life expectancy (Yu *et al.*, 2020).

To further investigate the role of miR-340 in ALS, human primary astrocyte cells were utilised due to their relevance to ALS. In particular, whilst ALS patient-derived astrocytes appear toxic to cocultured motor neurones, overexpression of NRF2 specifically in astrocytes and the upregulation of the antioxidant response appears to afford protection to motor neurones in ALS models, and extends SOD1<sup>G93A</sup> mice survival (Vargas *et al.*, 2008, 2013; Haidet-Phillips *et al.*, 2011). By inhibiting endogenous miR-340, we observed an increase in NRF2 protein levels, rendering miR-340 an attractive therapeutic target. This is the direction of dysregulation we expected with the use of a miR-340 inhibitor. We also observed a decrease in TBK1 protein levels which may be due to indirect effects as this is not the direction of dysregulation we expected with the miR-340 inhibitor (section 5.2.1). We speculated this could be through DYRK2 and DTX4, which both target TBK1 for proteasomal degradation and are predicted targets of miR-340. By inhibiting endogenous miR-340, the expression of DYRK2 and DTX4 may increase and lead to reduced TBK1 protein. Future work should determine whether *DYRK2* and/or *DTX4* are direct targets of miR-340 using the luciferase assay and western blotting. If found to be direct targets, this would support the hypothesis that the reduction of TBK1 by inhibition of miR-340 is by indirect effects.

By performing RNA sequencing of astrocytes with endogenous miR-340 inhibition, we detected significant expression changes in only six protein coding mRNAs and none overlapped with ALS and autophagy-related genes. We therefore repeated the experiment in HeLa cells, used in Chapter 4, though with overexpression of miR-340, and observed a significant change in expression of 1,826 mRNAs. Of these there was an overlap with over 15% of ALS-related genes from ALSod, including *UNC13A* which has recently been implicated as a therapeutic target for almost all ALS cases due to its connection with TDP-43 mislocalisation (Brown *et al.*, 2022; Ma *et al.*, 2022).

The potential mechanism of action by miR-340 on proteins we found altered by its overexpression (using western blotting in Chapter 4) may also be elucidated, by comparing to this quantitative mRNA sequencing data. For example, the expression of *NRF2* was altered significantly from quantitative mRNA sequencing, which validates previous data, that miR-340 overexpression reduced NRF2 protein. This

suggests that miR-340 targets *NRF2* mRNA for degradation. However, the levels the expression of *TBK1* mRNA was not altered, indicating possible involvement of translational inhibition of this mRNA by miR-340, rather than degradation (section 5.2.2). Future work could validate the effect of miR-340 overexpression on *TBK1* and *NRF2* mRNA levels with RT-qPCR.

Recently, the functional importance of distinguishing between potential 'direct' and 'indirect' targets of miRNAs was highlighted, as the expression of mRNAs upon decreasing miR-218 levels in mice, speculated to belong in these two distinct groups, was altered in an opposing manner (section 5.2.2.1). Briefly, as miR-218 genetic expression within mice decreased, the expression of *directly* targeted mRNAs increased, whilst the expression of *indirectly* targeted mRNAs decreased in a dose-sensitive manner. Based on the presence or absence of a miR-340-target prediction, mRNAs with significantly altered expression upon miR-340 overexpression were classed as direct or indirect targets of miR-340. *NRF2* and p62 were classed as direct targets of miR-340. In total, 42% of the ALS-relevant genes found with altered expression were classed as direct and expected (possessing miR-340 target predictions and therefore a likely MRE) and 33% were indirect (not possessing miR-340 target predictions and therefore unlikely a MRE). The remaining 25% were classed as direct but unexpected targets, possessing miR-340 target predictions but exhibiting an increased expression change in quantitative mRNA sequencing. Although this experiment was performed at a single concentration, this is a method which could be used in future quantitative mRNA sequencing projects investigating miRNA function. These two distinct classes of mRNAs may function independently in their contribution to disease.

The autophagy and exosomal pathways are closely related: they share key protein components such as ATG3, ATG5, ATG12 and ATG16L1; and the two pathways even converge when MVBs fuse with autophagosomes to form amphisomes (Pan *et al.*, 1985; Berg *et al.*, 1998; Murrow, Malhotra and Debnath, 2015; Guo *et al.*, 2017). TDP-43, SOD1 and *C9orf72* have all been implicated in the pathogenic spread of ALS *via* exosomes. We therefore sought to investigate the consequence of impaired autophagy on the protein composition of secreted exosomes. Ideally, the inhibition

of autophagy would be achieved by overexpression of miR-340 in HeLa cells, although in keeping with the Layfield laboratory's preliminary work on exosomes, N2A cells (which lack the miR-340-*Tbk1* interaction) were used. MiR-340 overexpression did not alter autophagic flux in live HeLa cells (Appendix 3) so as an alternative, we isolated and analysed exosomes from N2A cells treated with bafilomycin. To achieve this, exosomes from N2A cells were first successfully isolated and characterised using western blotting and TEM (section 6.2.1).

Three replicates each of control (DMSO treatment) and bafilomycin treated N2A-derived exosomes were analysed by semi-quantitative mass spectrometry (LC/MS/MS). The number of proteins unique to and present in all three replicates of DMSO treated N2A-derived exosomes was nine, whereas the number of proteins unique to and present in all replicates of bafilomycin treated N2A-derived exosomes was 323. 54 of these proteins were present in all three replicates of both DMSO and bafilomycin samples (section 6.2.2).

Comparison of the total detected proteins with ALS and autophagy-relevant proteins revealed *Tbk1* presence was detected only in bafilomycin treated N2A-derived exosome samples (two of three replicates) but no DMSO treated N2A-derived exosome samples. The presence of *Tbk1* in all three replicates was confirmed by western blotting and this also did not detect *Tbk1* in any DMSO sample. It was speculated that *Tbk1* loading was increased in exosomes upon bafilomycin-mediated inhibition of autophagy, although exosomal markers were increased in these samples compared to control samples, suggesting simply the number of secreted exosomes (containing *Tbk1*) was increased. This is in line with evidence suggesting treatment with bafilomycin increases cellular exosome secretion (Miao *et al.*, 2015; Oshima *et al.*, 2019).

An attempt to normalise exosomal markers from western blots of DMSO and bafilomycin exosome samples revealed only a three-fold increase in apparent exosome levels in one of the replicates. This demonstrated that at least there, *Tbk1* loading into exosomes may have been increased. For future analysis, NTA could be used to quantify the concentration of exosomes per sample to more accurately

determine whether bafilomycin treatment increased the loading of Tbk1 into exosomes. Therefore, this work provided insight into the dysregulation of pathways implicated in ALS and future work could investigate the exosomal protein consequences of autophagy inhibition using miR-340 overexpression in human cells.

## 7.1 Concluding Remarks

The work presented here provides a pipeline for a bioinformatic approach to select candidate miRNAs, which could be utilised for a range of diseases besides ALS. An investigation into the role of miR-340 in autophagy as a mechanism implicated in ALS, revealed its ability to impair autophagy, potentially through the ALS and autophagy relevant gene, *TBK1*. Further, the reduction of proteins downstream of TBK1 signalling suggests a more profound influence of miR-340 on cellular mechanisms.

The increase in NRF2 protein upon miR-340 inhibition in human astrocytes was shown. The ability to elevate NRF2 with the potential to increase antioxidant production and afford protection to neurones makes miR-340 an attractive therapeutic target.

Of known ALS-relevant genes, overexpression of miR-340 altered the expression of over 15% of these in HeLa cells, including *UNC13A*, recently associated with TDP-43 mislocalisation which implicates miR-340 as a potential therapeutic in ALS cases with TDP-43 mislocalisation (97%). A method to differentiate between direct and indirect mRNA targets of miR-340 (which could be applied to other miRNAs) was devised, using quantitative mRNA sequencing of HeLa cells overexpressing miR-340. This reveals potential mechanisms of action of miR-340.

The implication of ALS pathogenic spread *via* exosomes and the convergence of the autophagy pathway with exosome biogenesis suggests the relationship between autophagy dysfunction and the subsequent impact on exosomes should be investigated. Whilst the use of miR-340 to inhibit autophagy in this instance was not feasible, bafilomycin-mediated autophagy inhibition resulted in the presence of several autophagy and ALS genes of interest in exosomes secreted from neurone-like cells treated with bafilomycin though in no or fewer controls. This suggests miR-340-

mediated autophagy inhibition may also result in alterations of exosomal protein content which could have significant implications in ALS pathogenesis.

In summary, we have established a clear and novel role of an ALS and autophagy implicated miRNA, miR-340, in pathways of relevance to ALS. The work presented here contributes to the growing knowledge of the pathomechanisms in ALS, and provides evidence that miR-340 should be researched for its potential as a therapeutic in ALS.

## 7.2 Future Directions

Here we presented ALS patient dysregulated miRNAs and based on its relevance to the autophagy pathway, selected miR-340 for experimental validation. Future work could utilise this collection of known ALS-relevant miRNAs to select others for further experimental testing, perhaps based on their ability to target alternate pathways implicated in ALS. Indeed, the pipeline presented in section 3.2.5 could be applied to several pathways of interest in ALS (not just autophagy) to select a miRNA based on a high likelihood of targeting multiple ALS-implicated pathways.

In Chapter 4 we established a role of miR-340 in impairing autophagy and in targeting *TBK1* with downstream consequences in HeLa cells. We also confirmed the ability of miR-340 overexpression to reduce NRF2 protein levels, in line with current literature. In Chapter 5 we extended this beyond current knowledge, to show miR-340 inhibition resulted in increased NRF2 protein in human primary astrocyte cells. A significant and desirable outcome would be a subsequent decrease in ROS due to increased NRF2-mediated antioxidant gene expression. As discussed, we attempted to measure the ROS levels in astrocyte cells treated with miR-340 inhibitor and control, using a ROS indicator, H2DCFDA, though we were unable to obtain a rational response with several positive controls, suggesting the assay required further optimisation than we had the capacity to perform (section 5.2.1). Future work could use alternative ROS indicators, as a reduction in ROS upon miR-340 inhibition would solidify miR-340 in astrocytes as a potential therapeutic target.

In Chapter 5 we established a significant increase in *UNC13A* mRNA levels in HeLa cells with overexpressed miR-340 and future work should validate this. This may determine whether miR-340 overexpression could be of interest as a potential therapy to promote increased UNC13A protein, which could rescue reductions in neurotransmitter release and increase survival of ALS patients. The potential benefits of miR-340 inhibition discussed above contradict this data, where overexpression of miR-340 may be beneficial. The differences observed with miR-340 inhibition and overexpression could be explained by the differing cell types – primary astrocytes compared to HeLa cells. The increase in *UNC13A* levels should be validated by RT-qPCR in HeLa cells and subsequently analysed in astrocytes with miR-340 overexpression to determine if the *UNC13A* levels become decreased with miR-340 overexpression. If both advantageous, miR-340 inhibitors or mimics could be beneficial at different stages of disease.

Future work could also measure protein changes in exosomes secreted from human cells overexpressing miR-340. Of particular interest, changes in TDP-43, SOD1 and *C9orf72* derived DRPs should be monitored, since all have been implicated in the pathogenic spread of ALS *via* exosomes. This would determine whether miR-340 contributes to the spread of ALS toxicity *via* exosomes.

## Chapter 8 - References

- Abbracchio, M. P. and Ceruti, S. (2006) 'Roles of P2 receptors in glial cells: Focus on astrocytes', *Purinergic Signalling*. Springer, 2(4), pp. 595–604. doi: 10.1007/S11302-006-9016-0/FIGURES/1.
- Abel, O. *et al.* (2012) 'ALSoD: A user-friendly online bioinformatics tool for amyotrophic lateral sclerosis genetics', *Human mutation*. Hum Mutat, 33(9), pp. 1345–1351. doi: 10.1002/HUMU.22157.
- Abel, O. *et al.* (2013) 'Development of a Smartphone App for a Genetics Website: The Amyotrophic Lateral Sclerosis Online Genetics Database (ALSoD).', *JMIR mHealth and uHealth*. JMIR mHealth and uHealth, 1(2). doi: 10.2196/mhealth.2706.
- Abel, O. (no date) *ALSoD: Amyotrophic Lateral Sclerosis Online Genetics Database*. Available at: <http://alsod.iop.kcl.ac.uk/Statistics/report.aspx> (Accessed: 11 January 2019).
- Agarwal, V. *et al.* (2015) 'Predicting effective microRNA target sites in mammalian mRNAs', *eLife*, 4. doi: 10.7554/eLife.05005.
- Ahmed, Z. *et al.* (2007) 'Progranulin in frontotemporal lobar degeneration and neuroinflammation', *Journal of Neuroinflammation*. BioMed Central, p. 7. doi: 10.1186/1742-2094-4-7.
- Aizawa, H. *et al.* (2010) 'TDP-43 pathology in sporadic ALS occurs in motor neurons lacking the RNA editing enzyme ADAR2', *Acta Neuropathologica* 2010 120:1. Springer, 120(1), pp. 75–84. doi: 10.1007/S00401-010-0678-X.
- Akamatsu, M. *et al.* (2016) 'The AMPA receptor antagonist perampanel robustly rescues amyotrophic lateral sclerosis (ALS) pathology in sporadic ALS model mice', *Scientific Reports*. Nature Publishing Group, 6. doi: 10.1038/SREP28649.
- Akbari Dilmaghani, N. *et al.* (2021) 'Emerging role of microRNAs in the pathogenesis of amyotrophic lateral sclerosis', *Metabolic Brain Disease*. Springer, 36(5), pp. 737–749. doi: 10.1007/S11011-021-00697-5/TABLES/3.
- Akkoc, Y. and Gozuacik, D. (2020) 'MicroRNAs as major regulators of the autophagy pathway', *Biochimica et Biophysica Acta - Molecular Cell Research*. doi: 10.1016/j.bbamcr.2020.118662.
- Al-Sarraj, S. *et al.* (2011) 'P62 positive, TDP-43 negative, neuronal cytoplasmic and intranuclear inclusions in the cerebellum and hippocampus define the pathology of C9orf72-linked FTL and MND/ALS', *Acta Neuropathologica*. Springer, 122(6), pp. 691–702. doi: 10.1007/s00401-011-0911-2.
- Alarcón, C. R. *et al.* (2015) 'N6-methyladenosine marks primary microRNAs for processing.', *Nature*. NIH Public Access, 519(7544), pp. 482–5. doi: 10.1038/nature14281.
- Alemu, E. A. *et al.* (2012) 'ATG8 family proteins act as scaffolds for assembly of the ULK complex: Sequence requirements for LC3-interacting region (LIR) motifs', *Journal of Biological Chemistry*. American Society for Biochemistry and Molecular Biology, 287(47), pp. 39275–39290. doi: 10.1074/jbc.M112.378109.
- Algaber, A. *et al.* (2021) 'Targeting FHL2-E-cadherin axis by miR-340-5p attenuates colon cancer cell migration and invasion', *Oncology Letters*. Spandidos Publications, 22(2). doi: 10.3892/OL.2021.12898.
- Amick, J., Roczniak-Ferguson, A. and Ferguson, S. M. (2016) 'C9orf72 binds SMCR8, localizes to lysosomes, and regulates mTORC1 signaling', *Molecular Biology of the Cell*. American Society for Cell Biology, 27(20), pp. 3040–3051. doi: 10.1091/mbc.E16-01-0003.
- Amin, N. D. *et al.* (2021) *A hidden threshold in motor neuron gene networks revealed by modulation of miR-218 dose*, *Neuron*. doi: 10.1016/j.neuron.2021.07.028.
- An, T. *et al.* (2015) 'DYRK2 Negatively Regulates Type I Interferon Induction by Promoting TBK1 Degradation via Ser527 Phosphorylation', *PLOS Pathogens*. Public Library of Science, 11(9), p. e1005179. doi: 10.1371/JOURNAL.PPAT.1005179.
- Anderson, M. A. *et al.* (2016) 'Astrocyte scar formation AIDS central nervous system axon

- regeneration', *Nature*. Nature Publishing Group, 532(7598), pp. 195–200. doi: 10.1038/nature17623.
- de Andrade, H. M. T. *et al.* (2016) 'MicroRNAs-424 and 206 are potential prognostic markers in spinal onset amyotrophic lateral sclerosis', *Journal of the Neurological Sciences*. Elsevier, 368, pp. 19–24. doi: 10.1016/j.jns.2016.06.046.
- Aoki, Y. *et al.* (2017) 'C9orf72 and RAB7L1 regulate vesicle trafficking in amyotrophic lateral sclerosis and frontotemporal dementia', *Brain*. Oxford Academic, 140(4), pp. 887–897. doi: 10.1093/BRAIN/AWX024.
- Arenas, A. *et al.* (2021) 'FUS regulates autophagy by mediating the transcription of genes critical to the autophagosome formation', *Journal of neurochemistry*. NIH Public Access, 157(3), p. 752. doi: 10.1111/JNC.15281.
- Arroyo, J. D. *et al.* (2011) 'Argonaute2 complexes carry a population of circulating microRNAs independent of vesicles in human plasma.', *Proceedings of the National Academy of Sciences of the United States of America*. National Academy of Sciences, 108(12), pp. 5003–8. doi: 10.1073/pnas.1019055108.
- Ash, P. E. A. *et al.* (2013) 'Unconventional Translation of C9ORF72 GGGGCC Expansion Generates Insoluble Polypeptides Specific to c9FTD/ALS', *Neuron*. Cell Press, 77(4), pp. 639–646. doi: 10.1016/J.NEURON.2013.02.004.
- Augustin, I. *et al.* (1999) 'Munc13-1 is essential for fusion competence of glutamatergic synaptic vesicles', *Nature* 1999 400:6743. Nature Publishing Group, 400(6743), pp. 457–461. doi: 10.1038/22768.
- Ayala, Y. M. *et al.* (2011) 'TDP-43 regulates its mRNA levels through a negative feedback loop', *EMBO Journal*. European Molecular Biology Organization, 30(2), pp. 277–288. doi: 10.1038/emboj.2010.310.
- Babst, M. *et al.* (1997) 'Endosomal transport function in yeast requires a novel AAA-type ATPase, Vps4p.', *The EMBO journal*, 16(8), pp. 1820–1831. Available at: <https://www.ncbi.nlm.nih.gov/pmc/articles/PMC1169785/> (Accessed: 7 April 2020).
- Bach, M. *et al.* (2011) 'The serine/threonine kinase ULK1 is a target of multiple phosphorylation events.', *The Biochemical journal*. Portland Press Limited, 440(2), pp. 283–91. doi: 10.1042/BJ20101894.
- Baker, M. *et al.* (2006) 'Mutations in progranulin cause tau-negative frontotemporal dementia linked to chromosome 17', *Nature*. Nature Publishing Group, 442(7105), pp. 916–919. doi: 10.1038/nature05016.
- Bakkar, N. *et al.* (2015) 'RBM45 Modulates the Antioxidant Response in Amyotrophic Lateral Sclerosis through Interactions with KEAP1', *Molecular and Cellular Biology*. Mol Cell Biol, 35(14), pp. 2385–2399. doi: 10.1128/mcb.00087-15.
- Barbosa, M. *et al.* (2021) 'Recovery of Depleted miR-146a in ALS Cortical Astrocytes Reverts Cell Aberrancies and Prevents Paracrine Pathogenicity on Microglia and Motor Neurons', *Frontiers in Cell and Developmental Biology*. Frontiers Media S.A., 9. doi: 10.3389/fcell.2021.634355/FULL.
- Barker, H. V. *et al.* (2017) 'RNA Misprocessing in C9orf72-Linked Neurodegeneration', *Frontiers in Cellular Neuroscience*. Frontiers, 11, p. 195. doi: 10.3389/fncel.2017.00195.
- Barmada, S. J. *et al.* (2014) 'Autophagy induction enhances TDP43 turnover and survival in neuronal ALS models', *Nature Chemical Biology*. Nature Publishing Group, 10(8), pp. 677–685. doi: 10.1038/nchembio.1563.
- Bassell, G. J. *et al.* (1998) 'Sorting of beta-actin mRNA and protein to neurites and growth cones in culture', *The Journal of neuroscience : the official journal of the Society for Neuroscience*. J Neurosci, 18(1), pp. 251–265. doi: 10.1523/JNEUROSCI.18-01-00251.1998.
- Basso, M. *et al.* (2013) 'Mutant copper-zinc superoxide dismutase (SOD1) induces protein secretion pathway alterations and exosome release in astrocytes: Implications for disease spreading and motor neuron pathology in amyotrophic lateral sclerosis', *Journal of Biological Chemistry*. American Society for Biochemistry and Molecular Biology, 288(22), pp. 15699–15711. doi: 10.1074/jbc.M112.425066.

- Batista, A. F. R., Martínez, J. C. and Hengst, U. (2017) 'Intra-axonal Synthesis of SNAP25 Is Required for the Formation of Presynaptic Terminals', *Cell Reports*. Elsevier B.V., 20(13), pp. 3085–3098. doi: 10.1016/J.CELREP.2017.08.097/ATTACHMENT/721A0E37-6995-4A0D-A73D-38D737B673A3/MMC1.PDF.
- Beghi, E. *et al.* (2006) 'The epidemiology of ALS and the role of population-based registries', *Biochimica et Biophysica Acta (BBA) - Molecular Basis of Disease*. Elsevier, 1762(11–12), pp. 1150–1157. doi: 10.1016/J.BBADIS.2006.09.008.
- Behm-Ansmant, I. *et al.* (2006) 'mRNA degradation by miRNAs and GW182 requires both CCR4:NOT deadenylase and DCP1:DCP2 decapping complexes', *Genes and Development*. Cold Spring Harbor Laboratory Press, 20(14), pp. 1885–1898. doi: 10.1101/gad.1424106.
- Benigni, M. *et al.* (2016) 'Identification of miRNAs as Potential Biomarkers in Cerebrospinal Fluid from Amyotrophic Lateral Sclerosis Patients', *NeuroMolecular Medicine*. Springer US, 18(4), pp. 551–560. doi: 10.1007/s12017-016-8396-8.
- Bensimon, G. *et al.* (1994) 'A Controlled Trial of Riluzole in Amyotrophic Lateral Sclerosis', *New England Journal of Medicine*. Massachusetts Medical Society, 330(9), pp. 585–591. doi: 10.1056/NEJM199403033300901.
- Benussi, L. *et al.* (2016) 'Loss of exosomes in progranulin-associated frontotemporal dementia', *Neurobiology of Aging*. Elsevier, 40, pp. 41–49. doi: 10.1016/J.NEUROBIOLAGING.2016.01.001.
- Le Ber, I. *et al.* (2015) 'TBK1 mutation frequencies in French frontotemporal dementia and amyotrophic lateral sclerosis cohorts', *Neurobiology of Aging*. Elsevier, 36(11), pp. 3116.e5-3116.e8. doi: 10.1016/J.NEUROBIOLAGING.2015.08.009.
- Berg, T. O. *et al.* (1998) 'Isolation and Characterization of Rat Liver Amphisomes: EVIDENCE FOR FUSION OF AUTOPHAGOSOMES WITH BOTH EARLY AND LATE ENDOSOMES \*', *Journal of Biological Chemistry*. Elsevier, 273(34), pp. 21883–21892. doi: 10.1074/JBC.273.34.21883.
- Bernstein, E. *et al.* (2001) 'Role for a bidentate ribonuclease in the initiation step of RNA interference', *Nature*. Nature Publishing Group, 409(6818), pp. 363–366. doi: 10.1038/35053110.
- Betel, D. *et al.* (2010) 'Comprehensive modeling of microRNA targets predicts functional non-conserved and non-canonical sites', *Genome Biology*. BioMed Central, 11(8), p. R90. doi: 10.1186/gb-2010-11-8-r90.
- Bilsland, L. G. *et al.* (2010) 'Deficits in axonal transport precede ALS symptoms in vivo.', *Proceedings of the National Academy of Sciences of the United States of America*. National Academy of Sciences, 107(47), pp. 20523–8. doi: 10.1073/pnas.1006869107.
- Binker, M. G. *et al.* (2007) 'Arrested maturation of Neisseria -containing phagosomes in the absence of the lysosome-associated membrane proteins, LAMP-1 and LAMP-2', *Cellular Microbiology*. Cell Microbiol, 9(9), pp. 2153–2166. doi: 10.1111/j.1462-5822.2007.00946.x.
- van Blitterswijk, M. *et al.* (2015) 'Novel clinical associations with specific C9ORF72 transcripts in patients with repeat expansions in C9ORF72', *Acta Neuropathologica*. Springer Verlag, 130(6), pp. 863–876. doi: 10.1007/s00401-015-1480-6.
- Böing, A. N. *et al.* (2014) 'Single-step isolation of extracellular vesicles by size-exclusion chromatography', *Journal of Extracellular Vesicles*. Wiley-Blackwell, 3(1). doi: 10.3402/JEV.V3.23430.
- Bono, S., Feligioni, M. and Corbo, M. (2021) 'Impaired antioxidant KEAP1-NRF2 system in amyotrophic lateral sclerosis : NRF2 activation as a potential therapeutic strategy'. *Molecular Neurodegeneration*, pp. 1–26.
- Borchert, G. M., Lanier, W. and Davidson, B. L. (2006) 'RNA polymerase III transcribes human microRNAs', *Nature Structural & Molecular Biology*. Nature Publishing Group, 13(12), pp. 1097–1101. doi: 10.1038/nsmb1167.
- Borghero, G. *et al.* (2015) 'TBK1 is associated with ALS and ALS-FTD in Sardinian patients', *Neurobiology of Aging*. Elsevier Inc., 43, pp. 180.e1-180.e5. doi: 10.1016/j.neurobiolaging.2016.03.028.

- Bosco, D. A. *et al.* (2010) 'Wild-type and mutant SOD1 share an aberrant conformation and a common pathogenic pathway in ALS', *Nature Neuroscience*. Nature Publishing Group, 13(11), pp. 1396–1403. doi: 10.1038/nn.2660.
- Bose, J. K., Huang, C.-C. and Shen, C.-K. J. (2011) 'Regulation of autophagy by neuropathological protein TDP-43.', *The Journal of biological chemistry*. American Society for Biochemistry and Molecular Biology, 286(52), pp. 44441–8. doi: 10.1074/jbc.M111.237115.
- Brady, O. A. *et al.* (2011) 'Regulation of TDP-43 aggregation by phosphorylation and p62/SQSTM1', *Journal of Neurochemistry*. John Wiley & Sons, Ltd, 116(2), pp. 248–259. doi: 10.1111/J.1471-4159.2010.07098.X.
- Braun, J. E. *et al.* (2012) 'A direct interaction between DCP1 and XRN1 couples mRNA decapping to 5' exonucleolytic degradation', *Nature Structural and Molecular Biology*. Nature Publishing Group, 19(12), pp. 1324–1331. doi: 10.1038/nsmb.2413.
- Brenner, D. *et al.* (2019) 'Heterozygous Tbx1 loss has opposing effects in early and late stages of ALS in mice', *Journal of Experimental Medicine*. Rockefeller University Press, 216(2), pp. 267–278. doi: 10.1084/jem.20180729.
- Brettschneider, J. *et al.* (2013) 'Stages of pTDP-43 pathology in amyotrophic lateral sclerosis', *Annals of Neurology*. John Wiley & Sons, Ltd, 74(1), pp. 20–38. doi: 10.1002/ana.23937.
- Brown, A. L. *et al.* (2022) 'TDP-43 loss and ALS-risk SNPs drive mis-splicing and depletion of UNC13A', *Nature*. Nature Publishing Group, 603(7899), p. 131. doi: 10.1038/S41586-022-04436-3.
- Buratti, E. *et al.* (2004) 'Nuclear Factor TDP-43 Binds to the Polymorphic TG Repeats in CFTR Intron 8 and Causes Skipping of Exon 9: A Functional Link with Disease Penetrance', *The American Journal of Human Genetics*. Elsevier, 74(6), pp. 1322–1325. doi: 10.1086/420978.
- Buratti, E. *et al.* (2005) 'TDP-43 binds heterogeneous nuclear ribonucleoprotein A/B through its C-terminal tail: An important region for the inhibition of cystic fibrosis transmembrane conductance regulator exon 9 splicing', *Journal of Biological Chemistry*. American Society for Biochemistry and Molecular Biology, 280(45), pp. 37572–37584. doi: 10.1074/jbc.M505557200.
- Buratti, E. *et al.* (2010) 'Nuclear factor TDP-43 can affect selected microRNA levels', *The FEBS Journal*. John Wiley & Sons, Ltd, 277(10), pp. 2268–2281. doi: 10.1111/J.1742-4658.2010.07643.X.
- Byrne, S. *et al.* (2012) 'Cognitive and clinical characteristics of patients with amyotrophic lateral sclerosis carrying a C9orf72 repeat expansion: A population-based cohort study', *The Lancet Neurology*. Elsevier, 11(3), pp. 232–240. doi: 10.1016/S1474-4422(12)70014-5.
- C.N. Marchetto, M. *et al.* (2008) 'Non-Cell-Autonomous Effect of Human SOD1G37R Astrocytes on Motor Neurons Derived from Human Embryonic Stem Cells | Elsevier Enhanced Reader', *Cell Stem Cell*, 3(6), pp. 649–657. Available at: <https://reader.elsevier.com/reader/sd/pii/S1934590908005249?token=07E92BAC44FB4293F0B9A87F9F4EC1DF6BAB2E1206878FA011DDC2449A2D3A1A5BDC2604C6852BB0A38AF4A68674192F&originRegion=eu-west-1&originCreation=20210511150246> (Accessed: 11 May 2021).
- Caccamo, A. *et al.* (2009) 'Rapamycin rescues TDP-43 mislocalization and the associated low molecular mass neurofilament instability', *Journal of Biological Chemistry*. American Society for Biochemistry and Molecular Biology, 284(40), pp. 27416–27424. doi: 10.1074/jbc.M109.031278.
- Cadenas, E. and Davies, K. J. A. (2000) 'Mitochondrial free radical generation, oxidative stress, and aging', *Free Radical Biology and Medicine*. Pergamon, 29(3–4), pp. 222–230. doi: 10.1016/S0891-5849(00)00317-8.
- Campos-Melo, D. *et al.* (2013) 'Altered microRNA expression profile in amyotrophic lateral sclerosis: a role in the regulation of NFL mRNA levels', *Molecular Brain*. BioMed Central, 6(1), p. 26. doi: 10.1186/1756-6606-6-26.
- Campos-Melo, D., Hawley, Z. C. E. and Strong, M. J. (2018) 'Dysregulation of human NEFM and NEFH mRNA stability by ALS-linked miRNAs', *Molecular Brain*. BioMed Central Ltd., 11(1), p. 43. doi: 10.1186/s13041-018-0386-3.

- Capece, V. *et al.* (2015) 'Oasis: online analysis of small RNA deep sequencing data.', *Bioinformatics (Oxford, England)*. Oxford University Press, 31(13), pp. 2205–7. doi: 10.1093/bioinformatics/btv113.
- Carriedo, S. G. *et al.* (2000) 'AMPA Exposures Induce Mitochondrial Ca<sup>2+</sup> Overload and ROS Generation in Spinal Motor Neurons In Vitro', *The Journal of Neuroscience*. Society for Neuroscience, 20(1), p. 240. doi: 10.1523/JNEUROSCI.20-01-00240.2000.
- Carthew, R. W. and Sontheimer, E. J. (2009) 'Origins and Mechanisms of miRNAs and siRNAs', *Cell*. Cell Press, 136(4), pp. 642–655. doi: 10.1016/J.CELL.2009.01.035.
- Catanese, A. *et al.* (2019) 'Retinoic acid worsens ATG10-dependent autophagy impairment in TBK1-mutant hiPSC-derived motoneurons through SQSTM1/p62 accumulation', *Autophagy*. Taylor and Francis Inc., 15(10), pp. 1719–1737. doi: 10.1080/15548627.2019.1589257.
- Chairoungdua, A. *et al.* (2010) 'Exosome release of  $\beta$ -catenin: A novel mechanism that antagonizes Wnt signaling', *Journal of Cell Biology*. Rockefeller University Press, 190(6), pp. 1079–1091. doi: 10.1083/jcb.201002049.
- Chang, Y.-Y. and Neufeld, T. P. (2009) 'An Atg1/Atg13 complex with multiple roles in TOR-mediated autophagy regulation.', *Molecular biology of the cell*. American Society for Cell Biology, 20(7), pp. 2004–14. doi: 10.1091/mbc.e08-12-1250.
- Chang, Y. *et al.* (2008) 'Messenger RNA Oxidation Occurs Early in Disease Pathogenesis and Promotes Motor Neuron Degeneration in ALS', *PLOS ONE*. Public Library of Science, 3(8), p. e2849. doi: 10.1371/JOURNAL.PONE.0002849.
- Chaudhury, A., Chander, P. and Howe, P. H. (2010) 'Heterogeneous nuclear ribonucleoproteins (hnRNPs) in cellular processes: Focus on hnRNP E1's multifunctional regulatory roles.', *RNA (New York, N.Y.)*. Cold Spring Harbor Laboratory Press, 16(8), pp. 1449–62. doi: 10.1261/rna.2254110.
- Cheloufi, S. *et al.* (2010) 'A dicer-independent miRNA biogenesis pathway that requires Ago catalysis.', *Nature*. NIH Public Access, 465(7298), pp. 584–9. doi: 10.1038/nature09092.
- Chen, H. *et al.* (2014) 'Modeling ALS with iPSCs Reveals that Mutant SOD1 Misregulates Neurofilament Balance in Motor Neurons', *Cell stem cell*. NIH Public Access, 14(6), p. 796. doi: 10.1016/J.STEM.2014.02.004.
- Chen, H. *et al.* (2015) 'Human-derived neural progenitors functionally replace astrocytes in adult mice', *Journal of Clinical Investigation*. American Society for Clinical Investigation, 125(3), pp. 1033–1042. doi: 10.1172/JCI69097.
- Chen, L. *et al.* (2018) 'Identification of aberrant circulating miRNAs in Parkinson's disease plasma samples', *Brain and Behavior*. John Wiley & Sons, Ltd, 8(4), p. e00941. doi: 10.1002/brb3.941.
- Chen, Q. Y. *et al.* (2021) 'Exosomal Proteins and miRNAs as Mediators of Amyotrophic Lateral Sclerosis', *Frontiers in Cell and Developmental Biology*, 9(September). doi: 10.3389/fcell.2021.718803.
- Chen, X. *et al.* (2008) 'Characterization of microRNAs in serum: a novel class of biomarkers for diagnosis of cancer and other diseases', *Cell Research*. Nature Publishing Group, 18(10), pp. 997–1006. doi: 10.1038/cr.2008.282.
- Chen, Y. *et al.* (2016) 'Aberration of miRNAs Expression in Leukocytes from Sporadic Amyotrophic Lateral Sclerosis.', *Frontiers in molecular neuroscience*. Frontiers Media SA, 9, p. 69. doi: 10.3389/fnmol.2016.00069.
- Chendrimada, T. P. *et al.* (2005) 'TRBP recruits the Dicer complex to Ago2 for microRNA processing and gene silencing', *Nature*. Nature Publishing Group, 436(7051), pp. 740–744. doi: 10.1038/nature03868.
- Cheng, L.-C. *et al.* (2009) 'miR-124 regulates adult neurogenesis in the subventricular zone stem cell niche.', *Nature neuroscience*. NIH Public Access, 12(4), pp. 399–408. doi: 10.1038/nn.2294.
- Cheng, X.-T. *et al.* (2015) 'Axonal autophagosomes recruit dynein for retrograde transport through fusion with late endosomes', *Journal of Cell Biology*. The Rockefeller University Press, 209(3), pp. 377–386. doi: 10.1083/JCB.201412046.

- Chiò, A. *et al.* (2012) 'Extensive genetics of ALS: a population-based study in Italy.', *Neurology*. American Academy of Neurology, 79(19), pp. 1983–9. doi: 10.1212/WNL.0b013e3182735d36.
- Chitiprolu, M. *et al.* (2018) 'A complex of C9ORF72 and p62 uses arginine methylation to eliminate stress granules by autophagy', *Nature Communications*. Nature Publishing Group, 9(1), pp. 1–18. doi: 10.1038/s41467-018-05273-7.
- Chou, C.-H. *et al.* (2018) 'miRTarBase update 2018: a resource for experimentally validated microRNA-target interactions', *Nucleic Acids Research*. Oxford University Press, 46(Database issue), p. D296. doi: 10.1093/NAR/GKX1067.
- Cirulli, E. T. *et al.* (2015) 'Exome sequencing in amyotrophic lateral sclerosis identifies risk genes and pathways', *Science*. American Association for the Advancement of Science, 347(6229), pp. 1436–1441. doi: 10.1126/science.aaa3650.
- Ciuffa, R. *et al.* (2015) 'The Selective Autophagy Receptor p62 Forms a Flexible Filamentous Helical Scaffold', *Cell Reports*. Cell Press, 11(5), pp. 748–758. doi: 10.1016/J.CELREP.2015.03.062.
- Clague, M. J. (2002) 'Membrane Transport : A Coat for Ubiquitin', 12(02), pp. 529–531.
- Clark, K. *et al.* (2009) 'Use of the pharmacological inhibitor BX795 to study the regulation and physiological roles of TBK1 and I $\kappa$ B Kinase  $\epsilon$ : A distinct upstream kinase mediates ser-172 phosphorylation and activation', *Journal of Biological Chemistry*. Elsevier, 284(21), pp. 14136–14146. doi: 10.1074/jbc.M109.000414.
- Clayton, A. *et al.* (2011) 'Cancer Exosomes Express CD39 and CD73, Which Suppress T Cells through Adenosine Production', *The Journal of Immunology*. The American Association of Immunologists, 187(2), pp. 676–683. doi: 10.4049/jimmunol.1003884.
- Cloutier, F. *et al.* (2015) 'MicroRNAs as Potential Circulating Biomarkers for Amyotrophic Lateral Sclerosis', *Journal of Molecular Neuroscience*. Springer US, 56(1), pp. 102–112. doi: 10.1007/s12031-014-0471-8.
- Cocucci, E. and Meldolesi, J. (2015) 'Ectosomes and exosomes: shedding the confusion between extracellular vesicles', *Trends in Cell Biology*. Elsevier Current Trends, 25(6), pp. 364–372. doi: 10.1016/J.TCB.2015.01.004.
- Colombrita, C. *et al.* (2009) 'TDP-43 is recruited to stress granules in conditions of oxidative insult', *Journal of Neurochemistry*. John Wiley & Sons, Ltd, 111(4), pp. 1051–1061. doi: 10.1111/j.1471-4159.2009.06383.x.
- Cooper-Knock, J. *et al.* (2012) 'Clinico-pathological features in amyotrophic lateral sclerosis with expansions in C9ORF72', *A JOURNAL OF NEUROLOGY*, 135(3), pp. 751–764. doi: 10.1093/brain/awr365.
- Cooper-Knock, J. *et al.* (2014) 'Sequestration of multiple RNA recognition motif-containing proteins by C9orf72 repeat expansions', *Brain*. Narnia, 137(7), pp. 2040–2051. doi: 10.1093/brain/awu120.
- Cooper-Knock, J. *et al.* (2015) 'Antisense RNA foci in the motor neurons of C9ORF72-ALS patients are associated with TDP-43 proteinopathy', *Acta Neuropathologica*. Springer Berlin Heidelberg, 130(1), pp. 63–75. doi: 10.1007/s00401-015-1429-9.
- Copple, I. M. *et al.* (2010) 'Physical and Functional Interaction of Sequestosome 1 with Keap1 Regulates the Keap1-Nrf2 Cell Defense Pathway', *The Journal of biological chemistry*, 285(22), pp. 16782–16788. doi: 10.1074/jbc.M109.096545.
- Corradi, E. *et al.* (2020) 'Axonal precursor miRNAs hitchhike on endosomes and locally regulate the development of neural circuits', *The EMBO Journal*. European Molecular Biology Organization, 39(6). doi: 10.15252/EMBJ.2019102513.
- Costa Verdera, H. *et al.* (2017) 'Cellular uptake of extracellular vesicles is mediated by clathrin-independent endocytosis and macropinocytosis', *Journal of Controlled Release*. Elsevier, 266, pp. 100–108. doi: 10.1016/J.JCONREL.2017.09.019.
- Costes, S. V. *et al.* (2004) 'Automatic and Quantitative Measurement of Protein-Protein Colocalization

- in Live Cells', *Biophysical Journal*. Cell Press, 86(6), pp. 3993–4003. doi: 10.1529/BIOPHYSJ.103.038422.
- Cruts, M. *et al.* (2006) 'Null mutations in progranulin cause ubiquitin-positive frontotemporal dementia linked to chromosome 17q21', *Nature*. Nature Publishing Group, 442(7105), pp. 920–924. doi: 10.1038/nature05017.
- Cui, J. *et al.* (2012) 'NLRP4 negatively regulates type I interferon signaling by targeting the kinase TBK1 for degradation via the ubiquitin ligase DTX4', *Nature Immunology* 2012 13:4. Nature Publishing Group, 13(4), pp. 387–395. doi: 10.1038/ni.2239.
- D'Erchia, A. M. *et al.* (2017a) 'Massive transcriptome sequencing of human spinal cord tissues provides new insights into motor neuron degeneration in ALS.', *Scientific reports*. Nature Publishing Group, 7(1), p. 10046. doi: 10.1038/s41598-017-10488-7.
- D'Erchia, A. M. *et al.* (2017b) 'Massive transcriptome sequencing of human spinal cord tissues provides new insights into motor neuron degeneration in ALS.', *Scientific reports*. Nature Publishing Group, 7(1), p. 10046. doi: 10.1038/s41598-017-10488-7.
- Dajas-Bailador, F. *et al.* (2012) 'microRNA-9 regulates axon extension and branching by targeting Map1b in mouse cortical neurons', *Nature Neuroscience*. Nature Publishing Group, 15(5), pp. 697–699. doi: 10.1038/nn.3082.
- Van Damme, P. *et al.* (2007) 'Astrocytes regulate GluR2 expression in motor neurons and their vulnerability to excitotoxicity', *Proceedings of the National Academy of Sciences of the United States of America*. National Academy of Sciences, 104(37), pp. 14825–14830. doi: 10.1073/pnas.0705046104.
- Van Damme, P. *et al.* (2008) 'Progranulin functions as a neurotrophic factor to regulate neurite outgrowth and enhance neuronal survival', *Journal of Cell Biology*. J Cell Biol, 181(1), pp. 37–41. doi: 10.1083/jcb.200712039.
- Dardiotis, E. *et al.* (2018) 'The Role of MicroRNAs in Patients with Amyotrophic Lateral Sclerosis', *Journal of Molecular Neuroscience*. Springer US, pp. 1–12. doi: 10.1007/s12031-018-1204-1.
- Davidson, Y. *et al.* (2016) 'Neurodegeneration in frontotemporal lobar degeneration and motor neurone disease associated with expansions in C9orf72 is linked to TDP-43 pathology and not associated with aggregated forms of dipeptide repeat proteins', *Neuropathology and Applied Neurobiology*. Blackwell Publishing Ltd, 42(3), pp. 242–254. doi: 10.1111/nan.12292.
- Debanne, D. *et al.* (2011) 'Axon physiology', *Physiological Reviews*. American Physiological Society Bethesda, MD, 91(2), pp. 555–602. doi: 10.1152/PHYSREV.00048.2009/ASSET/IMAGES/LARGE/Z9J0021125790017.JPEG.
- Van Deerlin, V. M. *et al.* (2008) 'TARDBP mutations in amyotrophic lateral sclerosis with TDP-43 neuropathology: a genetic and histopathological analysis', *The Lancet Neurology*. Elsevier, 7(5), pp. 409–416. doi: 10.1016/S1474-4422(08)70071-1.
- Dehouck, M.-P. *et al.* (1990) 'An Easier, Reproducible, and Mass-Production Method to Study the Blood-Brain Barrier In Vitro', *Journal of Neurochemistry*. John Wiley & Sons, Ltd, 54(5), pp. 1798–1801. doi: 10.1111/j.1471-4159.1990.tb01236.x.
- Deitmer, J. W., Bröer, A. and Bröer, S. (2003) 'Glutamine efflux from astrocytes is mediated by multiple pathways', *Journal of Neurochemistry*. John Wiley & Sons, Ltd, 87(1), pp. 127–135. doi: 10.1046/j.1471-4159.2003.01981.x.
- DeJesus-Hernandez, M. *et al.* (2011) 'Expanded GGGGCC Hexanucleotide Repeat in Noncoding Region of C9ORF72 Causes Chromosome 9p-Linked FTD and ALS', *Neuron*. Cell Press, 72(2), pp. 245–256. doi: 10.1016/J.NEURON.2011.09.011.
- DeJesus-Hernandez, M. *et al.* (2017) 'In-depth clinico-pathological examination of RNA foci in a large cohort of C9ORF72 expansion carriers', *Acta Neuropathologica*. Springer Verlag, 134(2), pp. 255–269. doi: 10.1007/s00401-017-1725-7.
- Deng, Z. *et al.* (2019) 'ALS-FTLD-linked mutations of SQSTM1/p62 disrupt selective autophagy and

- NFE2L2/NRF2 anti-oxidative stress pathway', *Autophagy*. Taylor & Francis, pp. 1–15. doi: 10.1080/15548627.2019.1644076.
- Deng, Z. *et al.* (2020) 'ALS-FTLD-linked mutations of SQSTM1/p62 disrupt selective autophagy and NFE2L2/NRF2 anti-oxidative stress pathway', *Autophagy*. Taylor and Francis Inc., 16(5), pp. 917–931. doi: 10.1080/15548627.2019.1644076.
- Dervishi, I. *et al.* (2018) 'Protein-protein interactions reveal key canonical pathways, upstream regulators, interactome domains, and novel targets in ALS.', *Scientific reports*. Nature Publishing Group, 8(1), p. 14732. doi: 10.1038/s41598-018-32902-4.
- Diaz-Amarilla, P. *et al.* (2016) 'Electrophilic nitro-fatty acids prevent astrocyte-mediated toxicity to motor neurons in a cell model of familial amyotrophic lateral sclerosis via nuclear factor erythroid 2-related factor activation', *Free Radical Biology and Medicine*. Elsevier Inc., 95, pp. 112–120. doi: 10.1016/j.freeradbiomed.2016.03.013.
- Diekstra, F. P. *et al.* (2012) 'UNC13A is a modifier of survival in amyotrophic lateral sclerosis', *Neurobiology of Aging*. Elsevier, 33(3), pp. 630.e3-630.e8. doi: 10.1016/J.NEUROBIOLAGING.2011.10.029.
- Ding, X. *et al.* (2015) 'Exposure to ALS-FTD-CSF generates TDP-43 aggregates in glioblastoma cells through exosomes and TNTs-like structure', *Oncotarget*. Impact Journals, 6(27), pp. 24178–24191. doi: 10.18632/oncotarget.4680.
- Dobrowolny, G. *et al.* (2021) 'A longitudinal study defined circulating microRNAs as reliable biomarkers for disease prognosis and progression in ALS human patients', *Cell Death Discovery*. Nature Publishing Group, 7(1), p. 4. doi: 10.1038/S41420-020-00397-6.
- Dodson, P. D. and Forsythe, I. D. (2004) 'Presynaptic K<sup>+</sup> channels: electrifying regulators of synaptic terminal excitability', *Trends in Neurosciences*. Elsevier, 27(4), pp. 210–217. doi: 10.1016/J.TINS.2004.02.012.
- Dong, X. *et al.* (2018) 'miR-133a, directly targeted USP39, suppresses cell proliferation and predicts prognosis of gastric cancer', *Oncology Letters*. Spandidos Publications, 15(6), p. 8311. doi: 10.3892/OL.2018.8421.
- Doyle, L. M. and Wang, M. Z. (2019) 'Overview of Extracellular Vesicles, Their Origin, Composition, Purpose, and Methods for Exosome Isolation and Analysis', *Cells*. MDPI AG, 8(7), p. 727. doi: 10.3390/cells8070727.
- Doyle, L. and Wang, M. (2019) 'Overview of Extracellular Vesicles, Their Origin, Composition, Purpose, and Methods for Exosome Isolation and Analysis', *Cells*. MDPI AG, 8(7), p. 727. doi: 10.3390/cells8070727.
- Dringen, R., Pawlowski, P. G. and Hirrlinger, J. (2005) 'Peroxide detoxification by brain cells', in *Journal of Neuroscience Research*, pp. 157–165. doi: 10.1002/jnr.20280.
- Duan, W. *et al.* (2019) 'Deletion of Tbk1 disrupts autophagy and reproduces behavioral and locomotor symptoms of FTD-ALS in mice', *Aging*. Impact Journals LLC, 11(8), pp. 2457–2476. doi: 10.18632/aging.101936.
- Duffy, J. R., Peach, R. K. and Strand, E. A. (2007) 'Progressive Apraxia of Speech as a Sign of Motor Neuron Disease', *American Journal of Speech-Language Pathology*. American Speech-Language-Hearing Association, 16(3), p. 198. doi: 10.1044/1058-0360(2007/025).
- Emde, A. *et al.* (2015) 'Dysregulated miRNA biogenesis downstream of cellular stress and ALS-causing mutations: a new mechanism for ALS.', *The EMBO journal*. EMBO Press, 34(21), pp. 2633–51. doi: 10.15252/embj.201490493.
- Van Es, M. A. *et al.* (2009) 'Genome-wide association study identifies 19p13.3 (UNC13A) and 9p21.2 as susceptibility loci for sporadic amyotrophic lateral sclerosis', *Nature genetics*. Nat Genet, 41(10), pp. 1083–1087. doi: 10.1038/NG.442.
- Escola, J. M. *et al.* (1998) 'Selective enrichment of tetraspan proteins on the internal vesicles of multivesicular endosomes and on exosomes secreted by human B-lymphocytes', *Journal of Biological*

*Chemistry*. American Society for Biochemistry and Molecular Biology, 273(32), pp. 20121–20127. doi: 10.1074/jbc.273.32.20121.

Eskelinen, E.-L. (2006) 'Roles of LAMP-1 and LAMP-2 in lysosome biogenesis and autophagy', *Molecular Aspects of Medicine*. Pergamon, 27(5–6), pp. 495–502. doi: 10.1016/J.MAM.2006.08.005.

Eskelinen, E. L. *et al.* (2002) 'Role of LAMP-2 in lysosome biogenesis and autophagy', *Molecular Biology of the Cell*. American Society for Cell Biology, 13(9), pp. 3355–3368. doi: 10.1091/mbc.E02-02-0114.

Eulalio, A., Huntzinger, E. and Izaurralde, E. (2008) 'GW182 interaction with Argonaute is essential for miRNA-mediated translational repression and mRNA decay', *Nature Structural & Molecular Biology*. Nature Publishing Group, 15(4), pp. 346–353. doi: 10.1038/nsmb.1405.

Evers, M. M., Toonen, L. J. A. and van Roon-Mom, W. M. C. (2015) 'Antisense oligonucleotides in therapy for neurodegenerative disorders', *Advanced Drug Delivery Reviews*. Elsevier, 87, pp. 90–103. doi: 10.1016/J.ADDR.2015.03.008.

Fader, C. M. *et al.* (2007) 'Induction of Autophagy Promotes Fusion of Multivesicular Bodies with Autophagic Vacuoles in K562 Cells', *Traffic*. John Wiley & Sons, Ltd, 9(2), pp. 230–250. doi: 10.1111/j.1600-0854.2007.00677.x.

Fader, C. M. *et al.* (2009) 'TI-VAMP/VAMP7 and VAMP3/cellubrevin: two v-SNARE proteins involved in specific steps of the autophagy/multivesicular body pathways', *Biochimica et Biophysica Acta - Molecular Cell Research*. Elsevier, 1793(12), pp. 1901–1916. doi: 10.1016/j.bbamcr.2009.09.011.

Farg, M. A. *et al.* (2014) 'C9ORF72, implicated in amyotrophic lateral sclerosis and frontotemporal dementia, regulates endosomal trafficking', *Human Molecular Genetics*, 23(13), pp. 3579–3595. doi: 10.1093/hmg/ddu068.

Fecto, F., Yan, J., Vemula, S. P., Liu, E., Yang, Y., Chen, W., Zheng, J. G., Shi, Y., Siddique, N., Arrat, H., Donkervoort, S., Ajroud-Driss, S., Sufit, R. L., Heller, S. L., Deng, H.-X., *et al.* (2011) '&lt;emph type="ital"&gt;SQSTM1&lt;/emph&gt; Mutations in Familial and Sporadic Amyotrophic Lateral Sclerosis', *Archives of Neurology*. American Medical Association, 68(11), p. 1440. doi: 10.1001/archneurol.2011.250.

Fecto, F., Yan, J., Vemula, S. P., Liu, E., Yang, Y., Chen, W., Zheng, J. G., Shi, Y., Siddique, N., Arrat, H., Donkervoort, S., Ajroud-Driss, S., Sufit, R. L., Heller, S. L., Deng, H. X., *et al.* (2011) 'SQSTM1 mutations in familial and sporadic amyotrophic lateral sclerosis', *Archives of Neurology*. American Medical Association, 68(11), pp. 1440–1446. doi: 10.1001/archneurol.2011.250.

Feiler, M. S. *et al.* (2015) 'TDP-43 is intercellularly transmitted across axon terminals.', *The Journal of cell biology*. Rockefeller University Press, 211(4), pp. 897–911. doi: 10.1083/jcb.201504057.

Feit, H. *et al.* (1998) 'Vocal cord and pharyngeal weakness with autosomal dominant distal myopathy: Clinical description and gene localization to 5q31', *American Journal of Human Genetics*. Cell Press, 63(6), pp. 1732–1742. doi: 10.1086/302166.

De Felice, B. *et al.* (2012) 'A miRNA signature in leukocytes from sporadic amyotrophic lateral sclerosis', *Gene*. Elsevier, 508(1), pp. 35–40. doi: 10.1016/J.GENE.2012.07.058.

De Felice, B. *et al.* (2018) 'Wide-Ranging Analysis of MicroRNA Profiles in Sporadic Amyotrophic Lateral Sclerosis Using Next-Generation Sequencing', *Frontiers in Genetics*. Frontiers, 9, p. 310. doi: 10.3389/fgene.2018.00310.

Fevrier, B. *et al.* (2004) 'Cells release prions in association with exosomes', *Proceedings of the National Academy of Sciences of the United States of America*. National Academy of Sciences, 101(26), pp. 9683–9688. doi: 10.1073/pnas.0308413101.

Figueroa-Romero, C. *et al.* (2016) 'Expression of microRNAs in human post-mortem amyotrophic lateral sclerosis spinal cords provides insight into disease mechanisms.', *Molecular and cellular neurosciences*. NIH Public Access, 71, pp. 34–45. doi: 10.1016/j.mcn.2015.12.008.

Filimonenko, M. *et al.* (2007) 'Functional multivesicular bodies are required for autophagic clearance of protein aggregates associated with neurodegenerative disease', *Journal of Cell Biology*. The Rockefeller University Press, 179(3), pp. 485–500. doi: 10.1083/JCB.200702115.

- Fitzgerald, K. A. *et al.* (2003) 'IKKE and TBK1 are essential components of the IRF3 signalling pathway', *Nature Immunology*. Nature Publishing Group, 4(5), pp. 491–496. doi: 10.1038/ni921.
- Foggin, S. *et al.* (2019) 'Biological significance of microRNA biomarkers in ALS-innocent bystanders or disease culprits?', *Frontiers in Neurology*, 10(578). doi: 10.3389/fneur.2019.00578.
- Foster, A. D. *et al.* (2020) 'ALS-associated TBK1 variant p.G175S is defective in phosphorylation of p62 and impacts TBK1-mediated signalling and TDP-43 autophagic degradation', *Molecular and Cellular Neuroscience*. Academic Press Inc., 108, p. 103539. doi: 10.1016/j.mcn.2020.103539.
- Freischmidt, A. *et al.* (2013) *Systemic dysregulation of TDP-43 binding microRNAs in amyotrophic lateral sclerosis*. doi: 10.1186/2051-5960-1-42.
- Freischmidt, A. *et al.* (2014) 'Serum microRNAs in patients with genetic amyotrophic lateral sclerosis and pre-manifest mutation carriers', *Brain*. Oxford University Press, 137(11), pp. 2938–2950. doi: 10.1093/brain/awu249.
- Freischmidt, A., Wieland, T., *et al.* (2015) 'Haploinsufficiency of TBK1 causes familial ALS and frontotemporal dementia', *Nature Neuroscience*. Nature Publishing Group, 18(5), pp. 631–636. doi: 10.1038/nn.4000.
- Freischmidt, A., Müller, K., *et al.* (2015) 'Serum microRNAs in sporadic amyotrophic lateral sclerosis', *Neurobiology of Aging*. Elsevier, 36(9), pp. 2660.e15-2660.e20. doi: 10.1016/J.NEUROBIOLAGING.2015.06.003.
- Friedman, R. C. *et al.* (2009) 'Most mammalian mRNAs are conserved targets of microRNAs.', *Genome research*. Cold Spring Harbor Laboratory Press, 19(1), pp. 92–105. doi: 10.1101/gr.082701.108.
- Frizzo, M. E. dos S. *et al.* (2004) 'Riluzole Enhances Glutamate Uptake in Rat Astrocyte Cultures', *Cellular and Molecular Neurobiology 2004 24:1*. Springer, 24(1), pp. 123–128. doi: 10.1023/B:CEMN.0000012717.37839.07.
- Fu, M., Nirschl, J. J. and Holzbaaur, E. L. F. (2014) 'LC3 Binding to the Scaffolding Protein JIP1 Regulates Processive Dynein-Driven Transport of Autophagosomes', *Developmental cell*. NIH Public Access, 29(5), p. 577. doi: 10.1016/J.DEVCEL.2014.04.015.
- Fuentealba, R. A. *et al.* (2010) 'Interaction with polyglutamine aggregates reveals a Q/N-rich domain in TDP-43', *Journal of Biological Chemistry*. American Society for Biochemistry and Molecular Biology, 285(34), pp. 26304–26314. doi: 10.1074/jbc.M110.125039.
- Fumagalli, E. *et al.* (2008) 'Riluzole enhances the activity of glutamate transporters GLAST, GLT1 and EAAC1', *European Journal of Pharmacology*. Elsevier, 578(2–3), pp. 171–176. doi: 10.1016/J.EJPHAR.2007.10.023.
- Furukawa, M. and Xiong, Y. (2005) 'BTB Protein Keap1 Targets Antioxidant Transcription Factor Nrf2 for Ubiquitination by the Cullin 3-Roc1 Ligase', *Molecular and Cellular Biology*. American Society for Microbiology, 25(1), pp. 162–171. doi: 10.1128/mcb.25.1.162-171.2005.
- Furuya, N. *et al.* (2005) 'The Evolutionarily Conserved Domain of Beclin 1 is Required for Vps34 Binding, Autophagy, and Tumor Suppressor Function', *Autophagy*. Taylor & Francis, 1(1), pp. 46–52. doi: 10.4161/auto.1.1.1542.
- Futter, C. E. *et al.* (1996) 'Multivesicular endosomes containing internalized EGF-EGF receptor complexes mature and then fuse directly with lysosomes', *The Journal of Cell Biology*. The Rockefeller University Press, 132(6), p. 1011. doi: 10.1083/JCB.132.6.1011.
- Gal, J. *et al.* (2007) 'p62 Accumulates and Enhances Aggregate Formation in Model Systems of Familial Amyotrophic Lateral Sclerosis', *Journal of Biological Chemistry*. American Society for Biochemistry and Molecular Biology, 282(15), pp. 11068–11077. doi: 10.1074/JBC.M608787200.
- Gal, J. *et al.* (2009) 'Sequestosome 1/p62 links familial ALS mutant SOD1 to LC3 via an ubiquitin-independent mechanism', *Journal of Neurochemistry*. John Wiley & Sons, Ltd (10.1111), 111(4), pp. 1062–1073. doi: 10.1111/j.1471-4159.2009.06388.x.
- Gall, L. Le *et al.* (2020) 'Molecular and Cellular Mechanisms Affected in ALS', *Journal of Personalized*

*Medicine*. Multidisciplinary Digital Publishing Institute (MDPI), 10(3), pp. 1–34. doi: 10.3390/JPM10030101.

Garcia-Martin, R. *et al.* (2021) 'MicroRNA sequence codes for small extracellular vesicle release and cellular retention', *Nature* 2021 601:7893. Nature Publishing Group, 601(7893), pp. 446–451. doi: 10.1038/s41586-021-04234-3.

De Gassart, A. *et al.* (2003) 'Lipid raft-associated protein sorting in exosomes', *Blood*. Blood, 102(13), pp. 4336–4344. doi: 10.1182/blood-2003-03-0871.

Gatica, D., Lahiri, V. and Klionsky, D. J. (2018) 'Cargo Recognition and Degradation by Selective Autophagy', *Nature cell biology*. NIH Public Access, 20(3), p. 233. doi: 10.1038/S41556-018-0037-Z.

Ge, W. W. *et al.* (2005) 'Mutant Copper-Zinc Superoxide Dismutase Binds to and Destabilizes Human Low Molecular Weight Neurofilament mRNA', *Journal of Biological Chemistry*. Elsevier, 280(1), pp. 118–124. doi: 10.1074/JBC.M405065200.

Geiger, J. R. P. *et al.* (1995) 'Relative Abundance of Subunit mRNAs Determines Gating and Ca<sup>2+</sup> Permeability of AMPA Receptors in Principal Neurons and Interneurons in Rat CNS', *Neuron*, 15, pp. 193–204. Available at: <https://reader.elsevier.com/reader/sd/pii/0896627395900764?token=A390B6830F5A2D86AC6498A3E3BB8B626FA2F35CA729D14AE1A09740A81051462AEDD7BF41D0B4ADA5D4D73DC9AE0453&originRegion=eu-west-1&originCreation=20220215100017> (Accessed: 15 February 2022).

Gerbino, V. *et al.* (2020) 'The Loss of TBK1 Kinase Activity in Motor Neurons or in All Cell Types Differentially Impacts ALS Disease Progression in SOD1 Mice', *Neuron*. Elsevier Inc., pp. 1–17. doi: 10.1016/j.neuron.2020.03.005.

Ghetti, B. *et al.* (2015) 'Invited review: Frontotemporal dementia caused by microtubule-associated protein tau gene (MAPT) mutations: A chameleon for neuropathology and neuroimaging', *Neuropathology and Applied Neurobiology*. Blackwell Publishing Ltd, pp. 24–46. doi: 10.1111/nan.12213.

Gibbins, D. J. *et al.* (2009) 'Multivesicular bodies associate with components of miRNA effector complexes and modulate miRNA activity', *Nature Cell Biology* 2009 11:9. Nature Publishing Group, 11(9), pp. 1143–1149. doi: 10.1038/ncb1929.

Goljanek-whysall, K. *et al.* (2020) 'miR-181a regulates p62/SQSTM1, parkin, and protein DJ-1 promoting mitochondrial dynamics in skeletal muscle aging', *Aging Cell*, pp. 1–16. doi: 10.1111/acer.13140.

Gomes, C. *et al.* (2007) 'Evidence for secretion of Cu,Zn superoxide dismutase via exosomes from a cell model of amyotrophic lateral sclerosis', *Neuroscience Letters*. Elsevier, 428(1), pp. 43–46. doi: 10.1016/j.neulet.2007.09.024.

Gomes, C. *et al.* (2019) 'Cortical Neurotoxic Astrocytes with Early ALS Pathology and miR-146a Deficit Replicate Gliosis Markers of Symptomatic SOD1G93A Mouse Model', *Molecular neurobiology*. Mol Neurobiol, 56(3), pp. 2137–2158. doi: 10.1007/S12035-018-1220-8.

Gomes, C. *et al.* (2020) 'Astrocyte regional diversity in ALS includes distinct aberrant phenotypes with common and causal pathological processes', *Experimental cell research*. Exp Cell Res, 395(2). doi: 10.1016/J.YEXCR.2020.112209.

Gong, Y. H. *et al.* (2000) 'Restricted Expression of G86R Cu/Zn Superoxide Dismutase in Astrocytes Results in Astrocytosis But Does Not Cause Motoneuron Degeneration', *The Journal of Neuroscience*. Society for Neuroscience, 20(2), p. 660. doi: 10.1523/JNEUROSCI.20-02-00660.2000.

Goode, A., Rea, S., *et al.* (2016) 'ALS-FTLD associated mutations of SQSTM1 impact on Keap1-Nrf2 signalling', *Molecular and Cellular Neuroscience*. Academic Press Inc., 76, pp. 52–58. doi: 10.1016/j.mcn.2016.08.004.

Goode, A., Butler, K., *et al.* (2016) 'Defective recognition of LC3B by mutant SQSTM1/p62 implicates impairment of autophagy as a pathogenic mechanism in ALS-FTLD', *Autophagy*. Taylor & Francis, 12(7), pp. 1094–1104. doi: 10.1080/15548627.2016.1170257.

- Gracias, N. G., Shirkey-Son, N. J. and Hengst, U. (2014) 'Local translation of TC10 is required for membrane expansion during axon outgrowth', *Nature Communications* 2014 5:1. Nature Publishing Group, 5(1), pp. 1–13. doi: 10.1038/ncomms4506.
- Grad, L. I. *et al.* (2011) 'Intermolecular transmission of superoxide dismutase 1 misfolding in living cells', *Proceedings of the National Academy of Sciences of the United States of America*. National Academy of Sciences, 108(39), pp. 16398–16403. doi: 10.1073/pnas.1102645108.
- Grad, L. I. *et al.* (2014) 'Intercellular propagated misfolding of wild-type Cu/Zn superoxide dismutase occurs via exosome-dependent and -independent mechanisms', *Proceedings of the National Academy of Sciences of the United States of America*. National Academy of Sciences, 111(9), pp. 3620–3625. doi: 10.1073/pnas.1312245111.
- Graffmo, K. S. *et al.* (2013) 'Expression of wild-type human superoxide dismutase-1 in mice causes amyotrophic lateral sclerosis', *Human Molecular Genetics*. Oxford Academic, 22(1), pp. 51–60. doi: 10.1093/HMG/DDS399.
- Gregory, R. I. *et al.* (2004) 'The Microprocessor complex mediates the genesis of microRNAs', *Nature*. Nature Publishing Group, 432(7014), pp. 235–240. doi: 10.1038/nature03120.
- Griffiths-Jones, S. *et al.* (2008) 'miRBase: tools for microRNA genomics.', *Nucleic acids research*. Oxford University Press, 36(Database issue), pp. D154–8. doi: 10.1093/nar/gkm952.
- Grimson, A. *et al.* (2007) 'MicroRNA Targeting Specificity in Mammals: Determinants Beyond Seed Pairing', *Molecular cell*. NIH Public Access, 27(1), p. 91. doi: 10.1016/J.MOLCEL.2007.06.017.
- Guitart, K. *et al.* (2016) 'Improvement of neuronal cell survival by astrocyte-derived exosomes under hypoxic and ischemic conditions depends on prion protein', *Glia*. *Glia*, 64(6), pp. 896–910. doi: 10.1002/GLIA.22963.
- Guo, B. *et al.* (2014) 'O-GlcNAc-modification of SNAP-29 regulates autophagosome maturation', *Nature Cell Biology*. Nature Publishing Group, 16(12), pp. 1215–1226. doi: 10.1038/ncb3066.
- Guo, H. *et al.* (2017) 'Atg5 Disassociates the V1V0-ATPase to Promote Exosome Production and Tumor Metastasis Independent of Canonical Macroautophagy', *Developmental Cell*, 43(6), pp. 716–730.e7. doi: 10.1016/j.devcel.2017.11.018.
- Guo, Y. *et al.* (2013) 'The modest impact of transcription factor Nrf2 on the course of disease in an ALS animal model', *Laboratory Investigation*. Nature Publishing Group, 93(7), pp. 825–833. doi: 10.1038/labinvest.2013.73.
- Gwinn, D. M. *et al.* (2008) 'AMPK Phosphorylation of Raptor Mediates a Metabolic Checkpoint', *Molecular Cell*. Elsevier, 30(2), pp. 214–226. doi: 10.1016/j.molcel.2008.03.003.
- Ha, M. and Kim, V. N. (2014) 'Regulation of microRNA biogenesis', *Nature Reviews Molecular Cell Biology*. Nature Publishing Group, 15(8), pp. 509–524. doi: 10.1038/nrm3838.
- Haeusler, A. R. *et al.* (2014) 'C9orf72 nucleotide repeat structures initiate molecular cascades of disease', *Nature*. Nature Publishing Group, 507(7491), pp. 195–200. doi: 10.1038/nature13124.
- Haidet-Phillips, A. M. *et al.* (2011) 'Astrocytes from familial and sporadic ALS patients are toxic to motor neurons', *Nature Biotechnology*. NIH Public Access, 29(9), pp. 824–828. doi: 10.1038/nbt.1957.
- Hammond, S. M. (2015) 'An overview of microRNAs.', *Advanced drug delivery reviews*. NIH Public Access, 87, pp. 3–14. doi: 10.1016/j.addr.2015.05.001.
- Han, J. *et al.* (2004) 'The Drosha-DGCR8 complex in primary microRNA processing.', *Genes & development*. Cold Spring Harbor Laboratory Press, 18(24), pp. 3016–27. doi: 10.1101/gad.1262504.
- Han, J. *et al.* (2006) 'Molecular Basis for the Recognition of Primary microRNAs by the Drosha-DGCR8 Complex', *Cell*. Cell Press, 125(5), pp. 887–901. doi: 10.1016/J.CELL.2006.03.043.
- Hara, T. *et al.* (2006) 'Suppression of basal autophagy in neural cells causes neurodegenerative disease in mice', *Nature* 2006 441:7095. Nature Publishing Group, 441(7095), pp. 885–889. doi: 10.1038/nature04724.

- Hara, T. *et al.* (2008) 'FIP200, a ULK-interacting protein, is required for autophagosome formation in mammalian cells.', *The Journal of cell biology*. The Rockefeller University Press, 181(3), pp. 497–510. doi: 10.1083/jcb.200712064.
- Hashimoto, K. *et al.* (2016) 'TAK1 Regulates the Nrf2 Antioxidant System Through Modulating p62/SQSTM1', *Antioxidants and Redox Signaling*. Mary Ann Liebert Inc., 25(17), pp. 953–964. doi: 10.1089/ars.2016.6663.
- Hawley, Z. C. E., Campos-Melo, D. and Strong, M. J. (2019) 'MiR-105 and miR-9 regulate the mRNA stability of neuronal intermediate filaments. Implications for the pathogenesis of amyotrophic lateral sclerosis (ALS)', *Brain Research*. Elsevier, 1706, pp. 93–100. doi: 10.1016/J.BRAINRES.2018.10.032.
- He, L. and Hannon, G. J. (2004) 'MicroRNAs: small RNAs with a big role in gene regulation', *Nature Reviews Genetics*. Nature Publishing Group, 5(7), pp. 522–531. doi: 10.1038/nrg1379.
- He, Q. Q. *et al.* (2016) 'MicroRNA-127 targeting of mitoNEET inhibits neurite outgrowth, induces cell apoptosis and contributes to physiological dysfunction after spinal cord transection', *Scientific Reports*. Nature Publishing Group, 6. doi: 10.1038/srep35205.
- Helferich, A. M. *et al.* (2018) 'Dysregulation of a novel miR-1825/TBCB/TUBA4A pathway in sporadic and familial ALS', *Cellular and Molecular Life Sciences*. Birkhauser Verlag AG, 75(23), pp. 4301–4319. doi: 10.1007/S00018-018-2873-1/FIGURES/9.
- Hengst, U. *et al.* (2009) 'Axonal elongation triggered by stimulus-induced local translation of a polarity complex protein', *Nature Cell Biology* 2009 11:8. Nature Publishing Group, 11(8), pp. 1024–1030. doi: 10.1038/ncb1916.
- Henne, W. M., Buchkovich, N. J. and Emr, S. D. (2011) 'Developmental Cell The ESCRT Pathway'. doi: 10.1016/j.devcel.2011.05.015.
- Heo, J. M. *et al.* (2015) 'The PINK1-PARKIN Mitochondrial Ubiquitylation Pathway Drives a Program of OPTN/NDP52 Recruitment and TBK1 Activation to Promote Mitophagy', *Molecular Cell*. Cell Press, 60(1), pp. 7–20. doi: 10.1016/j.molcel.2015.08.016.
- Herman, A. B. *et al.* (2021) 'Reduction of lamin B receptor levels by miR-340-5p disrupts chromatin, promotes cell senescence and enhances senolysis', *Nucleic Acids Research*. Oxford Academic, 49(13), pp. 7389–7405. doi: 10.1093/NAR/GKAB538.
- Hettich, B. F. *et al.* (2020) 'Exosomes for Wound Healing: Purification Optimization and Identification of Bioactive Components', *Advanced Science*. John Wiley & Sons, Ltd, 7(23), p. 2002596. doi: 10.1002/ADVS.202002596.
- Hideyama, T. *et al.* (2012) 'Profound downregulation of the RNA editing enzyme ADAR2 in ALS spinal motor neurons', *Neurobiology of Disease*. Academic Press, 45(3), pp. 1121–1128. doi: 10.1016/J.NBD.2011.12.033.
- Higelin, J. *et al.* (2018) 'NEK1 loss-of-function mutation induces DNA damage accumulation in ALS patient-derived motoneurons', *Stem Cell Research*. Elsevier, 30, pp. 150–162. doi: 10.1016/J.SCR.2018.06.005.
- Hirst, J. *et al.* (2013) 'Interaction between AP-5 and the hereditary spastic paraplegia proteins SPG11 and SPG15', *Molecular Biology of the Cell*. The American Society for Cell Biology, 24(16), pp. 2558–2569. doi: 10.1091/MBC.E13-03-0170/ASSET/IMAGES/LARGE/2558FIG7.JPEG.
- Hoell, J. I. *et al.* (2011) 'RNA targets of wild-type and mutant FET family proteins', *Nature Structural & Molecular Biology*. Nature Publishing Group, 18(12), pp. 1428–1431. doi: 10.1038/nsmb.2163.
- Hosokawa, N. *et al.* (2009) 'Nutrient-dependent mTORC1 association with the ULK1-Atg13-FIP200 complex required for autophagy.', *Molecular biology of the cell*. American Society for Cell Biology, 20(7), pp. 1981–91. doi: 10.1091/mbc.e08-12-1248.
- Hou, W. *et al.* (2017) 'Inhibition of Beclin-1-Mediated Autophagy by MicroRNA-17-5p Enhanced the Radiosensitivity of Glioma Cells', *Oncology Research Featuring Preclinical and Clinical Cancer Therapeutics*, 25(1), pp. 43–53. doi: 10.3727/096504016X14719078133285.

- Hoye, Mariah L *et al.* (2017) 'MicroRNA Profiling Reveals Marker of Motor Neuron Disease in ALS Models', *The Journal of neuroscience : the official journal of the Society for Neuroscience*. Society for Neuroscience, 37(22), pp. 5574–5586. doi: 10.1523/JNEUROSCI.3582-16.2017.
- Hoye, Mariah L. *et al.* (2017) 'MicroRNA Profiling Reveals Marker of Motor Neuron Disease in ALS Models', *Journal of Neuroscience*. Society for Neuroscience, 37(22), pp. 5574–5586. doi: 10.1523/JNEUROSCI.3582-16.2017.
- Hoye, M. L. *et al.* (2018) 'Motor neuron-derived microRNAs cause astrocyte dysfunction in amyotrophic lateral sclerosis', *Brain*. Oxford Academic, 141(9), pp. 2561–2575. doi: 10.1093/BRAIN/AWY182.
- Hsu, C. *et al.* (2010) 'Regulation of exosome secretion by Rab35 and its GTPase-activating proteins TBC1D10A-C', *Journal of Cell Biology*. The Rockefeller University Press, 189(2), pp. 223–232. doi: 10.1083/jcb.200911018.
- Hu, H. Y. *et al.* (2009) 'Sequence features associated with microRNA strand selection in humans and flies.', *BMC genomics*. BioMed Central, 10, p. 413. doi: 10.1186/1471-2164-10-413.
- Huang, D. *et al.* (2015) 'miR-340 suppresses glioblastoma multiforme', *Oncotarget*. Impact Journals LLC, 6(11), pp. 9257–9270. doi: 10.18632/oncotarget.3288.
- Huang, Y., Guerrero-Preston, R. and Ratovitski, E. A. (2012) 'Phospho- $\Delta$ Np63 $\alpha$ -dependent regulation of autophagic signaling through transcription and micro-RNA modulation', *Cell Cycle*. Taylor & Francis, 11(6), pp. 1247–1259. doi: 10.4161/cc.11.6.19670.
- Huang, Z. *et al.* (2019) 'miR-340-FHL2 axis inhibits cell growth and metastasis in ovarian cancer', *Cell Death & Disease*, 10(5), p. 372. doi: 10.1038/s41419-019-1604-3.
- Hunziker, W., Simmen, T. and Höning, S. (1996) 'Trafficking of lysosomal membrane proteins in polarized kidney cells.', *Nephrologie*, 17(7), pp. 347–350. Available at: <https://europepmc.org/article/med/8987042> (Accessed: 27 April 2022).
- Huotari, J. and Helenius, A. (2011) 'Endosome maturation', *EMBO Journal*. EMBO J, pp. 3481–3500. doi: 10.1038/emboj.2011.286.
- Hurwitz, S. N. *et al.* (2016) 'Nanoparticle analysis sheds budding insights into genetic drivers of extracellular vesicle biogenesis', *Journal of Extracellular Vesicles*. Taylor and Francis Ltd., 5(1), p. 31295. doi: 10.3402/jev.v5.31295.
- Hutvagner, G. *et al.* (2001) 'A cellular function for the RNA-interference enzyme Dicer in the maturation of the let-7 small temporal RNA.', *Science (New York, N.Y.)*. American Association for the Advancement of Science, 293(5531), pp. 834–8. doi: 10.1126/science.1062961.
- Ichimura, Y. *et al.* (2000) 'A ubiquitin-like system mediates protein lipidation', *Nature*. Nature Publishing Group, 408(6811), pp. 488–492. doi: 10.1038/35044114.
- Ichimura, Y. *et al.* (2013) 'Phosphorylation of p62 Activates the Keap1-Nrf2 Pathway during Selective Autophagy', *Molecular Cell*. Cell Press, 51(5), pp. 618–631. doi: 10.1016/J.MOLCEL.2013.08.003.
- Iguchi, Y. *et al.* (2013) 'Loss of TDP-43 causes age-dependent progressive motor neuron degeneration', *A JOURNAL OF NEUROLOGY*, 136(5), pp. 1371–1382. doi: 10.1093/brain/awt029.
- Iguchi, Y. *et al.* (2016) 'Exosome secretion is a key pathway for clearance of pathological TDP-43', *Brain*. Narnia, 139(12), pp. 3187–3201. doi: 10.1093/brain/aww237.
- Iida, A. *et al.* (2012) 'Novel deletion mutations of OPTN in amyotrophic lateral sclerosis in Japanese', *Neurobiology of Aging*. Elsevier Inc., 33(8), pp. 1843.e19-1843.e24. doi: 10.1016/j.neurobiolaging.2011.12.037.
- Ikenaka, K. *et al.* (2013) 'dnc-1/dynactin 1 Knockdown Disrupts Transport of Autophagosomes and Induces Motor Neuron Degeneration', *PLoS ONE*. Edited by U. Pandey. Public Library of Science, 8(2), p. e54511. doi: 10.1371/journal.pone.0054511.
- Iko, Y. *et al.* (2004) 'Domain Architectures and Characterization of an RNA-binding Protein, TLS', *Journal of Biological Chemistry*. American Society for Biochemistry and Molecular Biology, 279(43),

pp. 44834–44840. doi: 10.1074/JBC.M408552200.

Inoue, Y. *et al.* (2021) 'The stimulator of interferon genes (STING) pathway is upregulated in striatal astrocytes of patients with multiple system atrophy', *Neuroscience Letters*. Elsevier, 757, p. 135972. doi: 10.1016/J.NEULET.2021.135972.

Ishigaki, S. *et al.* (2012) 'Position-dependent FUS-RNA interactions regulate alternative splicing events and transcriptions', *Scientific Reports*. Nature Publishing Group, 2, p. 529. doi: 10.1038/SREP00529.

Ishikawa, H., Ma, Z. and Barber, G. N. (2009) 'STING regulates intracellular DNA-mediated, type I interferon-dependent innate immunity', *Nature*. NIH Public Access, 461(7265), p. 788. doi: 10.1038/NATURE08476.

Ishimura, R., Tanaka, K. and Komatsu, M. (2014) 'Dissection of the role of p62/Sqstm1 in activation of Nrf2 during xenophagy', *FEBS Letters*. No longer published by Elsevier, 588(5), pp. 822–828. doi: 10.1016/J.FEBSLET.2014.01.045.

Ishtiaq, M. *et al.* (2014) 'Analysis of Novel NEFL mRNA Targeting microRNAs in Amyotrophic Lateral Sclerosis', *PLoS ONE*. Edited by P. J. Kahle. Public Library of Science, 9(1), p. e85653. doi: 10.1371/journal.pone.0085653.

Isogai, S. *et al.* (2011) 'Crystal Structure of the Ubiquitin-associated (UBA) Domain of p62 and Its Interaction with Ubiquitin', *The Journal of Biological Chemistry*. American Society for Biochemistry and Molecular Biology, 286(36), p. 31864. doi: 10.1074/JBC.M111.259630.

Itakura, E. *et al.* (2008) 'Beclin 1 forms two distinct phosphatidylinositol 3-kinase complexes with mammalian Atg14 and UVRAG.', *Molecular biology of the cell*. American Society for Cell Biology, 19(12), pp. 5360–72. doi: 10.1091/mbc.e08-01-0080.

Itakura, E., Kishi-Itakura, C. and Mizushima, N. (2012) 'The Hairpin-type Tail-Anchored SNARE Syntaxin 17 Targets to Autophagosomes for Fusion with Endosomes/Lysosomes', *Cell*. Cell Press, 151(6), pp. 1256–1269. doi: 10.1016/J.CELL.2012.11.001.

Itakura, E. and Mizushima, N. (2011) 'p62 Targeting to the autophagosome formation site requires self-oligomerization but not LC3 binding.', *The Journal of cell biology*. The Rockefeller University Press, 192(1), pp. 17–27. doi: 10.1083/jcb.201009067.

Ito, D. *et al.* (2011) 'Nuclear transport impairment of amyotrophic lateral sclerosis-linked mutations in FUS/TLS', *Annals of Neurology*. John Wiley & Sons, Ltd, 69(1), pp. 152–162. doi: 10.1002/ana.22246.

Itoh, K. *et al.* (1997) 'An Nrf2/small Maf heterodimer mediates the induction of phase II detoxifying enzyme genes through antioxidant response elements', *Biochemical and Biophysical Research Communications*. Academic Press Inc., 236(2), pp. 313–322. doi: 10.1006/bbrc.1997.6943.

Iwasaki, S. *et al.* (2010) 'Hsc70/Hsp90 Chaperone Machinery Mediates ATP-Dependent RISC Loading of Small RNA Duplexes', *Molecular Cell*. Cell Press, 39(2), pp. 292–299. doi: 10.1016/J.MOLCEL.2010.05.015.

Jahn, R. and Südhof, T. C. (2003) 'Membrane Fusion and Exocytosis', <http://dx.doi.org/10.1146/annurev.biochem.68.1.863>. Annual Reviews 4139 El Camino Way, P.O. Box 10139, Palo Alto, CA 94303-0139, USA, 68, pp. 863–911. doi: 10.1146/ANNUREV.BIOCHEM.68.1.863.

Jain, A. *et al.* (2010) 'p62/SQSTM1 Is a Target Gene for Transcription Factor NRF2 and Creates a Positive Feedback Loop by Inducing Antioxidant Response Element-driven Gene Transcription \*', *Journal of Biological Chemistry*. Elsevier, 285(29), pp. 22576–22591. doi: 10.1074/JBC.M110.118976.

Jan, A. T. *et al.* (2017) 'Perspective insights of exosomes in neurodegenerative diseases: A critical appraisal', *Frontiers in Aging Neuroscience*. Frontiers Media S.A. doi: 10.3389/fnagi.2017.00317.

Jensen, L. *et al.* (2016) 'Skeletal Muscle Remodelling as a Function of Disease Progression in Amyotrophic Lateral Sclerosis.', *BioMed research international*. Hindawi Limited, 2016, p. 5930621. doi: 10.1155/2016/5930621.

Ji, Y. *et al.* (2016) 'Evaluation of in vivo antitumor effects of low-frequency ultrasound-mediated miRNA-133a microbubble delivery in breast cancer', *Cancer Medicine*. Wiley-Blackwell, 5(9), p. 2534.

doi: 10.1002/CAM4.840.

Jiang, P. *et al.* (2014) 'The HOPS complex mediates autophagosome-lysosome fusion through interaction with syntaxin 17.', *Molecular biology of the cell*. American Society for Cell Biology, 25(8), pp. 1327–37. doi: 10.1091/mbc.E13-08-0447.

Jiang, S. *et al.* (2013) 'Secretory versus degradative autophagy: Unconventional secretion of inflammatory mediators', *Journal of Innate Immunity*. Karger Publishers, pp. 471–479. doi: 10.1159/000346707.

Jo, M. H. *et al.* (2015) 'Human Argonaute 2 Has Diverse Reaction Pathways on Target RNAs', *Molecular Cell*. Cell Press, 59(1), pp. 117–124. doi: 10.1016/J.MOLCEL.2015.04.027.

Johnson, J. O. *et al.* (2010) 'Exome Sequencing Reveals VCP Mutations as a Cause of Familial ALS', *Neuron*. Elsevier, 68(5), pp. 857–864. doi: 10.1016/j.neuron.2010.11.036.

Johnson, J. O. *et al.* (2014) 'Mutations in the Matrin 3 gene cause familial amyotrophic lateral sclerosis', *Nature Neuroscience*. Nature Publishing Group, 17(5), pp. 664–666. doi: 10.1038/nn.3688.

Joilin, G. *et al.* (2019) *An overview of microRNAs as biomarkers of ALS*. Available at: [www.frontiersin.org](http://www.frontiersin.org) (Accessed: 27 February 2019).

Joilin, G. *et al.* (2020) 'Identification of a potential non-coding RNA biomarker signature for amyotrophic lateral sclerosis', *Brain Communications*. Oxford Academic, 2(1). doi: 10.1093/BRAINCOMMS/FCAA053.

Jonas, P. *et al.* (1994) 'Differences in Ca<sup>2+</sup> Permeability of AMPA-type G lutamate Receptor Channels in Neocortical Neurons Caused by Differential G luR-B Subunit Expression', *Neuron*, 12, pp. 1281–1289. Available at: <https://reader.elsevier.com/reader/sd/pii/0896627394904448?token=6BFAB96E1503E70A2B6711B55A20E4096FB860F28A7DFEA69BC4D04BAD341296596A90E81754942949CC5A3F14282AF3&originRegion=eu-west-1&originCreation=20220215100158> (Accessed: 15 February 2022).

Jovičić, A. and Gitler, A. D. (2017) 'Distinct repertoires of microRNAs present in mouse astrocytes compared to astrocytesecreted exosomes', *PLoS ONE*. Public Library of Science, 12(2). doi: 10.1371/journal.pone.0171418.

Jung, C. H. *et al.* (2009) 'ULK-Atg13-FIP200 complexes mediate mTOR signaling to the autophagy machinery.', *Molecular biology of the cell*. American Society for Cell Biology, 20(7), pp. 1992–2003. doi: 10.1091/mbc.e08-12-1249.

Kabeya, Y. *et al.* (2004) 'LC3, GABARAP and GATE16 localize to autophagosomal membrane depending on form-II formation.', *Journal of cell science*. The Company of Biologists Ltd, 117(Pt 13), pp. 2805–12. doi: 10.1242/jcs.01131.

Kabuta, T., Suzuki, Y. and Wada, K. (2006) 'Degradation of amyotrophic lateral sclerosis-linked mutant Cu,Zn-superoxide dismutase proteins by macroautophagy and the proteasome.', *The Journal of biological chemistry*. American Society for Biochemistry and Molecular Biology, 281(41), pp. 30524–33. doi: 10.1074/jbc.M603337200.

Kakizuka, A. (2008) 'Roles of VCP in human neurodegenerative disorders', *Biochemical Society Transactions*. Portland Press, 36(1), pp. 105–108. doi: 10.1042/BST0360105.

Kamelgarn, M. *et al.* (2016) 'Proteomic analysis of FUS interacting proteins provides insights into FUS function and its role in ALS', *Biochimica et biophysica acta*. NIH Public Access, 1862(10), p. 2004. doi: 10.1016/J.BBADIS.2016.07.015.

Katsu, M. *et al.* (2019) 'MicroRNA expression profiles of neuron-derived extracellular vesicles in plasma from patients with amyotrophic lateral sclerosis', *Neuroscience Letters*. Elsevier, 708, p. 134176. doi: 10.1016/J.NEULET.2019.03.048.

Katzmann, D. J., Babst, M. and Emr, S. D. (2001) 'Ubiquitin-dependent sorting into the multivesicular body pathway requires the function of a conserved endosomal protein sorting complex, ESCRT-I', *Cell*. Cell Press, 106(2), pp. 145–155. doi: 10.1016/S0092-8674(01)00434-2.

- Kawahara, Y. and Mieda-Sato, A. (2012) 'TDP-43 promotes microRNA biogenesis as a component of the Drosha and Dicer complexes.', *Proceedings of the National Academy of Sciences of the United States of America*. National Academy of Sciences, 109(9), pp. 3347–52. doi: 10.1073/pnas.1112427109.
- Keerthikumar, S. *et al.* (2016) 'ExoCarta: A Web-Based Compendium of Exosomal Cargo', *Journal of Molecular Biology*. Academic Press, 428(4), pp. 688–692. doi: 10.1016/j.jmb.2015.09.019.
- Keller, A. *et al.* (2021) 'miRNATissueAtlas2: an update to the human miRNA tissue atlas', *Nucleic Acids Research*. Oxford University Press (OUP), (1). doi: 10.1093/NAR/GKAB808.
- Kim, H. J. *et al.* (2013) 'Mutations in prion-like domains in hnRNPA2B1 and hnRNPA1 cause multisystem proteinopathy and ALS', *Nature*. Nature Publishing Group, 495(7442), pp. 467–473. doi: 10.1038/nature11922.
- Kim, J. *et al.* (2004) 'Identification of many microRNAs that copurify with polyribosomes in mammalian neurons', *Proceedings of the National Academy of Sciences of the United States of America*. National Academy of Sciences, 101(1), pp. 360–365. doi: 10.1073/pnas.2333854100.
- Kim, J. *et al.* (2011) 'AMPK and mTOR regulate autophagy through direct phosphorylation of Ulk1', *Nature Publishing Group*, 13. doi: 10.1038/ncb2152.
- Kim, J. *et al.* (2013) 'Differential regulation of distinct Vps34 complexes by AMPK in nutrient stress and autophagy.', *Cell*. Elsevier, 152(1–2), pp. 290–303. doi: 10.1016/j.cell.2012.12.016.
- Kimura, S., Noda, T. and Yoshimori, T. (2008) 'Dynein-dependent movement of autophagosomes mediates efficient encounters with lysosomes', *Kimura S1, Noda T, Yoshimori T.*, 33(1), pp. 109–122.
- Kimura, T. *et al.* (2017) 'Dedicated SNAREs and specialized TRIM cargo receptors mediate secretory autophagy', *The EMBO Journal*. European Molecular Biology Organization, 36(1), p. 42. doi: 10.15252/EMBJ.201695081.
- Kirby, J. *et al.* (2016) 'The genetics of amyotrophic lateral sclerosis: current insights', *Degenerative Neurological and Neuromuscular Disease*. Dove Press, 6, p. 49. doi: 10.2147/DNND.S84956.
- Kirisako, T. *et al.* (2000) 'The reversible modification regulates the membrane-binding state of Apg8/Aut7 essential for autophagy and the cytoplasm to vacuole targeting pathway', *Journal of Cell Biology*. The Rockefeller University Press, 151(2), pp. 263–275. doi: 10.1083/jcb.151.2.263.
- Kirkin, V. *et al.* (2009) 'A Role for NBR1 in Autophagosomal Degradation of Ubiquitinated Substrates', *Molecular Cell*. Cell Press, 33(4), pp. 505–516. doi: 10.1016/J.MOLCEL.2009.01.020.
- Kishore, S. *et al.* (2011) 'A quantitative analysis of CLIP methods for identifying binding sites of RNA-binding proteins', *Nature methods*. Nat Methods, 8(7), pp. 559–567. doi: 10.1038/NMETH.1608.
- Kislauskis, E. H., Zhu, X. and Singer, R. H. (1994) 'Sequences responsible for intracellular localization of beta-actin messenger RNA also affect cell phenotype', *The Journal of cell biology*. J Cell Biol, 127(2), pp. 441–451. doi: 10.1083/JCB.127.2.441.
- Kiss, A. L. and Botos, E. (2009) 'Endocytosis via caveolae: alternative pathway with distinct cellular compartments to avoid lysosomal degradation?', *Journal of cellular and molecular medicine*. J Cell Mol Med, 13(7), pp. 1228–1237. doi: 10.1111/J.1582-4934.2009.00754.X.
- Klionsky, D. J. *et al.* (2016) 'Guidelines for the use and interpretation of assays for monitoring autophagy (3rd edition)', *Autophagy*. Taylor and Francis Inc., pp. 1–222. doi: 10.1080/15548627.2015.1100356.
- Kmetzsch, V. *et al.* (2021) 'Plasma microRNA signature in presymptomatic and symptomatic subjects with C9orf72-associated frontotemporal dementia and amyotrophic lateral sclerosis', *Journal of Neurology, Neurosurgery & Psychiatry*. BMJ Publishing Group Ltd, 92(5), pp. 485–493. doi: 10.1136/JNNP-2020-324647.
- Kobayashi, A. *et al.* (2004) 'Oxidative Stress Sensor Keap1 Functions as an Adaptor for Cul3-Based E3 Ligase To Regulate Proteasomal Degradation of Nrf2', *Molecular and Cellular Biology*. American Society for Microbiology, 24(16), pp. 7130–7139. doi: 10.1128/mcb.24.16.7130-7139.2004.

- Komander, D. and Rape, M. (2012) 'The Ubiquitin Code', *Annual Review of Biochemistry*. Annual Reviews, 81(1), pp. 203–229. doi: 10.1146/annurev-biochem-060310-170328.
- Komatsu, M. *et al.* (2006) 'Loss of autophagy in the central nervous system causes neurodegeneration in mice', *Nature*. Nature Publishing Group, 441(7095), pp. 880–884. doi: 10.1038/nature04723.
- Komatsu, M. *et al.* (2007) 'Essential role for autophagy protein Atg7 in the maintenance of axonal homeostasis and the prevention of axonal degeneration', *Proceedings of the National Academy of Sciences*. National Academy of Sciences, 104(36), pp. 14489–14494. doi: 10.1073/PNAS.0701311104.
- Komatsu, M. *et al.* (2010) 'The selective autophagy substrate p62 activates the stress responsive transcription factor Nrf2 through inactivation of Keap1', *Nature Cell Biology*. Nat Cell Biol, 12(3), pp. 213–223. doi: 10.1038/ncb2021.
- Kong, D. S. *et al.* (2009) 'Prognostic significance of c-Met expression in glioblastomas', *Cancer*. Cancer, 115(1), pp. 140–148. doi: 10.1002/cncr.23972.
- Koppers-Lalic, D. *et al.* (2014) 'Nontemplated nucleotide additions distinguish the small RNA composition in cells from exosomes', *Cell Reports*. Elsevier, 8(6), pp. 1649–1658. doi: 10.1016/j.celrep.2014.08.027.
- Korac, J. *et al.* (2012) 'Ubiquitin-independent function of optineurin in autophagic clearance of protein aggregates', *Journal of Cell Science*, 126, pp. 580–592. doi: 10.1242/jcs.114926.
- Korkmaz, G. *et al.* (2012) 'miR-376b controls starvation and mTOR inhibition-related autophagy by targeting ATG4C and BECN1', *Autophagy*. Taylor & Francis, 8(2), pp. 165–176. doi: 10.4161/auto.8.2.18351.
- Kosaka, N. *et al.* (2010) 'Secretory Mechanisms and Intercellular Transfer of MicroRNAs in Living Cells', *The Journal of Biological Chemistry*. American Society for Biochemistry and Molecular Biology, 285(23), p. 17442. doi: 10.1074/JBC.M110.107821.
- Kovanda, A. *et al.* (2018) 'Differential expression of microRNAs and other small RNAs in muscle tissue of patients with ALS and healthy age-matched controls', *Scientific Reports*. Nature Publishing Group, 8(1), p. 5609. doi: 10.1038/s41598-018-23139-2.
- Kozomara, A., Birgaoanu, M. and Griffiths-Jones, S. (2019) 'miRBase: from microRNA sequences to function', *Nucleic Acids Research*. Narnia, 47(D1), pp. D155–D162. doi: 10.1093/nar/gky1141.
- Kozomara, A. and Griffiths-Jones, S. (2014) 'miRBase: annotating high confidence microRNAs using deep sequencing data', *Nucleic Acids Research*. Oxford University Press, 42(D1), pp. D68–D73. doi: 10.1093/nar/gkt1181.
- Krek, A. *et al.* (2005) 'Combinatorial microRNA target predictions', *Nature Genetics*. Nature Publishing Group, 37(5), pp. 495–500. doi: 10.1038/ng1536.
- Kristen, A. V. *et al.* (2019) 'Patisiran, an RNAi therapeutic for the treatment of hereditary transthyretin-mediated amyloidosis', *Neurodegenerative disease management*. NLM (Medline), 9(1), pp. 5–23. doi: 10.2217/NMT-2018-0033/ASSET/IMAGES/LARGE/FIGURE4.JPEG.
- Kroemer, G., Mariño, G. and Levine, B. (2010) 'Autophagy and the integrated stress response', *Molecular cell*. NIH Public Access, 40(2), p. 280. doi: 10.1016/J.MOLCEL.2010.09.023.
- Krol, J., Loedige, I. and Filipowicz, W. (2010) 'The widespread regulation of microRNA biogenesis, function and decay', *Nature Reviews Genetics*. Nature Publishing Group, 11(9), pp. 597–610. doi: 10.1038/nrg2843.
- Kumar-Singh, S. (2011) 'Progranulin and TDP-43: Mechanistic links and future directions', in *Journal of Molecular Neuroscience*. Springer, pp. 561–573. doi: 10.1007/s12031-011-9625-0.
- Kumar, S. *et al.* (2019) 'Phosphorylation of Syntaxin 17 by TBK1 Controls Autophagy Initiation', *Developmental Cell*. Cell Press, 49(1), pp. 130–144.e6. doi: 10.1016/j.devcel.2019.01.027.
- Kwak, M.-K. *et al.* (2002) 'Enhanced Expression of the Transcription Factor Nrf2 by Cancer Chemopreventive Agents: Role of Antioxidant Response Element-Like Sequences in the nrf2 Promoter', *Molecular and Cellular Biology*. American Society for Microbiology, 22(9), pp. 2883–2892.

doi: 10.1128/mcb.22.9.2883-2892.2002.

Kwiatkowski, T. J. *et al.* (2009) 'Mutations in the FUS/TLS gene on chromosome 16 cause familial amyotrophic lateral sclerosis.', *Science (New York, N.Y.)*. American Association for the Advancement of Science, 323(5918), pp. 1205–8. doi: 10.1126/science.1166066.

Kye, M. J. *et al.* (2007) 'Somatodendritic microRNAs identified by laser capture and multiplex RT-PCR', *RNA*. Cold Spring Harbor Laboratory Press, 13(8), p. 1224. doi: 10.1261/RNA.480407.

Kye, M. J. and Gonçalves, I. do C. G. (2014) 'The role of miRNA in motor neuron disease', *Frontiers in Cellular Neuroscience*. Frontiers, 8, p. 15. doi: 10.3389/fncel.2014.00015.

Lagier-Tourenne, C., Polymenidou, M. and Cleveland, D. W. (2010) 'TDP-43 and FUS/TLS: emerging roles in RNA processing and neurodegeneration.', *Human molecular genetics*. Oxford University Press, 19(R1), pp. R46–64. doi: 10.1093/hmg/ddq137.

Lagos-Quintana, M. *et al.* (2001) 'Identification of Novel Genes Coding for Small Expressed RNAs', *Science (New York, N.Y.)*. American Association for the Advancement of Science, 294(5443), pp. 853–858. doi: 10.1126/science.286.5441.950.

Lai, C. *et al.* (2009) 'Regulation of endosomal motility and degradation by amyotrophic lateral sclerosis 2/alsin', *Molecular Brain*. BioMed Central, 2(1), p. 23. doi: 10.1186/1756-6606-2-23.

Lamark, T. *et al.* (1986) 'Cell Cycle NBR1 and p62 as cargo receptors for selective autophagy of ubiquitinated targets', *Cell Cycle*, 8(13), p. 13. doi: 10.4161/cc.8.13.8892.

Laplante, M. and Sabatini, D. M. (2009) 'mTOR signaling at a glance', *Journal of Cell Science*. Company of Biologists, 122(20), p. 3589. doi: 10.1242/JCS.051011.

Larabi, A. *et al.* (2013) 'Crystal Structure and Mechanism of Activation of TANK-Binding Kinase 1', *Cell Reports*. Cell Press, 3(3), pp. 734–746. doi: 10.1016/J.CELREP.2013.01.034.

Lattante, S. *et al.* (2015) 'Sqstm1 knock-down causes a locomotor phenotype ameliorated by rapamycin in a zebrafish model of ALS/FTLD', *Human Molecular Genetics*. Narnia, 24(6), pp. 1682–1690. doi: 10.1093/hmg/ddu580.

Lee, C.-T., Risom, T. and Strauss, W. M. (2007) 'Evolutionary Conservation of MicroRNA Regulatory Circuits: An Examination of MicroRNA Gene Complexity and Conserved MicroRNA-Target Interactions through Metazoan Phylogeny', *DNA and Cell Biology*, 26(4), pp. 209–218. doi: 10.1089/dna.2006.0545.

Lee, R. C., Feinbaum, R. L. and Ambros, V. (1993) 'The *C. elegans* heterochronic gene *lin-4* encodes small RNAs with antisense complementarity to *lin-14*', *Cell*. Cell Press, 75(5), pp. 843–854. doi: 10.1016/0092-8674(93)90529-Y.

Lee, Y. *et al.* (2003) 'The nuclear RNase III Drosha initiates microRNA processing', *Nature*. Nature Publishing Group, 425(6956), pp. 415–419. doi: 10.1038/nature01957.

Lee, Y. *et al.* (2004) 'MicroRNA genes are transcribed by RNA polymerase II.', *The EMBO journal*. EMBO Press, 23(20), pp. 4051–60. doi: 10.1038/sj.emboj.7600385.

Leidal, A. M. *et al.* (2020) 'The LC3-conjugation machinery specifies the loading of RNA-binding proteins into extracellular vesicles', *Nature Cell Biology*, 22(2), pp. 187–199. doi: 10.1038/s41556-019-0450-y.

Lerga, A. *et al.* (2001) 'Identification of an RNA binding specificity for the potential splicing factor TLS.', *The Journal of biological chemistry*. American Society for Biochemistry and Molecular Biology, 276(9), pp. 6807–16. doi: 10.1074/jbc.M008304200.

Levine, B., Sinha, S. and Kroemer, G. (2008) 'Bcl-2 family members: Dual regulators of apoptosis and autophagy', *Autophagy*. NIH Public Access, 4(5), p. 600. doi: 10.4161/auto.6260.

Levy, J. R. *et al.* (2006) 'A motor neuron disease-associated mutation in p150Glued perturbs dynactin function and induces protein aggregation', *Journal of Cell Biology*. The Rockefeller University Press, 172(5), pp. 733–745. doi: 10.1083/jcb.200511068.

- Li, C. *et al.* (2017) 'Downregulation of MicroRNA-193b-3p Promotes Autophagy and Cell Survival by Targeting TSC1/mTOR Signaling in NSC-34 Cells.', *Frontiers in molecular neuroscience*. Frontiers Media SA, 10, p. 160. doi: 10.3389/fnmol.2017.00160.
- Li, D.-B. *et al.* (2017) 'Plasma exosomal miR-422a and miR-125b-2-3p serve as biomarkers for ischemic stroke', *Current Neurovascular Research*. Bentham Science Publishers Ltd., 14(4). doi: 10.2174/1567202614666171005153434.
- Li, S. *et al.* (2017) 'MiR-340 Regulates Fibrinolysis and Axon Regrowth Following Sciatic Nerve Injury', *Molecular Neurobiology*. Humana Press Inc., 54(6), pp. 4379–4389. doi: 10.1007/s12035-016-9965-4.
- Liguori, M. *et al.* (2018) 'Dysregulation of MicroRNAs and Target Genes Networks in Peripheral Blood of Patients With Sporadic Amyotrophic Lateral Sclerosis', *Frontiers in Molecular Neuroscience*. Frontiers, 11, p. 288. doi: 10.3389/fnmol.2018.00288.
- Lillo, P. *et al.* (2011) 'How common are behavioural changes in amyotrophic lateral sclerosis?', *Amyotrophic Lateral Sclerosis*. Taylor & Francis, 12(1), pp. 45–51. doi: 10.3109/17482968.2010.520718.
- Lim, J. *et al.* (2015) 'Proteotoxic Stress Induces Phosphorylation of p62/SQSTM1 by ULK1 to Regulate Selective Autophagic Clearance of Protein Aggregates', *PLoS Genetics*. Edited by W. Yang. Public Library of Science, 11(2), p. e1004987. doi: 10.1371/journal.pgen.1004987.
- Lindmo, K. *et al.* (2008) 'The PI 3-kinase regulator Vps15 is required for autophagic clearance of protein aggregates', *Autophagy*. Taylor & Francis, 4(4), pp. 500–506. doi: 10.4161/auto.5829.
- Lindow, M. and Kauppinen, S. (2012) 'Discovering the first microRNA-targeted drug', *The Journal of Cell Biology*. The Rockefeller University Press, 199(3), p. 407. doi: 10.1083/JCB.201208082.
- Ling, J. P. *et al.* (2015) 'TDP-43 repression of nonconserved cryptic exons is compromised in ALS-FTD', *Science (New York, N.Y.)*. NIH Public Access, 349(6248), p. 650. doi: 10.1126/SCIENCE.AAB0983.
- Lingel, A. *et al.* (2003) 'Structure and nucleic-acid binding of the Drosophila Argonaute 2 PAZ domain', *Nature*. Nature Publishing Group, 426(6965), pp. 465–469. doi: 10.1038/nature02123.
- Liu, Q., Li, P. and Sun, Y. (2016) 'MicroRNA-340 Induces Apoptosis and Inhibits Metastasis of Ovarian Cancer Cells by Inactivation of NF- $\kappa$ B1', *Cell Physiol Biochem*, 38, pp. 1915–1927. doi: 10.1159/000445553.
- Liu, S. *et al.* (2015) 'Phosphorylation of innate immune adaptor proteins MAVS, STING, and TRIF induces IRF3 activation', *Science*. American Association for the Advancement of Science, 347(6227). doi: 10.1126/SCIENCE.AAA2630.
- Liu, Z. *et al.* (2018) 'ALS-associated E478G mutation in human OPTN (optineurin) promotes inflammation and induces neuronal cell death', *Frontiers in Immunology*. Frontiers Media S.A., 9(NOV). doi: 10.3389/fimmu.2018.02647.
- Lomen-Hoerth, C., Anderson, T. and Miller, B. (2002) 'The overlap of amyotrophic lateral sclerosis and frontotemporal dementia', *Neurology*. Lippincott Williams and Wilkins, 59(7), pp. 1077–1079. doi: 10.1212/WNL.59.7.1077.
- Long, J. *et al.* (2008) 'Ubiquitin recognition by the ubiquitin-associated domain of p62 involves a novel conformational switch.', *The Journal of biological chemistry*. American Society for Biochemistry and Molecular Biology, 283(9), pp. 5427–40. doi: 10.1074/jbc.M704973200.
- Lu, C. H. *et al.* (2015) 'Neurofilament light chain: A prognostic biomarker in amyotrophic lateral sclerosis', *Neurology*. American Academy of Neurology, 84(22), p. 2247. doi: 10.1212/WNL.0000000000001642.
- Lucci, C. *et al.* (2020) 'Spatiotemporal regulation of GSK3 $\beta$  levels by miRNA-26a controls axon development in cortical neurons', *Development (Cambridge)*. Company of Biologists Ltd, 147(3). doi: 10.1242/dev.180232.
- Ludwig, N. *et al.* (2016) 'Distribution of miRNA expression across human tissues.', *Nucleic acids research*. Oxford University Press, 44(8), pp. 3865–77. doi: 10.1093/nar/gkw116.

- De Luna, N. *et al.* (2020) 'Downregulation of miR-335-5P in Amyotrophic Lateral Sclerosis Can Contribute to Neuronal Mitochondrial Dysfunction and Apoptosis', *Scientific Reports*. Nature Research, 10(1). doi: 10.1038/s41598-020-61246-1.
- Lund, E. *et al.* (2004) 'Nuclear Export of MicroRNA Precursors', *Science*. American Association for the Advancement of Science, 301(5631), pp. 95–98. doi: 10.1126/science.1085242.
- Ma, J.-B., Ye, K. and Patel, D. J. (2004) 'Structural basis for overhang-specific small interfering RNA recognition by the PAZ domain', *Nature*. Nature Publishing Group, 429(6989), pp. 318–322. doi: 10.1038/nature02519.
- Ma, X. R. *et al.* (2022) 'TDP-43 represses cryptic exon inclusion in the FTD–ALS gene UNC13A', *Nature*. Nature Publishing Group, 603(7899), p. 124. doi: 10.1038/S41586-022-04424-7.
- Ma, Y. *et al.* (2016) 'Validation of downregulated microRNAs during osteoclast formation and osteoporosis progression', *Molecular Medicine Reports*. Spandidos Publications, 13(3), pp. 2273–2280. doi: 10.3892/mmr.2016.4765.
- Maday, S., Wallace, K. E. and Holzbaur, E. L. F. (2012) 'Autophagosomes initiate distally and mature during transport toward the cell soma in primary neurons', *Journal of Cell Biology*. The Rockefeller University Press, 196(4), pp. 407–417. doi: 10.1083/JCB.201106120.
- Magdziarek, M. *et al.* (2020) 'Re-examining how Munc13-1 facilitates opening of syntaxin-1'. doi: 10.1002/pro.3844.
- Magen, I. *et al.* (2021) 'Circulating miR-181 is a prognostic biomarker for amyotrophic lateral sclerosis', *Nature neuroscience*. Nat Neurosci, 24(11), pp. 1534–1541. doi: 10.1038/S41593-021-00936-Z.
- Mancuso, R. *et al.* (2014) 'Resveratrol Improves Motoneuron Function and Extends Survival in SOD1G93A ALS Mice', *Neurotherapeutics*. Springer US, 11(2), pp. 419–432. doi: 10.1007/s13311-013-0253-y.
- Mann, D. M. *et al.* (2013) 'Dipeptide repeat proteins are present in the p62 positive inclusions in patients with frontotemporal lobar degeneration and motor neurone disease associated with expansions in C9ORF72', *Acta Neuropathologica Communications*. Springer Nature, 1(1), p. 68. doi: 10.1186/2051-5960-1-68.
- Maruyama, H. *et al.* (2010) 'Mutations of optineurin in amyotrophic lateral sclerosis', *Nature*. Nature Publishing Group, 465(7295), pp. 223–226. doi: 10.1038/nature08971.
- Massey, A., Kiffin, R. and Cuervo, A. M. (2004) 'Pathophysiology of chaperone-mediated autophagy', *The international journal of biochemistry & cell biology*. Int J Biochem Cell Biol, 36(12), pp. 2420–2434. doi: 10.1016/J.BIOCEL.2004.04.010.
- Matsumoto, G. *et al.* (2011) 'Serine 403 Phosphorylation of p62/SQSTM1 Regulates Selective Autophagic Clearance of Ubiquitinated Proteins', *Molecular Cell*. Cell Press, 44(2), pp. 279–289. doi: 10.1016/J.MOLCEL.2011.07.039.
- McEwan, D. G. *et al.* (2015) 'PLEKHM1 Regulates Autophagosome-Lysosome Fusion through HOPS Complex and LC3/GABARAP Proteins', *Molecular Cell*. Cell Press, 57(1), pp. 39–54. doi: 10.1016/J.MOLCEL.2014.11.006.
- McMahon, H. T. and Boucrot, E. (2015) 'Membrane curvature at a glance', *Journal of Cell Science*. Company of Biologists Ltd, 128(6), pp. 1065–1070. doi: 10.1242/jcs.114454.
- Mei, T. *et al.* (2019) 'miR-340-5p: A potential direct regulator of Nrf2 expression in the post-exercise skeletal muscle of mice', *Molecular Medicine Reports*, 19(2), pp. 1340–1348. doi: 10.3892/mmr.2018.9762.
- Meijer, H. A., Smith, E. M. and Bushell, M. (2014) 'Regulation of miRNA strand selection: follow the leader?', *Biochemical Society transactions*. Portland Press Limited, 42(4), pp. 1135–40. doi: 10.1042/BST20140142.
- Melcher, T. *et al.* (1996) 'A mammalian RNA editing enzyme', *Nature*, 379.
- Meldolesi, J. (2018) 'Exosomes and Ectosomes in Intercellular Communication', *Current Biology*. Cell

Press, 28(8), pp. R435–R444. doi: 10.1016/J.CUB.2018.01.059.

Melino, G. (2005) 'Discovery of the ubiquitin proteasome system and its involvement in apoptosis', *Cell Death & Differentiation*. Nature Publishing Group, 12(9), pp. 1155–1157. doi: 10.1038/sj.cdd.4401740.

Menzies, F. M. *et al.* (2002) 'Selective loss of neurofilament expression in Cu/Zn superoxide dismutase (SOD1) linked amyotrophic lateral sclerosis', *Journal of Neurochemistry*. John Wiley & Sons, Ltd (10.1111), 82(5), pp. 1118–1128. doi: 10.1046/j.1471-4159.2002.01045.x.

Mercer, C. A., Kaliappan, A. and Dennis, P. B. (2009) 'A novel, human Atg13 binding protein, Atg101, interacts with ULK1 and is essential for macroautophagy', *Autophagy*, 5(5), pp. 649–662. doi: 10.4161/auto.5.5.8249.

Mesquita-Ribeiro, R. *et al.* (2021) 'Distinct small non-coding RNA landscape in the axons and released extracellular vesicles of developing primary cortical neurons and the axoplasm of adult nerves', <https://doi.org/10.1080/15476286.2021.2000792>. Taylor & Francis, 18(sup2), pp. 832–855. doi: 10.1080/15476286.2021.2000792.

Miao, Y. *et al.* (2015) 'A TRP Channel Senses Lysosome Neutralization by Pathogens to Trigger Their Expulsion', *Cell*. NIH Public Access, 161(6), p. 1306. doi: 10.1016/J.CELL.2015.05.009.

Michlewski, G. and Cáceres, J. F. (2019) 'Post-transcriptional control of miRNA biogenesis.', *RNA (New York, N.Y.)*. Cold Spring Harbor Laboratory Press, 25(1), pp. 1–16. doi: 10.1261/rna.068692.118.

Mijaljica, D., Prescott, M. and Devenish, R. J. (2011) 'Microautophagy in mammalian cells: revisiting a 40-year-old conundrum', *Autophagy*. *Autophagy*, 7(7), pp. 673–682. doi: 10.4161/AUTO.7.7.14733.

Minakaki, G. *et al.* (2018) 'Autophagy inhibition promotes SNCA/alpha-synuclein release and transfer via extracellular vesicles with a hybrid autophagosome-exosome-like phenotype', *Autophagy*. Taylor & Francis, 14(1), p. 98. doi: 10.1080/15548627.2017.1395992.

Mindell, J. A. (2012) 'Lysosomal acidification mechanisms', *Annual review of physiology*. *Annu Rev Physiol*, 74, pp. 69–86. doi: 10.1146/ANNUREV-PHYSIOL-012110-142317.

Mitchell, P. S. *et al.* (2008) 'Circulating microRNAs as stable blood-based markers for cancer detection', *Proceedings of the National Academy of Sciences of the United States of America*. National Academy of Sciences, 105(30), pp. 10513–10518. doi: 10.1073/pnas.0804549105.

Mitsumoto, H. *et al.* (2008) 'Oxidative stress biomarkers in sporadic ALS', *Amyotrophic lateral sclerosis : official publication of the World Federation of Neurology Research Group on Motor Neuron Diseases*. *Amyotroph Lateral Scler*, 9(3), pp. 177–183. doi: 10.1080/17482960801933942.

Mizushima, N. *et al.* (1998) 'A protein conjugation system essential for autophagy', *Nature*. Nature Publishing Group, 395(6700), pp. 395–398. doi: 10.1038/26506.

Mizushima, N. *et al.* (2003) 'In Vivo Analysis of Autophagy in Response to Nutrient Starvation Using Transgenic Mice Expressing a Fluorescent Autophagosome Marker', <https://doi.org/10.1091/mbc.e03-09-0704>. American Society for Cell Biology, 15(3), pp. 1101–1111. doi: 10.1091/MBC.E03-09-0704.

Mizushima, N. and Yoshimori, T. (2007) 'How to Interpret LC3 Immunoblotting', *Autophagy*, 542(6). doi: 10.4161/auto.4600.

Möbius, W. *et al.* (2002) 'Immunoelectron microscopic localization of cholesterol using biotinylated and non-cytolytic perfringolysin O', *Journal of Histochemistry and Cytochemistry*. Histochemical Society Inc., 50(1), pp. 43–55. doi: 10.1177/002215540205000105.

Moinova, H. R. and Mulcahy, T. (1999) 'Up-Regulation of the Human  $\gamma$ -Glutamylcysteine Synthetase Regulatory Subunit Gene Involves Binding of Nrf-2 to an Electrophile Responsive Element', *Biochemical and Biophysical Research Communications*, 261, pp. 661–668. Available at: <https://reader.elsevier.com/reader/sd/pii/S0006291X99911099?token=63E41837EF5B15E66AF2DD32F38794565450D9ACD152934D743CB11B1A4AD6D20717A3487C5C9325DDE62412C048A07D&originRegion=eu-west-1&originCreation=20210416100450> (Accessed: 16 April 2021).

- Molliex, A. *et al.* (2015) 'Phase Separation by Low Complexity Domains Promotes Stress Granule Assembly and Drives Pathological Fibrillization', *Cell*. Cell Press, 163(1), pp. 123–133. doi: 10.1016/j.cell.2015.09.015.
- Montecalvo, A. *et al.* (2012) 'Mechanism of transfer of functional microRNAs between mouse dendritic cells via exosomes', *Blood*. American Society of Hematology, 119(3), pp. 756–766. doi: 10.1182/blood-2011-02-338004.
- Moore, A. S. and Holzbaur, E. L. F. (2016) 'Dynamic recruitment and activation of ALS-associated TBK1 with its target optineurin are required for efficient mitophagy', *Proceedings of the National Academy of Sciences*. National Academy of Sciences, 113(24), pp. E3349–E3358. doi: 10.1073/PNAS.1523810113.
- Morgan, S. and Orrell, R. W. (2016) 'Pathogenesis of amyotrophic lateral sclerosis', *British Medical Bulletin*. Oxford University Press, 119(1), pp. 87–98. doi: 10.1093/bmb/ldw026.
- Mori, K. *et al.* (2013) 'hnRNP A3 binds to GGGGCC repeats and is a constituent of p62-positive/TDP43-negative inclusions in the hippocampus of patients with C9orf72 mutations', *Acta Neuropathologica*. Springer-Verlag, 125(3), pp. 413–423. doi: 10.1007/s00401-013-1088-7.
- Morita, E. *et al.* (2007) 'Human ESCRT and ALIX proteins interact with proteins of the midbody and function in cytokinesis', *EMBO Journal*. Nature Publishing Group, 26(19), pp. 4215–4227. doi: 10.1038/sj.emboj.7601850.
- Morlando, M. *et al.* (2012) 'FUS stimulates microRNA biogenesis by facilitating co-transcriptional Drosha recruitment', *The EMBO Journal*, 31, pp. 4502–4510. doi: 10.1038/emboj.2012.319.
- Mulcahy, L. A., Pink, R. C. and Carter, D. R. F. (2014) 'Routes and mechanisms of extracellular vesicle uptake', <https://doi.org/10.3402/jev.v3.24641>. Taylor & Francis, 3(1). doi: 10.3402/JEV.V3.24641.
- Müller, A. J. and Proikas-Cezanne, T. (2015) 'Function of human WIPI proteins in autophagosomal rejuvenation of endomembranes?', *FEBS Letters*. No longer published by Elsevier, 589(14), pp. 1546–1551. doi: 10.1016/J.FEBSLET.2015.05.008.
- Murrow, L., Malhotra, R. and Debnath, J. (2015) 'ATG12-ATG3 Interacts with Alix to Promote Basal Autophagic Flux and Late Endosome Function', *Nature cell biology*. NIH Public Access, 17(3), p. 300. doi: 10.1038/NCB3112.
- Muscaritoli, M. *et al.* (2012) 'Nutritional and metabolic support in patients with amyotrophic lateral sclerosis', *Nutrition*. Elsevier, 28(10), pp. 959–966. doi: 10.1016/J.NUT.2012.01.011.
- N'Diaye, E. N. *et al.* (2009) 'PLIC proteins or ubiquilins regulate autophagy-dependent cell survival during nutrient starvation', *EMBO reports*. John Wiley & Sons, Ltd, 10(2), pp. 173–179. doi: 10.1038/EMBOR.2008.238.
- Nagai, M. *et al.* (2007) 'Astrocytes expressing ALS-linked mutated SOD1 release factors selectively toxic to motor neurons', *Nature Neuroscience*. Nature Publishing Group, 10(5), pp. 615–622. doi: 10.1038/nn1876.
- Neumann, M. *et al.* (2006) 'Ubiquitinated TDP-43 in frontotemporal lobar degeneration and amyotrophic lateral sclerosis.', *Science (New York, N.Y.)*. American Association for the Advancement of Science, 314(5796), pp. 130–3. doi: 10.1126/science.1134108.
- Neumann, M. *et al.* (2009) 'A new subtype of frontotemporal lobar degeneration with FUS pathology', *A JOURNAL OF NEUROLOGY*, 132(11), pp. 2922–2931. doi: 10.1093/brain/awp214.
- Nguyen, D. K. H., Thombre, R. and Wang, J. (2019) 'Autophagy as a common pathway in amyotrophic lateral sclerosis', *Neuroscience Letters*. Elsevier, 697, pp. 34–48. doi: 10.1016/J.NEULET.2018.04.006.
- Nguyen, T. A. *et al.* (2015) 'Functional anatomy of the human microprocessor', *Cell*. Cell Press, 161(6), pp. 1374–1387. doi: 10.1016/j.cell.2015.05.010.
- Nishiyama, J. *et al.* (2007) 'Aberrant Membranes and Double-Membrane Structures Accumulate in the Axons of Atg5-Null Purkinje Cells before Neuronal Death', <https://doi.org/10.4161/auto.4964>. Taylor & Francis, 3(6), pp. 591–596. doi: 10.4161/AUTO.4964.

- Nonaka, T. *et al.* (2013) 'Article Prion-like Properties of Pathological TDP-43 Aggregates from Diseased Brains', *CellReports*, 4, pp. 124–134. doi: 10.1016/j.celrep.2013.06.007.
- Oakes, J. A., Davies, M. C. and Collins, M. O. (2017) 'TBK1: a new player in ALS linking autophagy and neuroinflammation', *Molecular Brain*. BioMed Central Ltd., 10(1), pp. 1–10. doi: 10.1186/s13041-017-0287-x.
- Olagnier, D. *et al.* (2018) 'Nrf2 negatively regulates STING indicating a link between antiviral sensing and metabolic reprogramming', *Nature Communications*. Nature Publishing Group, 9(1), pp. 1–13. doi: 10.1038/s41467-018-05861-7.
- Orlacchio, A. *et al.* (2010) 'SPATACSIN mutations cause autosomal recessive juvenile amyotrophic lateral sclerosis', *Brain*, 133(2), pp. 591–598. Available at: <https://academic.oup.com/brain/article/133/2/591/290773> (Accessed: 6 April 2020).
- Osaka, M., Ito, D. and Suzuki, N. (2016) 'Disturbance of proteasomal and autophagic protein degradation pathways by amyotrophic lateral sclerosis-linked mutations in ubiquilin 2', *Biochemical and Biophysical Research Communications*. Elsevier B.V., 472(2), pp. 324–331. doi: 10.1016/j.bbrc.2016.02.107.
- Oshima, M. *et al.* (2019) 'Reciprocal regulation of chaperone-mediated autophagy/microautophagy and exosome release', *Biological and Pharmaceutical Bulletin*, 42(8), pp. 1394–1401. doi: 10.1248/bpb.b19-00316.
- Ostrowski, M. *et al.* (2010) 'Rab27a and Rab27b control different steps of the exosome secretion pathway', *Nature Cell Biology*. Nat Cell Biol, 12(1), pp. 19–30. doi: 10.1038/ncb2000.
- Otake, K., Kamiguchi, H. and Hirozane, Y. (2019) 'Identification of biomarkers for amyotrophic lateral sclerosis by comprehensive analysis of exosomal mRNAs in human cerebrospinal fluid', *BMC Medical Genomics*. BioMed Central, 12(1), p. 7. doi: 10.1186/s12920-019-0473-z.
- Otomo, A. *et al.* (2011) 'Defective relocalization of ALS2/alsin missense mutants to Rac1-induced macropinosomes accounts for loss of their cellular function and leads to disturbed amphisome formation', *FEBS Letters*. John Wiley & Sons, Ltd, 585(5), pp. 730–736. doi: 10.1016/j.febslet.2011.01.045.
- Pajares, M. *et al.* (2016) 'Transcription factor NFE2L2/NRF2 is a regulator of macroautophagy genes', *Autophagy*. Taylor and Francis Inc., 12(10), pp. 1902–1916. doi: 10.1080/15548627.2016.1208889.
- Pan, B. T. *et al.* (1985) 'Electron microscopic evidence for externalization of the transferrin receptor in vesicular form in sheep reticulocytes', *The Journal of cell biology*. J Cell Biol, 101(3), pp. 942–948. doi: 10.1083/JCB.101.3.942.
- Pankiv, S. *et al.* (2007) 'p62/SQSTM1 binds directly to Atg8/LC3 to facilitate degradation of ubiquitinated protein aggregates by autophagy.', *The Journal of biological chemistry*. American Society for Biochemistry and Molecular Biology, 282(33), pp. 24131–45. doi: 10.1074/jbc.M702824200.
- Pankiv, S. *et al.* (2010) 'FYCO1 is a Rab7 effector that binds to LC3 and PI3P to mediate microtubule plus end-directed vesicle transport.', *The Journal of cell biology*. The Rockefeller University Press, 188(2), pp. 253–69. doi: 10.1083/jcb.200907015.
- Panwar, B., Omenn, G. S. and Guan, Y. (2017) 'miRmine: a database of human miRNA expression profiles', *Bioinformatics*. Oxford Academic, 33(10), pp. 1554–1560. doi: 10.1093/BIOINFORMATICS/BTX019.
- Paraskevopoulou, M. D. *et al.* (2013) 'DIANA-microT web server v5.0: service integration into miRNA functional analysis workflows.', *Nucleic acids research*. Oxford University Press, 41(Web Server issue), pp. W169–W173. doi: 10.1093/nar/gkt393.
- Patel, A. *et al.* (2015) 'A Liquid-to-Solid Phase Transition of the ALS Protein FUS Accelerated by Disease Mutation', *Cell*. Cell Press, 162(5), pp. 1066–1077. doi: 10.1016/j.cell.2015.07.047.
- Pathan, M. *et al.* (2019) 'Vesiclepedia 2019: A Compendium of RNA, Proteins, Lipids and Metabolites in Extracellular Vesicles - PubMed', *Nucleic Acids Research*, pp. D516–D519. Available at:

<https://pubmed.ncbi.nlm.nih.gov/30395310/> (Accessed: 8 April 2020).

Pattingre, S. *et al.* (2005) 'Bcl-2 Antiapoptotic Proteins Inhibit Beclin 1-Dependent Autophagy', *Cell*. Cell Press, 122(6), pp. 927–939. doi: 10.1016/J.CELL.2005.07.002.

Pegoraro, V., Merico, A. and Angelini, C. (2017) 'Micro-RNAs in ALS muscle: Differences in gender, age at onset and disease duration', *Journal of the Neurological Sciences*. Elsevier, 380, pp. 58–63. doi: 10.1016/J.JNS.2017.07.008.

Peng, W. *et al.* (2021) 'Microglia-Derived Exosomes Improve Spinal Cord Functional Recovery after Injury via Inhibiting Oxidative Stress and Promoting the Survival and Function of Endothelial Cells'. doi: 10.1155/2021/1695087.

Perea, G. and Araque, A. (2005) 'Properties of synaptically evoked astrocyte calcium signal reveal synaptic information processing by astrocytes', *Journal of Neuroscience*. Society for Neuroscience, 25(9), pp. 2192–2203. doi: 10.1523/JNEUROSCI.3965-04.2005.

Peretti, D. *et al.* (2008) 'Coordinated Lipid Transfer between the Endoplasmic Reticulum and the Golgi Complex Requires the VAP Proteins and Is Essential for Golgi-mediated Transport', *Molecular Biology of the Cell*. American Society for Cell Biology, 19(9), p. 3871. doi: 10.1091/MBC.E08-05-0498.

Peterson, T. R. *et al.* (2009) 'DEPTOR is an mTOR inhibitor frequently overexpressed in multiple myeloma cells and required for their survival', *Cell*. Cell, 137(5), pp. 873–886. doi: 10.1016/J.CELL.2009.03.046.

Phuyal, S. *et al.* (2014) 'Regulation of exosome release by glycosphingolipids and flotillins', *FEBS Journal*. Blackwell Publishing Ltd, 281(9), pp. 2214–2227. doi: 10.1111/febs.12775.

Di Pietro, L. *et al.* (2017) 'Potential therapeutic targets for ALS: MIR206, MIR208b and MIR499 are modulated during disease progression in the skeletal muscle of patients.', *Scientific reports*. Nature Publishing Group, 7(1), p. 9538. doi: 10.1038/s41598-017-10161-z.

Pilli, M. *et al.* (2012) 'TBK-1 Promotes Autophagy-Mediated Antimicrobial Defense by Controlling Autophagosome Maturation', *Immunity*. Cell Press, 37(2), pp. 223–234. doi: 10.1016/J.IMMUNI.2012.04.015.

Pinto, S. *et al.* (2017) 'Exosomes from NSC-34 cells transfected with hSOD1-G93A are enriched in mir-124 and drive alterations in microglia phenotype', *Frontiers in Neuroscience*. Frontiers Research Foundation, 11(MAY). doi: 10.3389/fnins.2017.00273.

Pinzón, N. *et al.* (2017) 'MicroRNA target prediction programs predict many false positives', *Genome Research*. Cold Spring Harbor Laboratory Press, 27(2), pp. 234–245. doi: 10.1101/GR.205146.116/-/DC1.

Piscopo, P. *et al.* (2018) 'Circulating miR-127-3p as a Potential Biomarker for Differential Diagnosis in Frontotemporal Dementia', *Journal of Alzheimer's Disease*. IOS Press, 65(2), pp. 455–464. doi: 10.3233/JAD-180364.

Polymenidou, M. *et al.* (2011) 'Long pre-mRNA depletion and RNA missplicing contribute to neuronal vulnerability from loss of TDP-43', *Nature Neuroscience* 2011 14:4. Nature Publishing Group, 14(4), pp. 459–468. doi: 10.1038/nn.2779.

Porta, S. *et al.* (2018) 'Patient-derived frontotemporal lobar degeneration brain extracts induce formation and spreading of TDP-43 pathology in vivo', *Nature Communications*. Nature Publishing Group, 9(1), pp. 1–15. doi: 10.1038/s41467-018-06548-9.

Prabakaran, T. *et al.* (2018) 'Attenuation of cGAS - STING signaling is mediated by a p62/SQSTM1-dependent autophagy pathway activated by TBK1', *The EMBO Journal*. EMBO, 37(8). doi: 10.15252/embj.201797858.

Prasad, D. *et al.* (1994) 'TLS/FUS fusion domain of TLS/FUS-erg chimeric protein resulting from the t(16;21) chromosomal translocation in human myeloid leukemia functions as a transcriptional activation domain.', *Oncogene*, 9(12), pp. 3717–3729. Available at: <https://europepmc.org/abstract/med/7970732> (Accessed: 26 March 2019).

- Qi, S. *et al.* (2015) 'Structure of the Human Atg13-Atg101 HORMA Heterodimer: an Interaction Hub within the ULK1 Complex.', *Structure (London, England : 1993)*. NIH Public Access, 23(10), pp. 1848–1857. doi: 10.1016/j.str.2015.07.011.
- Qian, Z. *et al.* (2020) 'Excess administration of miR-340-5p ameliorates spinal cord injury-induced neuroinflammation and apoptosis by modulating the P38-MAPK signaling pathway', *Brain, Behavior, and Immunity*. Academic Press, 87, pp. 531–542. doi: 10.1016/J.BBI.2020.01.025.
- Rademakers, R. *et al.* (2008) 'Common variation in the miR-659 binding-site of GRN is a major risk factor for TDP43-positive frontotemporal dementia', *Human Molecular Genetics*, 17(23), pp. 3631–3642. Available at: <https://www.ncbi.nlm.nih.gov/pmc/articles/PMC2581433/> (Accessed: 6 April 2020).
- Radi, R. (2013) 'Peroxynitrite, a stealthy biological oxidant', *The Journal of biological chemistry*. J Biol Chem, 288(37), pp. 26464–26472. doi: 10.1074/JBC.R113.472936.
- Raheja, R. *et al.* (2018) 'Correlating serum micrnas and clinical parameters in amyotrophic lateral sclerosis', *Muscle & Nerve*. Wiley-Blackwell, 58(2), pp. 261–269. doi: 10.1002/mus.26106.
- Raman, R. *et al.* (2015) 'Gene expression signatures in motor neurone disease fibroblasts reveal dysregulation of metabolism, hypoxia-response and RNA processing functions', *Neuropathology and Applied Neurobiology*. Wiley/Blackwell (10.1111), 41(2), pp. 201–226. doi: 10.1111/nan.12147.
- Ramesh, N. and Pandey, U. B. (2017) 'Autophagy Dysregulation in ALS: When Protein Aggregates Get Out of Hand.', *Frontiers in molecular neuroscience*. Frontiers Media SA, 10, p. 263. doi: 10.3389/fnmol.2017.00263.
- Ramírez-Jarquín, U. N. *et al.* (2017) 'Chronic infusion of SOD1G93A astrocyte-secreted factors induces spinal motoneuron degeneration and neuromuscular dysfunction in healthy rats', *Journal of Cellular Physiology*. John Wiley & Sons, Ltd, 232(10), pp. 2610–2615. doi: 10.1002/JCP.25827.
- Ramirez, C. *et al.* (2008) 'Fatigue in amyotrophic lateral sclerosis: Frequency and associated factors', *Amyotrophic Lateral Sclerosis*, 9(2), pp. 75–80. doi: 10.1080/17482960701642502.
- Rao, P., Benito, E. and Fischer, A. (2013) 'MicroRNAs as biomarkers for CNS disease', *Frontiers in Molecular Neuroscience*. Frontiers Media SA, 6(NOV). doi: 10.3389/fnmol.2013.00039.
- Rea, S. L. *et al.* (2013) 'New Insights Into the Role of Sequestosome 1/p62 Mutant Proteins in the Pathogenesis of Paget's Disease of Bone', *Endocrine Reviews*. Narnia, 34(4), pp. 501–524. doi: 10.1210/er.2012-1034.
- Reaume, A. G. *et al.* (1996) 'Motor neurons in Cu/Zn superoxide dismutase-deficient mice develop normally but exhibit enhanced cell death after axonal injury', *Nature Genetics*. Nature Publishing Group, 13(1), pp. 43–47. doi: 10.1038/ng0596-43.
- Reczko, M. *et al.* (2012) 'Functional microRNA targets in protein coding sequences', *Bioinformatics*. Oxford University Press, 28(6), pp. 771–776. doi: 10.1093/bioinformatics/bts043.
- Rehwinkel, J. *et al.* (2005) 'A crucial role for GW182 and the DCP1:DCP2 decapping complex in miRNA-mediated gene silencing.', *RNA (New York, N.Y.)*. Cold Spring Harbor Laboratory Press, 11(11), pp. 1640–7. doi: 10.1261/rna.2191905.
- Reid, G. *et al.* (2013) 'Restoring expression of miR-16: a novel approach to therapy for malignant pleural mesothelioma', *Annals of oncology : official journal of the European Society for Medical Oncology*. Ann Oncol, 24(12), pp. 3128–3135. doi: 10.1093/ANNONC/MDT412.
- Reid, G. *et al.* (2016) 'Clinical development of TargomiRs, a miRNA mimic-based treatment for patients with recurrent thoracic cancer', *Epigenomics*. Future Medicine Ltd., 8(8), pp. 1079–1085. doi: 10.2217/EPI-2016-0035/ASSET/IMAGES/LARGE/FIGURE2.JPEG.
- Renton, A. E. *et al.* (2011) 'A Hexanucleotide Repeat Expansion in C9ORF72 Is the Cause of Chromosome 9p21-Linked ALS-FTD', *Neuron*. Cell Press, 72(2), pp. 257–268. doi: 10.1016/J.NEURON.2011.09.010.
- Van Rheenen, W. *et al.* (2012) 'Hexanucleotide repeat expansions in C9ORF72 in the spectrum of

motor neuron diseases', *Neurology*. Lippincott Williams and Wilkins, 79(9), pp. 878–882. doi: 10.1212/WNL.0b013e3182661d14.

Ricci, C., Marzocchi, C. and Battistini, S. (2018) 'MicroRNAs as Biomarkers in Amyotrophic Lateral Sclerosis', *Cells*. Multidisciplinary Digital Publishing Institute, 7(11), p. 219. doi: 10.3390/cells7110219.

Richter, B. *et al.* (2016) 'Phosphorylation of OPTN by TBK1 enhances its binding to Ub chains and promotes selective autophagy of damaged mitochondria.', *Proceedings of the National Academy of Sciences of the United States of America*. National Academy of Sciences, 113(15), pp. 4039–44. doi: 10.1073/pnas.1523926113.

Riffo-Campos, Á. L., Riquelme, I. and Brebi-Mieville, P. (2016) 'Tools for Sequence-Based miRNA Target Prediction: What to Choose?', *International journal of molecular sciences*. Multidisciplinary Digital Publishing Institute (MDPI), 17(12), p. 1987. doi: 10.3390/ijms17121987.

Ringholz, G. M. *et al.* (2005) 'Prevalence and patterns of cognitive impairment in sporadic ALS', *Neurology*. Lippincott Williams and Wilkins, 65(4), pp. 586–590. doi: 10.1212/01.wnl.0000172911.39167.b6.

Robbins, P. D. and Morelli, A. E. (2014) 'Regulation of Immune Responses by Extracellular Vesicles', *Nature reviews. Immunology*. NIH Public Access, 14(3), p. 195. doi: 10.1038/NRI3622.

Roberts, R. C., Roche, J. K. and McCullumsmith, R. E. (2014) 'Localization of excitatory amino acid transporters EAAT1 and EAAT2 in human postmortem cortex: a light and electron microscopic study', *Neuroscience*. NIH Public Access, 277, p. 522. doi: 10.1016/J.NEUROSCIENCE.2014.07.019.

Robins, H., Li, Y. and Padgett, R. W. (2005) 'Incorporating structure to predict microRNA targets', *Proceedings of the National Academy of Sciences of the United States of America*. National Academy of Sciences, 102(11), p. 4006. doi: 10.1073/PNAS.0500775102.

Rosen, D. R. *et al.* (1993) 'Mutations in Cu/Zn superoxide dismutase gene are associated with familial amyotrophic lateral sclerosis', *Nature*. Nature Publishing Group, 362(6415), pp. 59–62. doi: 10.1038/362059a0.

Rotem, N. *et al.* (2017) 'ALS along the Axons - Expression of coding and noncoding RNA differs in axons of ALS models', *Scientific Reports*. Nature Publishing Group, 7. doi: 10.1038/srep44500.

Rothenberg, C. *et al.* (2010) 'Ubiquilin functions in autophagy and is degraded by chaperone-mediated autophagy', *Human Molecular Genetics*, 19(16), pp. 3219–32. Available at: <https://www.ncbi.nlm.nih.gov/pmc/articles/PMC2908472/> (Accessed: 3 April 2020).

Rothstein, J. D. *et al.* (1995) 'Selective loss of glial glutamate transporter GLT-1 in amyotrophic lateral sclerosis', *Annals of Neurology*. John Wiley & Sons, Ltd, 38(1), pp. 73–84. doi: 10.1002/ana.410380114.

Rothstein, J. D. (2017) 'Bench to Bedside Edaravone: A New Drug Approved for ALS', *Cell*, 171, p. 725. doi: 10.1016/j.cell.2017.10.011.

Roush, S. and Slack, F. J. (2008) 'The let-7 family of microRNAs', *Trends in Cell Biology*. Elsevier Current Trends, 18(10), pp. 505–516. doi: 10.1016/J.TCB.2008.07.007.

Ruby, J. G., Jan, C. H. and Bartel, D. P. (2007) 'Intronic microRNA precursors that bypass Drosha processing.', *Nature*. NIH Public Access, 448(7149), pp. 83–6. doi: 10.1038/nature05983.

Rudnick, N. D. *et al.* (2017) 'Distinct roles for motor neuron autophagy early and late in the SOD1G93A mouse model of ALS.', *Proceedings of the National Academy of Sciences of the United States of America*. National Academy of Sciences, 114(39), pp. E8294–E8303. doi: 10.1073/pnas.1704294114.

Russell, A. P. *et al.* (2013) 'Disruption of skeletal muscle mitochondrial network genes and miRNAs in amyotrophic lateral sclerosis', *Neurobiology of Disease*. Academic Press, 49, pp. 107–117. doi: 10.1016/J.NBD.2012.08.015.

Russell, R. C., Tian, Y., Yuan, H., Park, H. W., Chang, Y. Y., *et al.* (2013) 'ULK1 induces autophagy by phosphorylating Beclin-1 and activating VPS34 lipid kinase', *Nature Cell Biology*. NIH Public Access, 15(7), pp. 741–750. doi: 10.1038/ncb2757.

Russell, R. C., Tian, Y., Yuan, H., Park, H. W., Chang, Y.-Y., *et al.* (2013) 'ULK1 induces autophagy by

phosphorylating Beclin-1 and activating VPS34 lipid kinase', *Nature Cell Biology*. Nature Publishing Group, 15(7), pp. 741–750. doi: 10.1038/ncb2757.

Ryu, H.-H. *et al.* (2014) 'Autophagy regulates amyotrophic lateral sclerosis-linked fused in sarcoma-positive stress granules in neurons', *Neurobiology of Aging*. Elsevier, 35(12), pp. 2822–2831. doi: 10.1016/J.NEUROBIOLAGING.2014.07.026.

Saccon, R. A. *et al.* (2013) 'Is SOD1 loss of function involved in amyotrophic lateral sclerosis?', *Brain*. Oxford University Press, 136(8), p. 2342. doi: 10.1093/BRAIN/AWT097.

Sama, R. R. K. *et al.* (2013) 'FUS/TLS assembles into stress granules and is a prosurvival factor during hyperosmolar stress', *Journal of Cellular Physiology*. John Wiley & Sons, Ltd, 228(11), pp. 2222–2231. doi: 10.1002/jcp.24395.

Sang, Q. *et al.* (2013) 'Identification of MicroRNAs in Human Follicular Fluid: Characterization of MicroRNAs That Govern Steroidogenesis in Vitro and Are Associated With Polycystic Ovary Syndrome in Vivo', *The Journal of Clinical Endocrinology & Metabolism*. Oxford University Press, 98(7), pp. 3068–3079. doi: 10.1210/jc.2013-1715.

Sang, W. S. *et al.* (2007) 'Astrocyte glycogen sustains neuronal activity during hypoglycemia: Studies with the glycogen phosphorylase inhibitor CP-316,819 ([R-R\*,S\*]-5-chloro-N-[2-hydroxy-3-(methoxymethylamino)-3-oxo-1-(phenylmethyl)propyl]-1H-indole-2-carboxamide)', *Journal of Pharmacology and Experimental Therapeutics*. American Society for Pharmacology and Experimental Therapeutics, 321(1), pp. 45–50. doi: 10.1124/jpet.106.115550.

Sardiello, M. *et al.* (2009) 'A gene network regulating lysosomal biogenesis and function', *Science*. American Association for the Advancement of Science, 325(5939), pp. 473–477. doi: 10.1126/science.1174447.

Sareen, D. *et al.* (2013) 'Targeting RNA foci in iPSC-derived motor neurons from ALS patients with a C9ORF72 repeat expansion', *Science Translational Medicine*. NIH Public Access, 5(208), p. 208ra149. doi: 10.1126/scitranslmed.3007529.

Sarlette, A. *et al.* (2008) 'Nuclear Erythroid 2-Related Factor 2-Antioxidative Response Element Signaling Pathway in Motor Cortex and Spinal Cord in Amyotrophic Lateral Sclerosis', *Journal of Neuropathology & Experimental Neurology*. Oxford Academic, 67(11), pp. 1055–1062. doi: 10.1097/NEN.0b013e31818b4906.

Sasaki, S. (2011) 'Autophagy in Spinal Cord Motor Neurons in Sporadic Amyotrophic Lateral Sclerosis', *Journal of Neuropathology & Experimental Neurology*. Oxford Academic, 70(5), pp. 349–359. doi: 10.1097/NEN.0b013e3182160690.

Sasaki, S., Horie, Y. and Iwata, M. (2007) 'Mitochondrial alterations in dorsal root ganglion cells in sporadic amyotrophic lateral sclerosis', *Acta Neuropathologica*. Springer, 114(6), pp. 633–639. doi: 10.1007/S00401-007-0299-1/FIGURES/11.

Satoh, J. I., Kino, Y. and Niida, S. (2015) 'MicroRNA-Seq data analysis pipeline to identify blood biomarkers for alzheimer's disease from public data', *Biomarker Insights*. Libertas Academica Ltd., 2015(10), pp. 21–31. doi: 10.4137/BMI.S25132.

Saucier, D. *et al.* (2018) 'Identification of a circulating miRNA signature in extracellular vesicles collected from amyotrophic lateral sclerosis patients', *Brain Research*. Elsevier. doi: 10.1016/J.BRAINRES.2018.12.016.

Saucier, D. *et al.* (2019) 'Identification of a circulating miRNA signature in extracellular vesicles collected from amyotrophic lateral sclerosis patients', *Brain Research*. Elsevier, 1708, pp. 100–108. doi: 10.1016/J.BRAINRES.2018.12.016.

Schmidt, E. R. E., Pasterkamp, R. J. and van den Berg, L. H. (2009) 'Axon guidance proteins: Novel therapeutic targets for ALS?', *Progress in Neurobiology*. Pergamon, 88(4), pp. 286–301. doi: 10.1016/J.PNEUROBIO.2009.05.004.

Schwarz, D. S. *et al.* (2003) 'Asymmetry in the Assembly of the RNAi Enzyme Complex', *Cell*. Cell Press, 115(2), pp. 199–208. doi: 10.1016/S0092-8674(03)00759-1.

- Scotter, E. L., Chen, H.-J. and Shaw, C. E. (2015) 'TDP-43 Proteinopathy and ALS: Insights into Disease Mechanisms and Therapeutic Targets'. doi: 10.1007/s13311-015-0338-x.
- Seibenhener, M. L. *et al.* (2004) 'Sequestosome 1/p62 is a polyubiquitin chain binding protein involved in ubiquitin proteasome degradation.', *Molecular and cellular biology*. American Society for Microbiology Journals, 24(18), pp. 8055–68. doi: 10.1128/MCB.24.18.8055-8068.2004.
- Sekhar, K. R., Rachakonda, G. and Freeman, M. L. (2010) 'Cysteine-based regulation of the CUL3 adaptor protein Keap1', *Toxicology and Applied Pharmacology*. Academic Press, pp. 21–26. doi: 10.1016/j.taap.2009.06.016.
- Sellier, C. *et al.* (2016) 'Loss of C9ORF72 impairs autophagy and synergizes with polyQ Ataxin-2 to induce motor neuron dysfunction and cell death.', *The EMBO journal*. EMBO Press, 35(12), pp. 1276–97. doi: 10.15252/embj.201593350.
- Seto, A. G. *et al.* (2018) 'Cobomarsen, an oligonucleotide inhibitor of miR-155, co-ordinately regulates multiple survival pathways to reduce cellular proliferation and survival in cutaneous T-cell lymphoma', *British journal of haematology*. Br J Haematol, 183(3), pp. 428–444. doi: 10.1111/BJH.15547.
- Sharma, S. *et al.* (2003) 'Triggering the interferon antiviral response through an IKK-related pathway', *Science*. American Association for the Advancement of Science, 300(5622), pp. 1148–1151. doi: 10.1126/science.1081315.
- Shatunov, A. *et al.* (2010) 'Chromosome 9p21 in sporadic amyotrophic lateral sclerosis in the UK and seven other countries: A genome-wide association study', *The Lancet Neurology*. Elsevier, 9(10), pp. 986–994. doi: 10.1016/S1474-4422(10)70197-6.
- Shaw, P. J. *et al.* (1995) 'Oxidative damage to protein in sporadic motor neuron disease spinal cord', *Annals of Neurology*. Ann Neurol, 38(4), pp. 691–695. doi: 10.1002/ana.410380424.
- Shi, L. *et al.* (2014) 'miR-340 reverses cisplatin resistance of hepatocellular carcinoma cell lines by targeting Nrf2-dependent antioxidant pathway', *Asian Pacific Journal of Cancer Prevention*, 15(23), pp. 10439–10444. doi: 10.7314/APJCP.2014.15.23.10439.
- Shibata, N. *et al.* (2001) 'Morphological evidence for lipid peroxidation and protein glycoxidation in spinal cords from sporadic amyotrophic lateral sclerosis patients', *Brain Research*. Elsevier, 917(1), pp. 97–104. doi: 10.1016/S0006-8993(01)02926-2.
- Shintani, T. *et al.* (1999) *Apg10p, a novel protein-conjugating enzyme essential for autophagy in yeast*, *The EMBO Journal*. Available at: <https://www.ncbi.nlm.nih.gov/pmc/articles/PMC1171594/pdf/005234.pdf> (Accessed: 30 November 2018).
- Silverman, J. M. *et al.* (2019) 'CNS-derived extracellular vesicles from superoxide dismutase 1 (SOD1) G93A ALS mice originate from astrocytes and neurons and carry misfolded SOD1', *Journal of Biological Chemistry*. American Society for Biochemistry and Molecular Biology Inc., 294(10), pp. 3744–3759. doi: 10.1074/jbc.RA118.004825.
- Singh, A. *et al.* (2006) 'Glutathione Peroxidase 2, the Major Cigarette Smoke-Inducible Isoform of GPX in Lungs, Is Regulated by Nrf2', *American Journal of Respiratory Cell and Molecular Biology*. American Thoracic Society, 35(6), p. 639. doi: 10.1165/RCMB.2005-0325OC.
- Siracusa, J., Koulmann, N. and Banzet, S. (2018) 'Circulating myomiRs: a new class of biomarkers to monitor skeletal muscle in physiology and medicine.', *Journal of cachexia, sarcopenia and muscle*. Wiley-Blackwell, 9(1), pp. 20–27. doi: 10.1002/jcsm.12227.
- Skehel, P. A. *et al.* (1995) 'A VAMP-Binding Protein from Aplysia Required for Neurotransmitter Release', *Science*. American Association for the Advancement of Science, 269(5230), pp. 1580–1583. doi: 10.1126/SCIENCE.7667638.
- Smith, B. N. *et al.* (2014) 'Exome-wide rare variant analysis identifies TUBA4A mutations associated with familial ALS', *Neuron*. Cell Press, 84(2), pp. 324–331. doi: 10.1016/j.neuron.2014.09.027.
- Sohel, M. H. (2016) 'Extracellular/Circulating MicroRNAs: Release Mechanisms, Functions and Challenges', *Achievements in the Life Sciences*. No longer published by Elsevier, 10(2), pp. 175–186.

doi: 10.1016/J.ALS.2016.11.007.

Soifer, H. S. *et al.* (2012) 'Silencing of Gene Expression by Gymnotic Delivery of Antisense Oligonucleotides', *Methods in Molecular Biology*. Springer, New York, NY, 815, pp. 333–346. doi: 10.1007/978-1-61779-424-7\_25.

Sommer, B. *et al.* (1991) 'RNA editing in brain controls a determinant of ion flow in glutamate-gated channels', *Cell*, 67(1), pp. 11–19. doi: 10.1016/0092-8674(91)90568-J.

Song, J.-J. *et al.* (2004) 'Crystal structure of Argonaute and its implications for RISC slicer activity.', *Science (New York, N.Y.)*. American Association for the Advancement of Science, 305(5689), pp. 1434–7. doi: 10.1126/science.1102514.

Soo, K. Y. *et al.* (2015) 'ALS-associated mutant FUS inhibits macroautophagy which is restored by overexpression of Rab1', *Cell Death Discovery*. Nature Publishing Group, 1(1), p. 15030. doi: 10.1038/cddiscovery.2015.30.

Spillantini, M. G. *et al.* (1997) 'Familial multiple system tauopathy with presenile dementia: A disease with abundant neuronal and glial tau filaments', *Proceedings of the National Academy of Sciences of the United States of America*. National Academy of Sciences, 94(8), pp. 4113–4118. doi: 10.1073/pnas.94.8.4113.

Spreux-Varoquaux, O. *et al.* (2002) 'Glutamate levels in cerebrospinal fluid in amyotrophic lateral sclerosis: A reappraisal using a new HPLC method with coulometric detection in a large cohort of patients', *Journal of the Neurological Sciences*, 193(2), pp. 73–78. doi: 10.1016/S0022-510X(01)00661-X.

Stallings, N. R. *et al.* (2010) 'Progressive motor weakness in transgenic mice expressing human TDP-43', *Neurobiology of Disease*. Academic Press, 40(2), pp. 404–414. doi: 10.1016/J.NBD.2010.06.017.

Stein, C. A. *et al.* (2010) 'Efficient gene silencing by delivery of locked nucleic acid antisense oligonucleotides, unassisted by transfection reagents', *Nucleic Acids Research*. Oxford University Press, 38(1), p. e3. doi: 10.1093/NAR/GKP841.

Stenoien, D. L. and Brady, S. T. (1999) *Discovery and Conceptual Development of Fast and Slow Axonal Transport*.

Stewart, H. *et al.* (2012) 'Clinical and pathological features of amyotrophic lateral sclerosis caused by mutation in the C9ORF72 gene on chromosome 9p', *Acta Neuropathologica*. NIH Public Access, 123(3), pp. 409–417. doi: 10.1007/s00401-011-0937-5.

Stuffers, S. *et al.* (2009) 'Multivesicular endosome biogenesis in the absence of ESCRTs', *Traffic*. Traffic, 10(7), pp. 925–937. doi: 10.1111/j.1600-0854.2009.00920.x.

Subramanian, S. L. *et al.* (2015) 'Integration of extracellular RNA profiling data using metadata, biomedical ontologies and Linked Data technologies.', *Journal of extracellular vesicles*. Taylor & Francis, 4, p. 27497. doi: 10.3402/jev.v4.27497.

Sullivan, P. M. *et al.* (2016) 'The ALS/FTLD associated protein C9orf72 associates with SMCR8 and WDR41 to regulate the autophagy-lysosome pathway', *Acta Neuropathologica Communications*. BioMed Central, 4(1), p. 51. doi: 10.1186/s40478-016-0324-5.

Sun, L. *et al.* (2013) 'Cyclic GMP-AMP synthase is a cytosolic DNA sensor that activates the type I interferon pathway', *Science (New York, N.Y.)*. Science, 339(6121), pp. 786–791. doi: 10.1126/SCIENCE.1232458.

Sundaramoorthy, V. *et al.* (2015) 'Defects in optineurin- and myosin VI-mediated cellular trafficking in amyotrophic lateral sclerosis', *Human Molecular Genetics*. Narnia, 24(13), pp. 3830–3846. doi: 10.1093/hmg/ddv126.

Suzuki *et al.* (2001) 'The pre-autophagosomal structure organized by concerted functions of APG genes is essential for autophagosome formation', *The EMBO Journal*. EMBO Press, 20(21), pp. 5971–5981. doi: 10.1093/emboj/20.21.5971.

Suzuki, K. *et al.* (2001) 'The pre-autophagosomal structure organized by concerted functions of APG

- genes is essential for autophagosome formation\_\_\_\_', *The EMBO Journal*, 20(21), pp. 5971–5981.
- Suzuki, N. *et al.* (2010) 'FALS with FUS mutation in Japan, with early onset, rapid progress and basophilic inclusion', *Journal of Human Genetics*. Nature Publishing Group, 55(4), pp. 252–254. doi: 10.1038/jhg.2010.16.
- Szaro, B. G. and Strong, M. J. (2010) 'Post-transcriptional control of neurofilaments: New roles in development, regeneration and neurodegenerative disease', *Trends in Neurosciences*. Elsevier, pp. 27–37. doi: 10.1016/j.tins.2009.10.002.
- Taguchi, Y.-H. and Wang, H. (2018) 'Exploring microRNA Biomarker for Amyotrophic Lateral Sclerosis.', *International journal of molecular sciences*. Multidisciplinary Digital Publishing Institute (MDPI), 19(5). doi: 10.3390/ijms19051318.
- Takahashi, A. *et al.* (2017) 'Exosomes maintain cellular homeostasis by excreting harmful DNA from cells', *Nature Communications* 2017 8:1. Nature Publishing Group, 8(1), pp. 1–16. doi: 10.1038/ncomms15287.
- Takahashi, I. *et al.* (2015) 'Identification of plasma microRNAs as a biomarker of sporadic Amyotrophic Lateral Sclerosis', *Molecular Brain*. BioMed Central, 8(1), p. 67. doi: 10.1186/s13041-015-0161-7.
- Takahashi, M. *et al.* (1997) 'The role of glutamate transporters in glutamate homeostasis in the brain', *The Journal of experimental biology*. J Exp Biol, 200(Pt 2), pp. 401–409. doi: 10.1242/JEB.200.2.401.
- Takuma, H. *et al.* (1999) 'Reduction of GluR2 RNA editing, a molecular change that increases calcium influx through AMPA receptors, selective in the spinal ventral gray of patients with amyotrophic lateral sclerosis', *Annals of Neurology*, 46(6), pp. 806–815.
- Tan, J. M. M. *et al.* (2008) 'Lysine 63-linked ubiquitination promotes the formation and autophagic clearance of protein inclusions associated with neurodegenerative diseases', *Human Molecular Genetics*. Narnia, 17(3), pp. 431–439. doi: 10.1093/hmg/ddm320.
- Tan, X. *et al.* (2020) 'MiR-340 Reduces the Accumulation of Amyloid- $\beta$  Through Targeting BACE1 ( $\beta$ -site Amyloid Precursor Protein Cleaving Enzyme 1) in Alzheimer's Disease', *Current neurovascular research*. Curr Neurovasc Res, 17(1), pp. 86–92. doi: 10.2174/1567202617666200117103931.
- Tanaka, Y. and Chen, Z. J. (2012) 'STING Specifies IRF3 phosphorylation by TBK1 in the Cytosolic DNA Signaling Pathway', *Science signaling*. NIH Public Access, 5(214), p. ra20. doi: 10.1126/SCISIGNAL.2002521.
- Tanida, I. *et al.* (1999) 'Apg7p/Cvt2p: A Novel Protein-activating Enzyme Essential for Autophagy', *Molecular Biology of the Cell*. Edited by R. W. Schekman, 10(5), pp. 1367–1379. doi: 10.1091/mbc.10.5.1367.
- Tanzer, A. and Stadler, P. F. (2004) 'Molecular Evolution of a MicroRNA Cluster', *Journal of Molecular Biology*. Academic Press, 339(2), pp. 327–335. doi: 10.1016/J.JMB.2004.03.065.
- Tao, Q.-Q., Wei, Q. and Wu, Z.-Y. (2018) 'Sensory nerve disturbance in amyotrophic lateral sclerosis', *Life Sciences*. Pergamon, 203, pp. 242–245. doi: 10.1016/J.LFS.2018.04.052.
- Tasca, E. *et al.* (2016) 'Circulating microRNAs as biomarkers of muscle differentiation and atrophy in ALS', *Clinical Neuropathology*, 35(01), pp. 22–30. doi: 10.5414/NP300889.
- Tateishi, T. *et al.* (2010) 'Multiple system degeneration with basophilic inclusions in Japanese ALS patients with FUS mutation', *Acta Neuropathologica*. Acta Neuropathol, 119(3), pp. 355–364. doi: 10.1007/s00401-009-0621-1.
- Teis, D., Saksena, S. and Emr, S. D. (2008) 'Ordered assembly of the ESCRT-III complex on endosomes is required to sequester cargo during MVB formation', *Developmental cell*. Dev Cell, 15(4), pp. 578–589. doi: 10.1016/J.DEVCEL.2008.08.013.
- Thadani, R. and Tammi, M. T. (2006) 'MicroTar: predicting microRNA targets from RNA duplexes', *BMC Bioinformatics*. BioMed Central, 7(Suppl 5), p. S20. doi: 10.1186/1471-2105-7-S5-S20.
- Thomsen, G. M. *et al.* (2014) 'The past, present and future of stem cell clinical trials for ALS', *Experimental Neurology*. Academic Press, 262, pp. 127–137. doi: 10.1016/J.EXPNEUROL.2014.02.021.

- Thurston, T. L. M. (2009) 'The tbk1 adaptor and autophagy receptor ndp52 restricts the proliferation of ubiquitin-coated bacteria', *Nature Immunology*. Nat Immunol, 10(11), pp. 1215–1222. doi: 10.1038/ni.1800.
- Tian, T. *et al.* (2014) 'Exosome Uptake through Clathrin-mediated Endocytosis and Macropinocytosis and Mediating miR-21 Delivery', *The Journal of Biological Chemistry*. American Society for Biochemistry and Molecular Biology, 289(32), p. 22258. doi: 10.1074/JBC.M114.588046.
- Tokuda, E. *et al.* (2016) 'Low autophagy capacity implicated in motor system vulnerability to mutant superoxide dismutase', *Acta Neuropathologica Communications*. BioMed Central, 4(1), p. 6. doi: 10.1186/s40478-016-0274-y.
- Tong, K. I. *et al.* (2006) 'Keap1 Recruits Neh2 through Binding to ETGE and DLG Motifs: Characterization of the Two-Site Molecular Recognition Model', *Molecular and Cellular Biology*. American Society for Microbiology, 26(8), pp. 2887–2900. doi: 10.1128/mcb.26.8.2887-2900.2006.
- Tong, K. I. *et al.* (2007) 'Different Electrostatic Potentials Define ETGE and DLG Motifs as Hinge and Latch in Oxidative Stress Response', *Molecular and Cellular Biology*. American Society for Microbiology, 27(21), pp. 7511–7521. doi: 10.1128/mcb.00753-07.
- Trajkovic, K. *et al.* (2008) 'Ceramide triggers budding of exosome vesicles into multivesicular endosomes', *Science*. American Association for the Advancement of Science, 319(5867), pp. 1244–1247. doi: 10.1126/science.1153124.
- Truesdell, S. S. *et al.* (2012) 'MicroRNA-mediated mRNA Translation Activation in Quiescent Cells and Oocytes Involves Recruitment of a Nuclear microRNP', *Scientific Reports 2012 2:1*. Nature Publishing Group, 2(1), pp. 1–12. doi: 10.1038/srep00842.
- Tsutsumi, A. *et al.* (2011) 'Recognition of the pre-miRNA structure by Drosophila Dicer-1', *Nature Structural & Molecular Biology*. Nature Publishing Group, 18(10), pp. 1153–1158. doi: 10.1038/nsmb.2125.
- Turchinovich, A. *et al.* (2011) 'Characterization of extracellular circulating microRNA', *Nucleic Acids Research*. Oxford University Press, 39(16), pp. 7223–7233. doi: 10.1093/nar/gkr254.
- Turchinovich, A. *et al.* (2013) 'Circulating miRNAs: cell-cell communication function?', *Frontiers in genetics*. Frontiers Media SA, 4, p. 119. doi: 10.3389/fgene.2013.00119.
- Uchida, Y. *et al.* (2013) 'MiR-133a induces apoptosis through direct regulation of GSTP1 in bladder cancer cell lines', *Urologic oncology*. Urol Oncol, 31(1), pp. 115–123. doi: 10.1016/J.UROLONC.2010.09.017.
- Udagawa, T. *et al.* (2015) 'FUS regulates AMPA receptor function and FTLD/ALS-associated behaviour via GluA1 mRNA stabilization', *Nature Communications*. Nature Publishing Group, 6(1), p. 7098. doi: 10.1038/ncomms8098.
- Valadi, H. *et al.* (2007) 'Exosome-mediated transfer of mRNAs and microRNAs is a novel mechanism of genetic exchange between cells', *Nature Cell Biology*. Nature Publishing Group, 9(6), pp. 654–659. doi: 10.1038/ncb1596.
- Valapala, M. and Vishwanatha, J. K. (2011) 'Lipid raft endocytosis and exosomal transport facilitate extracellular trafficking of annexin A2', *The Journal of biological chemistry*. J Biol Chem, 286(35), pp. 30911–30925. doi: 10.1074/JBC.M111.271155.
- Valentine, J. S., Doucette, P. A. and Zittin Potter, S. (2005) 'COPPER-ZINC SUPEROXIDE DISMUTASE AND AMYOTROPHIC LATERAL SCLEROSIS', *Annual Review of Biochemistry*. Annual Reviews, 74(1), pp. 563–593. doi: 10.1146/annurev.biochem.72.121801.161647.
- Vance, C. *et al.* (2009) 'Mutations in FUS, an RNA Processing Protein, Cause Familial Amyotrophic Lateral Sclerosis Type 6', *Science*. American Association for the Advancement of Science, 323(5918), pp. 1208–1211. doi: 10.1126/SCIENCE.1165942.
- Varcianna, A. *et al.* (2019) 'Micro-RNAs secreted through astrocyte-derived extracellular vesicles cause neuronal network degeneration in C9orf72 ALS', *EBioMedicine*. Elsevier, 40, p. 626. doi: 10.1016/J.EBIOM.2018.11.067.

- Varga, R. E. *et al.* (2015) 'In Vivo Evidence for Lysosome Depletion and Impaired Autophagic Clearance in Hereditary Spastic Paraplegia Type SPG11', *PLoS Genetics*. Public Library of Science, 11(8). doi: 10.1371/journal.pgen.1005454.
- Vargas, M. R. *et al.* (2006) 'Increased glutathione biosynthesis by Nrf2 activation in astrocytes prevents p75NTR-dependent motor neuron apoptosis', *Journal of Neurochemistry*. J Neurochem, 97(3), pp. 687–696. doi: 10.1111/j.1471-4159.2006.03742.x.
- Vargas, M. R. *et al.* (2008) 'Nrf2 activation in astrocytes protects against neurodegeneration in mouse models of familial amyotrophic lateral sclerosis', *Journal of Neuroscience*. Society for Neuroscience, 28(50), pp. 13574–13581. doi: 10.1523/JNEUROSCI.4099-08.2008.
- Vargas, M. R. *et al.* (2013) 'Absence of Nrf2 or Its Selective Overexpression in Neurons and Muscle Does Not Affect Survival in ALS-Linked Mutant hSOD1 Mouse Models', *PLoS ONE*. Public Library of Science, 8(2), p. 56625. doi: 10.1371/journal.pone.0056625.
- Vickers, K. C. *et al.* (2011) 'MicroRNAs are transported in plasma and delivered to recipient cells by high-density lipoproteins.', *Nature cell biology*. NIH Public Access, 13(4), pp. 423–33. doi: 10.1038/ncb2210.
- Villarroya-Beltri, C. *et al.* (2013a) 'Sumoylated hnRNPA2B1 controls the sorting of miRNAs into exosomes through binding to specific motifs', *Nature Communications*, 4. doi: 10.1038/ncomms3980.
- Villarroya-Beltri, C. *et al.* (2013b) 'Sumoylated hnRNPA2B1 controls the sorting of miRNAs into exosomes through binding to specific motifs', *Nature Communications 2013 4:1*. Nature Publishing Group, 4(1), pp. 1–10. doi: 10.1038/ncomms3980.
- Villarroya-Beltri, C. *et al.* (2014) 'Sorting it out: Regulation of exosome loading', *Seminars in Cancer Biology*. Academic Press, pp. 3–13. doi: 10.1016/j.semcancer.2014.04.009.
- Vlachos, I. S. *et al.* (2015) 'DIANA-miRPath v3.0: deciphering microRNA function with experimental support', *Nucleic acids research*, 1(43), pp. W460–W466. Available at: <https://www.ncbi.nlm.nih.gov/pmc/articles/PMC4489228/> (Accessed: 5 May 2020).
- De vos, K. J. *et al.* (2007) 'Familial amyotrophic lateral sclerosis-linked SOD1 mutants perturb fast axonal transport to reduce axonal mitochondria content', *Human molecular genetics*. Hum Mol Genet, 16(22), pp. 2720–2728. doi: 10.1093/HMG/DDM226.
- Wakabayashi, K. *et al.* (2014) 'Analysis of microRNA from archived formalin-fixed paraffin-embedded specimens of amyotrophic lateral sclerosis', *Acta Neuropathologica Communications*. BioMed Central, 2, p. 173. doi: 10.1186/S40478-014-0173-Z.
- Wakabayashi, N. *et al.* (2003) 'Keap1-null mutation leads to postnatal lethality due to constitutive Nrf2 activation', *Nature Genetics*. Nature Publishing Group, 35(3), pp. 238–245. doi: 10.1038/ng1248.
- Waller, R., Goodall, E. F., *et al.* (2017) 'Serum miRNAs miR-206, 143-3p and 374b-5p as potential biomarkers for amyotrophic lateral sclerosis (ALS)', *Neurobiology of Aging*. Elsevier, 55, pp. 123–131. doi: 10.1016/J.NEUROBIOLAGING.2017.03.027.
- Waller, R., Wyles, M., *et al.* (2017) 'Small RNA Sequencing of Sporadic Amyotrophic Lateral Sclerosis Cerebrospinal Fluid Reveals Differentially Expressed miRNAs Related to Neural and Glial Activity.', *Frontiers in neuroscience*. Frontiers Media SA, 11, p. 731. doi: 10.3389/fnins.2017.00731.
- Wang, J. *et al.* (2018) 'MicroRNA-199a inhibits cellular autophagy and downregulates IFN- $\beta$  expression by targeting TBK1 in Mycobacterium bovis infected cells', *Frontiers in Cellular and Infection Microbiology*. Frontiers Media S.A., 8(JUL). doi: 10.3389/fcimb.2018.00238.
- Wang, P. *et al.* (2019) 'Macrophage achieves self-protection against oxidative stress-induced ageing through the Mst-Nrf2 axis', *Nature Communications*. Nature Publishing Group, 10(1). doi: 10.1038/S41467-019-08680-6.
- Wang, S. *et al.* (2011) 'Synapsin I Is an Oligomannose-Carrying Glycoprotein, Acts As an Oligomannose-Binding Lectin, and Promotes Neurite Outgrowth and Neuronal Survival When Released via Glia-Derived Exosomes', *The Journal of Neuroscience*. Society for Neuroscience, 31(20), p. 7275. doi: 10.1523/JNEUROSCI.6476-10.2011.

- Wang, T. *et al.* (2020) 'MSC-derived exosomes protect against oxidative stress-induced skin injury via adaptive regulation of the NRF2 defense system', *Biomaterials*. Biomaterials, 257. doi: 10.1016/J.BIOMATERIALS.2020.120264.
- Wang, W. *et al.* (2016) 'The inhibition of TDP-43 mitochondrial localization blocks its neuronal toxicity', *Nature Medicine*. doi: 10.1038/nm.4130.
- Wang, Y. *et al.* (2009) 'Nucleation, propagation and cleavage of target RNAs in Ago silencing complexes', *Nature*. Nature Publishing Group, 461(7265), pp. 754–761. doi: 10.1038/nature08434.
- Watts, C. R. and Vanryckeghem, M. (2001) 'Laryngeal dysfunction in Amyotrophic Lateral Sclerosis: a review and case report.', *BMC ear, nose, and throat disorders*. BioMed Central, 1(1), p. 1. doi: 10.1186/1472-6815-1-1.
- Weber, J. A. *et al.* (2010) 'The microRNA spectrum in 12 body fluids.', *Clinical chemistry*. NIH Public Access, 56(11), pp. 1733–41. doi: 10.1373/clinchem.2010.147405.
- Webster, C. P. *et al.* (2016) 'The C9orf72 protein interacts with Rab1a and the ULK 1 complex to regulate initiation of autophagy', *The EMBO Journal*. EMBO, 35(15), pp. 1656–1676. doi: 10.15252/embj.201694401.
- Wei, Y. (2014) 'Autophagic induction of amyotrophic lateral sclerosislinked Cu/Zn superoxide dismutase 1 G93A mutant in NSC34 cells', *Neural Regeneration Research*. Medknow Publications and Media Pvt. Ltd., 9(1), p. 16. doi: 10.4103/1673-5374.125325.
- Weishaupt, J. H. *et al.* (2013) 'A novel optineurin truncating mutation and three glaucoma-associated missense variants in patients with familial amyotrophic lateral sclerosis in Germany', *Neurobiology of Aging*. Elsevier, 34(5), pp. 1516.e9-1516.e15. doi: 10.1016/J.NEUROBIOLAGING.2012.09.007.
- Weishaupt, J. H., Hyman, T. and Dikic, I. (2016) 'Common Molecular Pathways in Amyotrophic Lateral Sclerosis and Frontotemporal Dementia', *Trends in Molecular Medicine*. doi: 10.1016/j.molmed.2016.07.005.
- Weisiger, R. A. and Fridovich, I. (1973) 'Mitochondrial Superoxide Dismutase SITE OF SYNTHESIS AND INTRAMITOCHONDRIAL LOCALIZATION\*', *THE JOURNAL OF BIOLOGICAL CHEMISTRY*, 248(13), pp. 4793–4796. doi: 10.1016/S0021-9258(19)43735-6.
- Wen, X. *et al.* (2018) 'MicroRNA-421 suppresses the apoptosis and autophagy of hippocampal neurons in epilepsy mice model by inhibition of the TLR/MYD88 pathway', *Journal of Cellular Physiology*. Wiley-Liss Inc., 233(9), pp. 7022–7034. doi: 10.1002/jcp.26498.
- Westergard, T. *et al.* (2016) 'Cell-to-Cell Transmission of Dipeptide Repeat Proteins Linked to C9orf72-ALS/FTD', *Cell Reports*. Elsevier B.V., 17(3), pp. 645–652. doi: 10.1016/j.celrep.2016.09.032.
- Wightman, B., Ha, I. and Ruvkun, G. (1993) 'Posttranscriptional regulation of the heterochronic gene *lin-14* by *lin-4* mediates temporal pattern formation in *C. elegans*', *Cell*. Cell Press, 75(5), pp. 855–862. doi: 10.1016/0092-8674(93)90530-4.
- Wilcke, M. *et al.* (2000) 'Rab11 regulates the compartmentalization of early endosomes required for efficient transport from early endosomes to the trans-golgi network.', *The Journal of cell biology*, 151(6), pp. 1207–20. doi: 10.1083/jcb.151.6.1207.
- Wild, A. C., Moinova, H. R. and Mulcahy, R. T. (1999) 'Regulation of  $\gamma$ -glutamylcysteine synthetase subunit gene expression by the transcription factor Nrf2', *Journal of Biological Chemistry*. Elsevier, 274(47), pp. 33627–33636. doi: 10.1074/jbc.274.47.33627.
- Wild, P. *et al.* (2011) 'Phosphorylation of the autophagy receptor optineurin restricts Salmonella growth.', *Science (New York, N.Y.)*. American Association for the Advancement of Science, 333(6039), pp. 228–33. doi: 10.1126/science.1205405.
- Williamson, T. L. and Cleveland, D. W. (1999) 'Slowing of axonal transport is a very early event in the toxicity of ALS-linked SOD1 mutants to motor neurons', *Nature Neuroscience* 1999 2:1. Nature Publishing Group, 2(1), pp. 50–56. doi: 10.1038/4553.
- Wils, H. *et al.* (2010) 'TDP-43 transgenic mice develop spastic paralysis and neuronal inclusions

characteristic of ALS and frontotemporal lobar degeneration', *Proceedings of the National Academy of Sciences of the United States of America*. National Academy of Sciences, 107(8), pp. 3858–3863. doi: 10.1073/pnas.0912417107.

De Winter, F. *et al.* (2006) 'Elsevier Enhanced Reader', *Molecular and Cellular Neuroscience*, 32, pp. 102–117. Available at: <https://reader.elsevier.com/reader/sd/pii/S1044743106000662?token=FF6170A816DC284AFA177C1E9E293EEF9437AE9EE849E245C168D34A4B723A7A0FAB0E79CD40476E420862AA6470031A&originRegion=eu-west-1&originCreation=20211124162024> (Accessed: 24 November 2021).

Winton, M. J. *et al.* (2008) 'A90V TDP-43 variant results in the aberrant localization of TDP-43 in vitro.', *FEBS letters*. NIH Public Access, 582(15), pp. 2252–6. doi: 10.1016/j.febslet.2008.05.024.

Witke, W. (2004) 'The role of profilin complexes in cell motility and other cellular processes', *Trends in Cell Biology*. Elsevier, pp. 461–469. doi: 10.1016/j.tcb.2004.07.003.

Wong, Y. C. and Holzbaur, E. L. F. (2015) 'Temporal dynamics of PARK2/parkin and OPTN/optineurin recruitment during the mitophagy of damaged mitochondria', *Autophagy*. Taylor & Francis, 11(2), pp. 422–424. doi: 10.1080/15548627.2015.1009792.

Wren, M. C. *et al.* (2015) 'Frontotemporal dementia-associated N279K tau mutant disrupts subcellular vesicle trafficking and induces cellular stress in iPSC-derived neural stem cells', *Molecular Neurodegeneration*. BioMed Central, 10(1). doi: 10.1186/S13024-015-0042-7.

Wu, H. *et al.* (2012) 'MiR-20a and miR-106b negatively regulate autophagy induced by leucine deprivation via suppression of ULK1 expression in C2C12 myoblasts', *Cellular Signalling*. Pergamon, 24(11), pp. 2179–2186. doi: 10.1016/J.CELLSIG.2012.07.001.

Wu, J. *et al.* (2013) 'Cyclic GMP-AMP is an endogenous second messenger in innate immune signaling by cytosolic DNA', *Science (New York, N.Y.)*. Science, 339(6121), pp. 826–830. doi: 10.1126/SCIENCE.1229963.

Wu, L. S., Cheng, W. C. and Shen, C. K. J. (2012) 'Targeted depletion of TDP-43 expression in the spinal cord motor neurons leads to the development of amyotrophic lateral sclerosis-like phenotypes in mice', *Journal of Biological Chemistry*. American Society for Biochemistry and Molecular Biology, 287(33), pp. 27335–27344. doi: 10.1074/jbc.M112.359000.

Wu, Y., Deng, W. and Klinke, D. J. (2015) 'Exosomes: Improved methods to characterize their morphology, RNA content, and surface protein biomarkers', *The Analyst*. NIH Public Access, 140(19), p. 6631. doi: 10.1039/C5AN00688K.

Wu, Z. *et al.* (2011) 'miR-340 inhibition of breast cancer cell migration and invasion through targeting of oncoprotein c-Met', *Cancer*. John Wiley & Sons, Ltd, 117(13), pp. 2842–2852. doi: 10.1002/cncr.25860.

Wurzer, B. *et al.* (2015) 'Oligomerization of p62 allows for selection of ubiquitinated cargo and isolation membrane during selective autophagy.', *eLife*. eLife Sciences Publications, Ltd, 4, p. e08941. doi: 10.7554/eLife.08941.

Xia, Q. *et al.* (2016) 'TDP-43 loss of function increases TFEB activity and blocks autophagosome-lysosome fusion', *The EMBO Journal*. EMBO Press, 35(2), pp. 121–142. doi: 10.15252/embj.201591998.

Xian, P. *et al.* (2019) 'Mesenchymal stem cell-derived exosomes as a nanotherapeutic agent for amelioration of inflammation-induced astrocyte alterations in mice', *Theranostics*. Ivyspring International Publisher, 9(20), pp. 5956–5975. doi: 10.7150/THNO.33872.

Xiao, J. *et al.* (2011) 'MiR-204 regulates cardiomyocyte autophagy induced by ischemia-reperfusion through LC3-II.', *Journal of biomedical science*. BioMed Central, 18(1), p. 35. doi: 10.1186/1423-0127-18-35.

Xu, D. *et al.* (2018) 'TBK1 Suppresses RIPK1-Driven Apoptosis and Inflammation during Development and in Aging In Brief', *Cell*, 174, pp. 1477-1491.e19. doi: 10.1016/j.cell.2018.07.041.

Xu, H.-L. *et al.* (2018) 'Lentian up-regulates microRNA-340 to promote apoptosis and autophagy of

human osteosarcoma cells', *International Journal of Clinical and Experimental Pathology*. e-Century Publishing Corporation, 11(8), p. 3876.

Y, O. *et al.* (2019) 'Enhanced oxidative stress and the treatment by edaravone in mice model of amyotrophic lateral sclerosis', *Journal of neuroscience research*. J Neurosci Res, 97(5), pp. 607–619. doi: 10.1002/JNR.24368.

Yang, C. *et al.* (2016) 'Mutant PFN1 causes ALS phenotypes and progressive motor neuron degeneration in mice by a gain of toxicity', *Proceedings of the National Academy of Sciences of the United States of America*. National Academy of Sciences, 113(41), pp. E6209–E6218. doi: 10.1073/pnas.1605964113.

Yang, J. *et al.* (2018) 'MicroRNA-181a inhibits autophagy by targeting Atg5 in hepatocellular carcinoma.', *Frontiers in bioscience (Landmark edition)*, 23, pp. 388–396. Available at: <http://www.ncbi.nlm.nih.gov/pubmed/28930552> (Accessed: 3 May 2019).

Yang, L. *et al.* (2014) 'Self-assembled FUS binds active chromatin and regulates gene transcription.', *Proceedings of the National Academy of Sciences of the United States of America*. National Academy of Sciences, 111(50), pp. 17809–14. doi: 10.1073/pnas.1414004111.

Yang, L. *et al.* (2018) 'MiR-340-5p is a potential prognostic indicator of colorectal cancer and modulates ANXA3', *European Review for Medical and Pharmacological Sciences*, 22, pp. 4837–4845.

Yang, M. *et al.* (2016) 'A C9ORF72/SMCR8-containing complex regulates ULK1 and plays a dual role in autophagy', *Science Advances*. American Association for the Advancement of Science, 2(9), p. e1601167. doi: 10.1126/sciadv.1601167.

Yang, X. *et al.* (2013) 'mir-30d Regulates multiple genes in the autophagy pathway and impairs autophagy process in human cancer cells.', *Biochemical and biophysical research communications*. NIH Public Access, 431(3), pp. 617–22. doi: 10.1016/j.bbrc.2012.12.083.

Yang, Y. *et al.* (2001) 'The gene encoding alsin, a protein with three guanine-nucleotide exchange factor domains, is mutated in a form of recessive amyotrophic lateral sclerosis', *Nature genetics*. Nat Genet, 29(2), pp. 160–165. doi: 10.1038/NG1001-160.

Yang, Z. *et al.* (2006) 'Atg22 Recycles Amino Acids to Link the Degradative and Recycling Functions of Autophagy', *Molecular Biology of the Cell*. Edited by J. Brodsky, 17(12), pp. 5094–5104. doi: 10.1091/mbc.e06-06-0479.

Yang, Z. and Klionsky, D. J. (2010) 'Mammalian autophagy: core molecular machinery and signaling regulation.', *Current opinion in cell biology*. NIH Public Access, 22(2), pp. 124–31. doi: 10.1016/j.cecb.2009.11.014.

Yao, L. *et al.* (2019) 'MicroRNA-124 regulates the expression of p62/p38 and promotes autophagy in the inflammatory pathogenesis of Parkinson's disease', *The FASEB Journal*. John Wiley and Sons Inc., 33(7), pp. 8648–8665. doi: 10.1096/fj.201900363R.

Yi, R. *et al.* (2003) 'Exportin-5 mediates the nuclear export of pre-microRNAs and short hairpin RNAs.', *Genes & development*. Cold Spring Harbor Laboratory Press, 17(24), pp. 3011–6. doi: 10.1101/gad.1158803.

Yoda, M. *et al.* (2010) 'ATP-dependent human RISC assembly pathways', *Nature Structural & Molecular Biology*. Nature Publishing Group, 17(1), pp. 17–23. doi: 10.1038/nsmb.1733.

Yoshioka, Y. *et al.* (2013) 'Comparative marker analysis of extracellular vesicles in different human cancer types', *Journal of Extracellular Vesicles*. Wiley-Blackwell, 2(1). doi: 10.3402/JEV.V2I0.20424.

Yu, C. H. *et al.* (2020) 'TDP-43 Triggers Mitochondrial DNA Release via mPTP to Activate cGAS/STING in ALS', *Cell*. Cell Press, 183(3), pp. 636-649.e18. doi: 10.1016/j.cell.2020.09.020.

Yu, Y. *et al.* (2012) 'microRNA 30A promotes autophagy in response to cancer therapy.', *Autophagy*. Taylor & Francis, 8(5), pp. 853–5. doi: 10.4161/auto.20053.

Zaborowski, M. P. *et al.* (2015) 'Editor's Choice: Extracellular Vesicles: Composition, Biological Relevance, and Methods of Study', *Bioscience*, 65(8), pp. 783–797. Available at:

<https://www.ncbi.nlm.nih.gov/pmc/articles/PMC4776721/> (Accessed: 8 April 2020).

Zeng, Y. (2006) 'Principles of micro-RNA production and maturation', *Oncogene*. Nature Publishing Group, 25(46), pp. 6156–6162. doi: 10.1038/sj.onc.1209908.

Zeng, Y. and Cullen, B. R. (2003) 'Sequence requirements for micro RNA processing and function in human cells.', *RNA (New York, N.Y.)*. Cold Spring Harbor Laboratory Press, 9(1), pp. 112–23. doi: 10.1261/RNA.2780503.

Zhang, C. *et al.* (2019) 'Structural basis of STING binding with and phosphorylation by TBK1', *Nature*. NIH Public Access, 567(7748), p. 394. doi: 10.1038/S41586-019-1000-2.

Zhang, D. *et al.* (2018) 'Edaravone attenuates oxidative stress induced by chronic cerebral hypoperfusion injury: role of ERK/Nrf2/HO-1 signaling pathway', *Neurological Research*. Taylor and Francis Ltd., 40(1), pp. 1–10. doi: 10.1080/01616412.2017.1376457.

Zhang, D. D. and Hannink, M. (2003) 'Distinct Cysteine Residues in Keap1 Are Required for Keap1-Dependent Ubiquitination of Nrf2 and for Stabilization of Nrf2 by Chemopreventive Agents and Oxidative Stress', *Molecular and Cellular Biology*. American Society for Microbiology (ASM), 23(22), p. 8137. doi: 10.1128/MCB.23.22.8137-8151.2003.

Zhang, F. *et al.* (2007) 'Interaction between familial Amyotrophic Lateral Sclerosis (ALS)-linked SOD1 mutants and the dynein complex', *Journal of Biological Chemistry*. American Society for Biochemistry and Molecular Biology, 282(22), pp. 16691–16699. doi: 10.1074/jbc.M609743200.

Zhang, H. *et al.* (2004) 'Single Processing Center Models for Human Dicer and Bacterial RNase III', *Cell*. Cell Press, 118(1), pp. 57–68. doi: 10.1016/J.CELL.2004.06.017.

Zhang, H. *et al.* (2005) 'Human Dicer preferentially cleaves dsRNAs at their termini without a requirement for ATP', *The EMBO Journal*. EMBO Press, 24, pp. 138–148. doi: 10.1093/emboj/cdf582.

Zhang, T. *et al.* (2018) 'FUS Regulates Activity of MicroRNA-Mediated Gene Silencing', *Molecular Cell*. Cell Press, 69(5), pp. 787–801.e8. doi: 10.1016/J.MOLCEL.2018.02.001.

Zhang, X. *et al.* (2018) 'Novel role of miR-133a-3p in repressing gastric cancer growth and metastasis via blocking autophagy-mediated glutaminolysis', *Journal of Experimental and Clinical Cancer Research*. BioMed Central Ltd., 37(1). doi: 10.1186/s13046-018-0993-y.

Zhang, Xiaojie *et al.* (2011) 'Rapamycin treatment augments motor neuron degeneration in SOD1 G93A mouse model of amyotrophic lateral sclerosis) Rapamycin treatment augments motor neuron degeneration in SOD1 G93A mouse model of amyotrophic lateral sclerosis', *Autophagy*, 7(4), pp. 412–425. doi: 10.4161/auto.7.4.14541.

Zhang, Xu *et al.* (2013) 'Cyclic GMP-AMP Containing Mixed Phosphodiester Linkages Is An Endogenous High-Affinity Ligand for STING', *Molecular Cell*. Cell Press, 51(2), pp. 226–235. doi: 10.1016/J.MOLCEL.2013.05.022.

Zhang, Y. *et al.* (2019) 'Exosomes: biogenesis, biologic function and clinical potential', *Cell & Bioscience*. BioMed Central, 9(1), p. 19. doi: 10.1186/s13578-019-0282-2.

Zhang, Y. *et al.* (2021) 'Cerebellar Kv3.3 potassium channels activate TANK-binding kinase 1 to regulate trafficking of the cell survival protein Hax-1', *Nature communications*. Nat Commun, 12(1). doi: 10.1038/S41467-021-22003-8.

Zhao, P. *et al.* (2018) 'Up-regulation of miR-340-5p promotes progression of thyroid cancer by inhibiting BMP4', *Journal of endocrinological investigation*. J Endocrinol Invest, 41(10), pp. 1165–1172. doi: 10.1007/S40618-018-0848-6.

Zhao, Y. *et al.* (2019) 'Vitamin D Alleviates Rotavirus Infection through a MicroRNA-155-5p Mediated Regulation of the TBK1/IRF3 Signaling Pathway In Vivo and In Vitro', *International Journal of Molecular Sciences*. Multidisciplinary Digital Publishing Institute (MDPI), 20(14). doi: 10.3390/IJMS20143562.

Zheng, Y. *et al.* (2020) 'MiR-340-5p alleviates oxygen-glucose deprivation/reoxygenation-induced neuronal injury via PI3K/Akt activation by targeting PDCD4', *Neurochemistry International*. Pergamon, 134, p. 104650. doi: 10.1016/J.NEUINT.2019.104650.

- Zhong, Y. *et al.* (2009) 'Distinct regulation of autophagic activity by Atg14L and Rubicon associated with Beclin 1–phosphatidylinositol-3-kinase complex', *Nature Cell Biology*. Nature Publishing Group, 11(4), pp. 468–476. doi: 10.1038/ncb1854.
- Zhou, F. *et al.* (2018) 'Screening the expression characteristics of several miRNAs in G93A-SOD1 transgenic mouse: altered expression of miRNA-124 is associated with astrocyte differentiation by targeting Sox2 and Sox9', *Journal of Neurochemistry*. John Wiley & Sons, Ltd (10.1111), 145(1), pp. 51–67. doi: 10.1111/jnc.14229.
- Zhou, J. *et al.* (2015) 'microRNA-340-5p Functions Downstream of Cardiotrophin-1 to Regulate Cardiac Eccentric Hypertrophy and Heart Failure via Target Gene Dystrophin', *International Heart Journal*, 56(4), pp. 454–458.
- Zhou, W. *et al.* (2014) 'Cancer-secreted miR-105 destroys vascular endothelial barriers to promote metastasis', *Cancer cell*. NIH Public Access, 25(4), p. 501. doi: 10.1016/J.CCR.2014.03.007.
- Zhou, Y. *et al.* (2013) 'ALS-associated FUS mutations result in compromised FUS alternative splicing and autoregulation.', *PLoS genetics*. Public Library of Science, 9(10), p. e1003895. doi: 10.1371/journal.pgen.1003895.
- Zhu, H. *et al.* (2009) 'Regulation of autophagy by a beclin 1-targeted microRNA, miR-30a, in cancer cells.', *Autophagy*. Taylor & Francis, 5(6), pp. 816–23. Available at: <http://www.ncbi.nlm.nih.gov/pubmed/19535919> (Accessed: 3 May 2019).
- Zhu, X. *et al.* (2013) 'Identification of micro-RNA networks in end-stage heart failure because of dilated cardiomyopathy', *Journal of Cellular and Molecular Medicine*. J Cell Mol Med, 17(9), pp. 1173–1187. doi: 10.1111/jcmm.12096.
- Zipper, L. M. and Timothy Mulcahy, R. (2002) 'The Keap1 BTB/POZ dimerization function is required to sequester Nrf2 in cytoplasm', *Journal of Biological Chemistry*. Elsevier, 277(39), pp. 36544–36552. doi: 10.1074/jbc.M206530200.
- Zitvogel, L. *et al.* (1998) 'Eradication of established murine tumors using a novel cell-free vaccine: Dendritic cell-derived exosomes', *Nature Medicine*. Nature Publishing Group, 4(5), pp. 594–600. doi: 10.1038/nm0598-594.

## Chapter 9 -Appendices

### Appendix 1: Features of studies comparing miRNA levels in ALS patients and healthy controls.

*Studies are organised chronologically, with newest first. Note both familial and sporadic ALS patients are used in some studies and the variation in the samples obtained from patients. Also note the variation in the techniques used for miRNA detection or quantification, and functional or bioinformatic assessments.*

Study	Sample	Participants	Main Methods and Techniques
Saucier et al., 2018	Extracellular Vesicles from Plasma	Next generation sequencing with 14 ALS patients and 12 HCs.  Quantification with 12 ALS and 3 HCs.	miRNA expression levels identified through next generation sequencing (NGS). Quantification performed using reverse transcription and digital droplet PCR.  Prediction of gene targets performed by TargetScan 7.1 and human miRanda algorithm. Functional relevance assessed with DAVID.
Taguchi and Wang 2018	Serum	9 fALS, 18 sALS, 18 ALS mutation carriers and 17 HCs.	miRNA expression profiles produced by Freidschmidt et al. 2014, were subject to principal component analysis – based unsupervised feature extraction. KEGG pathway enrichment analysis performed on the downregulated miRNAs.
Kovanda et al., 2018	Muscle biopsies	11 ALS patient muscle biopsies and 11 HCs.	NGS was followed by differential expression analysis of miRNAs. miRNA analysis performed using Tarbase and KEGG and Gene ontology (GO) analysis performed.

Raheja et al., 2018	Serum	20 sALS patients, 3 fALS patients and 30 HCs.	miRNA detection performed using RT-PCR.
Liguori et al., 2018	Peripheral blood	Discovery phase using 6 sALS and 5 HCs and validation with 50 sALS patients and 15 HCs.	High- throughput NGS and a subset validated using qRT-qPCR. Gene targets were predicted using miRtarbase and DIANA-Tarbase and pathway analysis was performed using DAVID.
De Felice et al., 2018	Neuromuscular junction and blood leukocytes	45 sALS patients and 25 HCs.	Samples analysed by next generation sequencing and a selection were validated by qRT-PCR. Target prediction performed using TargetScan and Pictar. KEGG and GO analysis were performed.
D'Erchia et al., 2017	Ventral horns of the lumbar spinal cord from post mortems	11 sALS and 7 HCs	Transcriptomes sequenced with RNA-seq and validated with qRT-PCR. Differentially expressed genes identified using CuffDiff2 and DEseq2. Ingenuity pathway and GO analysis performed.
Waller et al., 2017a	CSF	32 sALS patients and 10 healthy controls with 6 neurological controls (MS patients) combined.	qPCR and small RNA sequencing and qPCR was used in validation. The online platforms Oasis 2.0 (Capece <i>et al.</i> , 2015) and Genboree (Subramanian <i>et al.</i> , 2015) were used to analyse the small RNA sequencing data.
Waller et al., 2017b	Serum	27 sALS patients, and 25 HCs. Validation in 23 sALS patients and 22 HCs.	The expression levels of 750 miRNAs were determined using Taqman arrays and qPCR was performed on these miRNAs. Validation qPCR was performed on a selection of 27 miRNAs.

Di Pietro et al., 2017	Skeletal muscle	14 ALS patients and 24 healthy controls	RNA isolated using TaqMan microRNA Reverse Transcription kit and quantified using specific probes. Functional characterisation of one miRNA performed in cells.
Pegoraro et al., 2017	Skeletal muscle	13 sALS patients and 5 HCs	qRT-PCR performed on extracted miRNA.
Figueroa-Romero et al., 2016	Spinal cord from post mortems	12 sALS and 12 HCs.	TaqMan OpenArray miRNA profiling was performed and differential expression was confirmed with qPCR. Validation performed by qPCR. Validated miRNA targets obtained from TarBase and predicted targets from TargetScan and microrna.org
Benigni et al., 2016	CSF	24 sALS patients and 24 HCs.	Quantitative reverse transcription PCR identified deregulated miRNAs. miRNA profiling was performed by qRT-PCR and validated by RT-PCR.
Jensen et al., 2016	Skeletal muscle	5 ALS patients and 7 healthy controls.	Reverse transcription performed using TaqMan MicroRNA Reverse Transcription Kit. miRNA analysis performed using specific primers for skeletal muscle specific miRNAs.
Tasca et al., 2016	Muscle specific miRNAs in serum	14 sALS patients and 8 HCs	Expression levels quantified using qRT-PCR.

Chen et al., 2016	Leukocytes	5 Chinese sALS patients and 5 healthy controls.  Validation in 83 sALS patients with 61 HCs.	Microarray analysis identified differentially expressed miRNAs and validation was performed on all these miRNAs by RT-PCR. Target genes were predicted using TargetScan, PicTar, miRanda, PITA and RNA22. GO analysis was also performed.
de Andrade et al., 2016	Skeletal muscle and plasma	Skeletal muscle expression analysis: 5 sALS and 5 healthy controls. Plasma expression analysis; 39 sALS and 39 HCs.	Microarray analysis identified differentially expressed miRNAs from ALS patient's muscle. Three miRNAs were validated in RT-qPCR in muscle. Targets predicted using miRGen algorithm.
Raman et al., 2015	Fibroblasts	6 sALS, 6 PLS (primary lateral sclerosis) and 6 HCs.  Validation: 11 ALS, 6PALS and 10 HCs.	Microarray analysis identified differentially expressed miRNAs. DAVID and GO analysis were applied to differentially expressed transcripts. Validation performed using qRT-PCR.
Emde et al., 2015	Motor neurones of spinal cords	8 sALS, 9 non-neurodegeneration controls.	Taqman microarray and qPCR identified 667 miRNAs. RT-qPCR used to assess expression changes.
Takahashi et al., 2015	Plasma	Microarray cohort: 16 sALS patients and 10 HCs. Validation cohort: 48 sALS patients and 30 HCs	3D-Gene microarray analysis using around 1800 probes identified differentially expressed miRNAs, some which were validated in qRT-PCR.
Freischmidt et al., 2015	Serum	18 sALS patients and 16 healthy controls.	Microarray analysis with a focus on only downregulated miRNAs

		Validated by RT-qPCR in 20 sALS patients and 20 HCs. 13 fALS and 13 HCs used as a comparison group.	and validation was performed with qRT-PCR.
Freischmidt et al., 2014	Serum	Group 1: 9 fALS and 10 HCs.  Validation group: 13 fALS patients with 13 HCs.  Second validation group: 14 sALS patients with 14 HCs.	Microarray analysis measured the abundance of 1733 mature miRNAs. Validation of 4 miRNAs using qRT-PCR. A second validation was performed with the same 4 miRNAs by qRT-PCR. DREME tool used to identify two motifs frequently occurring in the downregulated miRNAs of fALS and ALS mutation carrying patients.
Wakabayashi et al., 2014	Formalin-fixed paraffin-embedded post mortem brain specimens	6 ALS patients and 4 healthy controls.	Microarray analysis performed on extracted RNA and analysed for differential expression. Bioinformatic predictions of target genes performed using miRmap. Ontology analysis performed using Metacore functional analysis and gene ontology analysis performed using the Gene Ontology Consortium web tool.
Ishtiaq et al., 2014	Ventral lumbar spinal cord	5 sALS patients and 5 healthy controls.	Small RNAs were isolated and sequencing library was generated. Sequencing revealed 80 putative novel miRNAs and only those predicted to target NEFL mRNA were considered. Following structural analysis, RT-PCR confirmed 10 miRNAs were differentially expressed. Further analysis performed using functional reporter assays and relative quantitative PCR.

Campos-Melo et al., 2013	Spinal cord	5 sALS patients and 3 healthy controls.	Taqman microarrays used to identify 664 miRNAs and a selection of miRNAs were validated using RT-qPCR. Ingenuity pathway analysis performed. Bioinformatic analysis performed using TargetScan and microrna.org to identify miRNAs with recognition elements in the 3'UTR of NEFL. Functional analysis performed using reporter assays and RT-qPCR.
Freischmidt et al., 2013	CSF and serum	22 ALS patients and 24 healthy controls.	RNA isolated and the levels of TDP-43 binding miRNAs measured by qPCR. Confirmation performed in lymphoblast cell lines from genetically defined ALS patients.
Russell et al., 2013	Skeletal muscle	14 ALS patients and 10 healthy controls.	Specific skeletal muscle enriched miRNAs reverse transcribed using specific primers and levels measured using specific primers and probes.

## Appendix 2: 27 papers' ALS-deregulated miRNAs.

<b>Kovanda et al, 2018</b>	miR-500a-3p	miR-26b-5p	miR-4505-5p	miR-1469-5p
miR-100-5p	miR-501-3p	miR-27b-3p	miR-4508-5p	miR-3940-5p
miR-125a-5p	miR-502-3p	miR-28-3p	miR-4725-3p	miR-4507-3p
miR-125-1-5p	miR-542-5p	miR-30b-5p		miR-4707-5p
miR-125b-5p	miR-5699-5p	miR-30c-5p	<b>Raheja et al, 2018</b>	miR-12813p
miR-1260a-5p	miR-584-5p	miR-342-3p	miR-101-3p	miR-455-3p
miR-126-5p	miR-625-3p	miR-409-3p	miR-16-2-3p	miR-4270-5p
miR-128-2-3p	miR-660-5p	miR-425-5p	miR-182-3p	miR-1825-3p
miR-1285-1-3p	miR-855-3p	miR-451a-5p	miR-188-5p	miR-4745-5p
miR-1285-2-3p	miR-99a-5p	miR-532-5p	miR-15b-3p	miR-4734-3p
miR-1303-3p	miR-542-3p	miR-550a-3p	miR-21-5p	miR-3613-5p
miR-132-5p		miR-584-5p	miR-22-3p	miR-4741-3p
miR-133a-1-3p	<b>Liguori et al, 2018</b>	miR-93-5p	miR-32-5p	miR-3185-5p
miR-133a-2-3p	let-7a-5p	<b>Freischmidt et al, 2014</b>	miR-34a-3p	miR-26a-5p
miR-150-5p	let-7d-5p	miR-455-3p	miR-525-5p	miR-451a-5p
miR-151a-5p	let-7f-5p	miR-4745-5p	miR-let-7a-5p	miR-181a-5p
miR-191-5p	let-7g-5p	miR-1915-3p	miR-let-7c-5p	miR-151a-5p
miR-199a-1-3p	let-7i-5p	miR-1825-3p	miR-let-7f-5p	miR-17-5p
miR-199a-2-3p	miR-103a-3p	miR-3613-5p	miR-107-3p	let-7i-5p
miR-199b-3p	miR-106b-3p	miR-3665-5p	miR-134-5p	miR-106a-5p
miR-212-5p	miR-128-3p	miR-3185-5p	miR-151a-5p	miR-2278-5p
miR-214-3p	miR-130a-3p	miR-4530-3p	miR-26a-5p	miR-99b-3p
miR-24-1-5p	miR-130b-3p	miR-1281-3p	miR-33a-3p	miR-760-3p
miR-26a-1-5p	miR-144-5p	miR-4734-3p	miR-340-5p	miR-584-5p
miR-26a-2-5p	miR-148a-3p	miR-4707-5p	miR-423-3p	let-7d-5p
miR-27a-5p	miR-148b-3p	miR-4497-5p	miR-7-1-3p	miR-3175-5p
miR-28-3p	miR-15a-5p	miR-1469-5p		miR-4306-3p
miR-3607-3p	miR-15b-5p	miR-4741-3p	<b>Taguchi et al, 2018</b>	miR-130b-3p
miR-362-5p	miR-151a-5p	miR-4787-5p	miR-3960-3p	miR-324-3p
miR-378a-3p	miR-151b-3p	miR-371b-5p	miR-3665-5p	miR-21-3p
miR-378d-2	miR-16-5p	miR-2861-3p	miR-4497-5p	miR-744-5p
miR-378c-5p	miR-181a-2-3p	miR-638-5p	miR-4787-3p	miR-25-3p
miR-378d-1	miR-182-5p	miR-4488-5p	miR-4466-5p	miR-4485-3p
miR-378d-3p	miR-183-5p	miR-3960-3p	miR-2861-3p	miR-378i-5p
miR-424-5p	miR-186-5p	miR-3940-5p	miR-638-5p	miR-652-3p
miR-450a-1-5p	miR-192-5p	miR-4466-5p	miR-4516-5p	miR-2392-3p
miR-450a-2-5p	miR-22-3p	miR-3196-5p	miR-4488-5p	let-7a-5p
miR-450b-5p	miR-221-3p	miR-4270-5p	miR-4508-5p	
miR-4662a-5p	miR-223-3p	miR-149-3p	miR-4530-3p	<b>D'Erchia et al, 2017</b>
miR-486-1-5p	miR-23a-3p	miR-4763-3p	miR-3196-5p	miR-577-5p
miR-486-2-5p	miR-25-3p	miR-4516-5p	miR-4763-3p	miR-182-5p
miR-494-3p	miR-26a-5p	miR-4507-3p		miR-485-5p

miR-124-3p miR-218-5p miR-183-5p miR-873-5p miR-133a-3p miR-487b-3p miR-219-5p miR-409-3p miR-889-3p miR-136-3p miR-410-3p miR-127-3p miR-148a-3p miR-155-5p miR-221-3p	<b>Ramen et al, 2015</b> miR-17-5p miR-20b-5p miR-106a-5p miR-107-3p miR-125a-3p miR-142-5p miR-149-5p miR-155-5p miR-219-1-3p miR-324-3p miR-362-5p miR-454-3p miR-484-5p miR-589-5p miR-598-3p miR-616-5p miR-618-5p miR-629-5p miR-636-3p	miR-2392-3p miR-4462-3p miR-338-3p miR-3616-3p miR-4688-5p miR-17-5p miR-106a-5p miR-4484-3p miR-29a-3p miR-4667-5p miR-30b-5p miR-4740-5p miR-1290-3p miR-3619-3p miR-1246-5p miR-3180-3p miR-4648-5p miR-4716-3p miR-940-3p miR-4787-3p miR-4697-5p miR-1231-5p miR-1915-5p miR-1203-5p miR-486-3p miR-3928-3p miR-3911-5p miR-760-3p miR-4281-3p miR-4428-3p	miR-1-3p miR-26a-5p miR-133a-3p miR-455-3p  <b>Pegoraro et al, 2017</b> miR-1-3p miR-206-3p miR-133a-3p miR-133b-3p miR-27a-3p miR-155-5p miR-146a-5p miR-221-3p  <b>Tasca et al, 2017</b> miR-206-3p miR-133a-3p miR-133b-3p miR-146a-5p miR-149-3p miR-27a-3p  <b>Chen et al, 2016</b> miR-193b-3p miR-34a-5p miR-100-5p miR-4485-3p miR-3690-5p miR-124-3p miR-183-5p miR-3935-3p miR-451-5p miR-4538-5p miR-4701-5p  <b>De Andrade et al, 2016</b> miR-4245p miR-503-5p miR-886-3p	miR-542-5p miR-34a-5p miR-886-5p miR-146b-5p miR-504-5p miR-21-5p miR-214-3p miR-183-5p  <b>Freischmidt et al, 2015</b> miR-1825-3p miR-1234-3p  <b>Ishtiaq et al, 2014</b> miR-b1336 miR-b2403 miR-b4652 miR-sb659* miR- b1123 miR-b2948 miR-b3265 miR-b5539 miR-sb1217* miR-sb3998  <b>Waller et al, 2017 (2)</b> miR-133a-3p miR-135b-5p miR-143-3p miR-144-3p miR-146b-3p miR-206-3p miR-20a-3p miR-214-3p miR-331-3p miR-374b-5p miR-518d-3p miR-551b-3p
<b>Waller et al, 2017</b> miR-124-3p miR-127-3p miR-143-3p miR-125b-2-3p miR-9-5p miR-27b-3p miR-486-5p Let-7f-5p miR-16-5p miR-28-3p miR-146a-5p miR-150-5p miR-378a-3p miR-142-5p miR-92a-5p	<b>Takahashi et al, 2015</b> miR-4258-5p miR-663b-3p miR-4649-5p miR-26b-5p miR-4299-3p miR-7f-5p miR-3187-5p miR-4496-3p	<b>Di Pietro et al, 2017</b> miR-133a-3p miR-1-3p miR-29c-3p miR-9-5p miR-208b-3p miR-206-3p miR-155-5p miR-23a-3p		
<b>Benigni et al, 2016</b> miR-15b-5p miR-21-5p miR-195-5p miR-148-3p let-7b-5p miR-181a-5p let-7a-5p let-7f-5p	<b>Wakabayashi et al, 2014</b> miR-494-3p miR-4257-3p miR-24-3p miR-4299-3p miR-1973-3p miR-4485-3p miR-3918-5p miR-4749-5p	<b>Jensen et al, 2016</b>		

<b>Figueroa-Romero et al, 2016</b>	miR-140-3p	miR-935-3p	miR-490-5p	miR-219a-2-3p
miR-142-5p	miR-625-3p	miR-577-5p	miR-6820-3p	miR-219a-5p
miR-155-5p	miR-382-5p		miR-323a-5p	miR-3622a-5p
miR-342-3p	miR-126-5p	<b>De Felice et al, 2018</b>	miR-409-5p	miR-24-1-5p
miR-125b-5p	miR-219-2-3p	miR-29b-3p	miR-574-5p	miR-379-3p
miR-30a-3p	miR-29b-2-5p	miR-23b-3p	miR-548v-3p	miR-1247-5p
let-7d-5p	miR-411-5p	miR-125a-5p	miR-302d-3p	miR-487b-3p
miR-125b-2-3p	miR-625-5p	miR-4301-5p	miR-6500-3p	miR-105-5p
miR-16-5p	miR-885-5p	miR-99b-5p	miR-190a-5p	miR-4524a-3p
let-7a-5p	miR-628-5p	miR-199b-5p	miR-504-5p	miR-132-3p
miR-532-5p	miR-592-5p	miR-1-3p	miR-411-5p	miR-487a-3p
let-7b-5p	miR-409-5p	miR-330-3p	miR-134-5p	miR-410-3p
miR-320b-3p	miR-127-3p	miR-98-3p	miR-655-3p	miR-23b-5p
miR-30d-5p	miR-210-3p	miR-769-5p	miR-485-3p	miR-4524a-5p
miR-20a-3p	miR-1233-3p	miR-181b-5p	miR-432-5p	miR-379-5p
miR-23b-3p	miR-598-3p	let-7b-5p	miR-375-3p	miR-485-5p
miR-502-3p	miR-330-5p	miR-381-3p	miR-200a-3p	miR-539-5p
miR-193b-3p	miR-338-5p	miR-519a-3p	miR-577-5p	miR-212-3p
let-7e-5p	miR-410-3p	miR-376c-3p	miR-4324-3p	miR-381-5p
let-7f-5p	miR-939-5p	miR-5701-5p	miR-1224-5p	miR-34c-3p
miR-204-5p	miR-432-5p	miR-3679-5p	miR-3622a-3p	miR-330-5p
miR-425-5p	miR-337-5p	miR-22-3p	miR-3960-3p	let-7e-5p
miR-340-3p	miR-18a-3p	miR-219b-5p	miR-181d-5p	miR-135b-5p
let-7g-5p	miR-539-5p	miR-320d-3p	let-7c-3p	miR-511-3p
miR-126-3p	miR-216b-5p	miR-320b-3p	miR-29c-5p	miR-299-5p
miR-27b-5p	miR-184-3p	miR-1224-3p	miR-373-3p	miR-302b-3p
miR-942-5p	miR-433-3p	miR-876-3p	miR-3065-5p	miR-490-3p
miR-424-3p	miR-543-3p	miR-6511b-3p	miR-369-3p	miR-770-5p
miR-222-3p	miR-218-5p	miR-195-3p	miR-3151-3p	miR-412-5p
miR-181a-2-3p	miR-148b-5p	miR-3117-5p	miR-181c-5p	miR-136-5p
miR-338-3p	miR-485-3p	miR-489-5p	miR-6507-5p	miR-7-2-3p
miR-409-3p	miR-154-5p	miR-1287-3p	miR-598-3p	miR-1299-3p
miR-512-3p	miR-136-3p	miR-548aw-5p	miR-323b-3p	miR-187-3p
miR-505-5p	miR-154-3p	miR-760-3p	miR-499a-3p	miR-1251-5p
miR-323a-3p	miR-133a-3p	miR-152-3p	miR-382-3p	miR-154-3p
miR-95-3p	miR-487b-3p	miR-1180-3p	miR-299-3p	miR-487a-5p
miR-34a-3p	miR-645-3p	miR-27b-3p	miR-758-5p	miR-132-5p
miR-638-5p	miR-138-5p	miR-154-5p	miR-1249-3p	miR-27b-5p
miR-769-5p	miR-133b-3p	miR-1287-5p	miR-190a-3p	miR-145-5p
miR-376c-3p	miR-138-2-3p	miR-3177-3p	miR-382-5p	miR-1973-3p
miR-766-3p	miR-139-5p	miR-193a-3p	miR-335-5p	miR-548ba-5p
miR-190a-5p	miR-584-5p	miR-29c-3p	miR-9-5p	miR-95-3p
	miR-654-3p	miR-193a-5p	miR-10b-5p	miR-489-3p
	miR-662-3p		miR-124-3p	miR-488-5p

miR-216b-5p	miR-10a-5p	miR-138-5p	miR-2115-5p	miR-671-5p
miR-488-3p	miR-129-1-3p	miR-3182-5p	miR-4732-5p	miR-505-5p
miR-143-5p	miR-138-2-3p	miR-100-5p	miR-550a-3p	miR-660-3p
miR-129-5p	miR-195-5p	miR-135a-5p	miR-5583-5p	miR-93-5p
miR-203a-3p	miR-338-5p	miR-9-3p	miR-301a-3p	miR-643-3p
miR-33b-5p	miR-34b-3p	miR-218-5p	let-7f-5p	miR-29b-1-5p
miR-1246-5p	miR-127-3p	let-7a-5p	miR-3613-3p	miR-548d-5p
miR-497-3p	miR-125b-1-3p	miR-101-3p	let-7i-5p	miR-33a-3p
miR-767-5p	miR-346-5p	miR-181a-5p	miR-194-5p	miR-185-3p
miR-193b-5p	miR-214-5p	miR-424-5p	miR-1306-5p	miR-151a-3p
miR-4488-3p	miR-10b-3p	miR-19b-3p	miR-590-5p	miR-205-5p
miR-206-3p	miR-483-3p	miR-423-5p	miR-454-3p	miR-5187-3p
miR-1185-5p	miR-92b-3p	miR-324-3p	miR-130a-3p	miR-6731-3p
miR-592-5p	miR-30c-2-3p	miR-185-5p	miR-17-3p	miR-92a-1-5p
miR-376a-5p	miR-377-3p	miR-183-5p	miR-576-5p	miR-584-5p
miR-193b-3p	miR-455-3p	miR-26a-5p	miR-19a-3p	miR-301a-5p
miR-3117-3p	miR-383-5p	miR-26b-5p	miR-628-3p	miR-150-5p
miR-4705-5p	miR-2114-5p	miR-296-5p	miR-140-5p	miR-1255a-5p
miR-323a-3p	miR-338-3p	miR-660-5p	miR-451a-5p	miR-493-5p
miR-337-5p	miR-1248-5p	miR-22-5p	miR-500a-3p	miR-4433-5p
miR-147b-3p	miR-885-5p	miR-548f-3p	miR-6502-5p	miR-4433-3p
let-7c-5p	miR-708-3p	miR-580-3p	miR-4646-3p	miR-103a-3p
miR-143-3p	miR-30a-3p	miR-194-3p	miR-4676-3p	miR-31-3p
miR-329-3p	miR-30a-5p	miR-106a-5p	miR-505-3p	miR-556-5p
miR-125a-3p	miR-204-3p	miR-4742-5p	miR-6770-5p	miR-16-2-3p
miR-539-3p	miR-138-1-3p	miR-374b-5p	miR-20b-5p	let-7f-1-3p
miR-153-3p	miR-1264-3p	miR-28-5p	miR-374a-5p	miR-2355-3p
miR-708-5p	miR-34a-3p	miR-199a-5p	miR-664b-3p	miR-30e-5p
miR-34a-5p	miR-184-3p	miR-148b-3p	miR-24-2-5p	let-7g-5p
miR-124-5p	miR-455-5p	miR-301b-3p	miR-20a-3p	miR-1301-3p
miR-433-3p	miR-137-3p	let-7f-2-3p	miR-548k-5p	miR-6513-3p
miR-935-3p	miR-196a-5p	miR-3074-5p	miR-664a-3p	let-7d-5p
miR-3200-3p	miR-149-5p	miR-1292-5p	miR-144-5p	miR-4785-3p
miR-127-5p	miR-99a-5p	miR-548d-3p	miR-362-5p	miR-6516-5p
miR-92b-5p	miR-34c-5p	miR-371b-5p	miR-4446-3p	miR-4422-5p
miR-136-3p	miR-125b-5p	miR-641-5p	let-7g-3p	miR-3617-5p
miR-615-3p	miR-887-3p	miR-4500-3p	miR-140-3p	miR-590-3p
miR-1912-5p	miR-99a-3p	miR-6514-3p	miR-24-3p	miR-532-3p
miR-497-5p	miR-125b-2-3p	miR-6764-3p	miR-1908-5p	miR-340-5p
miR-145-3p	miR-204-5p	miR-3614-5p	miR-1270-5p	miR-766-5p
miR-499a-5p	miR-129-2-3p	miR-324-5p	miR-624-5p	miR-188-3p
miR-376b-5p	miR-214-3p	miR-502-3p	miR-493-3p	miR-17-5p
miR-483-5p	miR-34b-5p	miR-1273c-5p	miR-31-5p	miR-542-5p
miR-4284-5p	miR-211-5p	miR-548a-3p	miR-4802-5p	miR-26b-3p

miR-370-3p	miR-182-5p	miR-4772-3p	miR-486-3p	miR-508-5p
miR-151a-5p	let-7d-3p	miR-28-3p	miR-627-5p	miR-558-3p
miR-579-3p	miR-374c-3p	miR-188-5p	miR-1260b-5p	miR-520e-3p
miR-378c-5p	miR-548ax-5p	miR-450a-5p	miR-155-5p	miR-524-5p
miR-18b-5p	miR-141-3p	miR-339-5p	miR-6503-5p	miR-548a-5p
miR-942-5p	miR-106b-5p	miR-1307-3p	miR-326-3p	miR-606-3p
miR-191-3p	miR-625-5p	miR-3194-5p	miR-5193-3p	miR-612-5p
miR-25-3p	miR-3667-5p	miR-423-3p	miR-941-3p	miR-624-5p
miR-30e-3p	miR-2355-5p	miR-3130-5p	miR-4433b-3p	miR-647-5p
miR-501-5p	miR-30d-5p	miR-192-5p	miR-486-5p	miR-373-5p
miR-876-5p	miR-224-3p	miR-23a-5p	miR-15a-3p	miR-506-3p
miR-548e-3p	miR-1273h-3p	miR-6803-3p	miR-652-5p	miR-518a-5p
miR-19b-1-5p	miR-93-3p	miR-16-5p	miR-1275-5p	miR-518e-3p
miR-4454-5p	miR-20b-3p	miR-877-3p	miR-1285-3p	miR-551a-3p
miR-1277-5p	miR-103a-2-5p	miR-378a-5p	miR-3615-3p	miR-890-5p
miR-126-3p	miR-5690-5p	miR-200c-3p	miR-150-3p	miR-1-3p
miR-3909-3p	miR-3607-5p	miR-4791-5p	miR-642a-5p	miR-9-5p
miR-3120-3p	miR-20a-5p	miR-221-5p	miR-766-3p	miR-10a-5p
miR-126-5p	miR-378a-3p	miR-181a-2-3p	miR-27a-5p	miR-10b-5p
miR-625-3p	miR-130b-3p	miR-21-3p	miR-342-3p	miR-15a-5p
miR-4802-3p	miR-3667-3p	miR-191-5p	miR-431-5p	miR-15b-5p
miR-96-5p	miR-4521-5p	miR-342-5p	miR-142-5p	miR-17-5p
miR-7977-5p	miR-197-3p	miR-15b-3p	miR-5684-5p	miR-18a-5p
miR-582-3p	miR-5100-3p	miR-130b-5p	miR-6503-3p	miR-18b-5p
miR-548a-5p	miR-425-5p	miR-1304-3p	miR-223-5p	miR-19a-3p
miR-3912-3p	miR-454-5p	miR-548w-5p	miR-223-3p	miR-19b-3p
miR-618-5p	miR-1537-3p	miR-629-3p	miR-4433b-5p	miR-20a-5p
miR-6802-3p	miR-331-5p	miR-4326-5p	miR-148a-3p	miR-20b-5p
miR-582-5p	miR-671-3p	miR-450b-5p	miR-4423-3p	miR-22-3p
miR-589-3p	miR-1256-3p	miR-425-3p	miR-144-3p	miR-23a-3p
miR-208a-3p	miR-27a-3p	miR-6852-5p	miR-3194-3p	miR-23b-3p
miR-424-3p	miR-642a-3p	miR-142-3p	miR-1296-5p	miR-24-3p
miR-106b-3p	miR-222-3p	miR-361-3p		miR-25-3p
miR-548o-3p	miR-652-3p	miR-503-5p	<b>Russel et al,</b>	miR-27a-3p
miR-21-5p	miR-335-3p	miR-3591-3p	<b>2013</b>	miR-27b-3p
miR-15a-5p	miR-339-3p	miR-4286-5p	miR-23a-3p	miR-28-3p
miR-532-5p	miR-146b-5p	miR-378d-5p	miR-29b-3p	miR-28-5p
miR-23a-3p	miR-1185-1-3p	miR-940-3p	miR-206-3p	miR-29a-3p
miR-6718-5p	miR-551a-3p	miR-484-5p	miR-455-3p	miR-29b-3p
miR-589-5p	miR-4695-3p	miR-221-3p		miR-29c-3p
miR-7-1-3p	miR-331-3p	miR-4772-5p	<b>Campos-Melo</b>	miR-30b-5p
miR-1285-5p	miR-1976-3p	miR-15b-5p	<b>et al, 2013</b>	miR-30c-5p
miR-92a-3p	miR-18a-5p	miR-224-5p	miR-16-2-3p	miR-31-5p
miR-6852-3p	miR-107-3p	miR-16-1-3p	miR-146a-3p	miR-34a-5p

miR-34c-5p	miR-152-3p	miR-326-3p	miR-455-5p	miR-579-3p
miR-92a-3p	miR-153-3p	miR-328-3p	miR-485-3p	miR-582-3p
miR-93-5p	miR-154-5p	miR-329-3p	miR-485-5p	miR-582-5p
miR-98-5p	miR-181a-5p	miR-330-3p	miR-487a-3p	miR-589-5p
miR-99a-5p	miR-181c-5p	miR-330-5p	miR-487b-3p	miR-597-5p
miR-99b-5p	miR-184-3p	miR-331-3p	miR-490-3p	miR-598-3p
miR-99b-3p	miR-185-5p	miR-331-5p	miR-491-5p	miR-604-3p
miR-100-5p	miR-188-3p	miR-335-5p	miR-494-3p	miR-618-5p
miR-101-3p	miR-190a-5p	miR-337-5p	miR-495-3p	miR-625-5p
miR-103a-3p	miR-192-5p	miR-338-3p	miR-499-5p	miR-625-3p
miR-105-5p	miR-193a-3p	miR-339-3p	miR-500a-3p	miR-627-5p
miR-106a-5p	miR-193a-5p	miR-339-5p	miR-501-5p	miR-629-5p
miR-106b-5p	miR-193b-3p	miR-340-5p	miR-502-3p	miR-642-
miR-107-3p	miR-194-5p	miR-342-5p	miR-502-5p	miR-651-5p
miR-122-5p	miR-197-3p	miR-345-5p	miR-503-5p	miR-652-3p
miR-124-3p	miR-198-5p	miR-346-5p	miR-504-5p	miR-654-3p
miR-125a-3p	miR-200a-3p	miR-361-5p	miR-505-3p	miR-654-5p
miR-125a-5p	miR-200b-3p	miR-362-3p	miR-511-3p	miR-655-3p
miR-125b-5p	miR-202-5p	miR-362-5p	miR-512-3p	miR-660-5p
miR-127-3p	miR-204-5p	miR-363-3p	miR-515-5p	miR-671-3p
miR-127-5p	miR-210-3p	miR-365-	miR-516b-5p	miR-708-5p
miR-128-3p	miR-211-5p	miR-367-3p	miR-517a-3p	miR-744-5p
miR-129-3p	miR-212-3p	miR-367-5p	miR-519a-3p	miR-758-3p
miR-129-5p	miR-215-5p	miR-369-3p	miR-519d-3p	miR-760-3p
miR-130a-3p	miR-216a-5p	miR-369-5p	miR-520a-3p	miR-873-5p
miR-130b-3p	miR-216b-5p	miR-370-3p	miR-520a-5p	miR-874-3p
miR-132-3p	miR-218-5p	miR-376a-3p	miR-520f-3p	miR-885-5p
miR-133a-3p	miR-218-2-3p	miR-377-3p	miR-532-3p	miR-887-3p
miR-133b-3p	miR-219-5p	miR-379-5p	miR-532-5p	miR-889-3p
miR-135a-5p	miR-219-2-3p	miR-380-3p	miR-539-3p	let-7a-5p
miR-135b-5p	miR-221-3p	miR-381-3p	miR-541-3p	let-7b-5p
miR-137-3p	miR-223-3p	miR-382-5p	miR-542-3p	let-7c-5p
miR-138-1-3p	miR-296-3p	miR-383-5p	miR-544-	let-7d-5p
miR-139-3p	miR-296-5p	miR-409-5p	miR-545-3p	let-7e-5p
miR-139-5p	miR-299-3p	miR-422a-5p	miR-548c-5p	
miR-140-5p	miR-299-5p	miR-423-5p	miR-548d-5p	<b>Freischmidt et</b>
miR-141-3p	miR-301a-3p	miR-424-5p	miR-550*	<b>al, 2013</b>
miR-142-3p	miR-301b-3p	miR-425-5p	miR-551b-3p	miR-132-5p
miR-142-5p	miR-302a-3p	miR-425-3p	miR-556-5p	miR-132-3p
miR-146b-3p	miR-302c-3p	miR-433-3p	miR-570-3p	miR-143-5p
miR-147b-3p	miR-320-	miR-448-3p	miR-574-3p	miR-143-3p
miR-148b-3p	miR-323-3p	miR-450a-5p	miR-576-3p	miR-574-5p
miR-149-5p	miR-324-3p	miR-450b-5p	miR-576-5p	let-7b-5p
miR-150-5p	miR-324-5p	miR-455-3p	miR-578-3p	

**Saucier et al,  
2018**

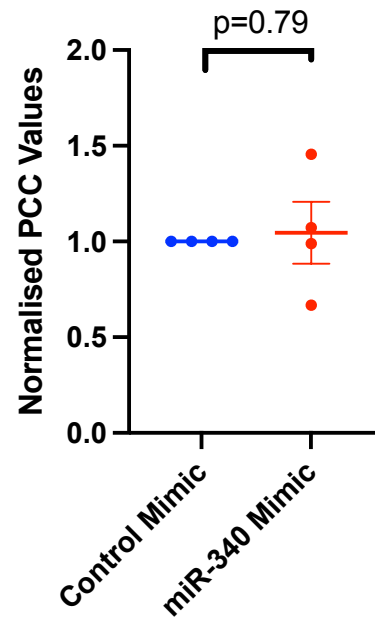
miR-532-3p  
miR-144-3p  
miR-15a-5p  
miR-363-3p  
miR-183-5p  
miR-4454-5p  
miR-9-1-5p  
miR-9-3-5p  
miR-338-3p  
miR-9-2-5p  
miR-100-5p  
miR-7977-5p  
miR-1246-5p  
miR-664a-5p  
miR-1290-3p  
miR-4286-5p  
miR-181b-1-5p  
miR-1260b-5p  
miR-181b-2-5p  
miR-127-3p  
let-7c-5p  
miR-181a-2-5p  
miR-181a-1-5p  
miR-199a-2-3p  
miR-199b-3p  
miR-199a-1-3p

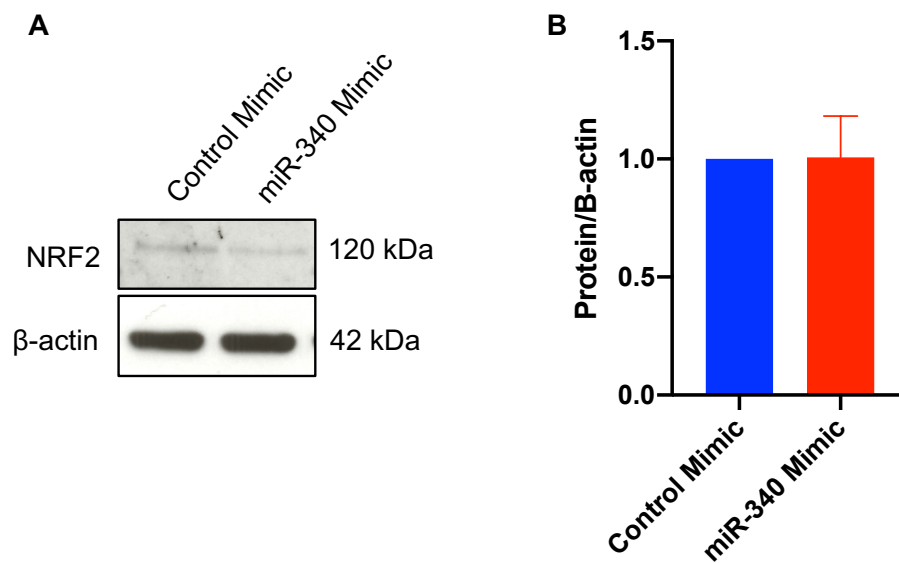
**Emde et al,  
2015**

miR-9-5p  
miR-124-3p

**Appendix 3: Live cell autophagic flux assay using N2A cells**

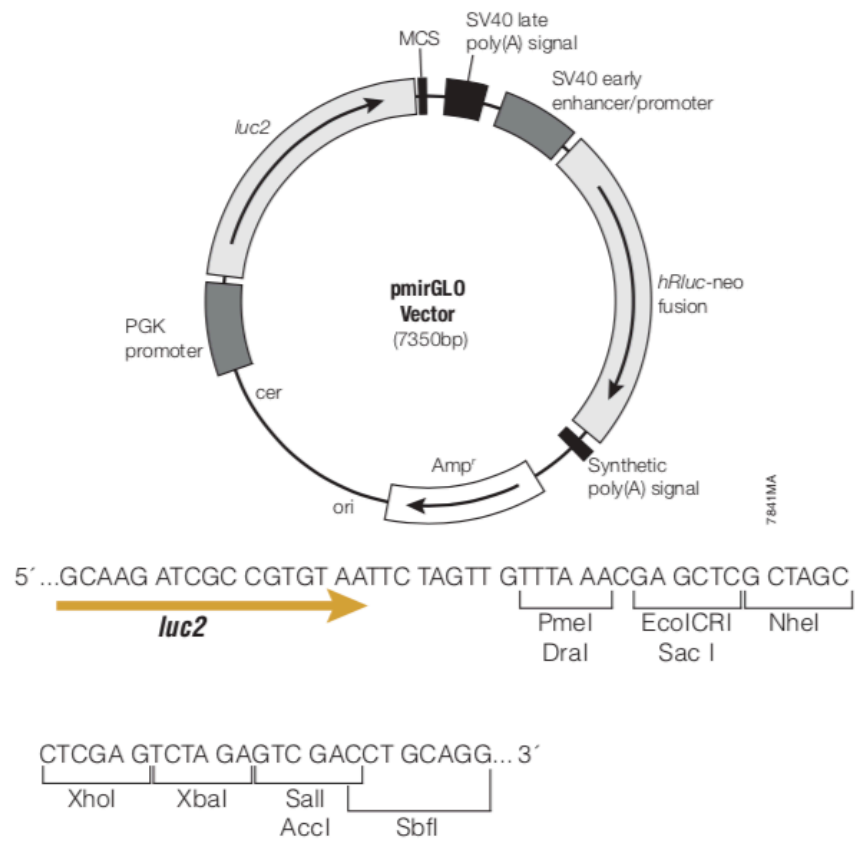
N2A cells were co-transfected with 100 ng mCherry-GFP-p62/SQSTM1 and 50 nM of either a negative control mimic or miR-340 mimic for 48 hours prior to visualisation by widefield microscopy using the DeltaVision microscope. Data is from four independent experiments and shows Mean  $\pm$  SEM.



**Appendix 4: Western blotting for NRF2 in N2A cells.**

A) A representative western blot of N2A cells transfected with 50 nM miR-340 mimic or inhibitor and respective negative controls for 48 hours. B) Densitometry analysis of western blots of N2A cells transfected with miR-340 mimic or negative mimic control. C) Densitometry analysis of western blots of N2A cells transfected with miR-340 inhibitor or negative inhibitor control. Data shows mean  $\pm$  SEM and is from a minimum of three independent experiments.

**Appendix 5: Plasmid map of pmirGLO vector used for the dual luciferase assay.**



**Appendix 6: COVID-19 Statement**

The COVID-19 pandemic resulted in an enforced 'stay at home' rule across the country, including our lab, in March 2020. This occurred 18 months into my PhD and coincided with a point at which several experiments were optimised and ready for performance. As a result, these experiments were delayed and resulted in a substantial set back for my planned work. The break resulted in six months away from the lab, and upon my return, left me with just one year of funded research time. I believe that significantly more research would have been performed during my PhD had the pandemic not occurred.

During the lockdown, I was able to write up as much work as I could, though since the majority of experiments were planned for the future, there was a limited amount I was able to achieve. However, I was able to work with my supervisors to plan and prioritise the experiments to be performed upon my return to work in September 2020. As a result, I was able to quickly return to a reasonable pace of work. However, I feel that due to the short period of time left on my PhD, I was unable to perform some experiments that would have provided a thorough conclusion to results chapters or areas of work. For example, I believe several of the experiments suggested as future work would have been incorporated into this thesis, had I not lost six months of funded research time.

Upon my return to work, the pandemic also resulted in maximum occupancy rules in labs, which led to our lab group physically moving location, which hindered some aspects of my work for several weeks. This maximum occupancy rule generally contributed to a slower pace of lab work for several months. For example, only one person could work in tissue culture at a time. Whilst this was not generally detrimental, it did require much more flexibility and planning of experiments than had been necessary pre-pandemic.

In summary the COVID-19 pandemic undeniably altered the course of my PhD. By thoroughly planning future experiments during the stay-at-home period, I was able to reduce the impact of the lockdown on my work as much as possible. However, had

six months of funded lab time not been lost, key concluding experiments would likely have been performed and strengthened several sections of my results chapters.